NORTH AMERICAN AVIATION, INC. SPACE and INFORMATION SYSTEMS DIVISION

SID 66-135

ANALYSIS OF WEBS OF PARTIAL-TENSION-FIELD BEAMS SUBJECTED TO LATERAL PRESSURE LOADINGS

April 1966

By

L. Kovalevsky
T. Furuike
L. A. Nelson
F. L. Rish

Prepared Under
Contract No. NAS8-20113 by
North American Aviation, Incorporated
Space and Information Systems Division,
Downey, California

For

George C. Marshall Space Flight Center,
Huntsville, Alabama

NATIONAL AERONAUTICS AND SPACE ADMINISTRATION,
WASHINGTON, D. C.

FOREWORD

This report was prepared by the Structural Sciences Department, Space and Information Systems Division, North American Aviation, Inc., Downey, California, under Contract NAS8-20113.

This program was conducted for the National Aeronautics and Space Administration, George C. Marshall Space Flight Center. Mr. James L. Lewis was the NASA technical monitor for the program. Mr. F. L. Rish of the Space and Information Systems Division was the program manager. The program was performed during the period May 1965 to March 1966.

The authors are indebted to Messrs. L. A. Harris, P. E. Franklin, D. J. Stone, and P. P. Radkowski for the overall guidance and technical review, to Mr. A. E. Zagorski for technical checking, Mr. R. M. Bereznak for IBM 7094 digital computer programming, and to Mr. R. W. Johnson for drafting and computations.

ABSTRACT

This report covers the derivation of a method of analysis for straight and curved partial-tension-field beams subjected to lateral pressure. In practical beams, the webs resist some diagonal compressive stress after buckling and thus act in an intermediate range between shear-resistant webs and pure-tension-field webs. These beams are termed partial-tension-field beams. The design and analysis of beams subjected to vertical stress is satisfactorily covered by the work done by Kuhn and Peterson. However, when the additional loading environment of lateral pressure is superimposed on the web of a beam in the partial-tension-field state, the effects on the stress field can only be approximated, resulting in undue conservatism. The method developed shows how the combination of shear and lateral loading affects both the web and uprights. The method relies principally on and is an extension of the work presented by Mr. Paul Kuhn in Stresses in Aircraft and Shell Structures, McGraw-Hill Book Co., Inc., 1956. The procedure covers both straight and curved beams, and illustrative numerical examples are provided.

SYMBOLS

a	Edge dimension of plate, in.
A	Area, in.^{2}
A_{FL}	Flange area, in.^{2}
A_U	Upright area, in.^{2}
A_{Ue}	Equivalent upright area, in.^{2}
b	Edge dimension of plate, in.
C_i	(i = 1, 2, 3) Stress concentration coefficients
c	Distance from neutral axis to outer fiber, in.
d	Distance between uprights in straight beam; distance between flanges in curved beam, in.
e	Eccentricity, in.
E	Young's modulus, psi
F	Force in flange, lb
G	Shear modulus, psi
G_p	Modified shear modulus (pure diagonal tension), psi
G^*	Modified shear modulus (postbuckling), psi
g_o	Vertical beam loading, lb/in.
h	Distance between flanges in straight beam; distance between uprights in curved beam, in.
H	Tensile load in catenary, lb
H_a, H_b	Force in the a and b directions, respectively, lb

i	Radius of gyration, in.; integer
I_{UF}	Moment of inertia of upper flange cross section with respect to centroidal axis, $in.^4$
I_{LF}	Moment of inertia of lower flange cross section with respect to centroidal axis, $in.^4$
k	Diagonal tension factor
k_1	Constant
k_{ss}	Buckling coefficient
ℓ	Distance between uprights, in.
L_e	Effective column length, in.
M	Moment, lb/in.
p	Pressure, psi
p_a	Partial pressure in the a direction, psi
p_b	Partial pressure in the b direction, psi
p_{cr}°	Critical external pressure on curved web, psi
P_U	Force in upright, lb
P_{FL}	Force in flange, lb
q	Distributed loading, lb/in.
R, r	Radii, in.
S	Vertical load, lb; initial length of catenary, in.
t	Web thickness, in.
u	$R + \delta$, in.
y	Deflection, in.
α	Diagonal tension angle, degrees
β	Angle, degrees; or coefficient.

Δ	Empirical stress correction factor
ρ	Radius of gyration, in.
δ	Deflection, in.
σ_a, σ_b	Stress in the a, b directions, respectively, psi
σ_c	Compressive stress, psi
σ_t	Tensile stress, psi
σ_U	Stress in upright, psi
σ_{FL}	Stress in flange, psi
σ_{CC}	Crippling stress, psi
$\sigma_{W\,max}$	Maximum stress in upright, psi
η_a	Pressure ratio, p_a/p
η_b	Pressure ratio, p_b/p
w	Angle; coefficient
τ	Shear stress, psi
τ_o	Shear stress corresponding to final vertical loading, g_o, psi
τ_{cr}	Critical shear stress, psi
τ^*	Combined loading critical shear, psi
μ	Poisson's ratio
->	Leads to

Other symbols are defined as they appear in the text.

CONTENTS

ILLUSTRATIONS

INTRODUCTION

Numerous theories and experimental test results are available in the literature on the strength analysis and stability analysis of tension field and partial-tension-field beams. The work of Kuhn (Reference 1) and Wagner (References 2, 3, and 4) is perhaps best known. The analysis of flat plates subjected to lateral pressure was investigated by Moness (Reference 5). Levy, Goldenberg, and Fibritosky (Reference 6) experimentally investigated the simply supported, long-rectangular, stiffened plate under combined axial load and normal pressure. Woolley, Corrick, and Levy (Reference 7) studied clamped-end conditions.

The above works omit treatment of combined vertical-lateral pressure loading. The objective of this study is to develop an analytical procedure for the analysis of straight and curved partial-tension-field beams subjected to combined vertical and lateral pressure loadings. The analysis is general in nature and is applicable to a variety of boundary conditions. The methods are valid for simple beams, cantilever beams, continuous beams, and other beam systems as long as the structure is properly idealized for the partial-tension-field beam analysis.

The first section of this study is a presentation of the state of the art of the theory for partial-tension-field beams which are loaded vertically. The second section deals with the lateral loading alone. The third section presents the stresses and deformations due to the interaction of vertical and lateral loading acting simultaneously. The fourth section presents the curved partial-tension-field beams. The appendix offers a set of illustrative examples, some derivations, and the necessary IBM 7094 computer programs to simplify the numerical solution of some parts of analysis.

1. PARTIAL-TENSION-FIELD BEAMS SUBJECTED TO VERTICAL LOADINGS

INTRODUCTION

This section presents a summary of the current theory of partial-tension-field beams subjected to vertical loadings. The design and analysis of partial-tension-field beams under vertical loadings are well established. The complete tension-web theory was developed by Wagner (References 2, 3, and 4) and partial-tension-field beam theory by Kuhn (Reference 1). There are other works in the same field, but in general they are usually extensions of the theories of Wagner and Kuhn. A summary of the available theory is needed as the basic foundation for the analysis of the interaction of the vertical loading with the lateral pressure loading, to be treated later.

WEBS

State of Stresses in the Web

Assume a rectangular web which is loaded by pure shear, τ. Figure 1 shows a family of Mohr circles for this loading condition. When the shear stress, τ, increases, the stress field for each increment can be pictorially represented by a Mohr circle. Each circle is equivalent to a certain fixed value of shear stress, τ_i.

From Figure 1 note that an element of the web oriented at an angle of 45 degrees will be subjected to an orthogonal system of axial stresses, one tension and the other compression. When the shear stress, τ, reaches a critical value of shear stress, τ_{cr}, the thin sheet buckles due to excessive diagonal compressive stress. Increases in applied load above this value are carried by diagonal tension stress in the web.

To facilitate analysis the nominal web shear, τ, is divided into a "true shear" part, τ_s, and a diagonal tension part, τ_{dt}.

$$\tau_{dt} = k\tau \qquad \tau_s = (1-k)\tau \text{ (For } \tau \geq \tau_{cr})$$

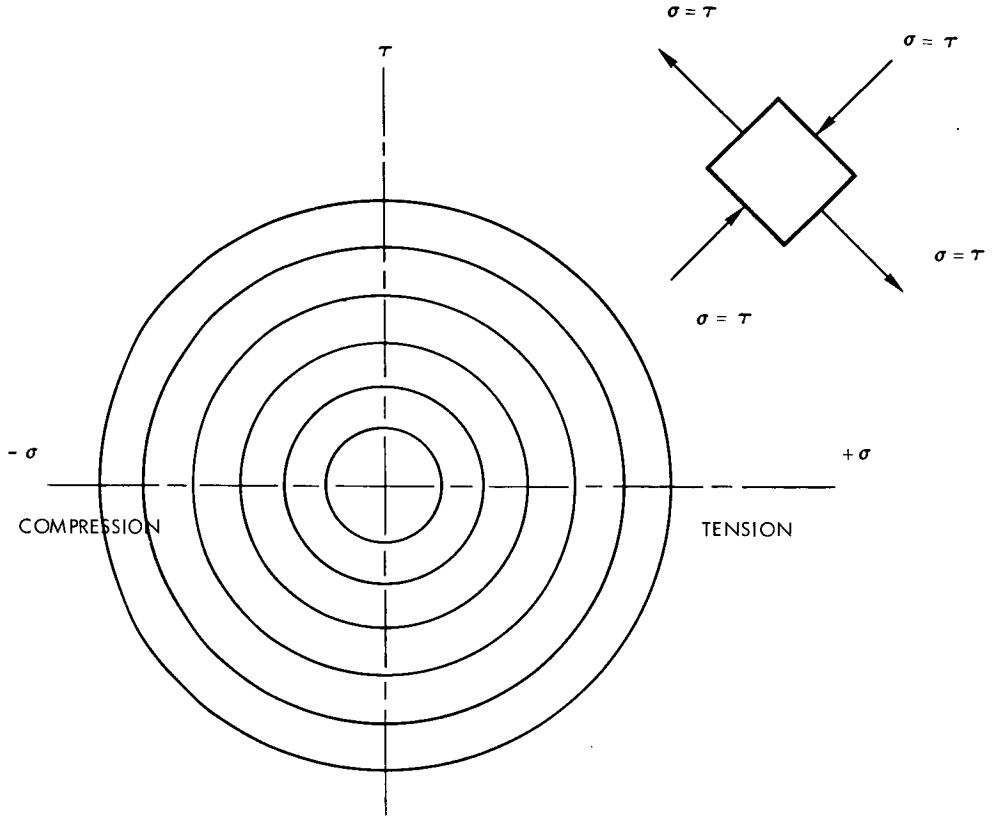

Figure 1. Family of Mohr Cirlces

where k is the diagonal-tension factor. For a given web system under a given load, the value of k is given by an empirical expression

$$k = \tanh\left(0.5 \log \frac{\tau}{\tau_{cr}}\right) \quad (\text{For } \tau \geqq \tau_{cr})$$

The ratio τ/τ_{cr} is called the loading ratio and is a ratio of the total applied load relative to that portion of the total load carried by the web in pure shear. Again to facilitate analysis, introduce the identity

$$\xi = \frac{\tau}{\tau_{cr}}$$

Two stages in the web behavior can be recognized: a prebuckling stage and a postbuckling stage. The prebuckling stage (Figure 1) is characterized by the following relationship:

$$\sigma_1 = \sigma_2 = \tau \text{ for } \xi \leq 1$$

where σ_1 is the principal compression stress
σ_2 is the principal tension stress
} inclined at 45 degrees to the horizontal

The postbuckling stage is characterized by the following relationship:

$$1 < \xi < \infty$$

A pure tension field condition can be approached only in extremely thin sheets. The analytical model (Figure 2) is assumed to carry only loads which are oriented in the diagonal direction, which is at an angle α; the angle α is the actual inclination of the buckles, approximately equal to 45 degrees. The principal stresses for a pure diagonal tension field are as follows:

$$\sigma_1 = 0 \quad \sigma_2 \cong 2\tau$$

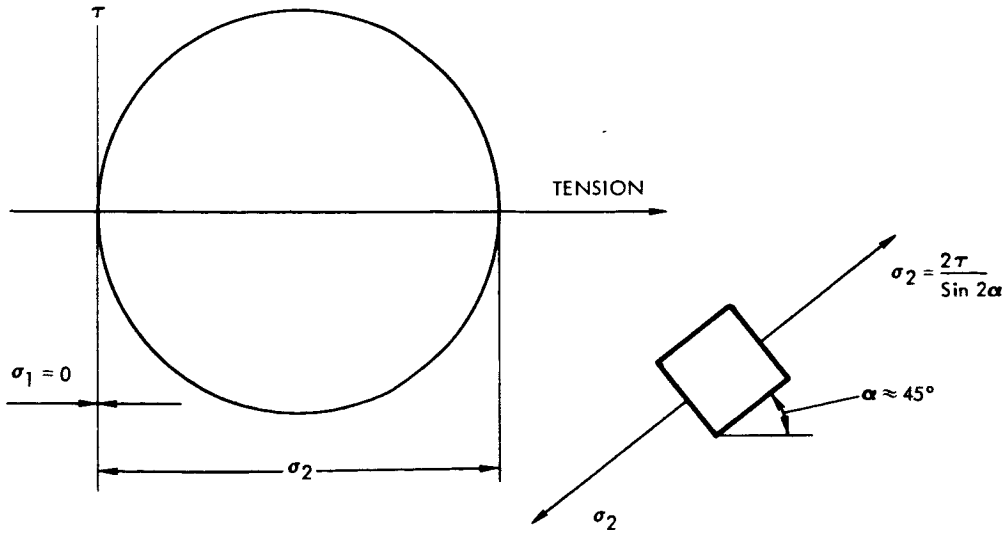

Figure 2. Mohr Circle for a Pure Tension Field

A pure tension-field condition never exists in actual structures. When the web buckles, the shear stresses at buckling will not disappear, but remain as the tension stresses increase (Figure 3). This condition may be represented by the superposition of the Mohr circles shown in Figures 1 and 2. Consequently, it is assumed that as the loading increases, the stress-field changes as is shown in Figure 1. When buckling occurs, the process is continued as is shown in Figure 3.

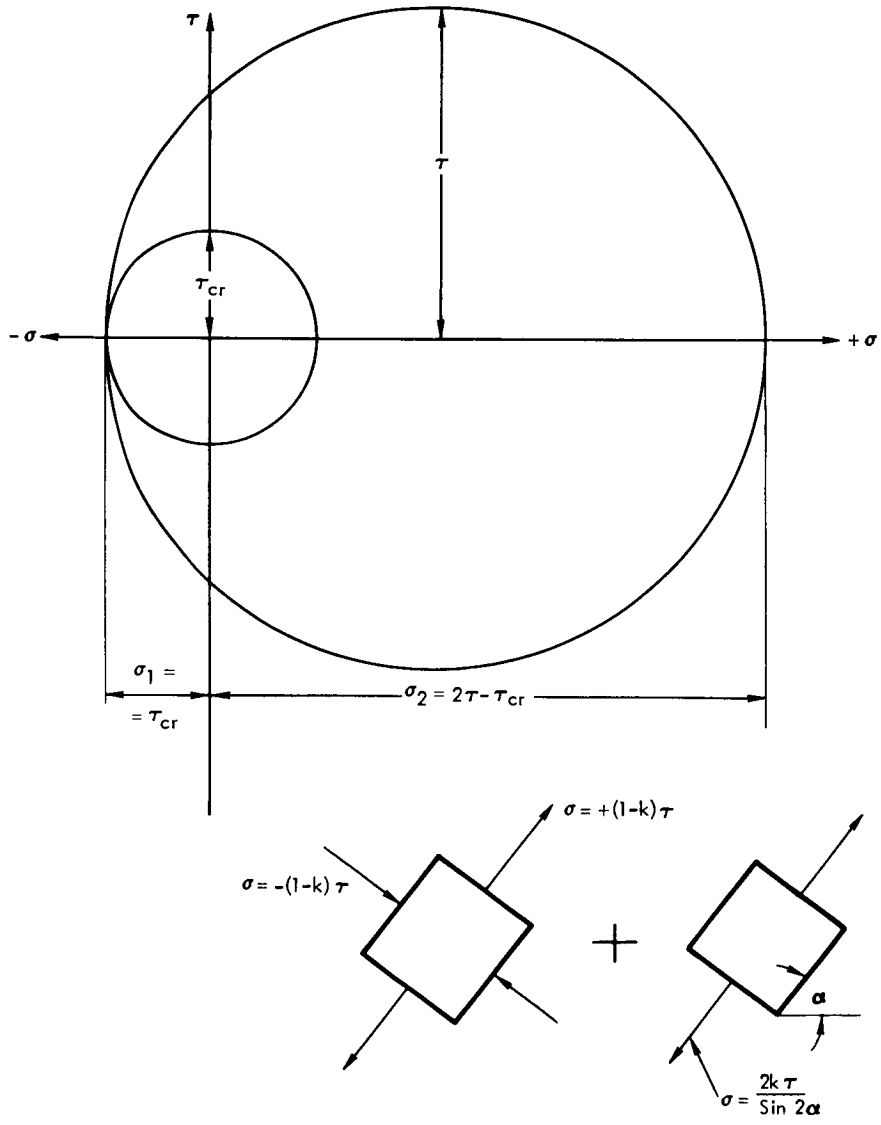

Figure 3. Superposition of Mohr Circles

The following relations characterize the behavior shown in Figure 3:

$$\sigma_2 = 2\tau - \tau_{cr} \; ; \quad \sigma_1 = -\tau_{cr}$$

For intermediate levels of loading, the behavior is shown by the family of Mohr circles shown in Figure 4.

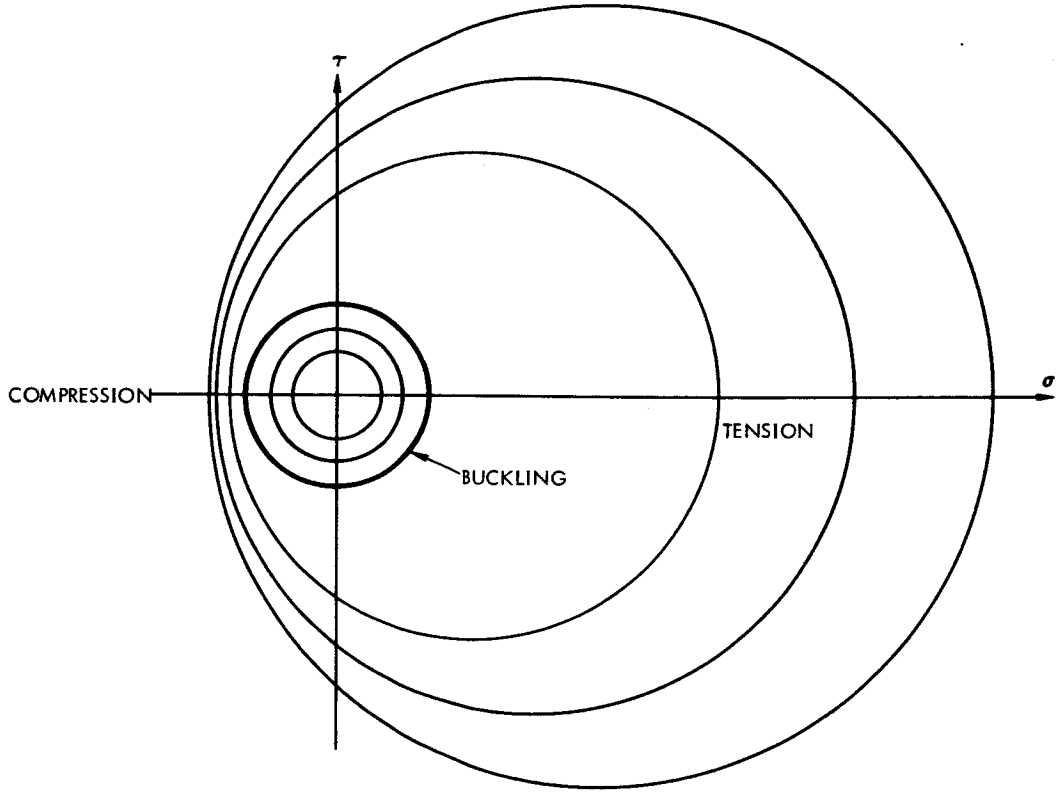

Figure 4. Family of Mohr Circles for Intermediate Levels of Loading

For the postbuckling case in which the loading ratio is larger than unity ($1 < \xi < \infty$), and the shear stress is larger than the critical shear stress ($\tau > \tau_{cr}$) the empirical diagonal tension factor k applies.

Figure 5 is helpful to determine k as function of the parameter τ/τ_{cr}. With the aid of the factor k the two components of any value of τ can be determined from Figure 1 and from Figure 2. The results can be superimposed according to Figure 3.

Consequently, according to Figure 3, the principal compression stress is

$$\sigma_c = -\tau(1-k)\sin 2\alpha$$

and tension stress is

$$\sigma_t = \frac{2k\tau}{\sin 2\alpha} + \tau(1-k)\sin 2\alpha$$

It is assumed that flanges are sufficiently rigid to produce essentially a uniform stress in the web.

The angle α is close to 45 degrees and usually varies from 41 to 49 degrees. This does not significantly affect the stresses σ_c and σ_t. This variation is mostly a function of rigidity of stiffeners and flanges.

If the uprights and flanges are considered rigid (Reference 8), then $\alpha = 45$ degrees.

$$\tan^2\alpha = \frac{1 + \frac{th}{A_{FL}}\frac{E}{E_{FL}}}{1 + \frac{t_d}{A_U}\frac{E}{E_{st}}\sin^2\alpha}$$

where

E = modulus of elasticity of material of web

E_{FL} = modulus of elasticity of material flanges

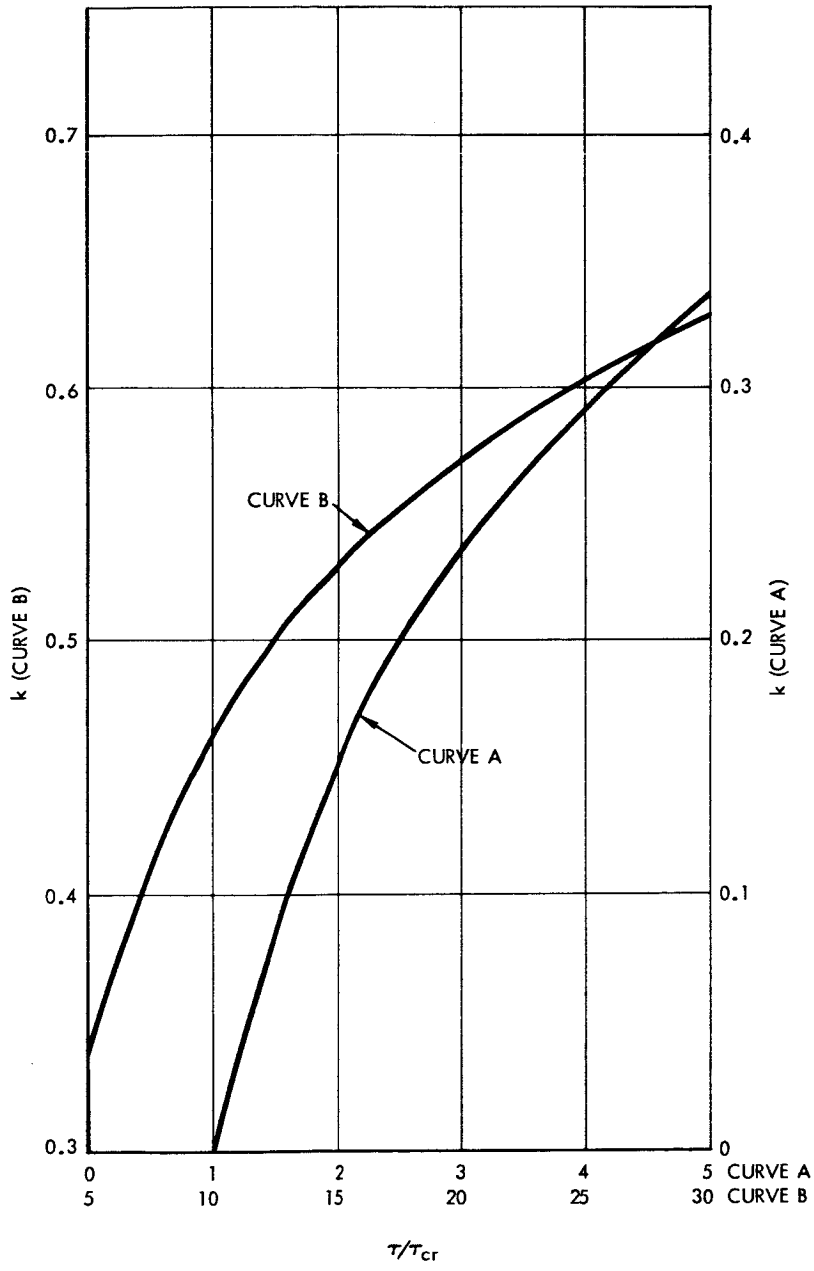

Figure 5. Graph of τ/τ_{cr} Versus k

E_{st} = modulus of elasticity of material of stiffeners

d = distance between the uprights

A_{FL} = areas of flanges

A_U = area of stiffeners

t = thickness of web

h = distance between the centers of gravity of flanges

If the flanges are sufficiently rigid, which is usually the case, the following simplified formula (Reference 8) can be used:

$$\tan \alpha = \sqrt[4]{\frac{1}{1 + \frac{dt}{A_U}}}$$

Figures 6 and 7 simplify the computations connected with the above formula.

The formulas for α are correct only for the ideal case of a pure tension field condition. For a partial tension field, the following formula (Reference 8) applies:

$$\tan^2 \alpha = \frac{1}{1 + \frac{k \tan \alpha}{\left[\frac{A_{U_e}}{dt} + 0.5\,(1-k)\right]\left[(1-k) + \frac{2k}{\sin 2\alpha}\right]}}$$

where

$$A_{U_e} = A_U \left[1 + \left(\frac{e}{\rho}\right)^2 \right]$$

e = eccentricity of stiffener

ρ = radius of gyration about area of web.

Figure 8 diagrams the solution of this equation.

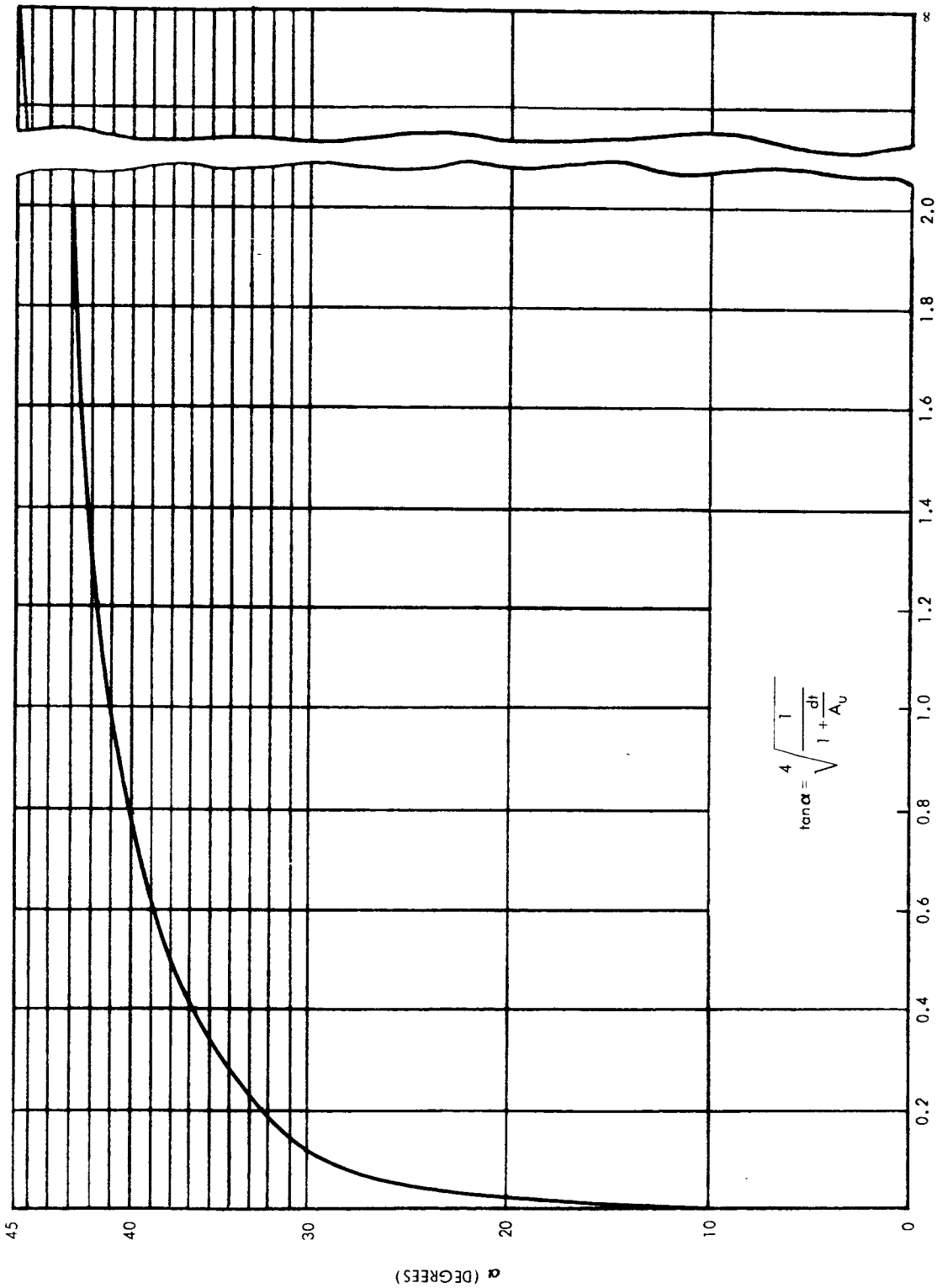

Figure 6. Angle of Diagonal Tension (α)

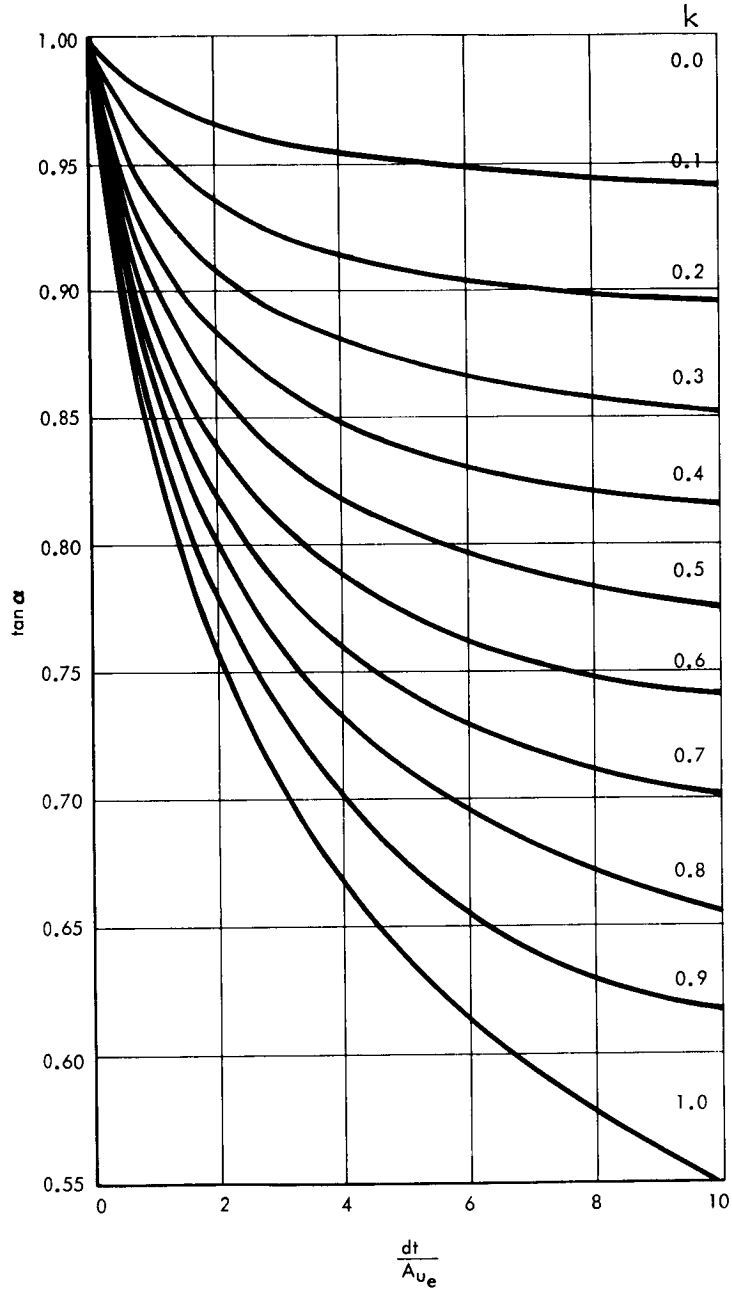

Figure 7. Tension-Field Factor and Angle of Diagonal Test

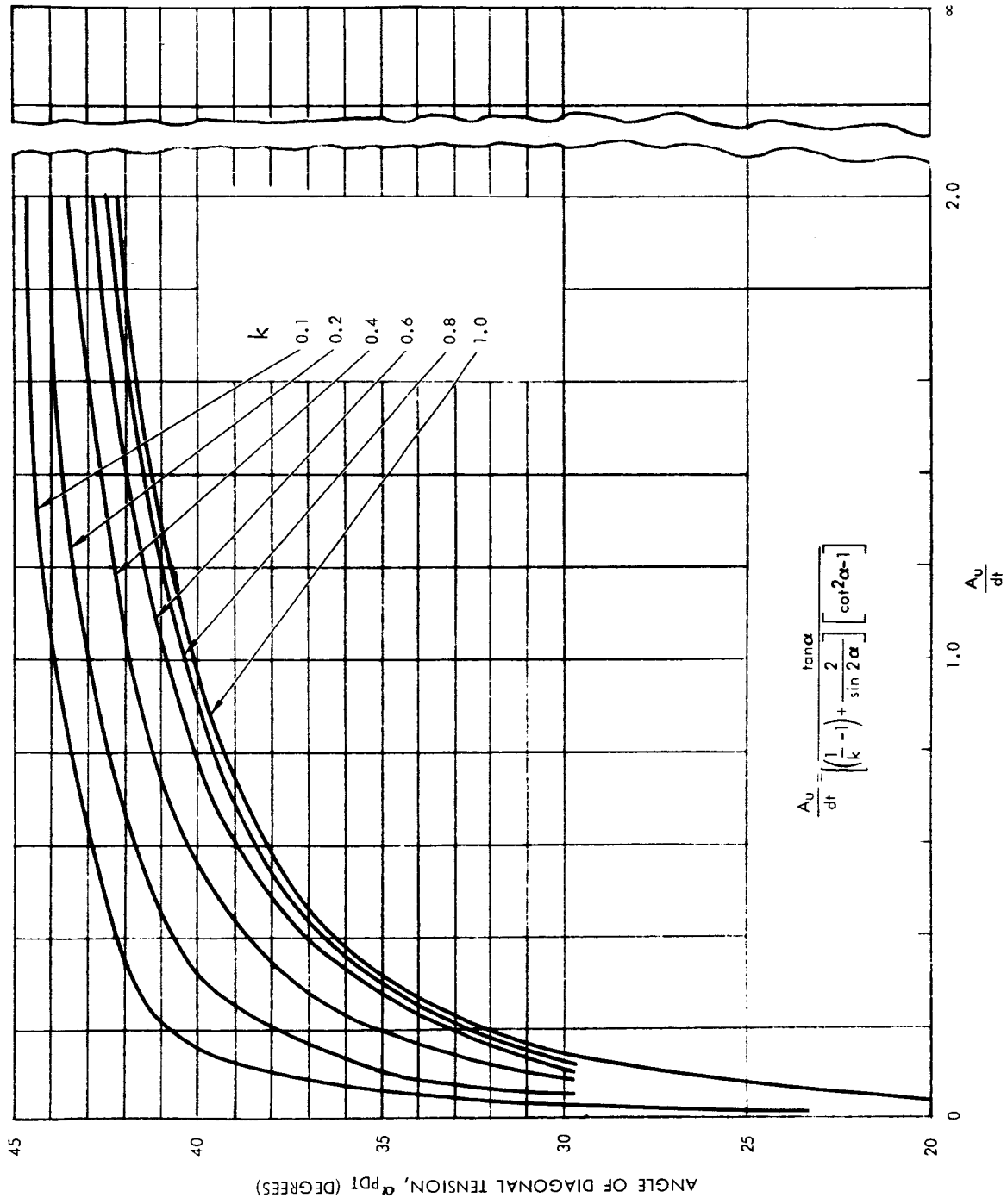

Figure 8. Graphical Solution of Case 2b

Flange deflection reduces the tensile stresses in the span between the stiffeners. This makes the distribution of stresses unequal as shown in Figure 9.

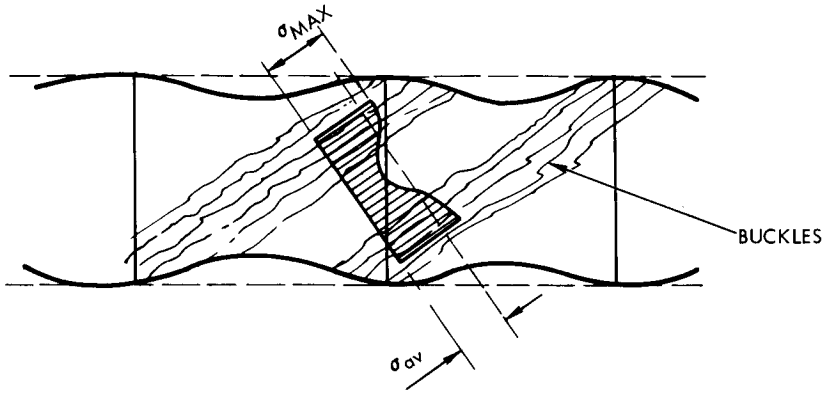

Figure 9. Unequal Distribution of Stresses

The maximum value of diagonal tensile stresses will be

$$\sigma_t^{max} = (1-k)\tau \sin 2\alpha + C_1 \frac{2k\tau}{\sin 2\alpha}$$

where C_1 is a coefficient given in Figure 10, as a function of parameter ωd. This parameter (Reference 8) is as given below:

$$\omega d = 1.25 d \sin\alpha \sqrt[4]{\frac{t}{h(I_{UF} + I_{LF})}}$$

Where I_{UF} and I_{LF} are the moments of inertia of the upper and lower flanges central axis. For the prebuckling stage, the shear modulus G of the material usually is used. For the condition of pure tension, the following equation is recommended to determine shear modulus G_p in the postbuckling stage

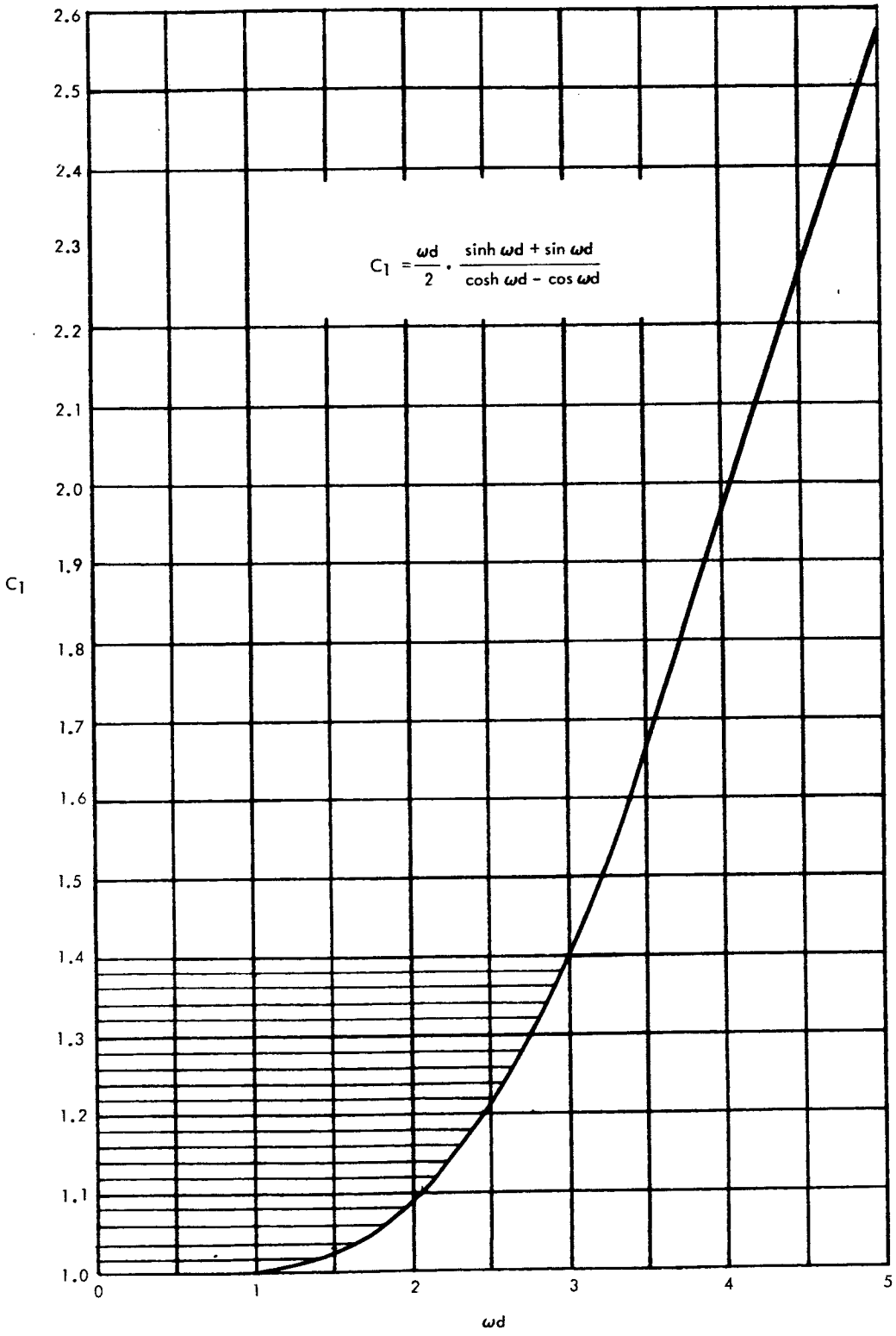

Figure 10. Coefficient C_1 Versus ωd

$$G_p = \frac{2}{3} \frac{G}{\sin^2 2\alpha}$$

This formula is graphically presented in Figure 11. For the post-buckling stage of the partial tension field beams, the following relation is used (Reference 1):

$$\frac{1}{G^*} = \frac{1-k}{G} + \frac{k}{G_p}$$

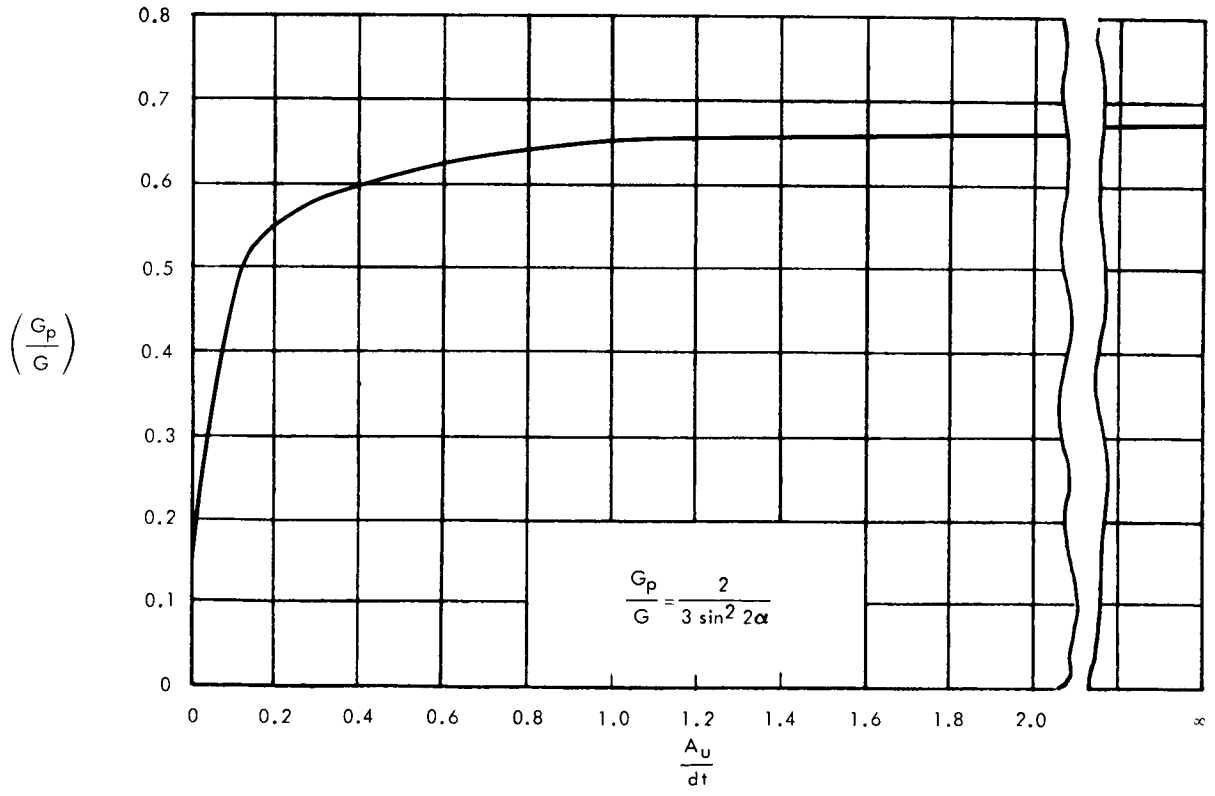

Figure 11. Effective Shear Modulus for the Case of Pure Diagonal Tension

where G* is a modified shear modulus (Reference 8), then

$$G^* = \frac{G}{(1-k) + \frac{3}{2}k \sin^2 2\alpha}$$

A plot of the above equation is shown in Figure 12. An additional coefficient will be introduced, which accounts for the reduction of the web strength due to rivet- or bolt-holes (Reference 8).

$$\beta = \frac{t_o - d_o}{t_o} = 1 - \frac{d_o}{t_o}$$

where

d_o = diameter of hole

t_o = distance of holes

The principal tensile stress σ_t then becomes

$$\sigma_t = \frac{\tau}{\beta}\left[(1-k)\sin 2\alpha + C_1 \frac{2k}{\sin 2\alpha}\right] < \sigma_{tu} \qquad (1-1)$$

where σ_{tu} is allowable stress (ultimate).

BUCKLING STRESS OF THE WEB

The following formula is suggested by Kuhn (Reference 1):

$$\tau_{cr_{elast}} = k_{ss} E \left(\frac{t}{d}\right)^2 \left[R_h + \frac{1}{2}(R_d - R_h)\left(\frac{d}{h}\right)^3 \right] \qquad (1-2)$$

where

k_{ss} = coefficient obtained from Figure 13.

R_h and R_d = empirical restraint coefficients for the vertical and horizontal edges of the web-panel, respectively, as given in Figure 14.

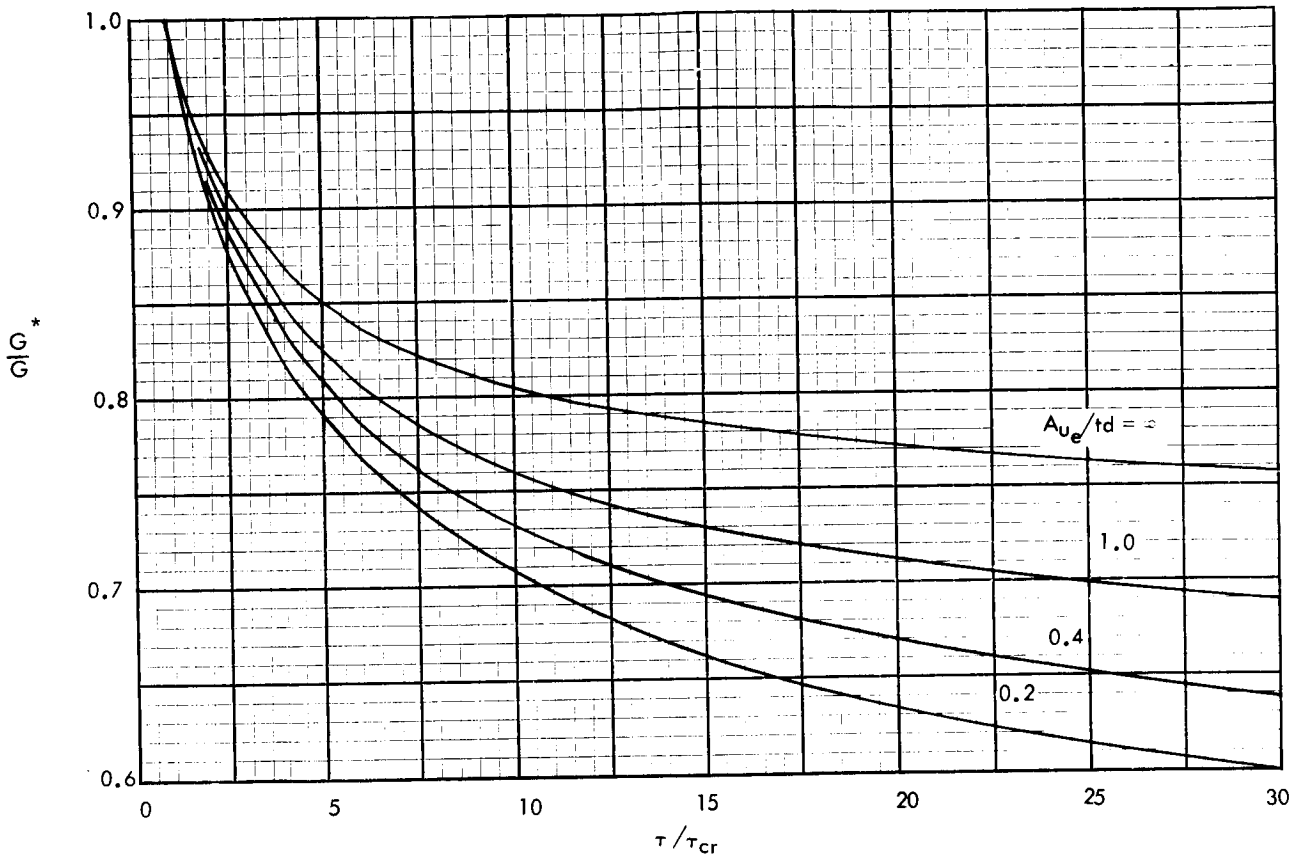

Figure 12. Effective Web Shear Modulus of Elasticity for Incomplete Diagonal Tension

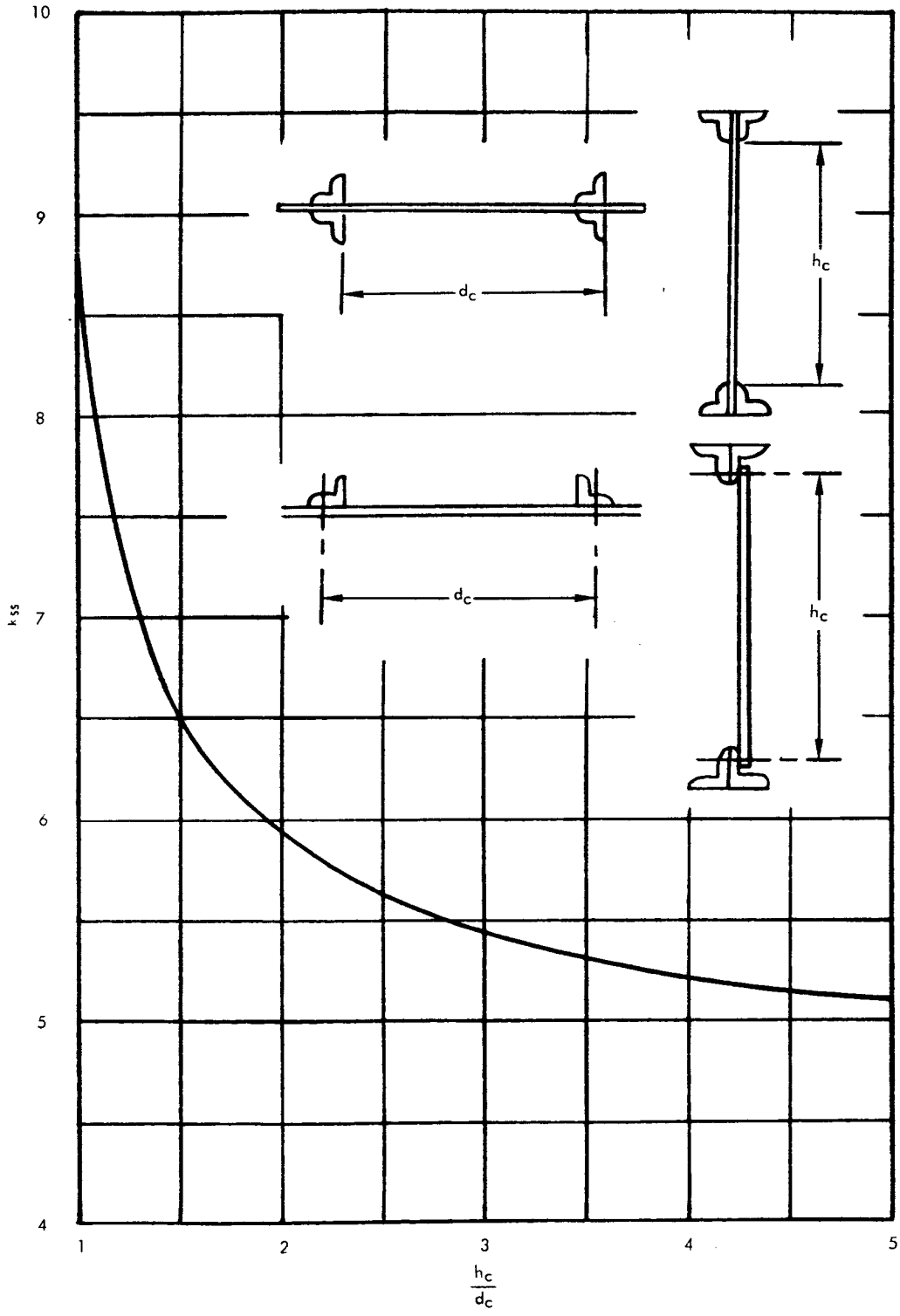

Figure 13. Buckling Coefficients, k_{ss}

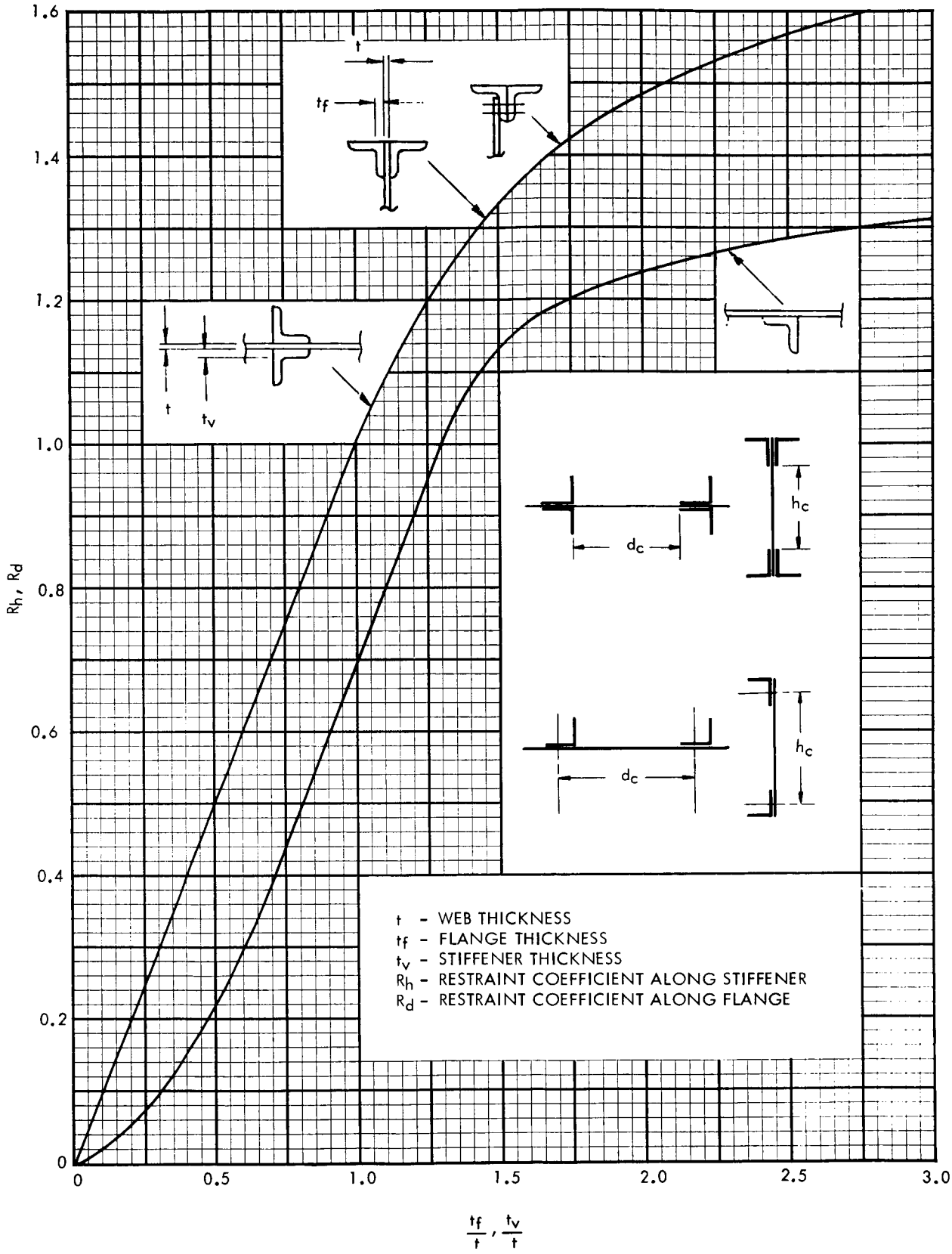

Figure 14. Empirical Edge Restraint Coefficients for Web Buckling Stresses

d = distance between the centers of gravity of the stiffeners

h = distance between the centers of gravity of flanges.

The formula is written for the case d < h. Otherwise, interchange d and h. For simply supported edges, use R = 1.0; for clamped edges, use R = 1.62.

For h and d, use "clear" values where "clear" values are the distance between flange edges. This is a deviation from the normal designation. The elastic stress, calculated with formula (1-2), shall be converted to τ_{cr} by considering plasticity correction, which is also presented in Figure 15.

The graphs presented in Reference 1 , page 58, will simplify the calculation considerably. These graphs are also given in Figures 13, 14, and 15. The graphs for allowable stress τ for aluminum (Figure 16) are given also. The k shown in Figure 16 is obtained from the equation on page 4 or from Figure 5.

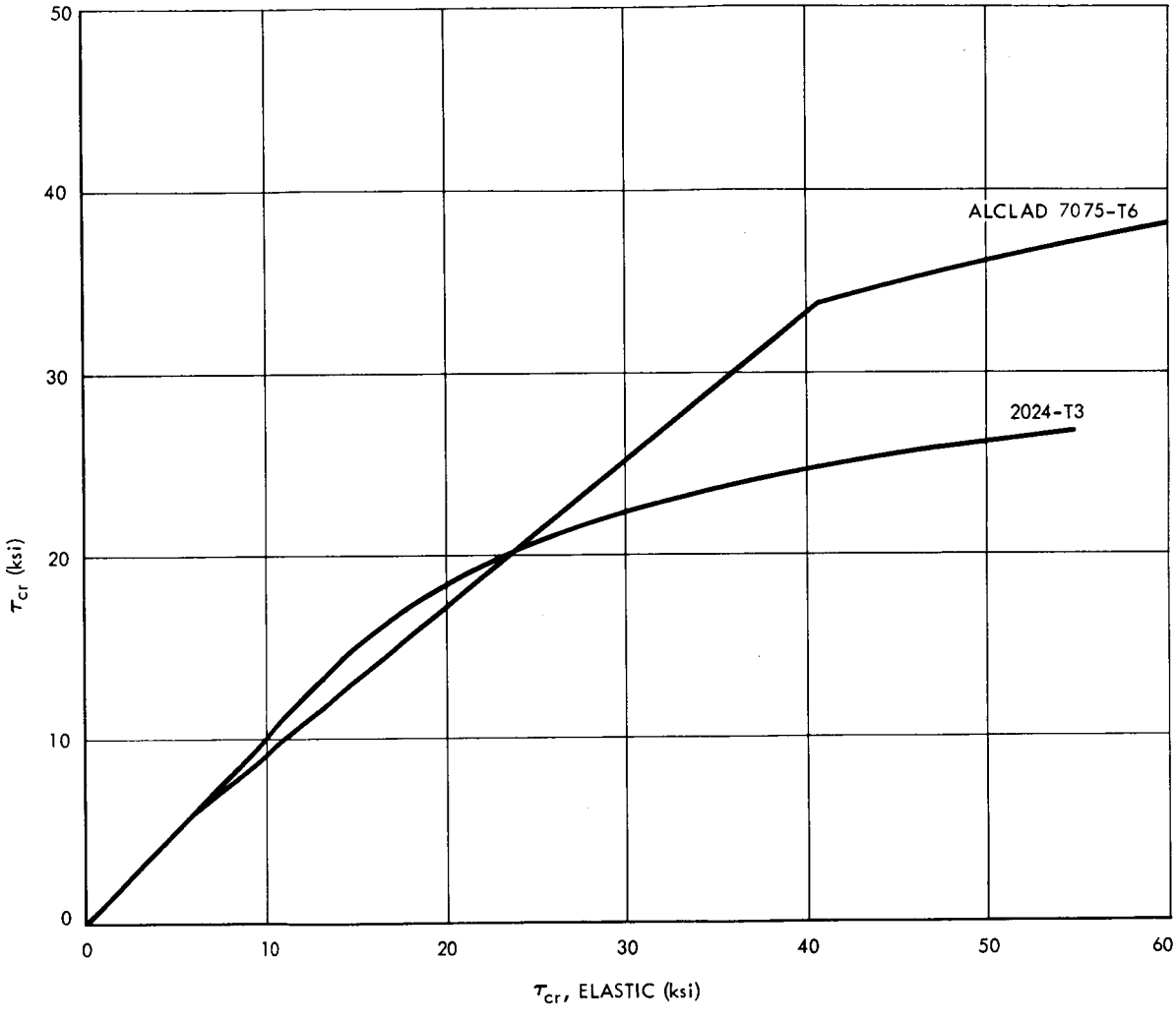

Figure 15. Plasticity Correction

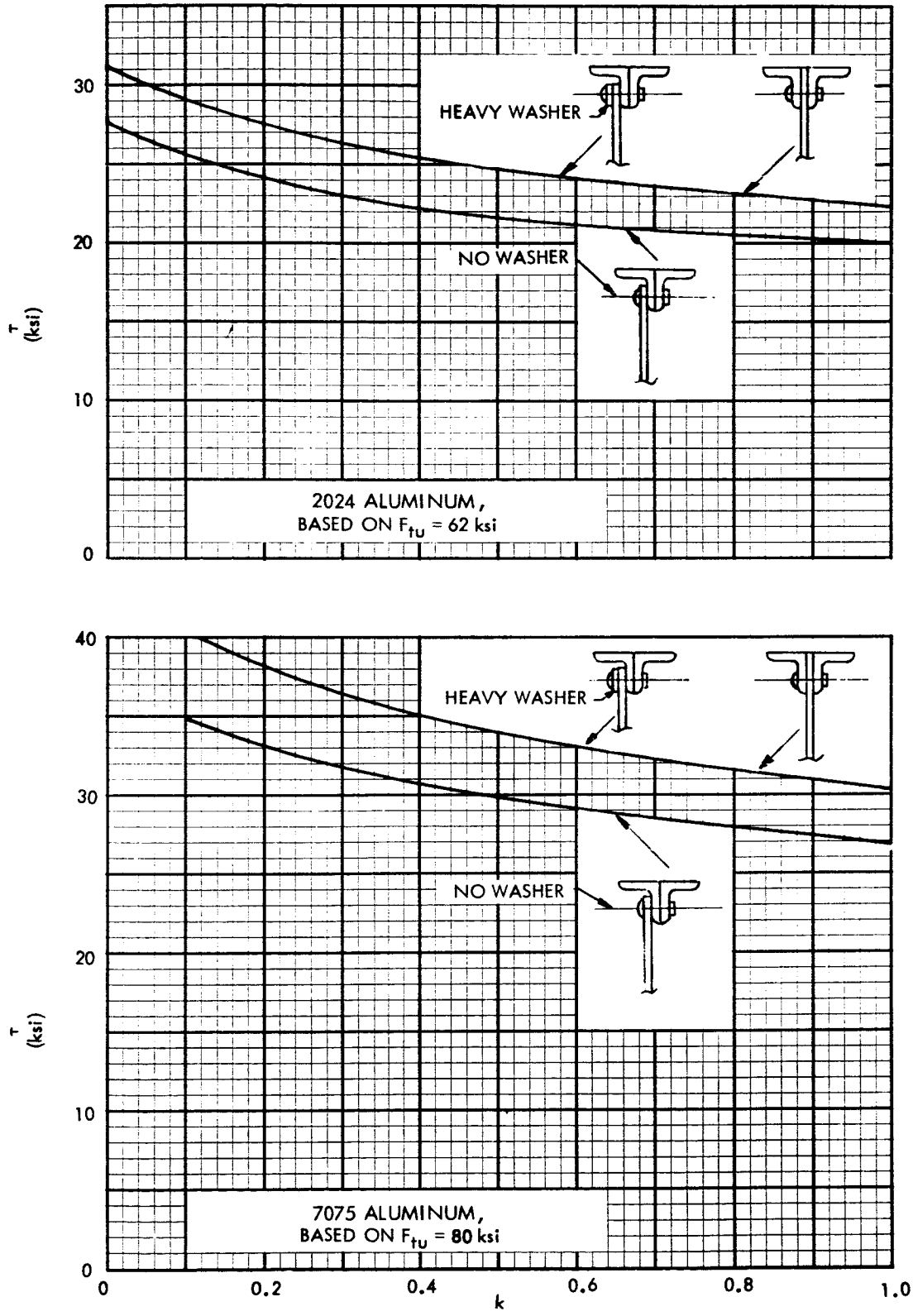

Figure 16. Allowable Web Stresses for 2024 and 7075 Aluminum at Room Temperature

UPRIGHTS

The uprights will be loaded according to the applicable postbuckling theory, either tension field or partial tension field.

PURE DIAGONAL TENSION

For the case of pure diagonal tension, Wagner's (References 2, 3, and 4) method of analysis is applicable. Hence, the force in the upright P_U which is applied by the web is

$$P_U = -S\frac{d}{h}\tan\alpha$$

where

S = shear force in the bay under consideration

d = spacing of uprights

h = distance between the centroids of flanges

Substituting $\tau = S/ht$, then

$$\sigma_u = -\frac{\tau dt}{A_{U_e}}\tan\alpha$$

where A_{u_e} is the area of upright. If the upright is eccentric with respect to the web, then

$$A_{U_e} = \frac{A_U}{1 + \left(\frac{e}{\rho}\right)^2}$$

where

A_U = the area of upright

e = the eccentricity

ρ = the radius of gyration of the area of upright with respect to the web centerline

On the basis of tests of Kuhn (Reference 1), the reduced, or effective, column length of the uprights may be taken as

$$L_e = \frac{h}{\sqrt{4 - 2d/h}} \quad \text{when } d < 1.5\,h$$

$$L_e = h \quad \text{when } d > 1.5\,h$$

INCOMPLETE DIAGONAL TENSION FIELD

For the case of incomplete diagonal tension, Kuhn's method of determining upright loading is applicable. For this case it is consistent to assume that the web may also carry compressive stresses parallel to the uprights. In other words, some effective width of web should be assumed to be stressed with the uprights. The effective width working with the uprights was determined experimentally by Kuhn to be

$$\frac{d_e}{d} = 0.5\,(1-k)$$

where d_e is the effective width. Correspondingly,

$$\sigma_U = -\frac{k\,\tau \tan \alpha}{A_{U_e}/dt + 0.5\,(1-k)}$$

σ_U is an average stress value along the length of the upright and is considered adequate as a basis for computing the column strength of the upright.

For investigation of the crippling strength of an upright, the maximum stress of $\sigma_{U_{max}}$ is needed, which occurs at midheight on the upright. The graph given by Kuhn (Reference 1) is helpful for obtaining stress ratio $\sigma_{U_{max}}/\sigma_U$ versus d/h for various values of k. (See Figure 17.) The effective length of the upright is given by

$$L_e = \frac{h}{\sqrt{1 + k^2\left(3 - \frac{2d}{h_u}\right)}} \quad \text{for } d < 1.5\,h$$

and

$$L_e = h \qquad \text{for } d > 1.5\,h$$

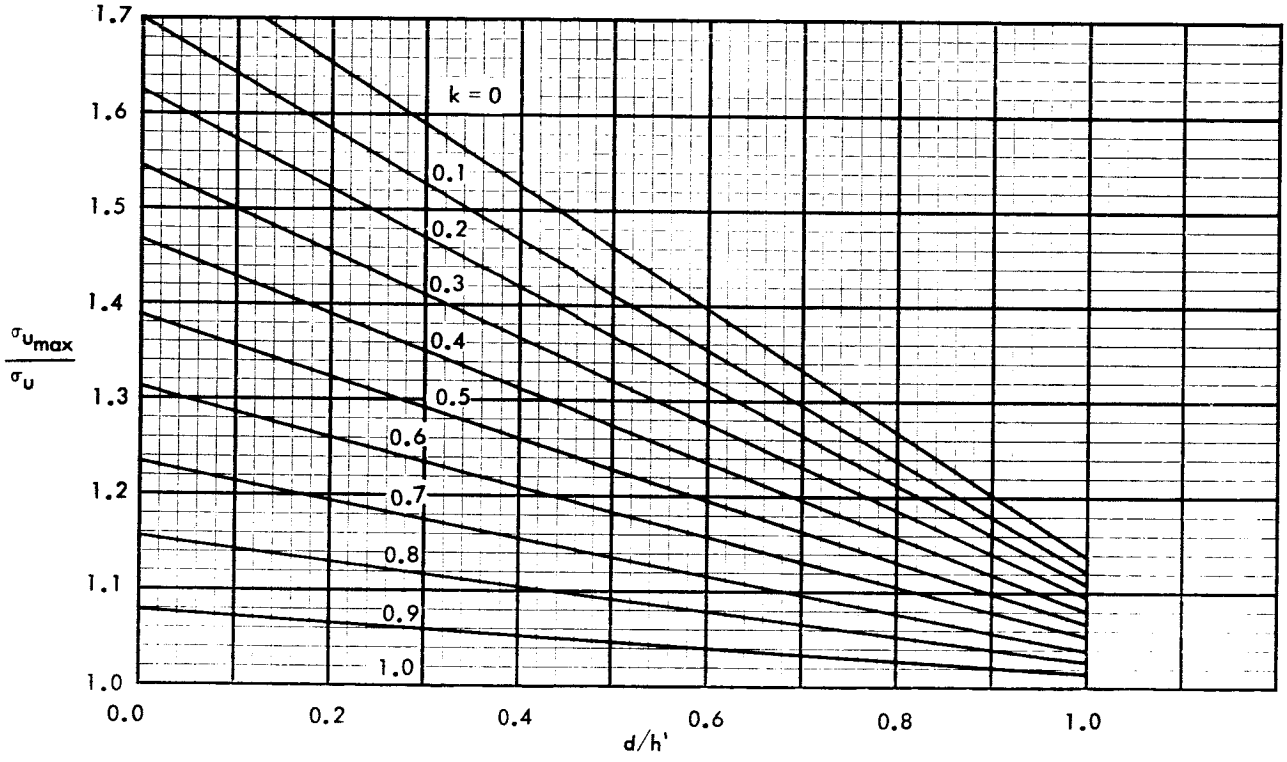

Figure 17. Ratio of Maximum to Average Stiffener Stress

Kuhn has stated that the nature of "column behavior" of single uprights is problematical, because excessive bowing rather than actual failures usually occurs. Consequently, it is recommended that the following limits be imposed:

1. $\sigma_U <$ column yield stress

2. The ratio $\sigma_U A_{U_e} / A_U <$ allowable stress for a column with the slenderness ratio $h/2\rho$.

Usually, however, the columns fail by forced crippling. For this type of failure, $\sigma_{U_{max}}$ is used as a criterion

$$\sigma_{U_{max}} < \sigma_o$$

where σ_o is allowable stress

$$\sigma_o = C k^{\frac{2}{3}} \left(\frac{t_U}{t}\right)^{\frac{1}{3}} \text{ kips/inch}^2$$

where

C = 21 for 2024-T3 double uprights

26 } for 7075-T6 double uprights

for 2024-T3 single uprights

32.5 for 7075-T6 single uprights

If σ_o is above the proportional limit, multiply it by E_{sec}/E taken from compression stress-strain curves.

Crippling

The above criterion was derived from the test data for uprights of angles, lipped-angle, and Z and lipped Z sections. Therefore, the empirical formula may be very conservative for hat sections since there are no outstanding free legs. The ultimate crippling stress of a closed section can be obtained by considering the local buckling behavior. Local upright buckling failure may exist when the legs or walls of the uprights are very thin. The stresses that would cause local buckling can be determined by determining the crippling stress when the upright is treated as a free column. The latter statement is applicable especially when the upright leg thickness is greater than the web thickness and when $A_U/t_w d$ is greater than approximately 0.2 thickness (where t_w is the web thickness in inches and d is the distance in inches between uprights). (See Table 1 obtained from Reference 9).

If the ratio of $A_U/t_w d$ is less than 0.2 for the section, then it is recommended that the interaction loads from the web to the upright be considered. By considering the combined web-upright-failure, we have

Table 1. Coefficient K (From Reference 9, Equation 2-7)

$\frac{h}{d}$	$\frac{EI_U}{dD} = 5$			$\frac{EI_U}{dD} = 10$			$\frac{EI_U}{dD} = 15$		
	$\frac{A_U}{dt_w} = 0.05$	$\frac{A_U}{dt_w} = 0.10$	$\frac{A_U}{dt_w} = 0.20$	$\frac{A_U}{dt_w} = 0.05$	$\frac{A_U}{dt_w} = 0.10$	$\frac{A_U}{dt_w} = 0.20$	$\frac{A_U}{dt_w} = 0.05$	$\frac{A_U}{dt_w} = 0.10$	$\frac{A_U}{dt_w} = 0.20$
0.6	16.5	16.5	16.5	16.5	16.5	16.5	16.5	16.5	16.5
0.8	15.4	14.6	13.0	16.8	16.8	16.8	16.8	16.8	16.8
1.0	12.0	11.1	9.72	16.0	16.0	15.8	16.0	16.0	16.0
1.2	9.83	9.06	7.88	15.3	14.2	12.4	16.5	16.5	16.5
1.4	8.62	7.91	6.82	12.9	12.0	10.3	16.1	15.7	13.6
1.6	8.01	7.38	6.32	11.4	10.5	9.05	14.7	13.6	11.8
1.8	7.84	7.19	6.16	10.6	9.7	8.35	13.2	12.2	10.5
2.0	7.96	7.29	6.24	10.2	9.35	8.03	12.4	11.4	9.80
2.2	8.28	7.58	6.50	10.2	9.30	7.99	12.0	11.0	9.45
2.4	8.79	8.06	6.91	10.4	9.49	8.15	11.9	10.9	9.37
2.6	9.27	8.50	7.28	10.8	9.86	8.48	12.1	11.1	9.53
2.8	8.62	7.91	6.31	11.4	10.4	8.94	12.5	11.5	9.85
3.0	8.31	7.62	6.53	12.0	11.1	9.52	13.1	12.0	10.3
3.2	8.01	7.38	6.32	11.4	10.5	9.05	13.9	12.7	10.9
3.6	7.84	7.19	6.16	10.6	9.7	8.35	13.2	12.2	10.5
4.0	7.96	7.29	6.24	10.2	9.35	8.03	12.4	11.4	10.8

Table 1. Coefficient K (From Reference 9, Equation 2-7) (Cont)

$\frac{h}{d}$	$\frac{EI_U}{dD} = 20$			$\frac{EI_U}{dD} = 25$		
	$\frac{A_U}{dt_w} = 0.05$	$\frac{A_U}{dt_w} = 0.10$	$\frac{A_U}{dt_w} = 0.20$	$\frac{A_U}{dt_w} = 0.05$	$\frac{A_U}{dt_w} = 0.10$	$\frac{A_U}{dt_w} = 0.20$
0.6	16.5	16.5	16.5	16.5	16.5	16.5
0.8	16.8	16.8	16.8	16.8	16.8	16.8
1.0	16.0	16.0	16.0	16.0	16.0	16.0
1.2	16.5	16.5	16.5	16.5	16.5	16.5
1.4	16.1	16.1	16.1	16.1	16.1	16.1
1.6	16.1	16.1	14.4	16.1	16.1	16.1
1.8	15.9	14.7	12.6	16.2	16.2	14.7
2.0	14.6	13.4	11.6	16.0	15.4	13.3
2.2	13.9	12.7	10.9	15.8	14.5	12.4
2.4	13.5	12.4	10.6	15.1	13.8	11.9
2.6	13.5	12.4	10.6	14.8	13.6	11.6
2.8	13.7	12.6	10.8	14.8	13.6	11.6
3.0	14.1	13.0	11.1	15.2	13.9	11.9
3.2	14.8	13.5	11.6	15.6	14.3	12.3
3.6	15.9	14.7	12.6	16.2	15.7	13.5
4.0	14.6	13.4	11.6	16.0	15.4	13.3

the case of "general elastic instability," since buckles occur in the uprights as well as the web. The general instability of web and upright for $A_U/t_w d \leq 0.2$ can be analyzed as a simply supported plate with longitudinal stiffeners (Figure 18). The critical stress can be represented (Reference 9) by

$$\sigma_{cr} = K \frac{\pi^2 D}{d^2 t_w} \tag{1-3}$$

where

D = flexural rigidity $= \frac{E t_w^3}{12 (1-\mu)}$ in. /lb

μ = Poisson's ratio

E = elastic modulus of elasticity, lb/in.^{2}

K = buckling coefficient (shown in Table 1).

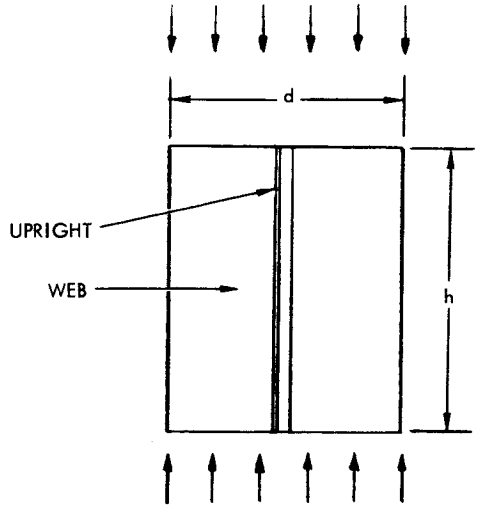

Figure 18. Simply Supported Plate With Longitudinal Stiffener

The values of buckling coefficient K are presented for various values of h/d ratios applicable to partial tension field beams and $A_U / t_w d \leq 0.2$

The buckling criteria for $A_U/t_w d \gtrsim 0.2$ is generally governed by the upright crippling. The ultimate crippling stress of a section (Reference 10) is

$$\sigma_{cc} = \frac{\sum_{i=1}^{N} A_i \, \sigma_{cc_i}}{\sum_{i=1}^{N} A_i} \qquad (1\text{-}4)$$

where σ_{cc_i} is the crippling stress (psi) of each of the several elements A_i is the corresponding cross-sectional areas (in.^{2}) and N is the number of elements of the upright cross section. Typical ultimate crippling curves for bare 7075-T6 aluminum alloy sheet are presented in Figure 19. Figures 19 through 21 show the relative influence of thermal soak environment (Reference 10).

To assure conservatism it is necessary to take $\sigma_{cc_i} = \sigma_o$ for the upright leg that is attached to the web. In this manner, the effect of the diagonal tension folds are properly accounted for. All other upright members (i.e., the outstanding leg of an angle-shaped stiffener) should have σ_{cc_i} determined from Figures 19 through 21 when using aluminum alloy 7075-T6.

Upright Instability as a Column Failure

Column failure criteria will govern when the stress in the upright σ_U equals the column-failing stress of the upright section. The slender ratio to be used is $d/2\rho$ (Reference 1). The buckling of the upright is enhanced by the lateral load imposed by the web action. For end-restrained web bay, a restraint coefficient (reduction in allowable stress) of at least 3.75 based upon tests should be used, compared to 4.0 based upon Moore and Westcoat (Reference 11).

Summary for the Design of Upright

The design of uprights is based upon satisfying

$$\tau_{cr} \Rightarrow \frac{\tau}{\tau_{cr}} \Rightarrow k \Rightarrow \sigma_U \Rightarrow \sigma_{U_{max}}$$

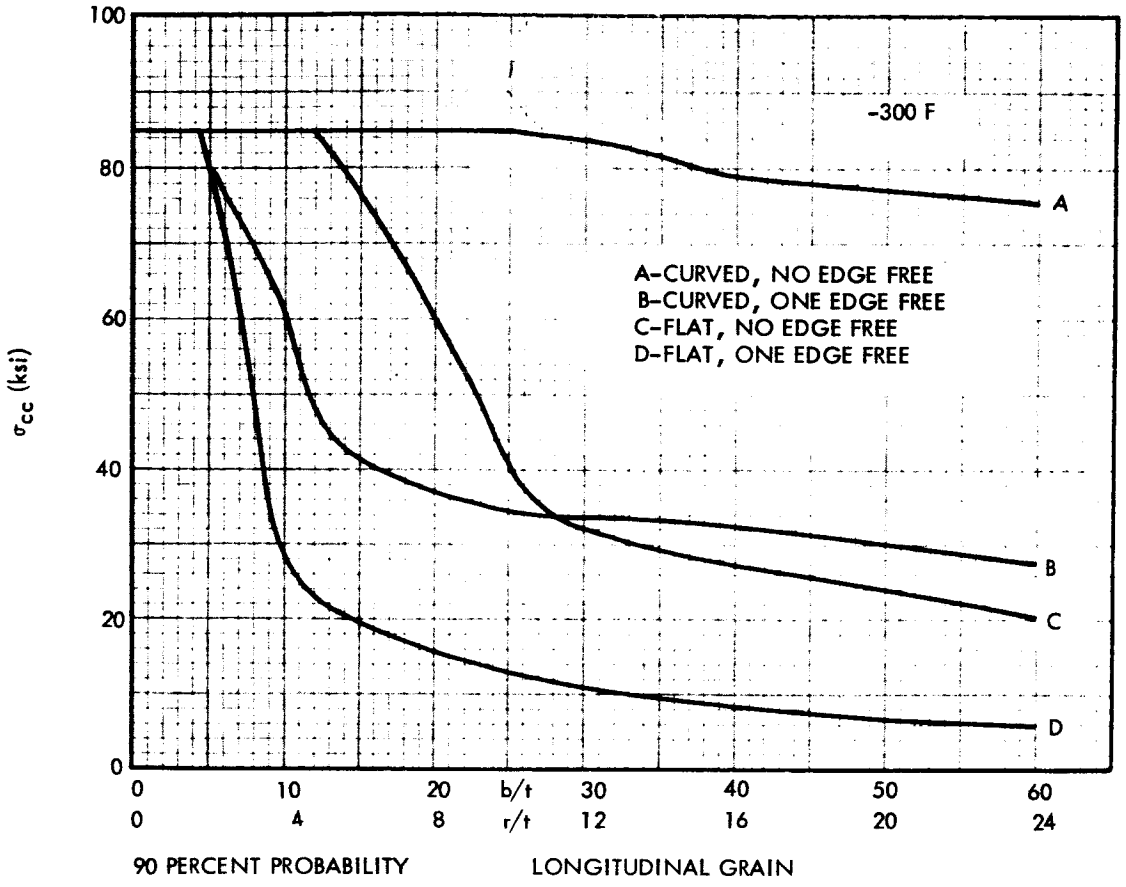

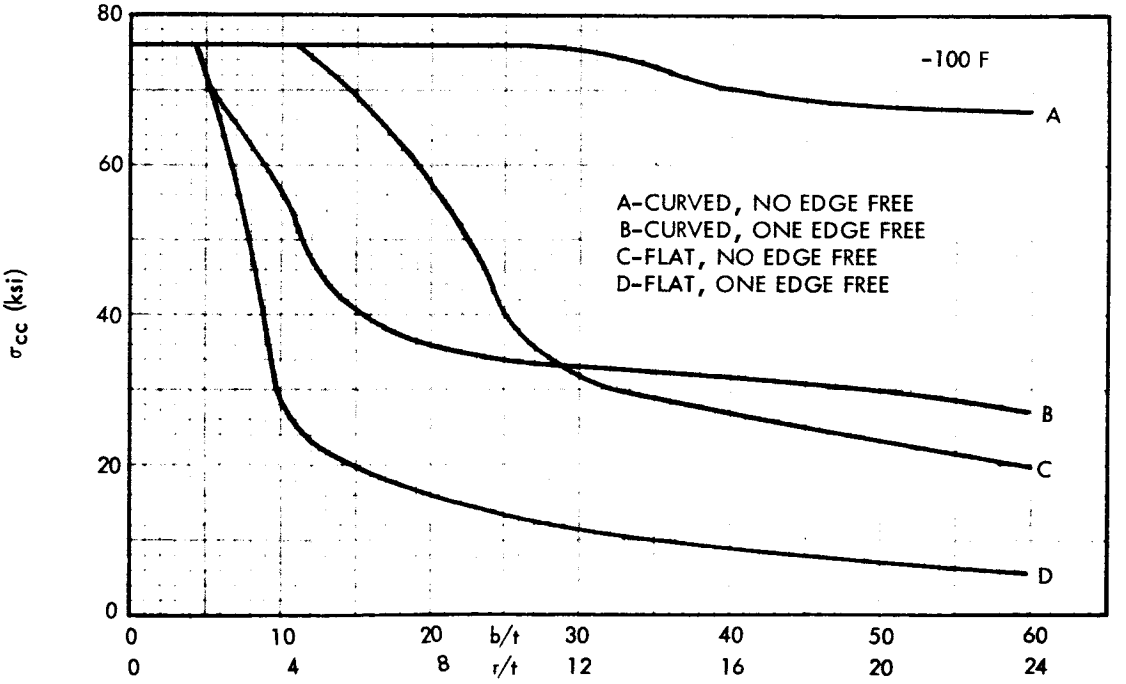

Figure 19. Ultimate Element Crippling Curves for Bare 7075-T6 Aluminum Alloy Sheet (-300, -100 F)

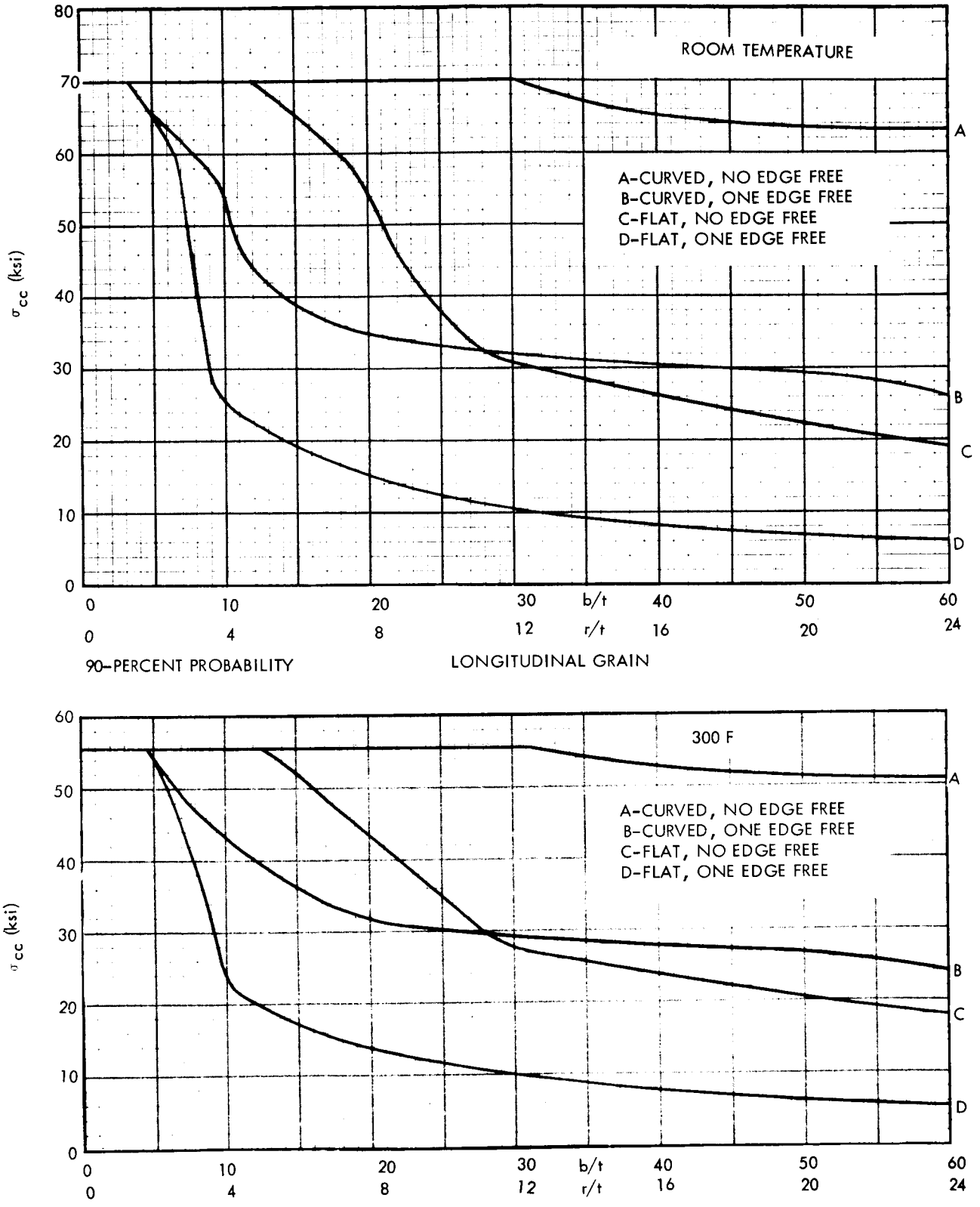

Figure 20. Ultimate Element Crippling Curves for Bare 7075-T6 Aluminum Alloy Sheet (Room Temperature, 300 F)

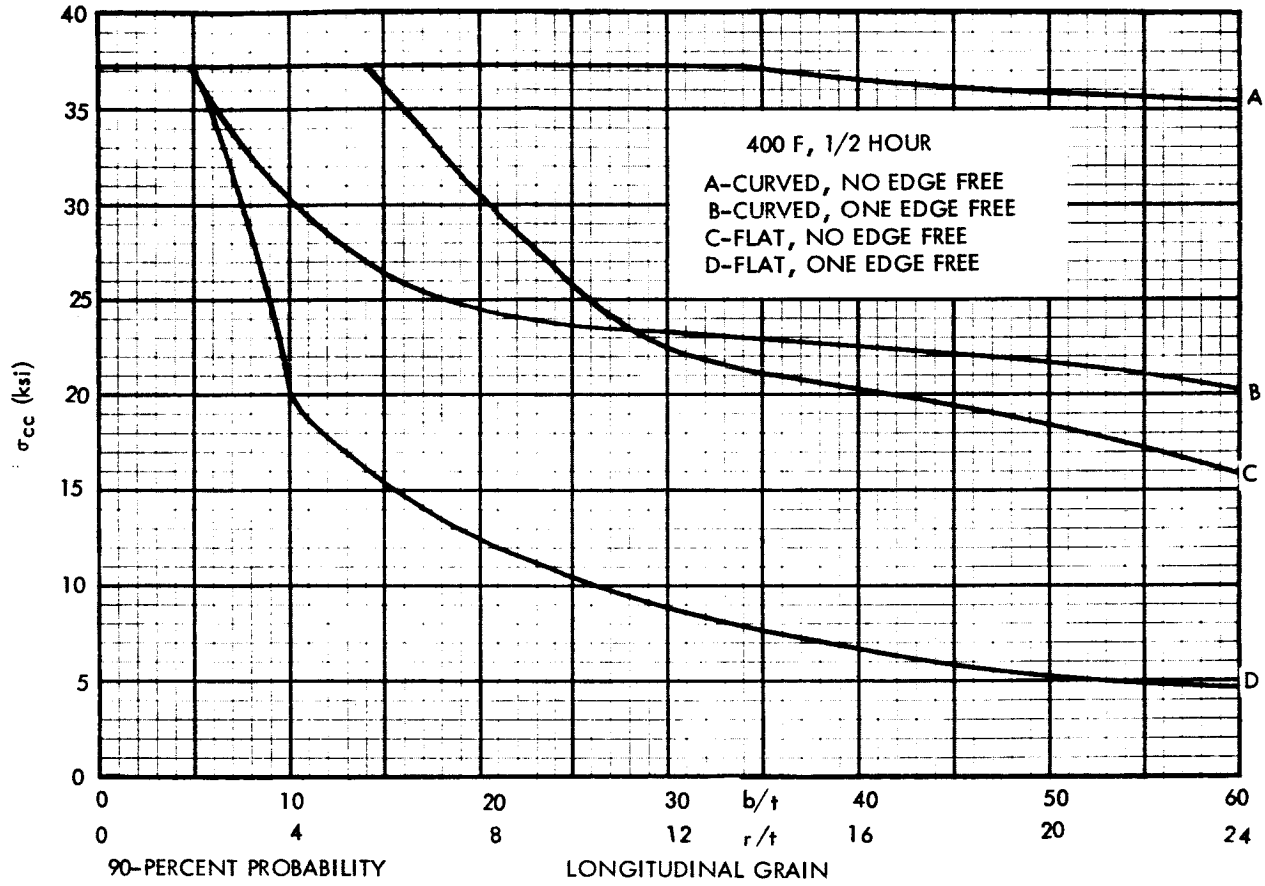

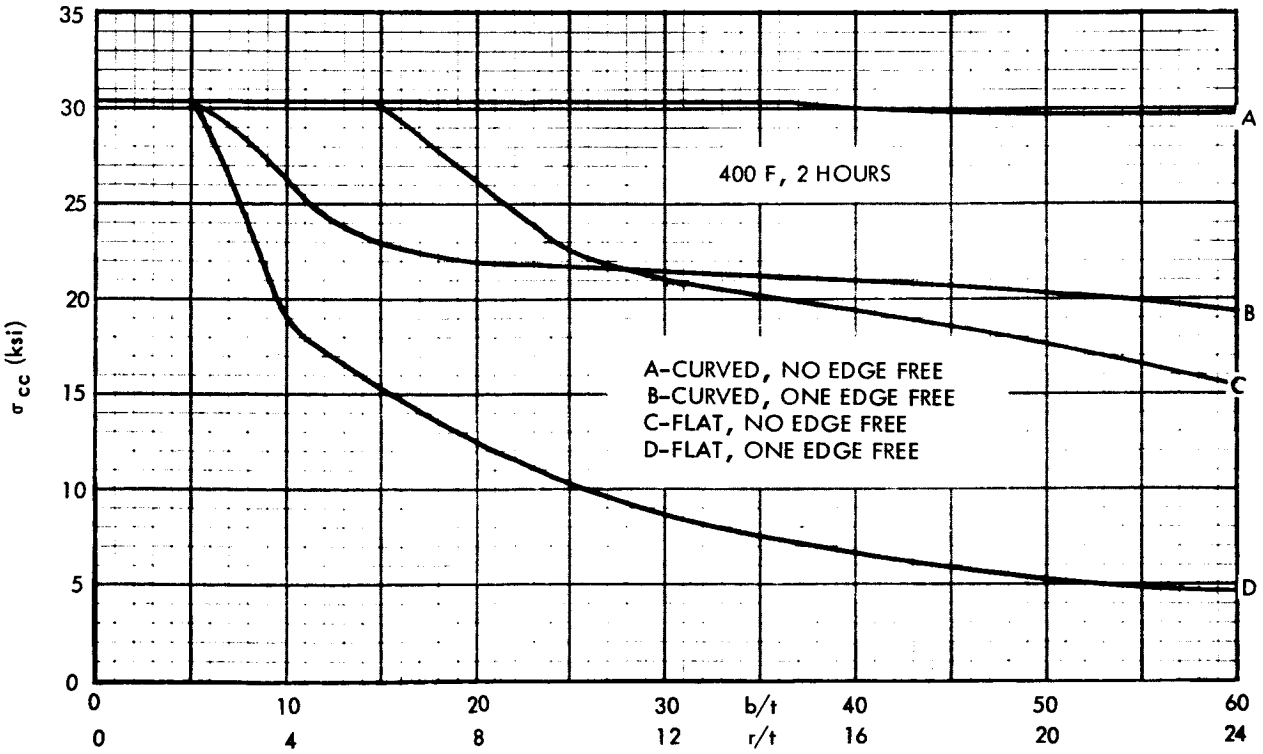

Figure 21. Ultimate Element Crippling Curves for Bare 7075-T6 Aluminum Alloy Sheet (400 F)

The following must be satisfied:

1. σ_U < column yield stress

2. $\frac{\sigma_U A_{U_e}}{A_U}$ < allowable stress for a column with the slenderness ratio $h_u/2\rho$

3. $\sigma_{U_{max}} < \sigma_o$ for open upright sections where

$$\sigma_o = Ck^{\frac{2}{3}} \left(\frac{t_u}{t}\right)^{1/3}$$

4. $\sigma_{U_{max}} < \sigma_{cr} = \frac{K\pi^2 D}{d^2 t_w}$ for $\frac{A_U}{t_w d} \lesssim 0.2$

5. $\sigma_{U_{max}} < \sigma_{cr} \approx \frac{\sum_{i=1}^{N} A_i \sigma_{cc_i}}{\sum_{i=1}^{N} A_i}$ for $\frac{A_U}{t_w d} \gtrsim 0.2$

FLANGES

PURE DIAGONAL TENSION

The force in flange is

$$F = \pm\frac{M}{h} - \frac{S}{2}\cot\alpha$$

Substituting

$$\tau = \frac{S}{ht}$$

then

$$\sigma_{FL} = -\frac{\tau ht}{2A_{FL}}\cot\alpha \qquad (1\text{-}1)$$

The vertical component of the web stresses σ acting on the flanges cause bending of the flanges between uprights. The flanges can be considered as continuous beams supported by the uprights. The primary maximum moment occurs at the uprights and is

$$\max M' = \frac{Sd^2 \tan\alpha}{12\ h}$$

At midbay the moment will be

$$M = \max M'/2$$

Because of redistribution of stresses in the web, max M will also be modified with indicated factor C_3 which is obtained from the graphs (Figure 22).

$$\max M = (C_3)\ (\max M')$$

$$\sigma_{max} = (1 + C_2)\frac{2\ S}{ht\ \sin 2\alpha}$$

C_3 is a function of flange-flexibility parameter ωd:

$$\omega d \approx 0.45\ d\ \sqrt[4]{\left(\frac{1}{I_t} + \frac{1}{I_c}\right)\frac{t}{h}}$$

Where t and c denote the tension and compression flanges respectively.

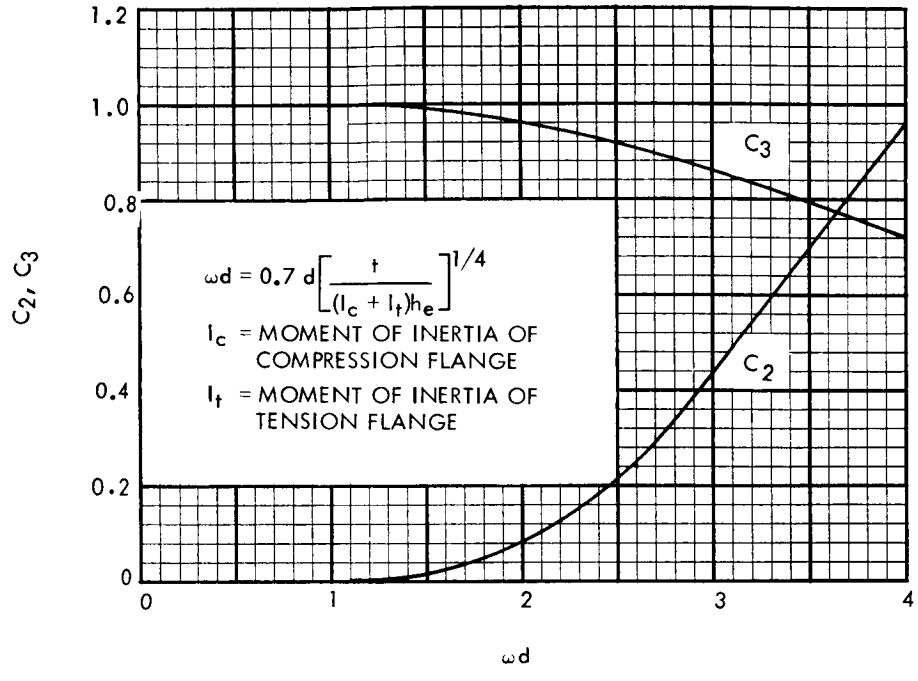

Figure 22. Stress Concentration Factors C_2 and C_3

INCOMPLETE DIAGONAL TENSION

The stress in the flange for the incomplete diagonal tension field beam (Reference 1) is as follows:

$$\sigma_F = -\frac{k\,\tau\,\cot\,\alpha}{\left(2A_{FL}/ht\right) + 0.5(1-k)}$$

This formula shall be used instead of Equation 1-1. All other formulas remain the same.

CONCLUSION

This concludes the summary of the state of the art. Additional informations may be found in References 12, 13, 14, 15, 16, and 17. The formulas and graphs which are presented cover the analysis of partial-tension-field beams that are loaded vertically. The next chapter deals with lateral loading only, so that both loadings can be combined later. The appropriate formulas and methods will be selected from existing literature.

II. ANALYSIS OF PARTIAL-TENSION-FIELD BEAMS SUBJECTED TO LATERAL PRESSURE LOADINGS

WEBS LOADED LATERALLY

INTRODUCTION

In this section the procedures to be used to determine the stresses and deformations in partial-tension-field beams subjected to lateral pressure are developed.

STRUCTURAL SYSTEM

Under the application of lateral loading, the thin web is treated as a plate which is attached to the flanges and uprights. Depending on the flexibility of the uprights, the web can be analyzed as a plate resting on rigid beams (or on the beams of negligible flexibility) or a plate, which is continuous over flexible beams (uprights). The flanges in this case always can be assumed to be rigid. Figure 23 illustrates the structural system consisting of a plate (web), crossbeams (uprights), and beams (flanges).

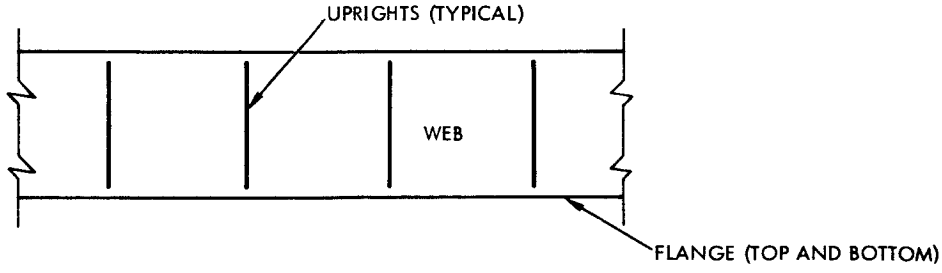

Figure 23. Structural System

In this report, webs that are able to resist bending are designated as thin webs. Such webs can be limited approximately by the relationship $b/t \leq 150$, where b and t are the longer side of web and thickness of web, respectively. The more exact limitation with corresponding explanation is given later in connection with Figure 24. Several solutions exist for this case, all based on small deflection theory. Webs which are unable to take bending are designated as very thin webs. For very thin webs, lateral loads are resisted by membrane stresses. The very thin webs are limited approximately by the relationship $b/t \geq 400$. The division into the two categories is also dependent on the loading intensity as will be explained later in connection with the Figure 24. There are numerous solutions for the first category. There are very few solutions for the second category and these are based on large deflection theory. There is a gap between these two categories which has no solution. The analyst must use his own judgment whether to use the thin or very thin solutions. This report deals primarily with very thin webs that are in a range of $b/t \approx 1000$. But for the sake of completeness the case of the thin web shall be considered also.

THIN WEBS

Several methods are presented in the literature which handle this problem. In the case where the web is thin, uprights and flanges for this partial loading are relatively rigid. The flat web is actually a two-dimensional equivalent of the beam (which is really a one-dimensional element). The flat web resists lateral loads, p, by means of direct stresses: shear stresses, bending stresses, and torsional stresses.

In the usual derivation of the differential equations for a flat plate, the following assumptions are made:

1. The material is homogeneous, isotropic, and elastic.

2. The least lateral dimension of the plate is at least 10 times the thickness. (In this case, the web is much thinner than that.)

3. A vertical element of the plate, before the bending, remains perpendicular to the middle surface of the plate after the bending.

4. Strains are small.

5. Strain of the middle surface is negligible.

To meet these assumptions, the deflections of the plate must be small when compared to the thickness. Sometimes the allowable limit of the deflections for validity of the thin plate equations is referred to as one-twentieth of the plate thickness; although, for most engineering problems,

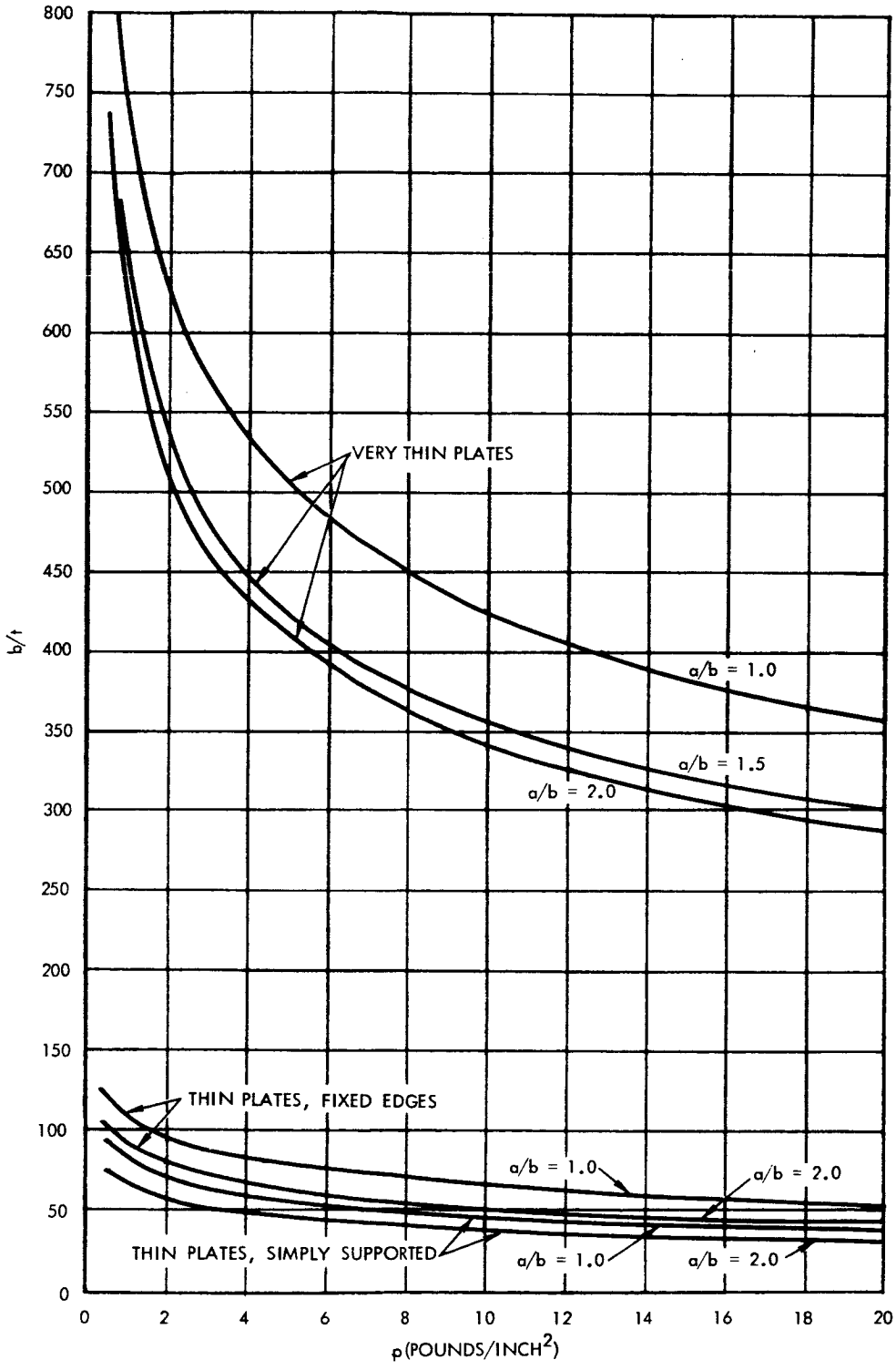

Figure 24. Limiting Regions for Plate Membrane and Thin Plate Theories

the calculated deflections, moments, and stresses are probably sufficiently accurate even though the deflections may be considerably larger. Some references suggest limiting the deflection to less than one-fifth of the plate thickness; this is a reasonable assumption.

Timoshenko's Method

Limited test data show that Timoshenko's thin plate equations (References 18 and 19) describe the behavior of plates reasonably well. Some error in deflection occurs at low loads since it is very difficult to obtain initially flat plates as structural elements. The low loads have a tendency to straighten out any initial waviness in the plate causing considerable error in the measured deflections. The equations, however, give reasonably accurate values for the stresses up to the proportional limit of the material. Beyond that stress the equations are not correct.

Timoshenko's method is recommended for plate analysis when the deflection will be small when compared to the thickness. The web is considered to be a rectangular plate with the edges clamped. This is a good approximation for webs stiffened with the equally spaced stiffeners because the rotation at the stiffeners by symetry is zero. Simply supported boundary conditions are considered also. Figure 25 shows designations for the plate. The following formulas are derived for thin plates (with the aforementioned characteristics) loaded with a uniformly distributed lateral pressure. The maximum deflection at the middle of the plate is:

$$\delta = \alpha \frac{pb^4}{Et^3}$$

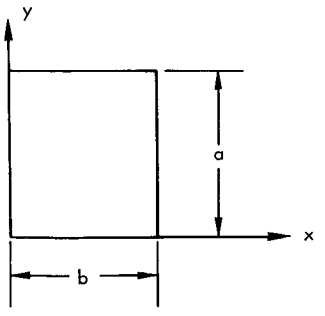

Figure 25. Axis Notation

The maximum moments in planes parallel to xz and yz axes, respectively, for the point ($x = b/2,\ y = a/2$), are

$$M_{x_{max}} = \beta\, pb^2 \quad \text{(in.-lb/in.)}$$

$$M_{y_{max}} = \beta_1\, pb^2 \quad \text{(in.-lb/in.)}$$

The maximum shearing stresses are:

$$Q_{x_{max}} = \gamma\, p\, b \text{ (lb/in.) at } (x = b/2,\ y = a/2)$$

$$Q_{y_{max}} = \gamma_1\, p\, b \text{ (lb/in.) at } (x = b/2,\ y = a)$$

The maximum vertical reactive forces along the side x = o or b are

$$V_{x_{max}} = \overline{\delta}\, p\, b \text{ (lb/in.) at } (x = b/2,\ y = a/2)$$

The values of the vertical reaction at the corner of the plate is

$$R = r\, pb^2 \quad \text{(lb)}$$

For all coefficients as listed above (α, β, γ, $\overline{\delta}$) see Figures 26 and 27, as given for the "built in" plates and "simply supported" plates.

Exact Solution

An exact solution is available which considers the continuity of the plate (web) in the x directions and which also takes into consideration the flexibility of the cross-beam (uprights in our case). This problem was solved by Tadahiko Kawai and Bruno Thürlimann in References 20 and 21. The solution is extremely complex and consequently, is not of much use to a practical analyst.

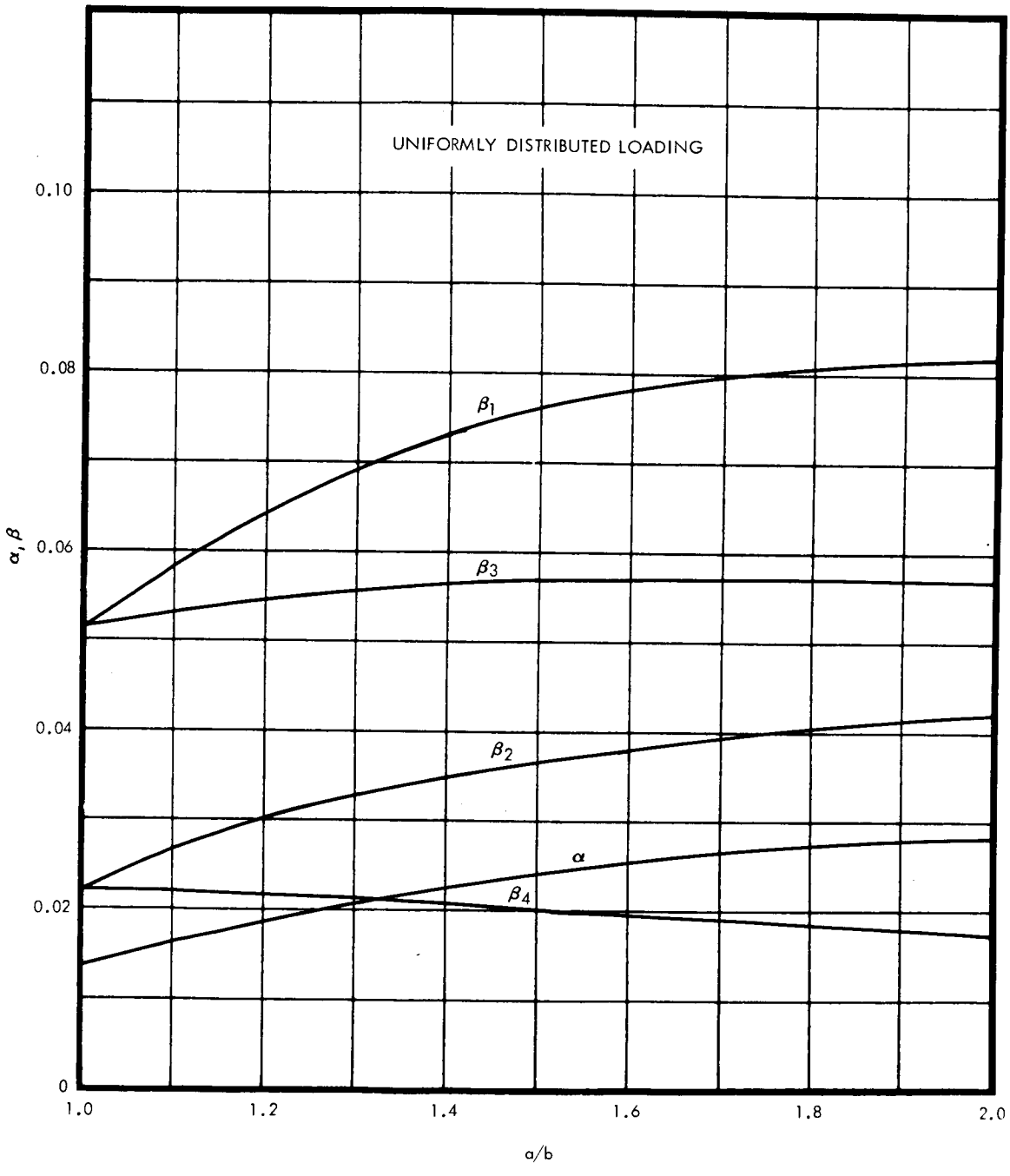

Figure 26. Coefficients for Plate Having Built-In Edges

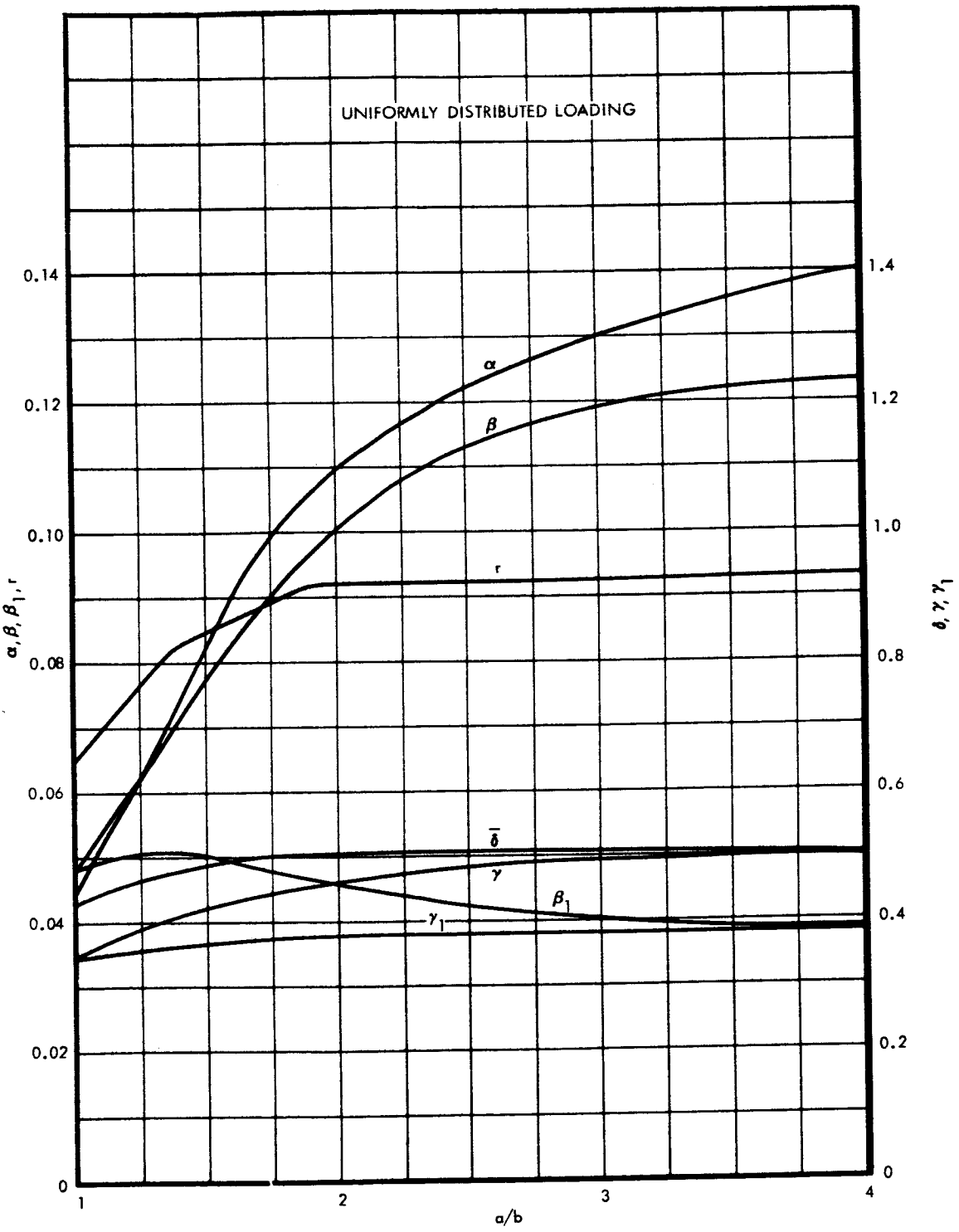

Figure 27. Coefficients for Simply Supported Plate

Summary and Conclusions

A method of analysis has been presented to predict the behavior of the webs under lateral pressure loadings in the prebuckling regime. The analysis is based upon the plate theory presented in References 18 and 19. The theory assumes that the deflections of the plate are small and that membrane stresses are neglected. This analysis should adequately describe the prebuckling behavior of beam webs which are within the thickness limitations previously discussed.

VERY THIN WEBS

Very thin webs offer a negligible resistance to bending and can be approximated by a membrane. The membrane is considered to be supported on four sides (flanges and uprights).

Square and Rectangular Membrane

Formulas for the membrane solution were derived for isotropic material by Prof. L. Föppl and are given in Reference 22. These formulas (Figure 28) were extended for application to rectangular membrane in References 19, 23, and 24.

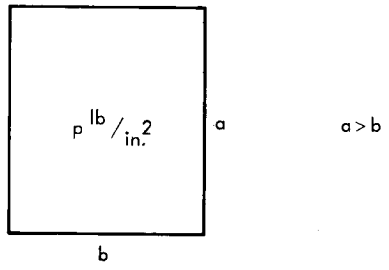

Figure 28. Square and Rectangular Membrane

The latter solution seems to give good agreement with the limited test values available, over a wider range of pressure. Also, since the formulas give larger and consequently more conservative values, it is suggested that they be used for the design of such membranes until more accurate test data are available.

For the deflection in the center of the panel

$$\delta = \eta_1 a \sqrt[3]{\frac{pa}{Et}} , \quad a > b$$

and for the stresses in the center of the panel:

$$\sigma_x = \eta_2 \sqrt[3]{U}$$

$$\sigma_y = \eta_3 \sqrt[3]{U}$$

where

$$U = p^2 E \frac{a^2}{t^2}$$

Similarly, for the stresses in the center of the short sides of the rectangle, the following is given:

$$\sigma_x = \eta_4 \sqrt[3]{U}$$

$$\sigma_y = \eta_5 \sqrt[3]{U}$$

and these formulas are applicable for the point, defined with the coordinates $x = b/2$, $y = o$ or a.

For the center of the long sides, they correspond to the coordinates $x = o$ or b, $y = a/2$, will be

$$\sigma_x = \eta_6 \sqrt[3]{U}$$

$$\sigma_y = \eta_7 \sqrt[3]{U}$$

The values η_i ($i = 1, 2, \ldots, 7$) are the coefficients, functions of a/b ratio and they are given in Figure 29. An additional graph, given in Figure 30, shows how the membrane theory agrees with the limited test results. The test specimen used was an aluminum-alloy plate 23.6 x 23.6 in. and 0.055 in. thick. The modulus of elasticity for this aluminum was

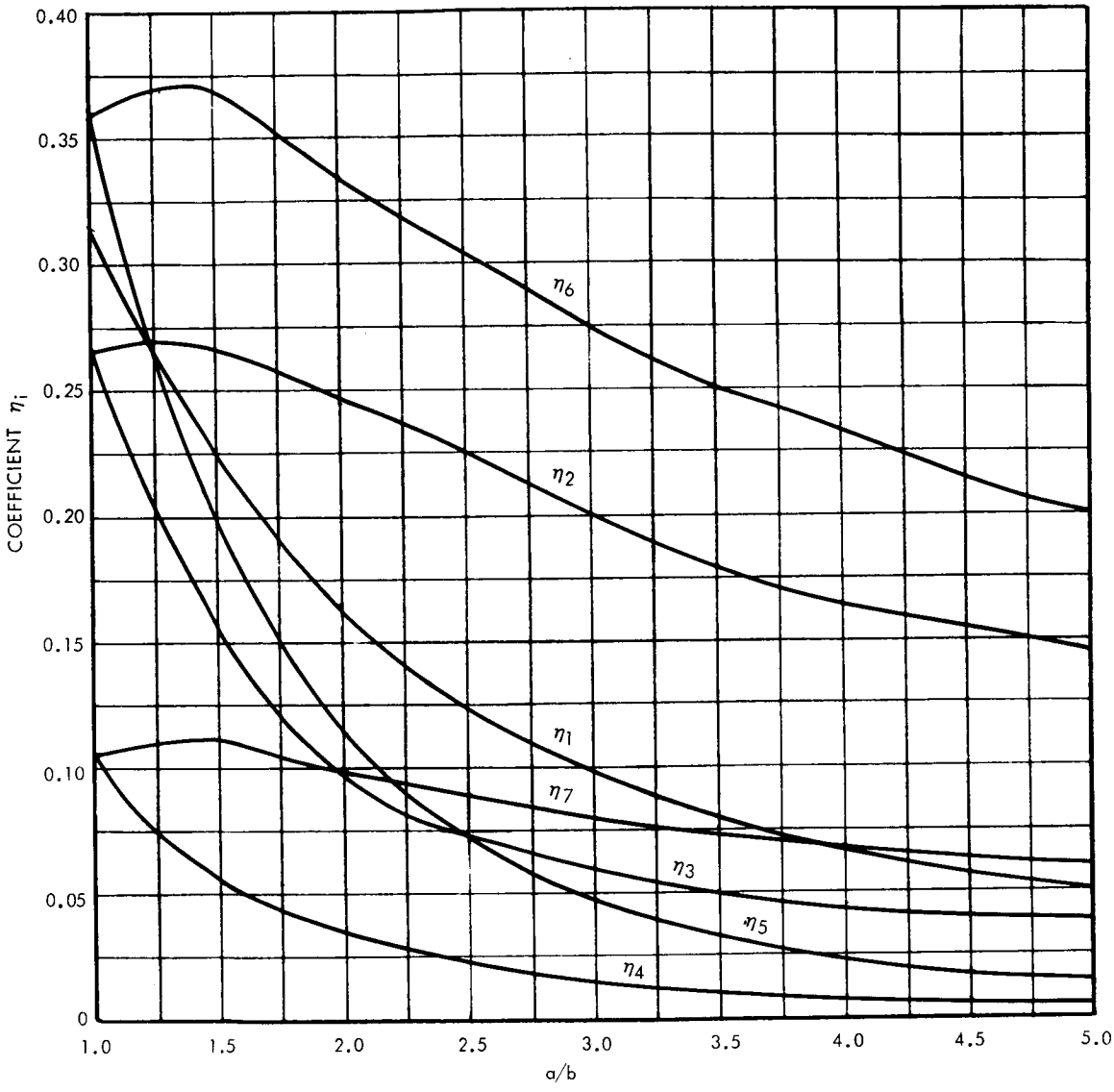

Figure 29. Coefficients for Uniformly Loaded Membrane

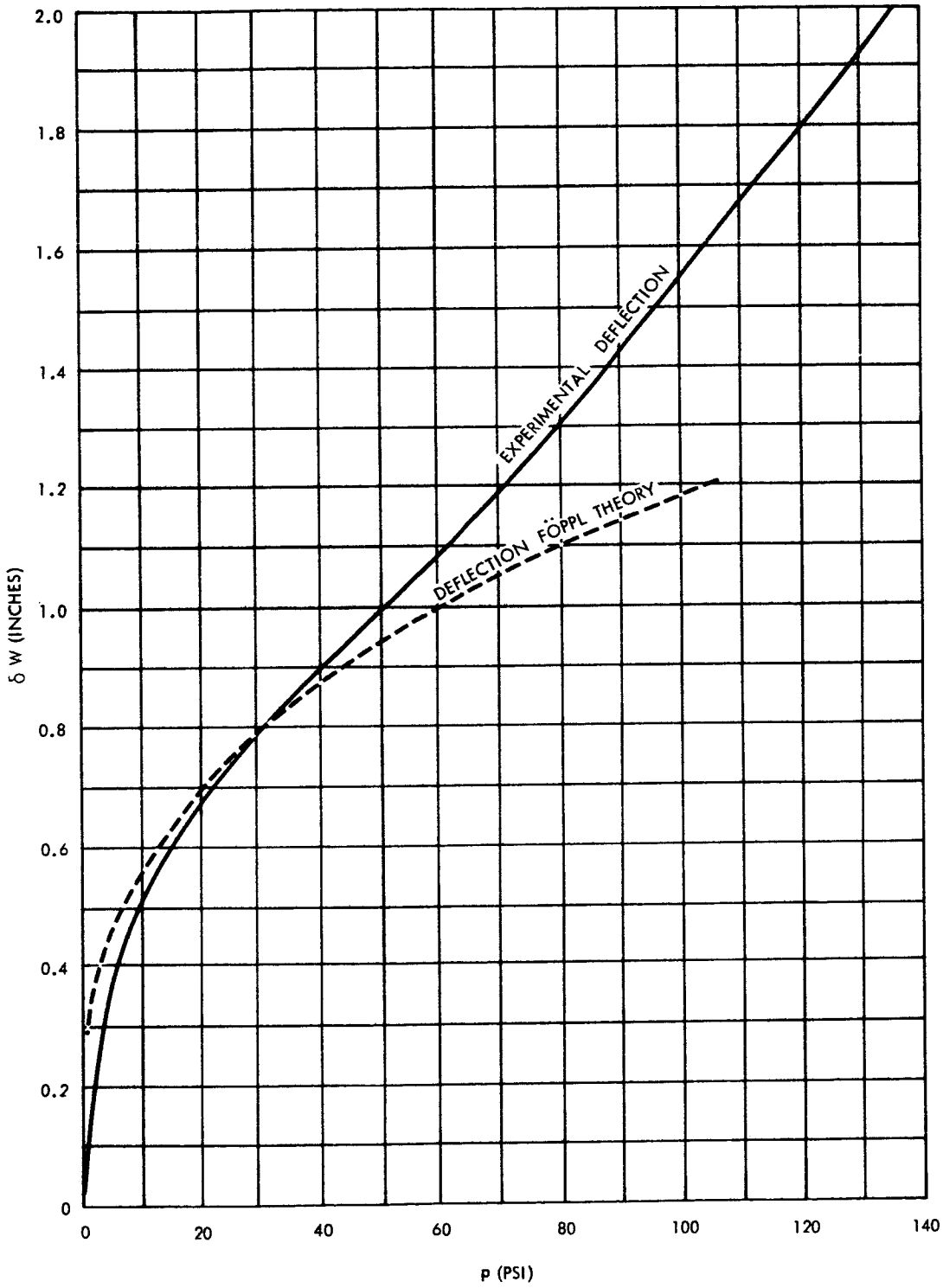

Figure 30. Comparison of Experimental and Theoretical Deflections

10.5×10^6 lb/in.^{2}. The plate was clamped at the edges, causing slight conservatism in the analytical results. The membrane equations will be assumed to be valied when the maximum deflection is equal or greater than ten times the thickness of the plate. In reality, however, these equations can be used whenever the deflection exceeds the thickness of the plate.

To determine which theory is to be used, b/t versus pressure is given (Figure 24), where, b is the smaller side of the plate, and t is the thickness. Figure 24 includes two sets of curves; one indicates the range of small deflection theory (thin plates), and the other the large deflection (membrane) theory which corresponds to the very thin plates. A design engineer, having the loading, p lb/in.^{2}, will be able to immediately choose the corresponding thickness, t, and design the web as a membrane or as a plate. If, however, the thickness, t, is prescribed in advance, the plate should be checked by both of above described theories and the more conservative result accepted.

CONCLUSION

In this section the behavior of webs under the influence of lateral loadings only has been studied. Distinction between thin and very thin webs was described. The discussion was applicable to all commonly used metallic structural materials.

UPRIGHTS AND FLANGES

INTRODUCTION

This section will consider tension-field beams under the influence of lateral loads without the presence of other loading. The response of uprights to lateral pressure loading on the beam will be discussed. Strength of uprights and the buckling of uprights will be analyzed. Similar discussions are provided for flanges.

ANALYSIS OF UPRIGHTS

Upright loading exists because of the application of lateral loads to the plane web system. The tensile stresses which exist in the thin webs tend to pull the flanges of the beam together, inducing compressive stresses in the uprights. The lateral load also induces bending stresses in the uprights as well as the flanges bending them out of the plane. As the lateral loads are increased, the loads may be reached where upright failure occurs due to compressive failure or column failure. At this stage, the partial-tension-field beam is considered to have failed.

Analysis Consideration for Uprights Other Than Stability Considerations

The stresses in the uprights for those uprights that are located on each side of the web can be determined from the elementary strength of materials when the tension field beam is subjected to lateral loads. Hence, upright stresses become

$$\sigma = \pm \frac{Mc}{I} + \frac{P}{A_e} \qquad (2\text{-}1)$$

where

I = cross-sectional moment of inertia, $in.^4$

M = bending moment, lb/in.

c = distance from the neutral axis to the outer most fiber, in.

P = compression load in the upright due to tension in the web, lb

A_e = cross sectional effective area of upright, $in.^2$

When the uprights are positioned only on one side of the web, then effective area to be used is

$$A_e = \frac{A_U}{1 + \left(\frac{e}{\rho}\right)^2} \tag{2-2}$$

where

A_U = cross-sectional area of upright, in.^{2}

e = distance from the web to the centroid of upright, in.

ρ = centroidal radius of gyration of the upright for bending normal to the plane of the web, in.

The moment of inertia is to be taken about the bending axis of the upright whether single or double uprights. First, consider the particular case of square panels, i.e., d = h, then the distribution of lateral load to the flanges and upright is shown in Figure 31.

where

$$q_{o_z} = pd$$

and

$$q_{o_w} = \frac{pd}{2}$$

For triangular distribution of the load acting on the upright, the upright (Figure 31(a)) can be considered as a beam column. For design purposes, the upright is taken to be pin-ended since the upright attachment to flange section and torsional restraint is small in most flange sections of diagonal tension field beams. The equations describing the behavior of the upright shown in Figure 31 are well known (Reference 25). The bending moment is then

$$M = C_1 \sin\frac{x}{j} + C_2 \cos\frac{x}{j} + f(q) \tag{2-3}$$

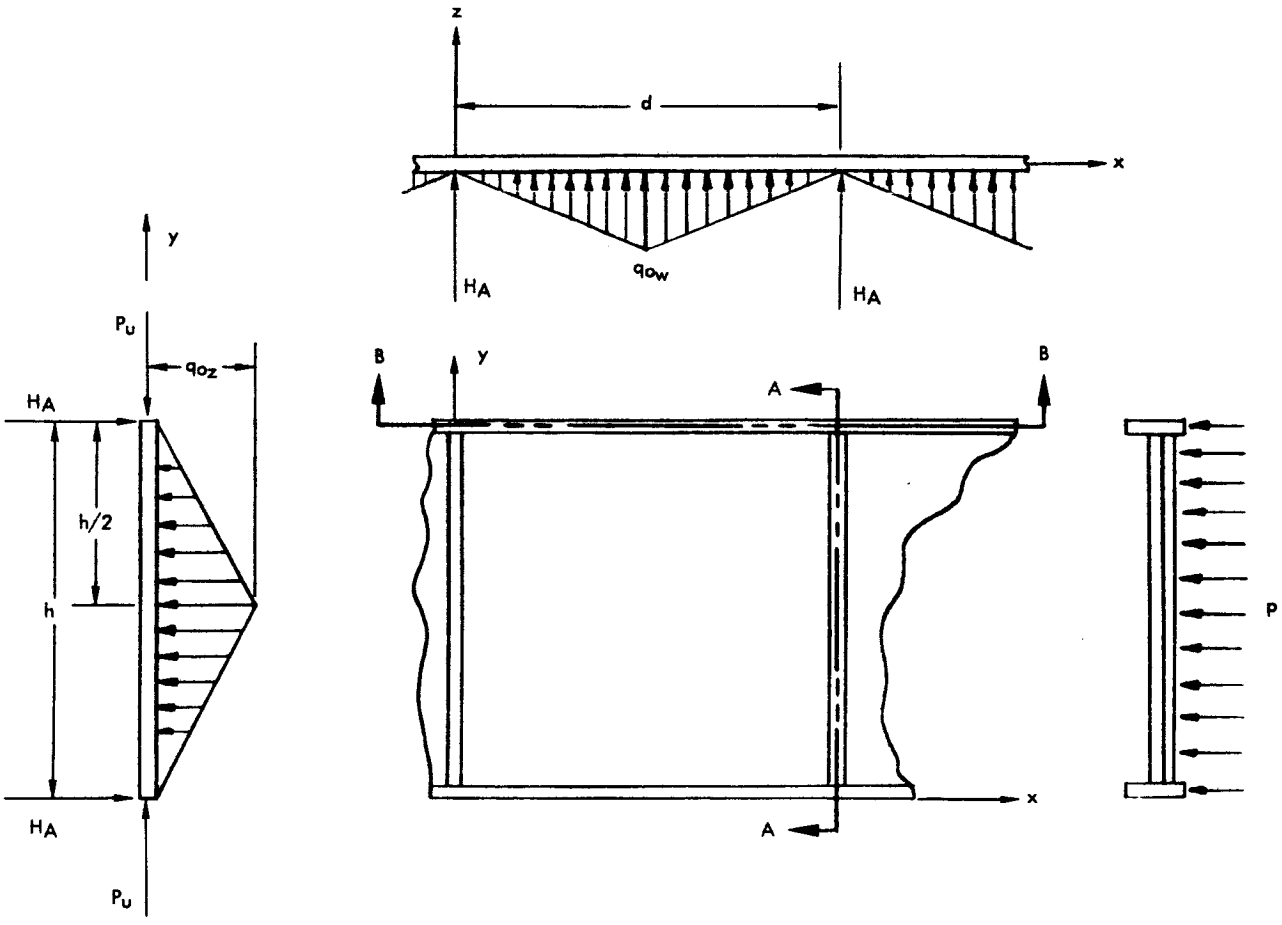

Figure 31. Forces Acting on Uprights (a) and Flanges (b)

where f(q) is a term containing q and j, x, and h but no axial load or end moments. Here x is the coordinate axis that measures distance along the upright height, and $j = \sqrt{EI/P_U}$. The values of C and f(q) are as follows:

For $x > \frac{h}{2}$

$$C_1 = -\frac{2qj^3}{h \cos\frac{h}{2j}} \qquad C_2 = 0 \qquad f(q) = \frac{2qjx^2}{h} \tag{2-4}$$

For $x > \frac{h}{2}$

$$C_1 = \frac{2qj^3 \cos\frac{h}{j}}{h\cos\frac{h}{2j}} \qquad C_2 = \frac{-4qj^3 \sin\frac{h}{2j}}{h} \qquad f(q) = 2qj^2\left(1-\frac{x}{h}\right) \qquad (2\text{-}5)$$

where

$$j^2 = \frac{EI}{P_U} \qquad (2\text{-}6)$$

The force P_U caused by the lateral load p can be determined from the web loading, T_v. The force, T_v, (See Figure 32) caused by the tension in the web is a function of the slope at each station along the upright and flange. For the very thin web system, the value of T_v can be obtained from the tensile stress distribution in the web system.

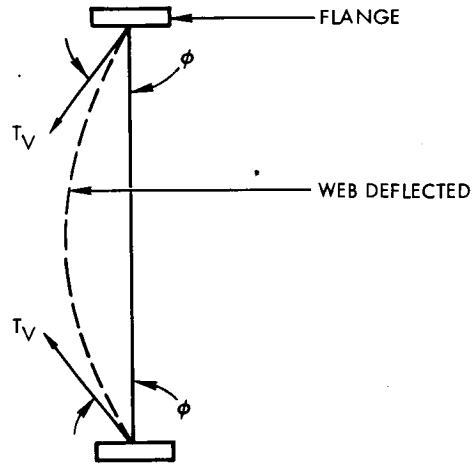

Figure 32. Web Tensile Force Creating Compressive Force in Uprights

The vertical load P_U induced in the upright due to only lateral-pressure is in almost all cases very small and can be neglected. The forces acting on upright for a rectangular web panel can now be approximated by those shown in Figure 33 where q = pd.

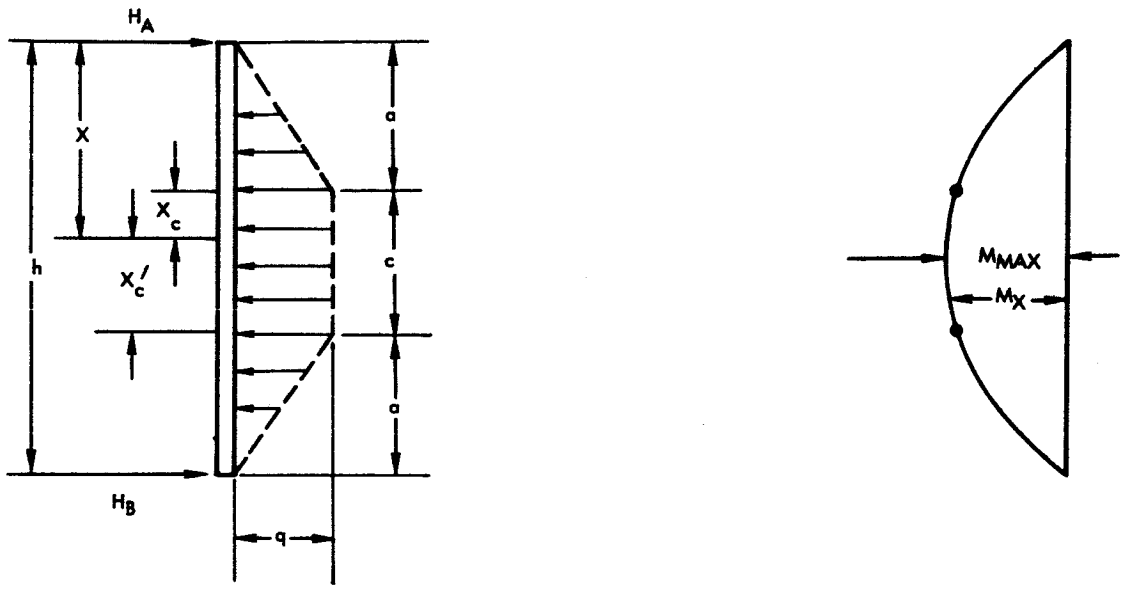

Figure 33. Upright Reaction

The reactions and deflection (Reference 26) for the case shown above are provided in Table 2.

One can use Table 2 to solve for the reaction for the case of triangular distribution by letting C = 0 and a = h/2.

With the aid of Table 2, the bending stress in the upright becomes

$$\sigma_{bend} = \pm \frac{Mc}{I}$$

where

c = distance between neutral axis to outermost fiber of upright, in.

I = cross-sectional moment of inertia of upright, $in.^4$

Table 2. Reaction and Deflections of Uprights

Reaction $H_A = H_B = \frac{q(h-a)}{2}$		
Location	Shear	Bending Moment
$x < a$	$Q_x = H_A - \frac{qx^2}{2a}$	$M_x = H_A x - \frac{qx^3}{6a}$
$x = a$	$Q_1 = \frac{qc}{2}$	$M_1 = \frac{qh^2}{6}\left[\frac{3a}{h} - 4\left(\frac{a}{h}\right)^2\right]$
$x > a$	$Q_x = \frac{qc}{2} - q(x-a)$	$M_x = M_1 + \frac{qx_c x_{c'}}{2}$
$x = \frac{h}{2}$	$Q = 0$	$M_{max} = q\left(\frac{h^2}{8} - \frac{a^2}{6}\right)$
Deflection $w_{max} = \frac{qh^4}{1920EI}\left[25 - 40\left(\frac{a}{h}\right)^2 + 16\left(\frac{a}{h}\right)^4\right]$		

Stability Consideration for Uprights

For laterally loaded partial-tension-field beams, the uprights are generally not subject to stability failure. The compressive load on the uprights due to lateral loading is generally extremely small in comparison to upright bending, and for design purposes it can be neglected.

The bending moment induces compressive stresses on one side and tensile stresses on the opposite side. If the uprights have very thin free edges on the compressive side, then local crippling may occur. This should be checked using the method outlined in Section I.

ANALYSIS OF THE FLANGES

The strength analysis of the flanges can be made using the elementary beam formulas or truss formulas. The stresses obtained are then combined with the local bending stresses caused by the tension in the web system. The local bending stresses are obtained by dividing the local bending moments by the section moduli of the individual flanges.

Strength Analysis of Flanges

The tensile force existing in the very thin web produces an approximate triangular load distribution on the flange. Consider only one bay as shown in Figure 34. The flange can be considered as a fixed-end beam with the end located at the upright-flange junction. The reactions for such a case are as follows (Reference 27):

$$M_o = \frac{5q_o d^2}{96} \tag{2-9}$$

$$R_o = \frac{1}{4} q_o d \tag{2-10}$$

which says that the maximum bending stresses exist at the upright flange junction region.

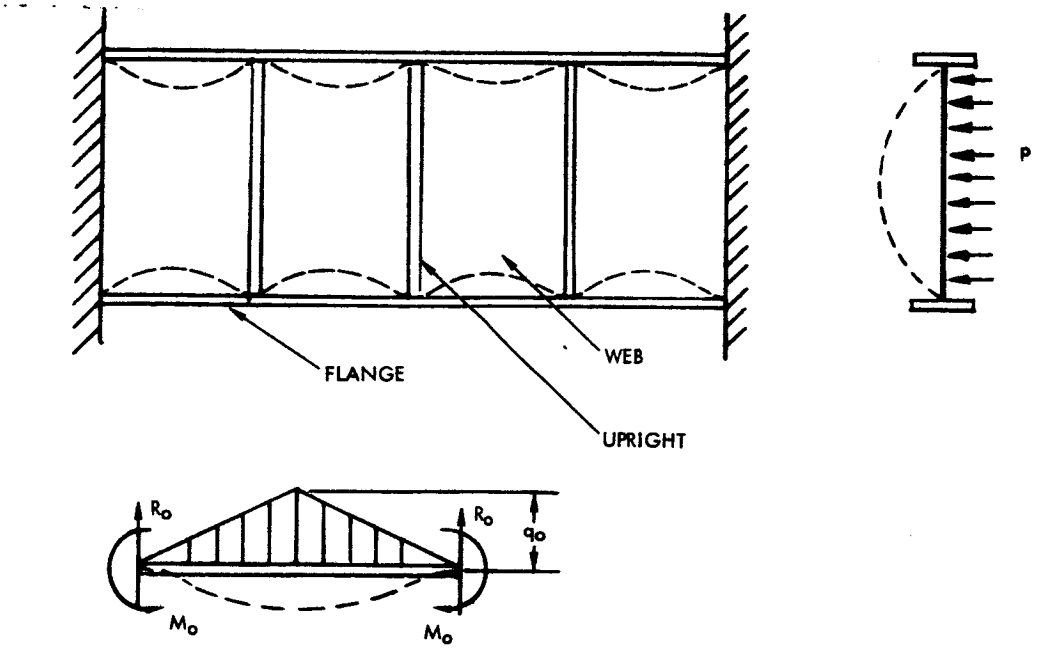

Figure 34. Strength Analysis of Flanges

The lateral deflection of the flange in the direction of the applied lateral pressure can be considered as a beam under triangular load and concentrated load as shown in Figure 35.

The reaction on the flange due to lateral pressure p is shown in Figure 35. In addition to the triangular load q (x) existing due to the load on the web, there exist concentrated lateral forces H caused by the reaction at the upright ends. Here q (x) is taken to be triangular load as a function of x, i. e., distance along the flange length.

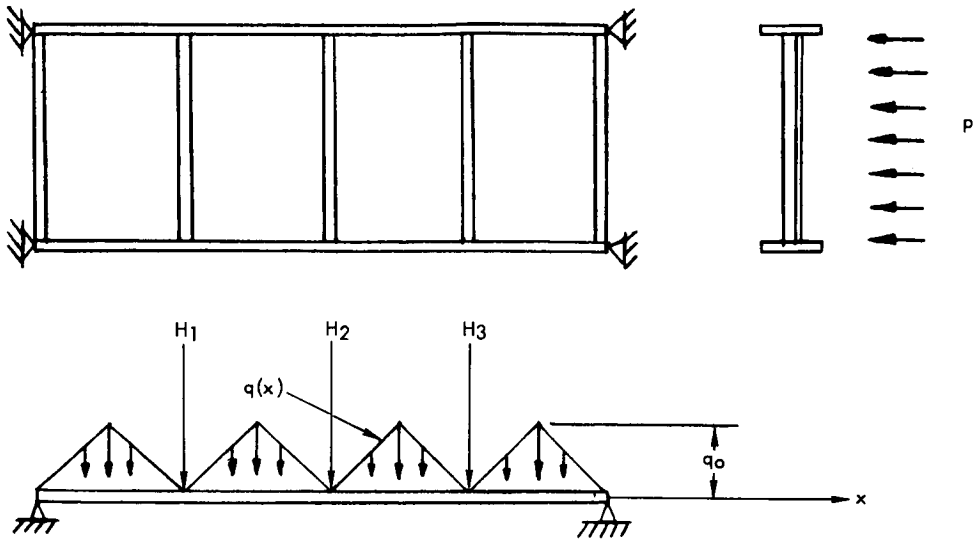

Figure 35. Reactions Acting on Flange Due to Lateral Pressure

Stability Consideration for Flanges

Lateral Instability of Flange

The lateral load acting on the beam induces compression and tension on the flange portion as shown in Figure 36. Since compressive force exist in the flange portion, this section must be investigated for stress and instability. The flange portion may be treated as a bending moment M caused by the lateral loading of the beam acting in its plane. This bending moment may buckle the flange out of the plane, i. e., sideways.

The bending moment must be less than the critical bending moment, otherwise, out-of-plane flange buckling will occur. The critical buckling moment for pin-end beam of Figure 37 is (Reference 28).

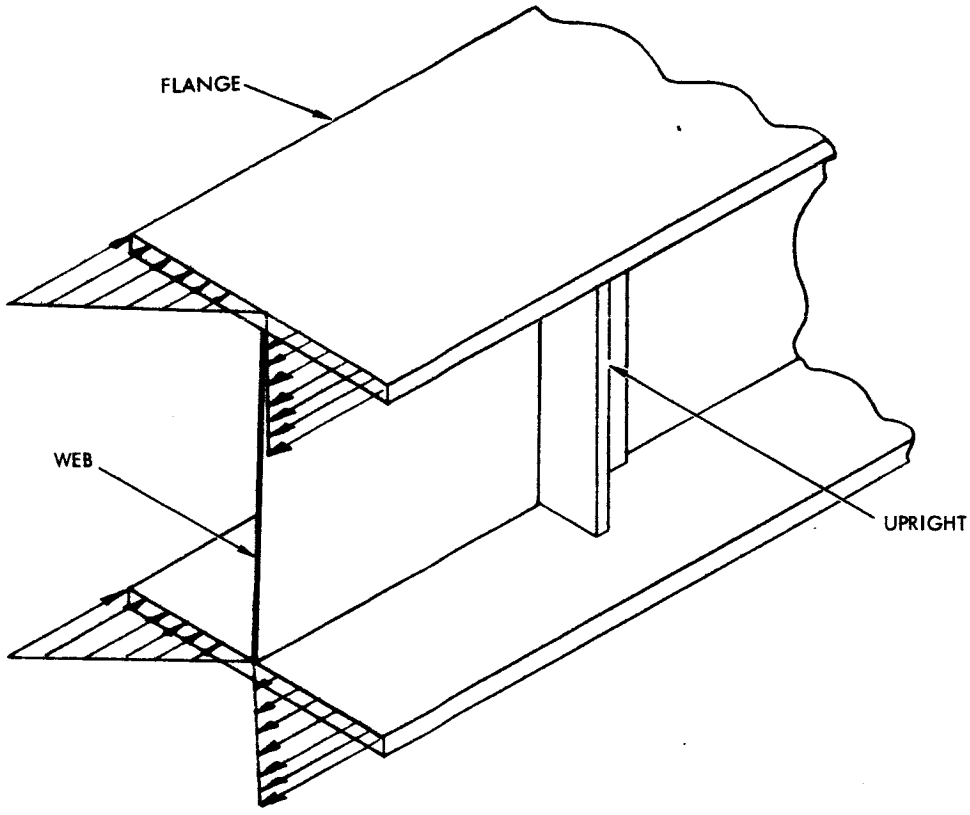

Figure 36. Laterally Loaded Tension Field Beam

$$M_{cr} = \frac{\pi\sqrt{GJEI_z}}{L} \qquad (2\text{-}11)$$

where

G = shear modulus, psi

J = torsional constant, $in.^4$

E = elastic modulus, psi

I = moment of inertia with respect to z-axis (Figure 37), $in.^4$

L = length of the beam between lateral supports, in.

GJ = torsional rigidity, $lb/in.^2$

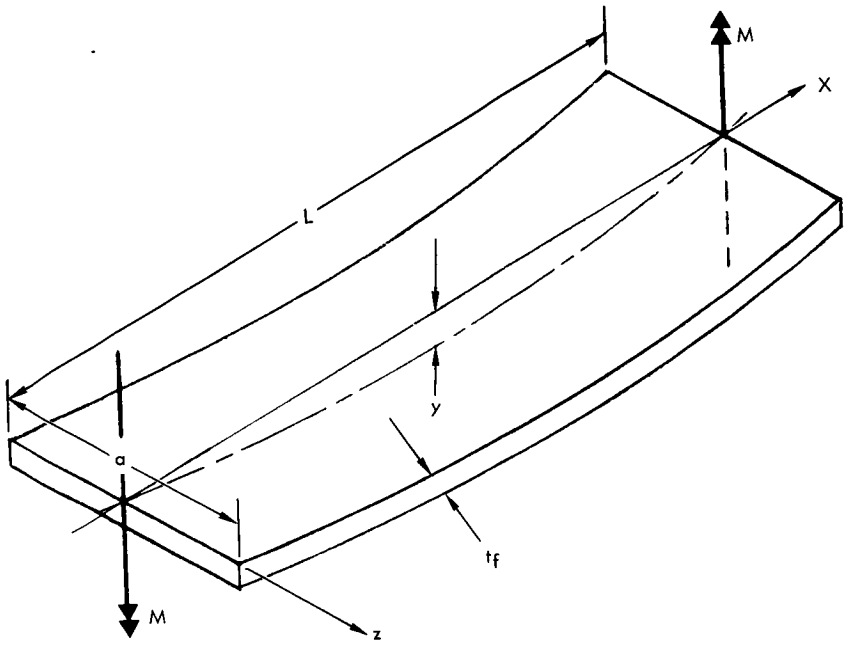

Figure 37. Moment of Inertia of Flange With Respect to Z-Axis, in.^{4}

The addition of lateral supports between end span will reduce the effective length and add some torsional restraint thus increasing the critical bending moment level. Since it is unlikely for the flange to buckle in this mode, the conservative assumption that uprights do not influence the buckling level is suggested. This is especailly appropriate since experimental data approaches the pin-end upright case rather than the fixed-end case.

Twisting of Flange

The maximum shear stress in the flange (Figure 38) due to twisting is (Reference 28).

$$\tau_{max} = \frac{3T}{at_f^2} \qquad (2\text{-}12)$$

where

a = flange width, in.

t_f = flange thickness, in.

T = maximum twisting moment, in. /lb

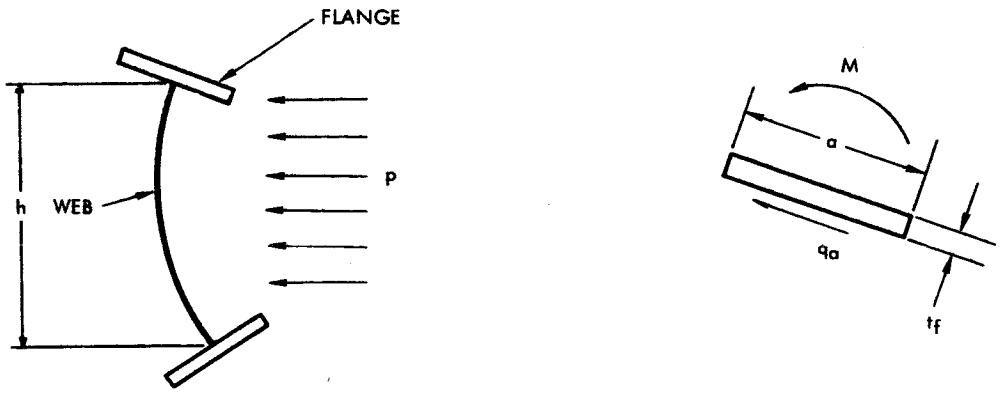

Figure 38. Maximum Shear Stress in the Flange Due to Twisting

The distributed twisting moment M_t is

$$M_t = \left(\frac{pA}{2L}\right)\left(\frac{t_f}{2}\right) \text{ (in. -lb/in.)}$$

therefore,

$$T_{max} = \frac{M_t L}{2} = \frac{pAt_f}{8} \text{ (in. -lb)} \qquad (2\text{-}13)$$

where $A = hL$ is the area in which the pressure is acting.

The maximum T that can be applied is when τ_{max} is taken to be equal to material allowable. Hence,

$$T_{max} = \tau_{max} \frac{at_f^2}{3}$$

when T is less than T_{max} the flange section being studied will not fail in torsion.

CONCLUSION

The methods for analyzing the uprights and flanges of a partial-tension-field beam subjected to lateral pressure loading have been developed in this section. The failure of uprights is due primarily to excessive bending such that the material allowable stress is exceeded. Crippling of the uprights should also be checked. For the flange portion, the stresses and the instability modes should be checked using the equations provided.

III. PARTIAL-TENSION-FIELD BEAMS LOADED VERTICALLY AND LATERALLY

Sections I and II have treated the behavior of partial-tension-field beams subjected to vertical loading or to lateral pressure loading. In this chapter analysis methods are developed which define response of partial-tension-field beams when these loadings are applied simultaneously.

WEBS

INTERACTION BETWEEN VERTICAL AND LATERAL LOADINGS

It is assumed that both vertical and lateral loadings act simultaneously on the beam. Both sets of stresses, as shown in the Figures 39 and 40, must be considered simultaneously.

In the prebuckled stage web stresses can be determined by simple superposition methods. It is noted that the compression in the diagonal direction, which causes buckles to form and the transition into the post-buckling stage, is diminished by the addition of the tension component resulting from the lateral loading. Consequently, the load range in which prebuckling analysis applies is increased. However, the post buckled case is of greater interest.

Postbuckled Stage

Under the application of vertical loads on the beam, the web will be stressed in shear. At the critical value of shear stress, τ_{cr}, the web will buckle. This is because the shear stress can be resolved into a compression stress, σ_c, in the diagonal direction causing buckling. The critical buckling value of shear stress, τ_{cr}, can be calculated knowing the material, size, and thickness of the web. The web can carry applied shear larger than the buckling shear by tension field behavior since the structural model changes when the web buckles.

Figure 41, diagram A, shows the increase of compression and tension stresses as a function of τ, which is a function of the vertical loading.

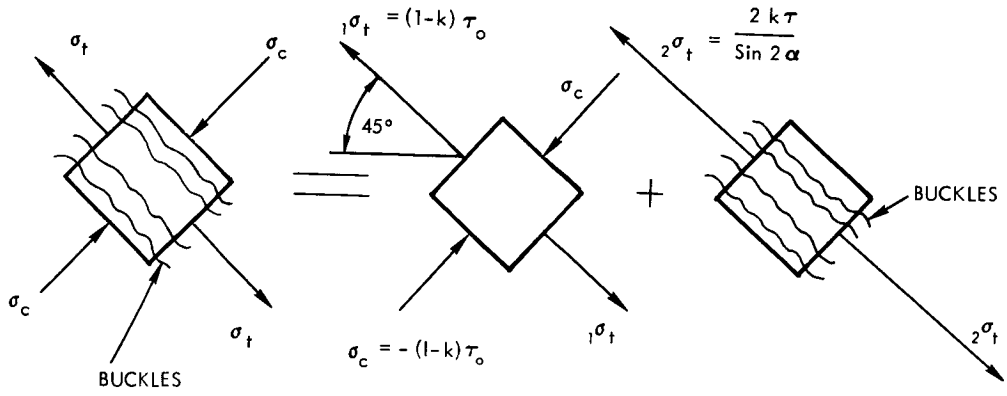

Figure 39. Stresses Due to Vertical Loading

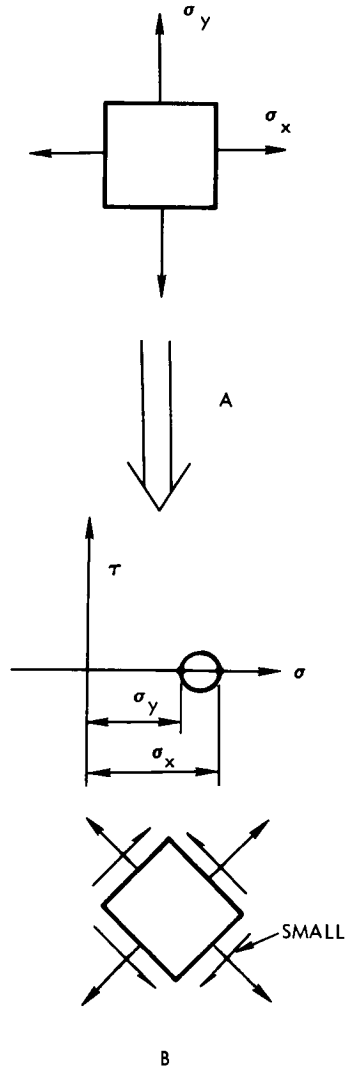

Figure 40. Stresses Due to Lateral Loading

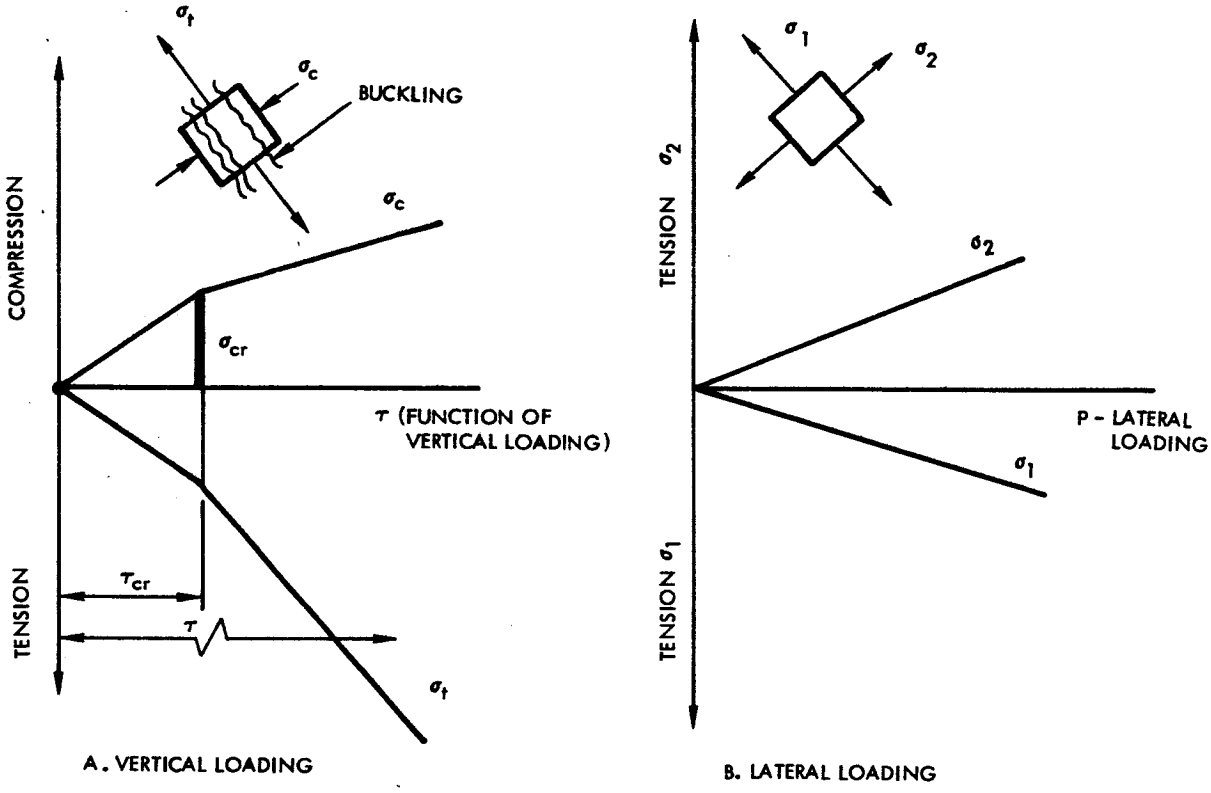

Figure 41. Diagrams of Stresses Versus Loadings

After σ_{cr} is reached, buckling occurs, and the compression stress will not be increased significantly. The tension stress, which is inclined at 90 degrees to the compression stress, will continue to increase (at a larger rate) because the model has now changed and nearly all increments of loading will be taken by tensional resistance of the web. Figure 41, diagram B, shows a similar relation between the lateral loading and the corresponding tensile stresses σ_1 and σ_2 as a function of lateral loading, which is designated by p (pressure).

To preclude web buckling, the combined interaction must satisfy the relationship:

$$\Delta\sigma = \left| -\sigma_c + \sigma_2 \right| < \left| -\sigma_{cr} \right| = \sigma_{max}$$

and this can be presented by the compression stress which is shown in Figure 42.

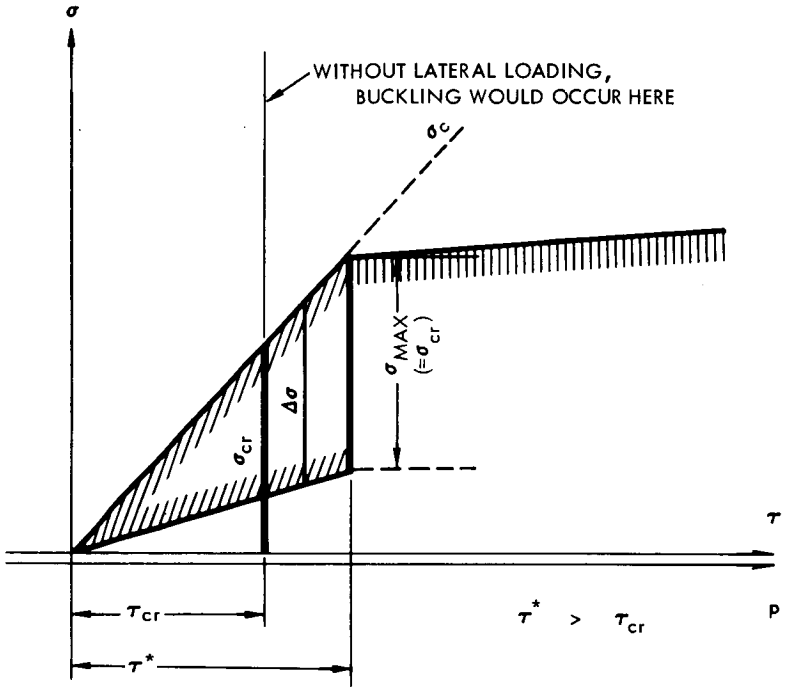

Figure 42. Combined Compression Stresses in Web

It is evident from this graph that the stability of the web increases due to lateral pressure, and buckling is postponed.

Interpretation of the Postbuckled Stage

The buckled web consists of a set of wrinkles that are oriented in the diagonal direction. The cross section through this set will indicate a wrinkled section which is similar to a corrugated metallic sheet. The corrugations are very small. The most fundamental question is: Which structural model is reasonable to use for the prediction of stresses in the buckled web that takes postbuckling stresses by diagonal tension. Test results and the observations of buckled webs are of significant help, showing that the compression stress σ_{cr} that caused buckling does not disappear with

the change of the model, but either remains constant or slightly increases with the increment of loading.

The aforementioned corrugation can not provide significant additional bending rigidity because of the negligibly small height of the corrugations. The small bending rigidity is negligible in comparison with the axial rigidity as shown in Figure 43.

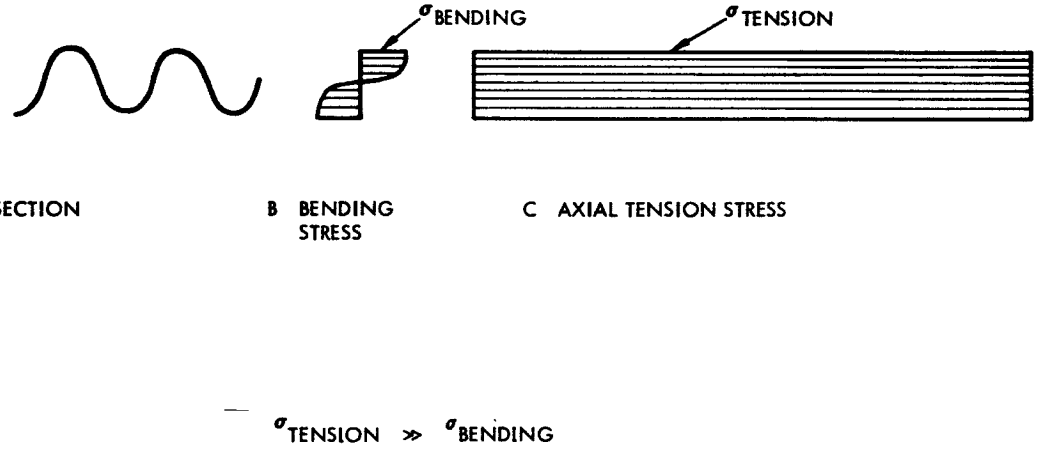

Figure 43. Stresses in Tensile Direction of Buckled Web

It is assumed that the buckled web can be idealized by a set of catenaries in the diagonal direction because of the negligible bending rigidity. The next section will describe the application of the physical model represented by the catenary.

ANALYSIS OF THE POSTBUCKLED WEB

Inextensible and Extensible Catenary

The web in the postbuckled state will be idealized in this analysis as a system of catenaries oriented along the wrinkles. The catenaries are assumed to carry the lateral pressure in the postbuckled stage.

The method of determining the stresses and deformations of an inextensible catenary is well known. Less known, however, is the case where the extensibility of the catenary is considered. Since the material is already wrinkled in the web of the partial-tension-field beam in the

postbuckling stage, it can be assumed that the deformations may be of considerable magnitude. In the case of a very thin web, the large deflection theory to determine the stresses in a membrane has already been dealt with. The extensible catenary actually presents another case of geometrical non-linearity (loading versus deflection); consequently, the linear approach can not be utilized.

This method of analysis was presented in Reference 28, which was later extended and modified considerably by NAA-S&ID. Figure 44 represents a general case of an extensible catenary that is loaded unsymmetrically. The distance between the loadings is arbitrary and the supports are on different elevations.

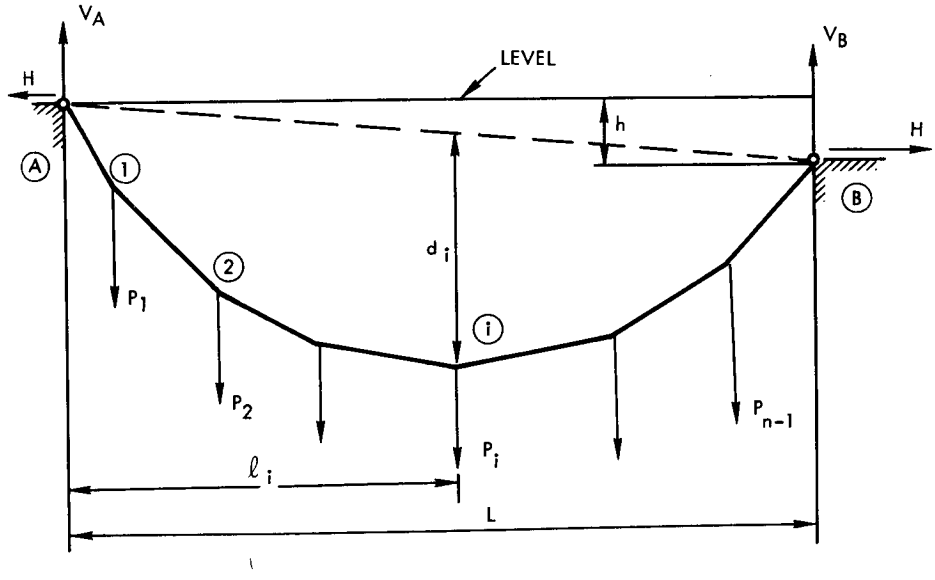

Figure 44. Unsymmetrically Loaded Catenary (General Case)

For our present purpose, it would be adequate to treat the simplest case of the catenary. This has the supports on the same level and is loaded with a uniformly distributed loading. Instead, we will describe the more general case as presented in Figure 44. This will be useful for possible future extension of this work. For instance, if hydrostatic pressure or some other distribution of the pressure is of interest, it is still possible to use this approach.

Suppose S is the known original length of the cable before it is placed in the position between the supports A and B. The equilibrium shape is not known at all; this depends upon the loading. A slight change in the loading

will be immediately followed by a change in the shape of the catenary. Under the loading shown in Figure 44, it can be observed that the deflected shape of the catenary depends only on the distribution of load, not on the magnitude. The stresses in the catenary depend upon both distribution and magnitude of the applied loads. If the extensibility is not negligible during loading, every point (i) will continue to change its vertical and horizontal coordinates. When the loading P_i reaches the final value, the shape of the catenary will be different from the original shape assumed by catenary at the beginning of the loading process. This final shape is designated as the extensible shape. The shape as it was originally noted at the beginning of the process is called the inextensible shape.

Under vertical loading, the horizontal movements of the load application points (i) on catenary are small in comparison with the vertical movements and, consequently, will be neglected. The following additional designations are made:

θ_i = angle between the catenary in the i^{th} bay and the horizontal

A = area of the cross section of the catenary

E = modulus of elasticity for the catenary

M_i = bending moment at the i^{th} load due to the force system, if H = O

H = horizontal component of reaction at supports A and B.

V = vertical reaction at A and B due to the loading.

F_i = vertical shear force in the i^{th} bay

S = initial length of catenary

d_i = initial location of the loaded point (i) measured from the reference line $\overline{AB}$. This value is not known in the beginning of the calculation, and is the function of S and loading P_i.

The reactions V_A and V_B are determined as follows:

$$V_A = R_A + H\frac{h}{L} = R_A + \alpha H$$

$$V_B = R_B - H\frac{h}{L} = R_B - \alpha H$$

where $h/L = \alpha$ and R_A and R_B are the reactions of the simply supported beam of span L loaded with applied loading.

The following formulas are known:

$$d_i = \frac{M_i}{H}$$

$$F_i = \frac{M_i - M_{i-1}}{\ell_i - \ell_{i-1}}$$

$$\tan \theta_i = \frac{F_i}{H} + \alpha$$

If the angle of inclination θ_i is not too large, instead of using the known relation $\text{Sec } \theta_i = \sqrt{1 + \tan^2 \theta_i}$, an approximate relation will be used:

$$\text{Sec } \theta_i \approx 1 + \frac{1}{2} \tan^2 \theta_i = 1 + \frac{1}{2}\left(\frac{F_i}{H} + \alpha\right)^2$$

In Reference 29 Pippard shows how the error varies with the angle θ:

θ	tan θ	Sec θ		Error (%)
		Accurate	Approximate	
0	0	1.0	1.0	0
10	0.1763	1.0154	1.0155	0.01
20	0.3639	1.0642	1.0662	0.19
30	0.5773	1.1547	1.1667	1.04
45	1.0	1.4142	1.5000	6.07
60	1.7320	2.0	2.5	25.0

Further, Pippard shows that the total length of the catenary when strained is

$$L\left(1 + \frac{1}{2}\alpha^2\right) + \frac{Z}{2H^2} \tag{3-1}$$

where

$$Z = \sum_1^n \left(\ell_1 - \ell_{i-1}\right) F_i^2 \tag{3-2}$$

If the tension in the catenary in the ith bay is designated by T_i, the increase in the length in this bay is

$$\frac{T_i\left(\ell_i - \ell_{i-1}\right) \operatorname{Sec} \theta_i}{AE}$$

Since

$$T_i = H \operatorname{Sec} \theta_i = \sqrt{H^2 + F_i^2}$$

the increase in the length of the catenary is

$$\frac{H}{AE} \sum_1^n \left(\ell_i - \ell_{i-1}\right) \operatorname{Sec}^2 \theta_i$$

The strained length is given by the following formula

$$S + \frac{H}{AE}\left[L\left(1 + \alpha^2\right) + \frac{Z}{H^2}\right] \tag{3-3}$$

Equating (3-1) and (3-3) leads to the cubic equation:

$$2H^3 L\left(1 + \alpha^2\right) + 2H^2 AE\left\{S - L\left(1 + \frac{1}{2}\alpha^2\right)\right\} + Z\left(2H - AE\right) = o$$

The term AE is much larger than the term H; therefore, the following approximation can be written:

$$2H^3 L\left(1 + \alpha^2\right) + 2H^2 AE\left\{S - L\left(1 + \frac{1}{2}\alpha^2\right)\right\} - ZAE = o \tag{3-4}$$

For any specified length of cable and distribution of load, H can be determined from Equation 3-4. Now assume that the cable is already pretensioned with a load H_o before any lateral load is applied. For this case, Equation 3-4 is modified to

$$2L(1+\alpha^2)\left(H^3 - H^2 H_o \frac{AE}{AE + H_o}\right) - ZAE = o \qquad (3-5)$$

because the extended length of the cable is equal to the span L, modified with the inclination factor $(1 + \frac{1}{2}\alpha^2)$

$$L(1+\frac{1}{2}\alpha^2) = S\left\{1 + \frac{H_o(1+\frac{1}{2}\alpha^2)}{AE}\right\}$$

If $\frac{AE}{AE + H_o} \approx 1$, Equation 3-5 may be simplified:

$$2L(1+\alpha^2)(H^3 - H^2 H_o) - ZAE = o \qquad (3-6)$$

H is the final tension under load (H_o is included in H). If the loads and spacings are both equal and A and B are at the same level (D = o, α = o, P_i = P) then

$$H = \sqrt[3]{\frac{AEP^2(n^2-1)}{24}} = 0.347 \sqrt[3]{AEP^2(n^2-1)}$$

n denotes the number of equal bays in the catenary.

If the loading is continuous and of uniform intensity p along the length AB, the shearing force at a distance X from A is

$$p\left(\frac{1}{2}L - x\right)\left(1 - \frac{1}{2}\alpha^2\right)$$

then

$$Z = p^2(1+\alpha^2)\int_o^L (\tfrac{1}{2}L - x)^2\,dx = \frac{p^2L^3(1+\alpha^2)}{12} \qquad (3-7)$$

$$H = \sqrt[3]{\frac{AEp^2L^2}{24}} = 0.347 \sqrt[3]{AEp^2L^2}$$

When H is known, the initial location of the loaded points below the reference line may be found from $d_i = M_i/H$ and, consequently, the loaded shape of the catenary determined. For determination of M_i the following method may be of help:

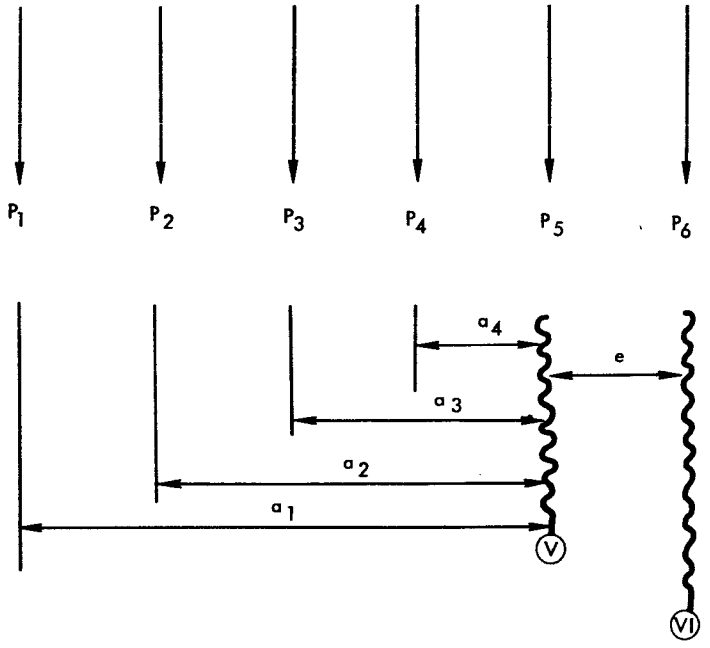

$$M_{\underline{v}} = P_1a_1 + P_2a_2 + P_3a_3 + P_4a_4; \quad F_v = \sum_1^5 P_i$$

$$M_{\underline{vi}} = P_1(a_1 + e) + P_2(a_2 + e) + P_3(a_3 + e) + P_4(a_4 + e) + P_5e$$

$$= \underbrace{(P_1a_1 + P_2a_2 + \ldots + P_4a_4)}_{M_{\underline{v}}} + \underbrace{(P_1e + \ldots + P_4e) + P_5e}_{e\sum_1^5 P_i}$$

Consequently,

$$M_{\underline{vi}} = M_{\underline{v}} + eF_{\underline{v}}$$

The moments can be calculated from this equation.

Consider the case of an equally distributed loading p on a catenary which is initially prestressed with load H_o before the loading p is applied.

From Equation 3-7

$$2L(1 + \alpha^2)(H^3 - H^2 H_o) - ZAE = o,$$

where

$$Z = \frac{1}{12} p^2 L^3 (1 + \alpha^2) \quad .$$

This leads to:

$$2L(1 + \alpha^2)(H^3 - H^2 H_o) - \frac{p^2 L^3 (1 + \alpha^2) AE}{12} = o.$$

After algebraic manipulation, this becomes:

$$H^3 - H_o H^2 - \frac{p^2 L^2 AE}{24} = o.$$

Designate $H_o = -a_2$,

$$\frac{p^2 L^2 AE}{24} = -a_o.$$

Then the cubic equation will be:

$$H^3 + a_2 H^2 + a_o = o. \qquad (3\text{-}8)$$

To determine the unknown value for the tension H in the cable, which is pretensioned with H_o and loaded with p, the roots of Equation 3-8 must be found.

Denote:

$$q = -\frac{1}{9} a_2^2 = -\left(\frac{H_o}{3}\right)^2$$

$$r = \frac{1}{6}(-3a_o) - \frac{1}{27} a_2^3 = \frac{p^2 L^2 AE}{48} - \left(\frac{H_o}{3}\right)^3$$

Then:

$$q^3 = -\left(\frac{H_o}{3}\right)^6$$

$$r^2 = \left(\frac{p^2L^2AE}{48}\right)^2 - 2\left(\frac{p^2L^2AE}{48}\right)\left(\frac{H_o}{3}\right)^3 + \left(\frac{H_o}{3}\right)^6$$

Adding the above equations:

$$q^3 + r^2 = \frac{p^2L^2AE}{48}\left[\frac{p^2L^2AE}{48} - 2\left(\frac{H_o}{3}\right)^3\right]$$

This is the governing equation for behavior of the catenary. The value of the quantity in the bracket will now be examined. Defining this quantity as Δ:

$$\Delta = \frac{p^2L^2AE}{48} - 2\left(\frac{H_o}{3}\right)^3$$

If $\Delta > 0$, there exists one real root and pair of complex conjugate roots. The above inequality may be expressed as: $p^2L^2AE > 3.56\,H_o^3$. If, however, $p^2L^2AE \leq 3.56\,H_o^3$ then all roots are real. To facilitate calculation of the roots, designate the following quantities:

$$S_1 = \left[r + \sqrt{q^3 + r^2}\right]^{1/3}$$

$$= \left[\frac{p^2L^2AE}{48} - \frac{H_o^3}{27} + pL\sqrt{\frac{AE}{48}}\sqrt{\frac{p^2L^2AE}{48} - \frac{H_o^3}{13.5}}\right]^{1/3}$$

$$S_2 = \left[r - \left(q^3 + r^2\right)^{1/2}\right]^{1/3}$$

$$= \left[\frac{p^2L^2AE}{48} - \frac{H_o^3}{27} - pL\sqrt{\frac{AE}{48}}\sqrt{\frac{p^2L^2AE}{48} - \frac{H_o^3}{13.5}}\right]^{1/3}$$

with these designations, the roots can be given in the general form:

$$H_1 = (S_1 + S_2) - \frac{a_2}{3} = (S_1 + S_2) + \frac{H_o}{3}$$

$$H_2 = -\frac{S_1 + S_2}{2} + \frac{H_o}{3} + \frac{i\sqrt{3}}{2}(S_1 - S_2)$$

$$H_3 = -\frac{S_1 + S_2}{2} + \frac{H_o}{3} - \frac{i\sqrt{3}}{2}(S_1 - S_2)$$

This leads to:

$$\left.\begin{aligned} H_1 &= S_1 + S_2 + \frac{H_o}{3} \\ H_2 &= S_1\left(\frac{i\sqrt{3} - 1}{2}\right) - S_2\left(\frac{i\sqrt{3} + 1}{2}\right) + \frac{H_o}{3} \\ H_3 &= S_2\left(\frac{i\sqrt{3} - 1}{2}\right) - S_1\left(\frac{i\sqrt{3} + 1}{2}\right) + \frac{H_o}{3} \end{aligned}\right\} \quad (3\text{-}9)$$

It is evident that the direct solution of Equations 3-5 and 3-8 appear to be involved; consequently, it may be simpler in some cases to solve these equations by a trial and error approach. The solution of the cubic equation is programmed for the IBM 7094 as part of the catenary analysis program discussed in Appendix C.

Numerical Example

A simple example will be calculated (Figure 45) where loading and dimensions are given.

Then $2H^3L + 2H^2AE(S - L) + Z(2H - AE) = o$ which is the equation to determine H for this case.

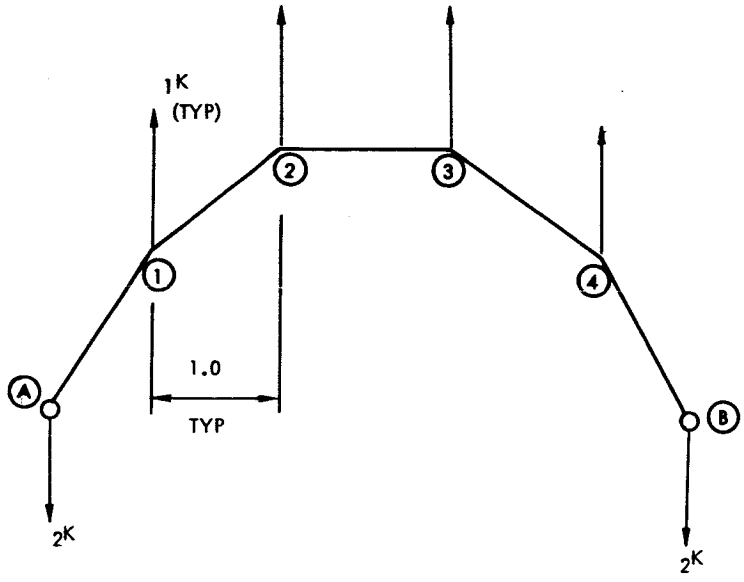

Figure 45. Numerical Example

	$\Delta \ell$	P_i	F_i	F_i^2	$\Delta \ell F_i^2$	$M_n = M_{n-1} + eF_{n-1}$
A		-2			0	0
	0.5		-2	4	2	
1		+1				-1 = -1
	1		-1	1	1	
2		+1				-1 - 1 = -2
	1		0	0	0	
3		+1				-2 + 0 = -2
	1		+1	1	1	
4		+1				-2 + 1 = -1
	0.5		+2	4	2	
B		-2				-1 + 1 = 0
			0		0	
					Z = 6	

Collect the terms:

$$\frac{1}{2}S = 0.65 + 1.15 + 0.50 = 2.30 \qquad S = 4.60 \qquad L = 4$$

Assume:

$$A = 0.5 \text{ in}^2$$
$$E = 8000 \text{ lb/in}^2$$
$$AE = 4000 \text{ lb.}$$
$$Z = 6$$

This leads to:

$$H^3 + 0.60\,H^2 + 1.50\,H = 3 \times 10^3$$

The solution is H = 1.00.

Now the new extensible shape can be easily found:

$$y_i = M_i/H$$

Actually, the buckled web consists of a set of many catenaries. If we want the stress/strain conditions in every strip, many calculations must be performed. The cubic equation to determine H can be solved with the trial and error method which is time consuming. If the time element is pressing, it would be useful to have a FORTRAN program. A program of this type is written and is discussed in Appendix C of this report.

Reactions on Uprights

If the buckled web is idealized by a set of catenaries in the diagonal direction, it will deliver to the uprights an inclined reaction which can be resolved into a horizontal component H and vertical component V. Each strip of the web, which is idealized by a catenary, will deliver this reaction. The FORTRAN Program, presented in Appendix C, will compute a set of reactions which correspond, as assumed, with each catenary.

FAILURE CRITERIA

It is apparent that the controlling factor in any case is the tension strength of the web, which is the ultimate limit to the loads carried by the beam. If only vertical loading is dealt with, then in the postbuckling stage, the web is stressed largely in tension and actual stress must be smaller than the strength of the material: $v\,\sigma_{actual} < \sigma_{ultimate}$. If the web is loaded up to σ_{ult}, no additional load can be accepted. The lateral loading also leads to the axially loaded catenary. In this case must be $_H\sigma_{act} < \sigma_{ult}$. If both vertical and lateral loadings are present, $_v\sigma_{act} + {}_H\sigma_{act} < \sigma_{ult}$.

For the case of a beam loaded with both vertical and lateral load, the nondimensional graph shown in Figure 46 is used.

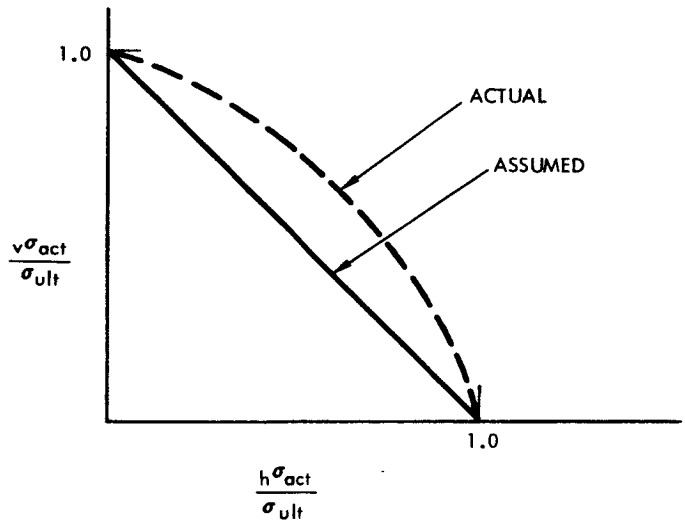

Figure 46. Interaction Graph

The straight line assumption is a reasonable simplification. In reality, the interaction curve is slightly curved because of the geometrical nonlinearity connected with the stresses and deflections of the catenary. However, assume that this effect is small. The straight line is also a conservative assumption because in an extensible catenary the extensibility reduces the stresses.

SIMULTANEOUS APPLICATION OF VERTICAL AND LATERAL LOADINGS

The basic assumption made by Paul Kuhn in Reference 1 is that all stresses that were developed in the prebuckling stage remain "frozen" in the web after buckling. After buckling occurre , the rate of increase of these stresses will be changed, so that the compression stresses will continue to increase but at a smaller rate than before buckling. The tension stresses, however, increase at a larger rate.

The question of increase of the compression stresses after buckling is disputable. Several investigators claimed that the compression stress after buckling remains constant. Wagner even suggested that the compression stresses drastically decrease, which leads to the safe conclusion to neglect them.

The behavior of stresses/deformations due to the lateral loading must be consistent with the assumption that was made by investigation of stresses/deformations due to vertical loading. Kuhn shows in Reference 1 that his assumption was made in accordance with numerous test results. Since this work is a continuation of the excellent work performed by Kuhn on vertical loading, it is logical to keep the same assumptions. This was done in the beginning of this section and all stresses that were developed in the web in the prebuckling stage were assumed to be frozen in the web. An increase in the vertical or lateral loading supplied just additional components to the frozen state of the stresses. This structural model, however, leads to the conclusion that the sequence of loading slightly influences the results. This influence from the practical point of view is not too significant, and from the theoretical point of view it is open to question.

Many arguments may be presented in favor or against the assumption that the sequence of loading influences the final state of stress. In reality, only a well performed testing program may prove it one way or another. Unfortunately, no such program is possible under this study. Consequently, it is difficult to answer this question with complete certainty.

Consequently, two procedures are outlined here. The first procedure is consistent with the assumption of frozen stresses; the second procedure deviates from this assumption, as will be explained later. The second procedure is independent of the path of loading and is consistent with the law of conservation of energy.

First Procedure

Since vertical and lateral loadings are applied simultaneously, buckling of the web may occur under some critical combination of shear and pressure (τ^*, p^*) where

τ^* = postponed critical shear due to the presence of p^* ($\tau^* > \tau_{cr}$)

p^* = part of lateral loading ($p^* \leq p_o$) which supports the web at buckling when τ^* is reached.

There are an infinite number of combinations of load (τ^*, p^*) under which buckling occurs. It is necessary to select in advance any value $\tau^* \geq \tau_{cr}$ or $p^* \leq p_o$ under which it is desired to get the web buckled. If τ^* is given in advance, then a corresponding p^* can be determined. If p^* is selected τ^* can be determined.

The characteristic equation for buckling is:

$$\tau^* \approx \tau_{cr} + \sigma^* \tag{3-10}$$

where σ^* is the tension in the compression (diagonal) direction, and depends on the lateral pressure loading.

This procedure takes into account the sequence of loading. The load deformation relationships are not linear; and the previously assumed linear variation of the stresses was a simplification, useful for small lateral loadings. This simplification will be removed here.

In the prebuckling stage τ_{cr} due to vertical loading only was determined. Two approaches can be used:

1. Determine the lateral loading p^* which buckles the web in combination with the assumed shear stress, τ^*.

   From Equation 3-10: $\sigma^* = \tau^* - \sigma_{cr}$. Now τ^* shall be transformed into components in a and b direction where a and b are the horizontal and vertical dimensions of the web respectively. In connection with Figure 47 the following formula can be used:

$$\sigma = \sigma_a \cos^2\theta + \sigma_b \sin^2\theta - 2\tau_{xy} \sin\theta \cos\theta$$

$$\tau = (\sigma_a - \sigma_b) \sin\theta \cos\theta + \tau_{xy} (\cos^2\theta - \sin^2\theta) \tag{3-11}$$

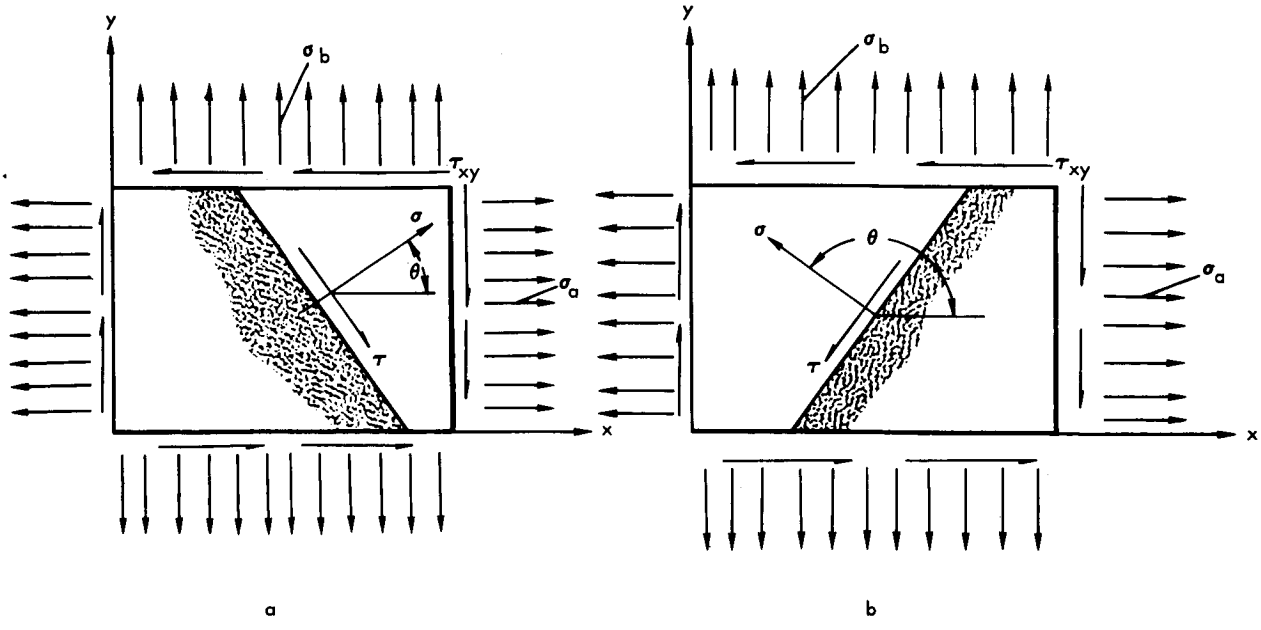

Figure 47. Stressed Element

τ can be neglected because τ_{xy} for our case is small. Consequently, the equation can be written:

$$\sigma_a^* A = \sigma_a^* l = \sigma^* \cos\theta \times l \cos\theta$$

$$\sigma_a^* = \sigma^* \cos^2\theta$$

Since $\theta = 45°$, the expression for the buckling stress in the a-direction is

$$\sigma_a^* = \sigma^* \times 0.71^2 = 0.505\,\sigma^* \approx 0.5\,\sigma^*$$

In order to find corresponding p^* the following formula is used:

$$\sigma_a^* = \eta_2 \sqrt[3]{p^2 E \frac{(\text{larger side of plate})^2}{t^2}}$$

and η_2 as function of the parameter a/b (where a > b) shall be obtained from Figure 29.

Then:

$$p^* = \frac{\sigma_a{}^* t}{\eta_2 \text{ (long side)}} \sqrt{\frac{\sigma_a{}^*}{\eta_2 E}}$$

2. Determine the shear stress τ^* which buckles the web in combination with the assumed lateral pressure p^*.

$U = (p^*)^2 E \frac{a^2}{t^2}$ to p^* corresponds; $a > b$

From Equation 3-10

$$\sigma^* = \frac{1}{2}(\eta_2 + \eta_3) \sqrt[3]{U}$$

Figure 48 leads to determination of the factor $\beta = 1/2(\eta_2 + \eta_3)$ as function of a/b $(a > b)$.

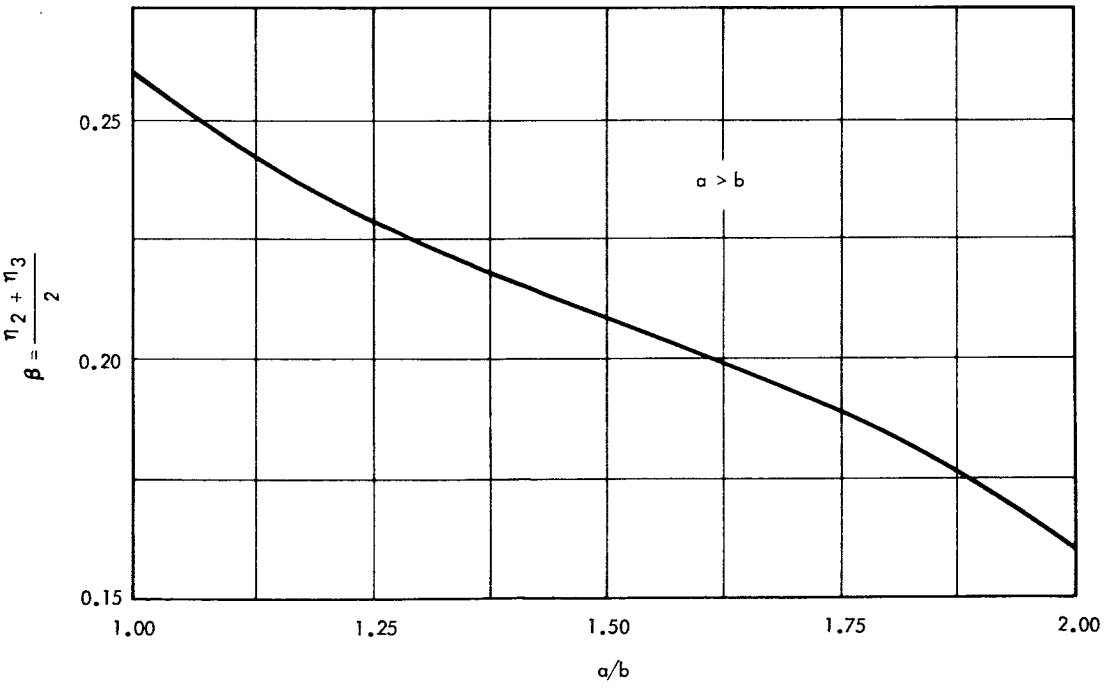

Figure 48. Coefficient β

Then

$$\gamma = \frac{\tau^*}{\tau_{cr}} = \frac{\tau_{cr}}{\tau_{cr}} + \frac{\sigma^*}{\tau_{cr}} = 1 + \frac{\beta}{\tau_{cr}} \sqrt[3]{U}$$

Finally

$$\tau^* = \gamma \tau_{cr} \tag{3-12}$$

Approaches 1 and 2 lead to a critical combination which causes buckling: (τ^*, p^*). Since the critical combination under which the buckling occurred is determined, the corresponded k factor can be found, which is designated by k^* in order to show that this factor is actually a function of τ_o/τ^* rather than τ_o/τ_{cr}. The rest of lateral loading (if any)

$$p'' = p - p^*$$

is taken by the set of catenaries. The rest of the vertical loading which is taken by the set of catenaries (changed model after buckling) corresponds to the difference $(\tau_o - \tau^*)$. Then in the usual manner

$$\frac{\tau_o}{\tau_*} \Rightarrow k^*$$

The compressive stress in diagonal direction:

1. Due to vertical loading:

$$\sigma_c = -\tau_o(1 - k^*) \sin 2\alpha$$

2. Due to lateral loading:

$$\sigma^* = \text{function of } (\sigma_a, \sigma_b)$$

Finally:

$$\sigma_I = -\tau_o(1 - k^*) \sin 2\alpha + \sigma^* \tag{3-13}$$

The tensile stresses, which are taken by set of catenaries:

1. Due to vertical loading:

$$\sigma_{II}' = \frac{2k^* \tau_o}{\sin 2\alpha} + \tau_o (1 - k^*) \sin 2\alpha + \sigma^* \qquad (3\text{-}14)$$

This stress component can be interpreted as a prestress in the catenaries.

2. Due to the lateral loading, the stress σ_{II}' is increased in the following manner:

The prestressed catenary has to support the rest of the lateral loading which was not taken during the prebuckling stage:

$$p'' = p_o - p^*$$

The appropriate formula given before, or the FORTRAN program leads to the determination of the tensile stress σ_{II} and final lateral deflection y. The input to the FORTRAN program is as follows:

The catenary, which has a length equal to the length of the diagonal, is prestressed with $H_o = \sigma_{II}'/A$, loaded with p'', and has the initial deflection δ from the prebuckling stage. The output will be final tensile prestressing H which leads to the final tensile stress in catenary $\sigma_{II} = H/l.t$, and the final deflection y.

The most important sequences of loading considered in the numerical examples are as follows:

1. Vertical and lateral loadings are concurrently applied in a linear manner.

2. Full vertical load is applied, followed by lateral load.

3. Full lateral load is applied, followed by vertical load.

From this study and as a result of many numerical examples, it was concluded that the sequence of loading has little effect on the results. The difference in results appears to be primarily due to the change of structural model from a plate to a set of catenaries with the preservation of the frozen stresses that existed at buckling. For a practical engineer these

differences are small. This discrepancy may be eliminated if the assumption of frozen stresses is slightly revised for lateral loading. The revised procedure follows.

Recommended Procedure

The physical behavior is reviewed first as was done on Figure 19.

It seems reasonable to assume, after buckling, that the entire lateral pressure load is carried by the catenaries. Consequently, at buckling the stresses due to lateral loading that existed in the prebuckling stage disappear and a new uniaxial stress system will develop. Since all of the lateral loading is taken now by the system of the catenaries, the compressive stresses in the diagonal direction due to lateral loading will be zero during the entire postbuckling stage. Figure 49 illustrates this. As before, the

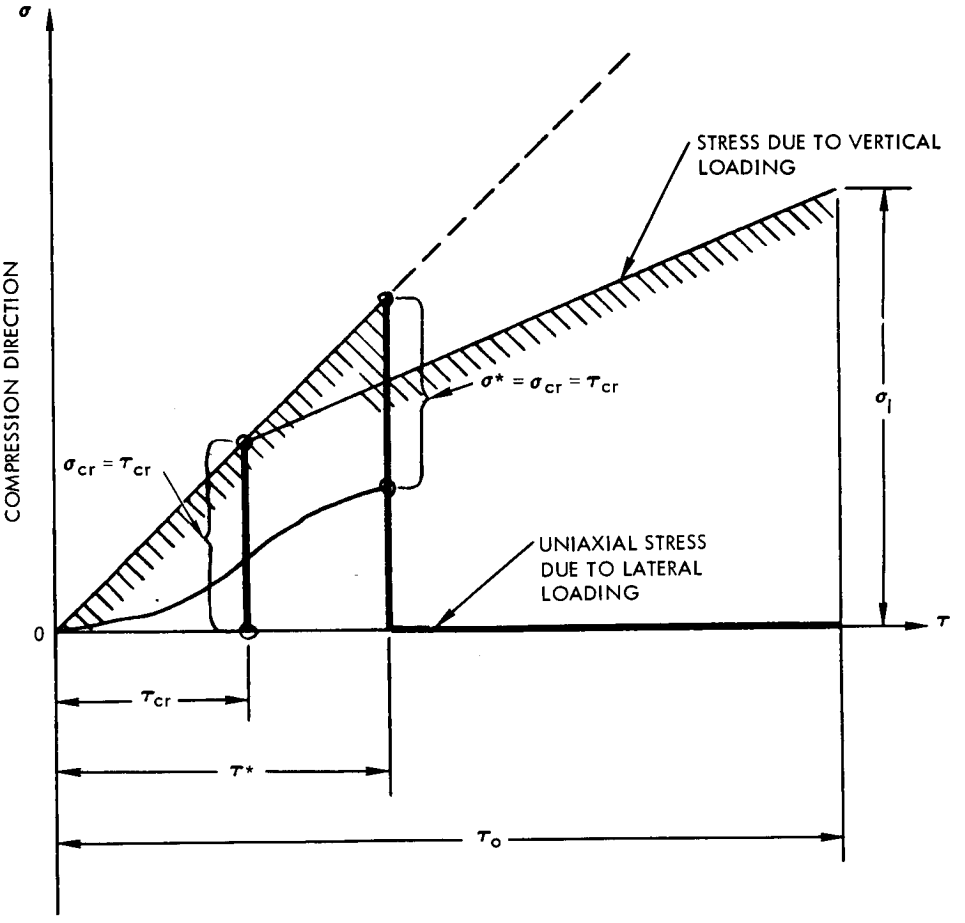

Figure 49. Compression Stresses Due to Vertical and Lateral Loading

lateral loading postpones buckling to an elevated value of shear, designated by τ^*. However, when buckling occurs the compressive component is the same as if the lateral loading were not present:

$$\sigma_I = \sigma_c = -\tau_o (1 - k) \sin 2\alpha$$

where k is the function of τ_o / τ_{cr} as was shown previously.

It is noted that at buckling there is a sudden drop in this compression stress. In the prebuckling stage, as before, the compression stress is

$$\sigma_I = -\sigma_c + {}_H\sigma_1$$

where

$$\sigma_c = \tau, \text{ where } \tau \leq \tau^*; \quad {}_H\sigma_1 \approx \frac{1}{2}(\sigma_a + \sigma_b)$$

for σ_a and σ_b use the formulas from Section $\hat{II}$:

$$\sigma_a = \eta_2 \sqrt[3]{U}, \quad \sigma_b = \eta_3 \sqrt[3]{U}$$

A similar discontinuity in the tension stresses appears at buckling as is evident from Figure 50.

In the presence of lateral loading buckling is postponed (line $\overline{a, b}$) and will occur at point b. After buckling the system changes and the tensile stress due to vertical loading immediately increases (point C). The tensile stress continues to follow the line determined by the vertical loading. Consequently, the tension stress due to vertical loading in the postbuckling stage is:

$$\sigma'_{II} = \sigma_t = \frac{2k\,\tau_o}{\text{Sin } 2\alpha} + \tau_o(1 - k) \sin 2\alpha$$

The entire lateral loading p_o is taken by a system of catenaries, shown in Figure 50. Again at buckling a discontinuity occurs because of the change in the structural model.

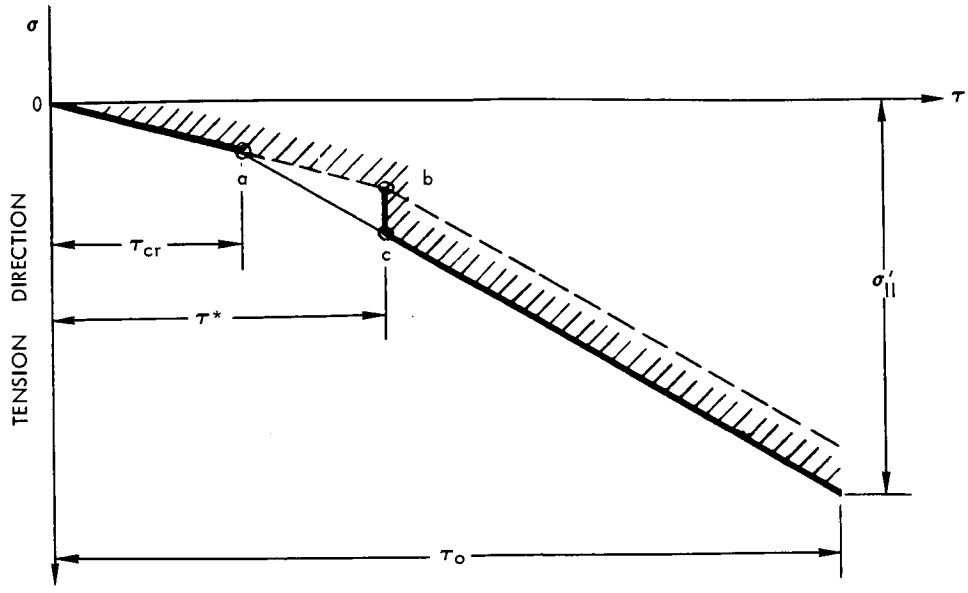

A. DUE TO VERTICAL LOADING IN PRESENCE OF LATERAL LOADING

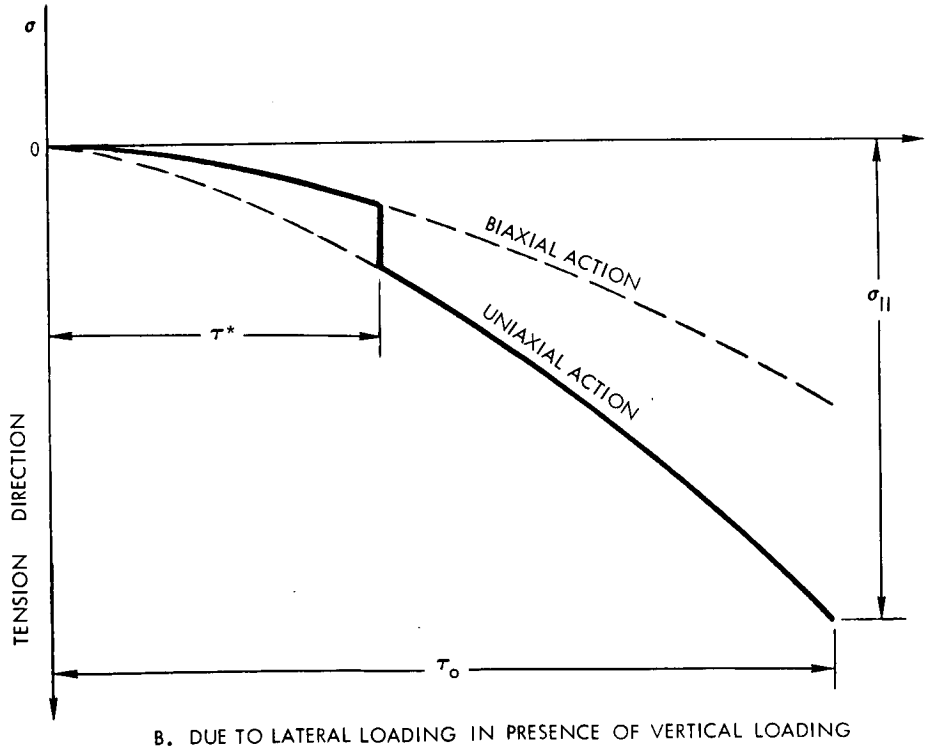

B. DUE TO LATERAL LOADING IN PRESENCE OF VERTICAL LOADING

Figure 50. Tension Stresses Due to Vertical and Lateral Loading

To determine the total tensile stress in the postbuckling range a catenary model is analyzed as before. The length of the corresponding diagonal is used for the span. The prestress $H_o = \sigma_{II}' A$; the loading p_o, which is a total lateral loading; the initial deflection is $\delta = o$ in accordance with this assumption. The FORTRAN program or the corresponding formula leads to the determination of σ_{II} (actually, the output of the FORTRAN is H, then $\sigma_{II} = H/lxt$) and final deflection y.

In the prebuckling state

$$\sigma_{II} = \sigma_t + {}_H\sigma_2$$

where

$$\sigma_t = \tau \leq \tau^*$$

$$H\sigma_1 \approx \frac{1}{2}(\sigma_a + \sigma_b)$$

for σ_a and σ_b see formulas in the Section II.

It is evident that this procedure is independent of the path of the loading. In this case the system clearly follows the law of conservation of energy.

Consequently, there is no necessity to determine the critical combination (τ^*, p^*) under which buckling occurs because this combination does not affect the final stresses. All that is needed is to examine whether the beam is in the pre- or postbuckling range and then to use the corresponding set of formulas.

In the Summary the analysis procedure is outlined. If for some reason the analyst wants to postpone buckling during loading, the entire p will be applied first and then τ^* will be determined in the previously outlined manner.

In Appendix B the procedure is illustrated with numerical example.

All cases examined described the approximate behavior of the partial-tension-field beam webs under combined loading conditions. For simplicity, a linear relation was assumed between increment of loadings, strains, and stresses. This relation may not be linear for certain loading and material combinations. In these cases, the tangent modulus will be used, and the curves representing the interaction diagrams will be curved lines rather than straight. The general approach holds for this case, also.

SUMMARY OF PROCEDURES

The procedure for the analysis of webs of partial-tension-field beams under vertical and lateral loading is summarized in the following section. The following formulas are presented for the analysis of the web.

Vertical Loading

The applied shear

$$\tau_o = V/th$$

The critical shear

$$\tau_{cr} = k_{ss} E \left(\frac{t}{d}\right)^2 \left[R_h + \frac{1}{2}(R_d - R_h)\left(\frac{d}{h}\right)^3\right]$$

If the web is in the prebuckling stage, $\tau_o \leq \tau_{cr}$

then

$$|\sigma_t| = |\sigma_c| = |\tau_o|$$

If the web is in the postbuckling stage, $\tau_o > \tau_{cr}$

then compute:

$$k = \tanh\left(0.5 \log \frac{\tau_o}{\tau_{cr}}\right)$$

To compute the effective area of the stiffener:

$$A_{U_e} = A_U \left[1 + \left(\frac{e}{j}\right)^2\right]$$

To determine the angle, α, use the parameter A_{U_e}/dt with Figure 8 (using A_{U_e} instead of A_U as indicated in graph). Then compute the stresses:

$$\sigma_c = -\tau_o (1-k) \sin 2\alpha$$

$$\sigma_t = \frac{2k\tau_o}{\sin 2\alpha} + \tau_o (1-k) \sin 2\alpha$$

Lateral Loading

Depending upon the loading, p_o, and the ratio, b/t, from Figure 24, utilizing the ratio of the web size, a/b, determine if a thin web or very thin web is being dealt with and use the formulas for thin plates or membranes, respectively.

These formulas give the stresses σ_x and σ_y. With the corresponding Mohr circles or using the formulas, find ${}_H\sigma_1$ and ${}_H\sigma_2$ for diagonal direction. Also, find the deflection in the middle of the plate, y.

Vertical and Lateral Loading

Check the compression stress in the diagonal direction.

If

$$\left|\sigma_c - {}_H\sigma_1\right| < \left|\tau_{cr}\right|$$

we are in the prebuckling stage. Then

$$\sigma_{c\ final} = -\sigma_c + {}_H\sigma_1$$

$$\sigma_{t\ final} = \sigma_t + {}_H\sigma_2$$

using Mohr's circle determine σ_{max} which must be $\leq \sigma$ ultimate tensile.

If

$$\left|\sigma_c - {}_H\sigma_1\right| > \left|\tau_{cr}\right|$$

we are then in the postbuckling stage.

First Procedure

It is desired that buckling shall occur at τ^* prescribed in advance.

Then

$$\sigma^* = \tau^* - \tau_{cr}$$

$$\sigma_a^* = 0.5\,\sigma^*$$

$$p^* = \frac{\sigma_a^*\, t}{\eta_2\,(\text{longer side})}\sqrt{\frac{\sigma_a^*}{\eta_2 E}}$$

In this way the critical combination (τ^*, p^*) is obtained.

It is desired that buckling shall occur at p^* prescribed in advance.

Then

$$U = (p^*)^2\, E\, \frac{(\text{longer side})^2}{t^2}$$

$$a/b \Rightarrow \beta \text{ (Figure 48, page 85)}$$

$$\sigma^* = \beta \sqrt[3]{U}$$

$$\tau^* = \left(1 + \frac{\beta}{\tau_{cr}}\sqrt[3]{U}\right)\tau_{cr}$$

In this way the critical combination (τ^*, p^*) is obtained.

Having the critical combination (τ^*, p^*) in both cases as was shown above, proceed as follows:

The deflection

$$\delta = \eta_1\,(\text{longer side})\sqrt[3]{\frac{p^*(\text{longer side})}{Et}}$$

will correspond to p^*

where η_1 is obtained from Figure 29.

Then the following lateral loading is taken by catenaries:

$$p'' = p_o - p^*$$

$$\tau_o / \tau^* \Rightarrow k^*$$

stresses:

$$\sigma_I = -\tau_o(1 - k^*) \sin 2\alpha + \sigma^*$$

$$\sigma_{II}' = \frac{2k^* \tau_o}{\sin 2\alpha} + \tau_o(1 - k^*) \sin 2\alpha + \sigma^*$$

Now using the computer program or the formulas with the following inputs: prestressing $H_o = \sigma_{II}' A$, lateral loading p'', initial deflection δ, σ_{II} and the final deflection, y can be obtained. Figure 51 clarifies usage of this procedure.

Recommended Procedure

It is assumed that the vertical and lateral loads are given. If

$$\left| \sigma_c - {}_H\sigma_1 \right| \leq \left| \tau_{cr} \right|$$

we are in the prebuckling stage.

Then

$$\sigma_I = -\sigma_c + {}_H\sigma_1$$

$$\sigma_{II} = \sigma_t + {}_H\sigma_2$$

where

$${}_H\sigma_1 \approx {}_H\sigma_2 \approx \frac{1}{2}(\sigma_a + \sigma_b)$$

$$\sigma_a = \eta_2 \sqrt[3]{U}$$

$$\sigma_b = \eta_3 \sqrt[3]{U}$$

$$U = p^2 E \frac{(\text{longer side})^2}{t^2}$$

If

$$\left|\sigma_c - {}_H\sigma_1\right| > \left|\tau_{cr}\right|$$

we are in the postbuckling stage.

There are many combinations of τ^* and p^* under which the web may buckle. The method for selecting the proper combination was previously explained. If the analyst is interested only in the final results, this combination is not important and the analysis can be continued without τ^*, p^*

τ_o / τ_{cr} leads to the determination of k

The compression stress is

$$\sigma_I = -\tau_o(1-k)\sin 2\alpha$$

The final tension stress, σ_{II}, is obtained as a result of the computer program or use of corresponding formulas. In order to use the computer program, the prestress load is to be used:

$$H_o = \sigma'_{II} A$$

where

$$\sigma'_{II} = \frac{2k\tau_o}{\sin 2\alpha} + \tau_o(1 - k)\sin 2\alpha$$

$$A = 1''xt$$

The total lateral load p_o shall be used for the loading p. Initial deflection is $\delta = o$. The output of the computer program is $H = \sigma_{II}/A$, and the final deflection is y. Figure 52 clarifies usage of this procedure.

CONCLUSIONS

The analysis of the simultaneous action of vertical and lateral loadings on partial-tension-field beams is presented in this section. For this analysis only straight beams were considered. Curved beams will be considered in Section IV.

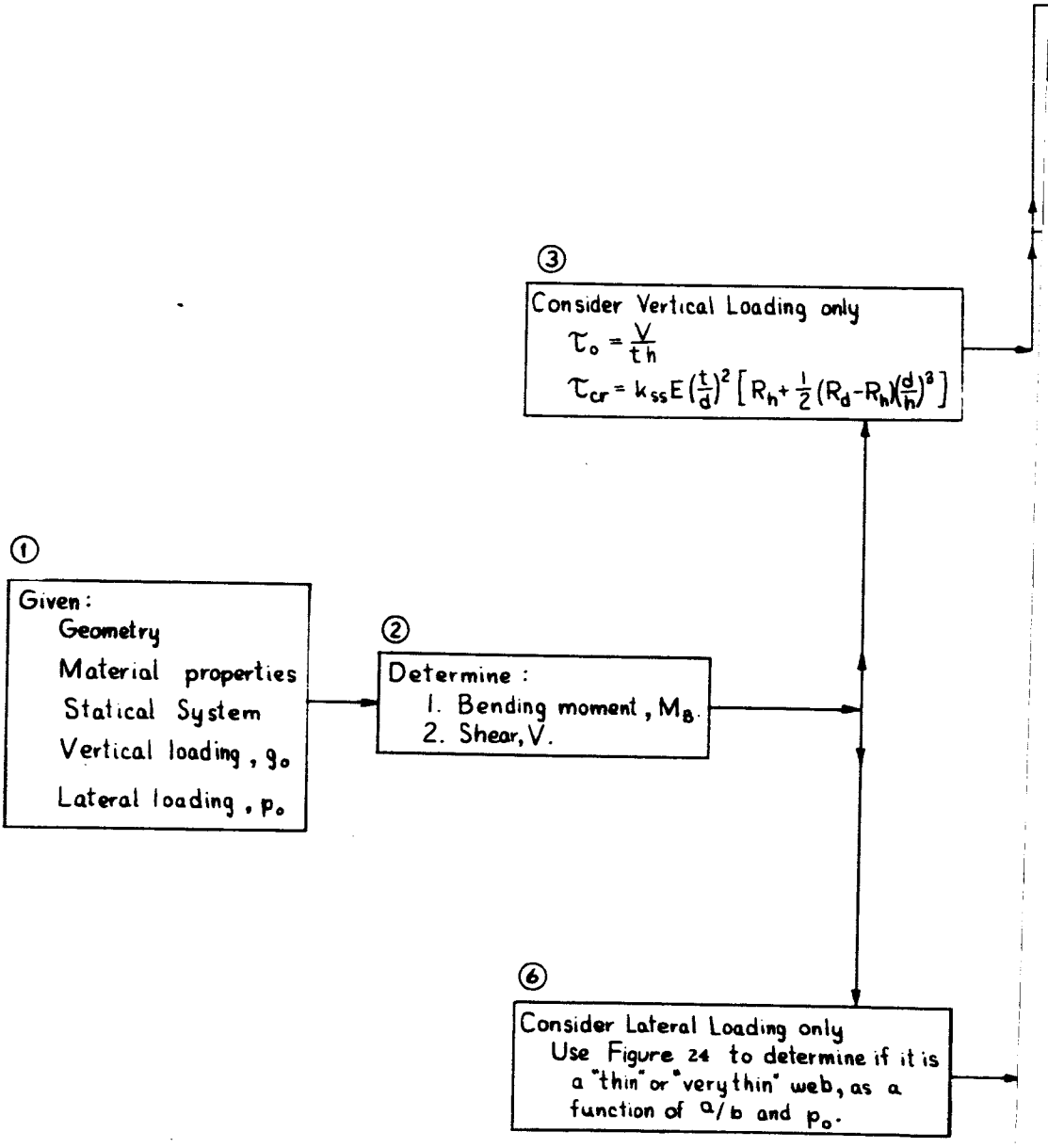
③
Consider Vertical Loading only
$\tau_o = \frac{V}{th}$
$\tau_{cr} = k_{ss} E \left(\frac{t}{d}\right)^2 \left[R_h + \frac{1}{2}(R_d - R_h)\left(\frac{d}{h}\right)^3 \right]$
①
Given:
Geometry
Material properties
Statical System
Vertical loading, g_o
Lateral loading, p_o
②
Determine:
1. Bending moment, M_B.
2. Shear, V.
⑥
Consider Lateral Loading only
Use Figure 24 to determine if it is a "thin" or "very thin" web, as a function of a/b and p_o.

97 ①

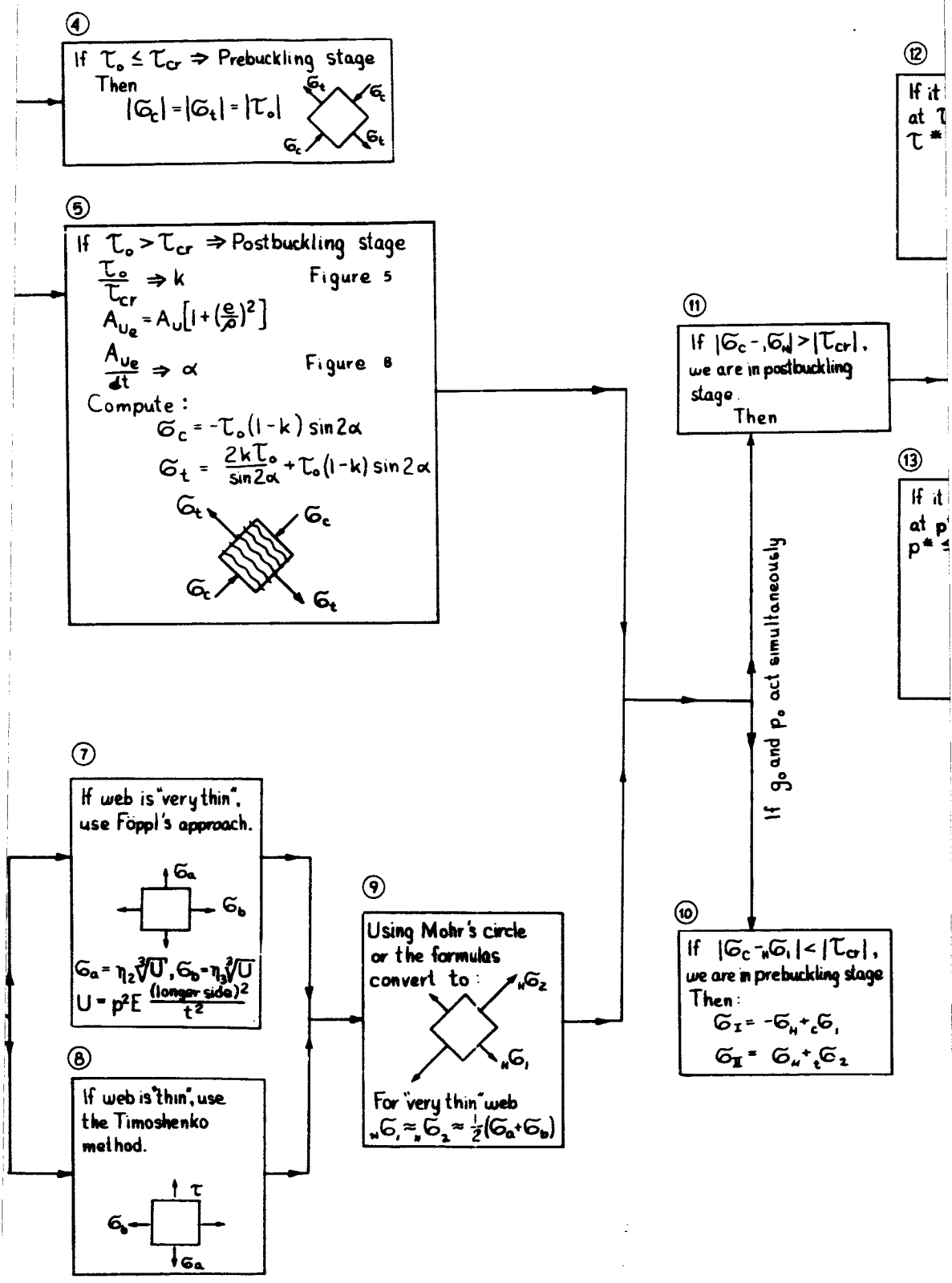
④
If $\tau_o \le \tau_{cr}$ ⇒ Prebuckling stage
Then
$|\sigma_c| = |\sigma_t| = |\tau_o|$
⑤
If $\tau_o > \tau_{cr}$ ⇒ Postbuckling stage
$\frac{\tau_o}{\tau_{cr}} \Rightarrow k$ Figure 5
$A_{U_e} = A_U\left[1+\left(\frac{e}{\rho}\right)^2\right]$
$\frac{A_{U_e}}{dt} \Rightarrow \alpha$ Figure 8
Compute:
$\sigma_c = -\tau_o(1-k)\sin 2\alpha$
$\sigma_t = \frac{2k\tau_o}{\sin 2\alpha} + \tau_o(1-k)\sin 2\alpha$
⑦
If web is "very thin", use Föppl's approach.
$\sigma_a = \eta_2\sqrt[3]{U}, \sigma_b = \eta_3\sqrt[3]{U}$
$U = p^2E\frac{(\text{longer side})^2}{t^2}$
⑧
If web is "thin", use the Timoshenko method.
⑨
Using Mohr's circle or the formulas convert to:
For "very thin" web
$_N\sigma_1 \approx {}_N\sigma_2 \approx \frac{1}{2}(\sigma_a+\sigma_b)$
⑪
If $|\sigma_c - {}_N\sigma_1| > |\tau_{cr}|$, we are in postbuckling stage.
Then
If g_o and p_o act simultaneously
⑩
If $|\sigma_c - {}_N\sigma_1| < |\tau_{cr}|$, we are in prebuckling stage
Then:
$\sigma_I = -\sigma_H + {}_c\sigma_1$
$\sigma_{II} = \sigma_H + {}_t\sigma_2$
⑫
If it
at τ
τ^*
⑬
If it
at p
p^*

Figure 51. Ge

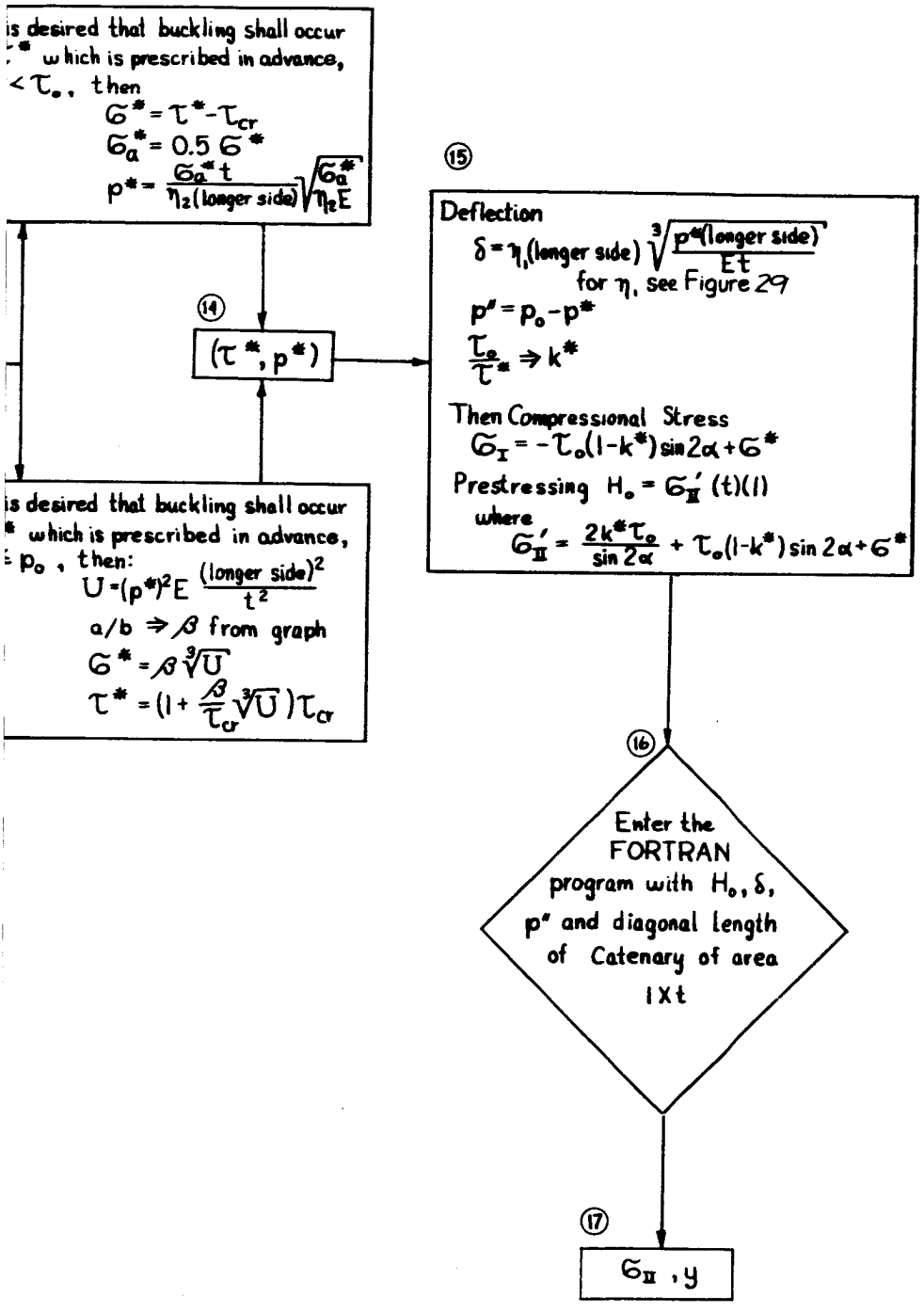
is desired that buckling shall occur
* which is prescribed in advance,
< τ_o , then
σ* = τ* - τ_cr
σ_a* = 0.5 σ*
p* = (σ_a* t / η_2(longer side)) √(σ_a* / η_2 E)
⑭
(τ*, p*)
is desired that buckling shall occur
* which is prescribed in advance,
= p_o , then:
U = (p*)² E (longer side)² / t²
a/b ⇒ β from graph
σ* = β ∛U
τ* = (1 + β/τ_cr ∛U) τ_cr
⑮
Deflection
δ = η_1(longer side) ∛(p*(longer side) / Et)
for η_1 see Figure 29
p'' = p_o - p*
τ_o/τ* ⇒ k*
Then Compressional Stress
σ_I = -τ_o(1-k*) sin 2α + σ*
Prestressing H_o = σ_II' (t)(1)
where
σ_II' = 2k*τ_o / sin 2α + τ_o(1-k*) sin 2α + σ*
⑯
Enter the FORTRAN program with H_o, δ, p'' and diagonal length of Catenary of area
1 X t
⑰
σ_II , y

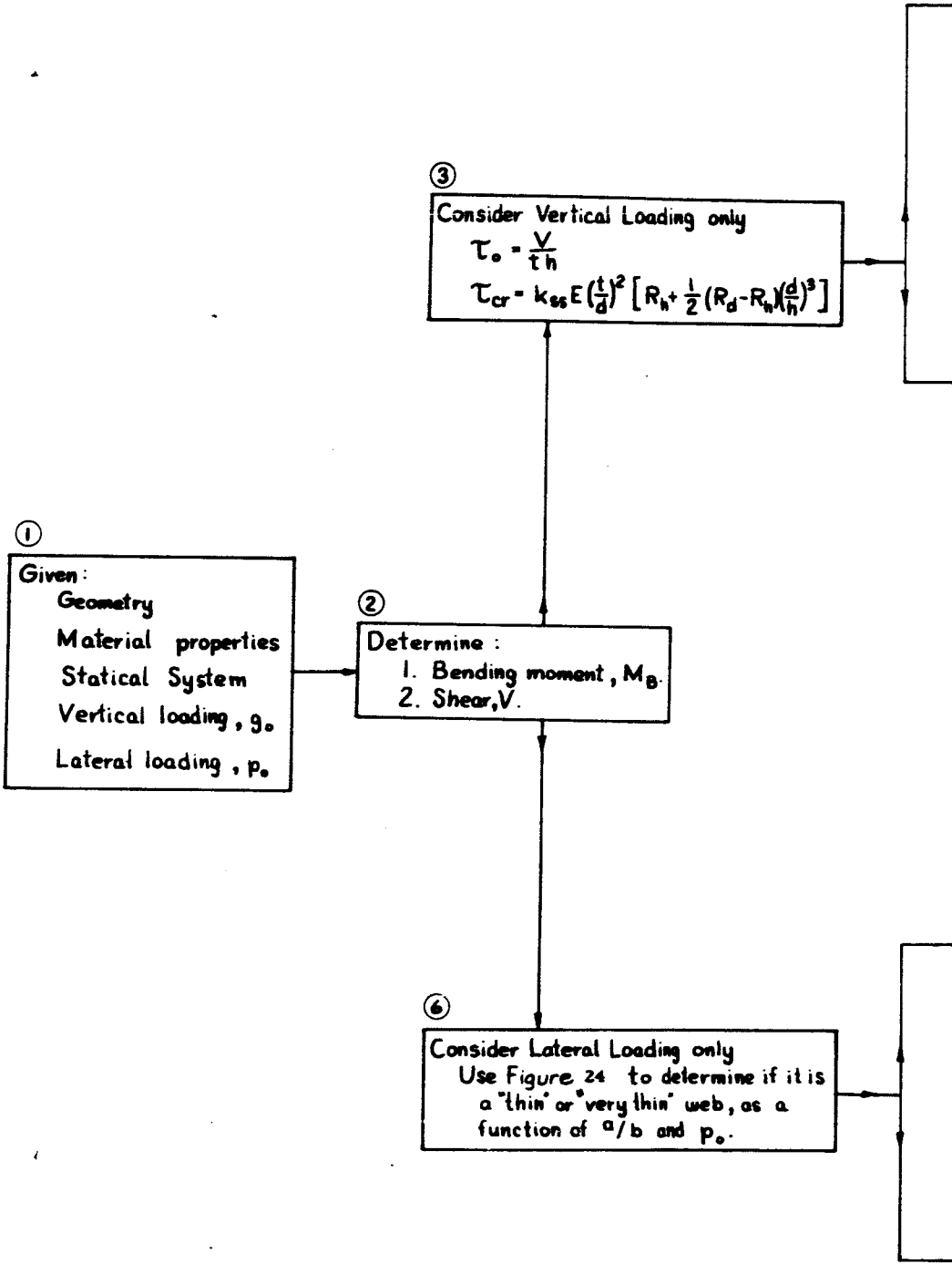
③
Consider Vertical Loading only
$\tau_o = \frac{V}{th}$
$\tau_{cr} = k_{ss} E \left(\frac{t}{d}\right)^2 \left[R_h + \frac{1}{2}(R_d - R_h)\left(\frac{d}{h}\right)^3\right]$
①
Given:
Geometry
Material properties
Statical System
Vertical loading, g_o
Lateral loading, p_o
②
Determine:
1. Bending moment, M_B.
2. Shear, V.
⑥
Consider Lateral Loading only
Use Figure 24 to determine if it is a "thin" or "very thin" web, as a function of a/b and p_o.

④

If $\tau_o \le \tau_{cr}$ ⇒ Prebuckling stage

Then

$$|\sigma_c| = |\sigma_t| = |\tau_o|$$

⑤

If $\tau_o > \tau_{cr}$ ⇒ Postbuckling stage

$\frac{\tau_o}{\tau_{cr}} \Rightarrow k$ Figure 5

$A_{U_e} = A_U\left[1+\left(\frac{e}{\rho}\right)^2\right]$

$\frac{A_{U_e}}{et} \Rightarrow \alpha$ Figure 8

Compute :

$$\sigma_c = -\tau_o(1-k)\sin 2\alpha$$

$$\sigma_t = \frac{2k\tau_o}{\sin 2\alpha} + \tau_o(1-k)\sin 2\alpha$$

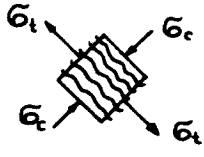

⑦

If web is "very thin", use Föppl's approach.

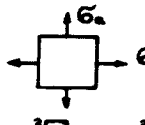

$\sigma_a = \eta_{12}\sqrt[3]{U}$, $\sigma_b = \eta_2\sqrt[3]{U}$

$U = p^2E\frac{(\text{longer side})^2}{t^2}$

⑧

If web is "thin", use the Timoshenko method.

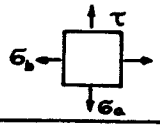

⑨

Using Mohr's circle or the formulas convert to :

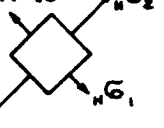

For "very thin" web

$\sigma_1 \approx \sigma_2 \approx \frac{1}{2}(\sigma_a + \sigma_b)$

⑪

IF

$|\sigma_c - \sigma_1| \le |\tau_{cr}|$ we

Then

$\sigma_I = -\sigma_c + \sigma_1$

$\sigma_{II} = \sigma_t + \sigma_2$

⑩

IF

$|\sigma_c - \sigma_1| \le |\tau_{cr}|$ w

st

$\frac{\tau_o}{\tau_{cr}} \Rightarrow k$

Then

$\sigma_I = -\tau_o(1-k)\sin 2\alpha$

$\sigma_{II}' = \frac{2k\tau_o}{\sin 2\alpha} + \tau_o(1-$

$H_o = \sigma_{II}'(t)(l)$

1002

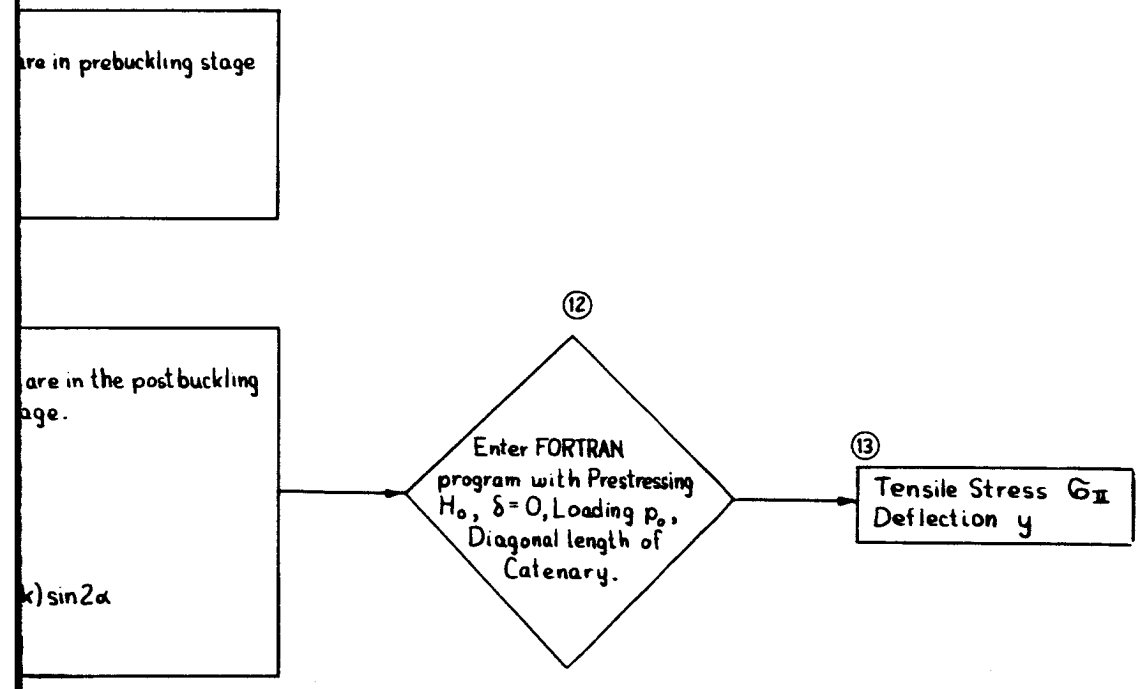

Figure 52. Recommended Procedure for Web Analysis

UPRIGHTS AND FLANGES

INTRODUCTION

The analysis and testing of partial-tension-field beams subjected to combined lateral and shear load has not previously been fully investigated. Kuhn, Peterson, and Levin (Reference 30) experimentally investigated shear loading. The test results were evaluated, and empirical relations were generated to analyze the partial-tension-field beam. The results are presented in Reference 30. A few theoretical considerations on the behavior of the web-upright flange under shear were investigated by various investigators. A significant analytical contribution was made by Denke (References 31 and 32) who used a strain energy approach to the tension-field beam subjected to shear loading.

Local phenomena associated with some of the phases were analytically considered by Denke. The effect of compressibility of the web that reduces the compressive strength in the upright is considered. The effects of diagonal-tension-field wrinkles on the bending of the uprights are also considered. In addition, the effects of cap bending between stiffeners and of flange and upright axial deformation were treated.

This section will consider the effect of the combined loading, i.e., lateral pressure and vertical loading on the partial-tension-field beam. Both stress analysis and a method for determining stability criteria for the upright are included in this section.

STRENGTH ANALYSIS OF UPRIGHTS

Consider the general case for which the web panels are rectangular. The tension-field beam (Figure 53) that is being considered here is subjected to both lateral pressure p and vertical load V at any stage of web behavior, but within the stability criteria of the upright. The stability criteria of the uprights will be discussed in the next section.

Double Uprights

Double uprights exist when uprights are located on both sides of the web. The upright can be analyzed as a beam column subjected to the various combinations of loading shown in Figures 53 through 58. The loading q(x) shown in Figures 54, 57, and 58 (xz plane) is that due to lateral pressure p. For design purposes, the trapezoidal distribution is represented by a

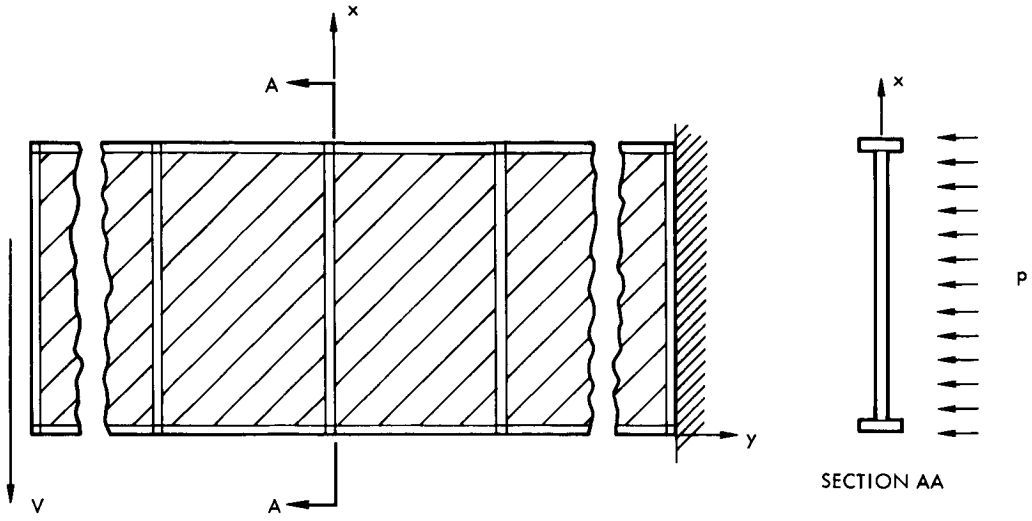

Figure 53. Tension-Field Beam Under Loading

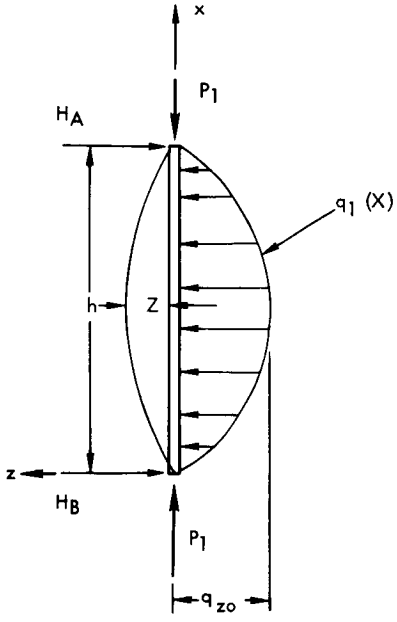

Figure 54. Upright Loading Due to Lateral Pressure (x-z Plane)

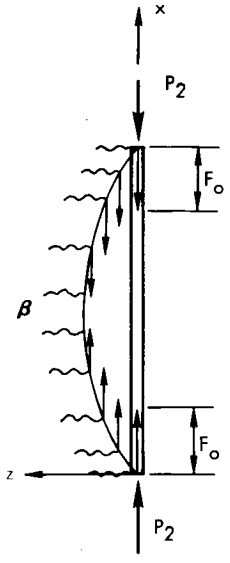

Figure 55. Upright Loading Due to Vertical Loading (x-z Plane)

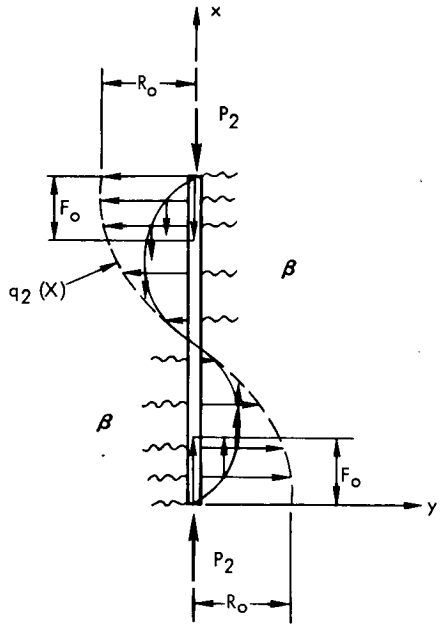

Figure 56. Upright Loading Due to Vertical Loading (x-y Plane)

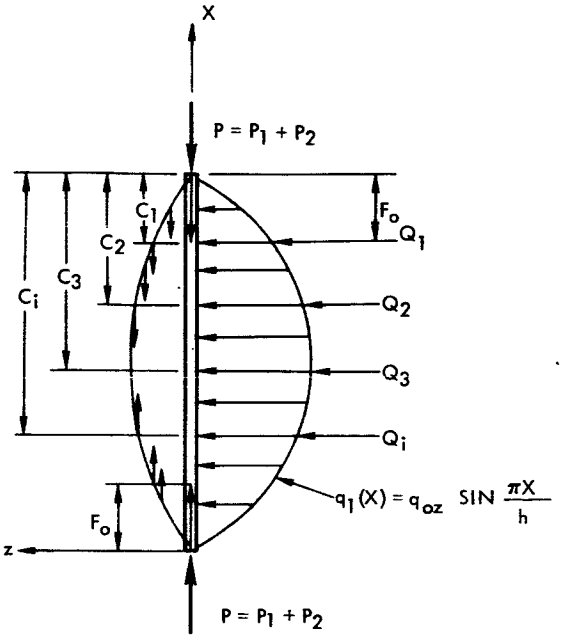

Figure 57. Combined Loading on Upright, xz Plane

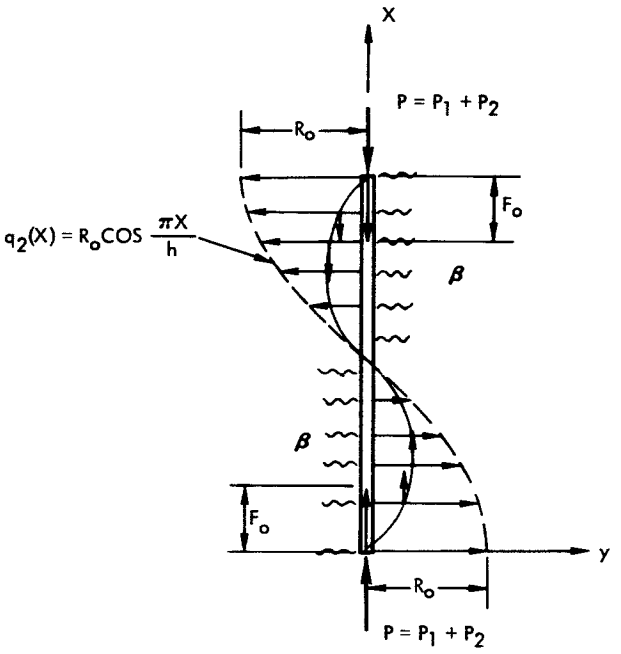

Figure 58. Combined Loading on Upright, xy Plane

sinusoidal loading with intensity q_{zo} acting on the upright in the direction of the applied lateral pressure load p. Thus, the distributed load can be represented by

$$q_1(x) = q_{zo} \sin \pi x/h$$

From simple geometry, the area of the trapezoid to the area of the sine curve is such that

$$q_{zo} = \frac{p\pi d\,(h - d/2)}{2h}$$

The distributed lateral forces (horizontal forces shown by Figure 58) represent the horizontal components of the net diagonal web forces acting on the upright. The intensity of this distributed force is R_o. For design purposes the distributed force can be represented by

$$q(x) = R_o \cos \frac{\pi x}{h} = (\sigma_t t_w \cos \alpha + \sigma_c t_w \sin \alpha) \cos \frac{\pi x}{h}$$

where σ_t and σ_c are tensile and compressive web stresses, t_w is the web thickness, α the diagonal fold angle (measured from flange), and force acts in the xy plane.

The concentrated lateral forces, Q_1, Q_2, Q_3, . . . , Q_i, represent the horizontal components of the diagonal web fold tension forces acting at the various locations, C_1, C_2, C_3, . . . , C_i, respectively, on the upright (see Figure 59). Thus, the forces, Q_1, Q_2, Q_3, . . . , Q_i, are considered as the components of the forces acting in the direction of the lateral pressure, i. e.,

$$Q_1 = T_1 \sin \phi_1 + T_1' \sin \phi_1'$$

$$Q_2 = T_2 \sin \phi_2 + T_2' \sin \phi_2'$$

. . . . . .

$$Q_i = T_i \sin \phi_i + T_i' \sin \phi_i'$$

where T_1, T_2, T_3, . . . , T_i and T_1', T_2', T_3', . . . , T_i' are the tensile forces in the web due to the shear force V and the lateral pressure p for the left and right side of the upright, respectively (Figure 59, diagram A). The values of T_1, T_2, . . . , T_i and T_1', T_2' . . . , T_i' and their corresponding slopes ϕ_1, ϕ_2, . . . , ϕ_i and ϕ_1', ϕ_2', . . . , ϕ_i', respectively, can be determined from the catenary analysis. However, these angles are relatively small such that $\sin \phi_i \approx \phi_i$ and $\sin \phi_i' \approx \phi_i'$. But for flat beams these are usually extremely small and generally neglected. Hence, Q_1, Q_2, . . . , Q_i are all zero.

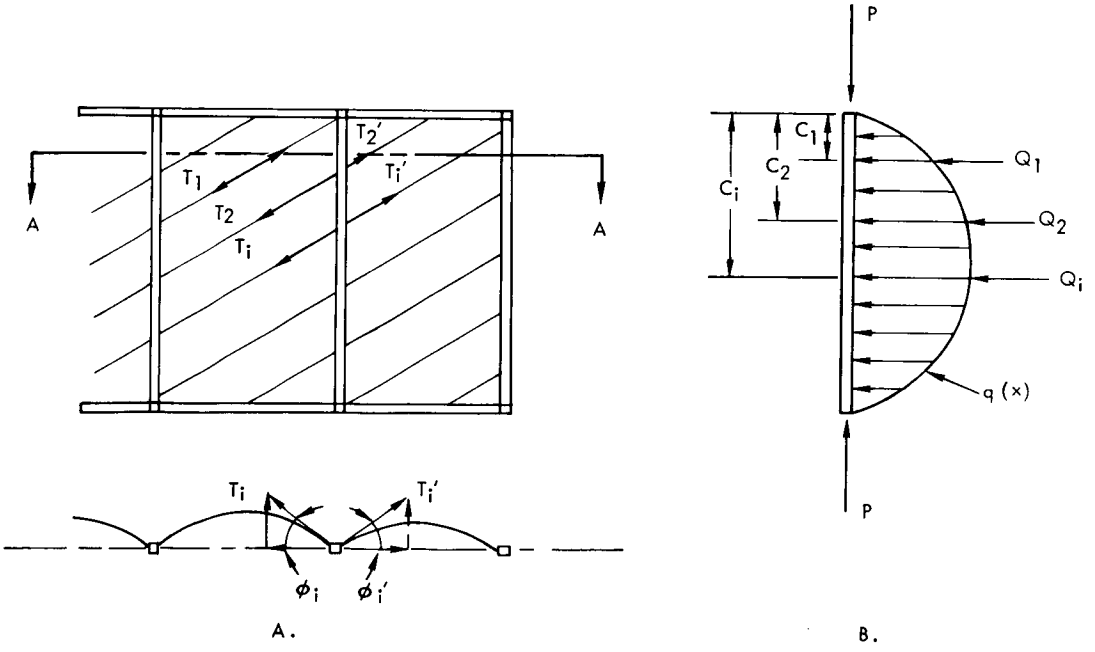

Figure 59. Lateral and Compressive Loads Acting on the Uprights

The vertical load at the ends of the upright is that due to P_1 and P_2 where P is defined as follows:

P_1 is the upright compression load due to tension in the web during lateral loading.

P_2 is the upright compression load due to vertical loading after the web buckles.

The distributed compressive force acting along the length of the upright is that due to the vertical component of the net forces acting on the upright due to the diagonal web-fold tensions. For design purposes, the distributed axial forces are taken to be distributed according to Figure 60, diagram B, i.e., the intensity of the force is F_o and is compressive (directed towards the center of upright). The force decreases linearly to zero at the center of the upright when the spacing of the uprights are uniform and such that $d \geq h$ and with complete diagonal folds. In almost all previous works in the literature, the distributed forces are assumed to be added and positioned as a concentrated force at the ends of the upright. Hence, for $d < h$ spacing of uprights and very incompletely developed diagonals, it is suggested that the distributed forces be added and taken at the ends to be conservative.

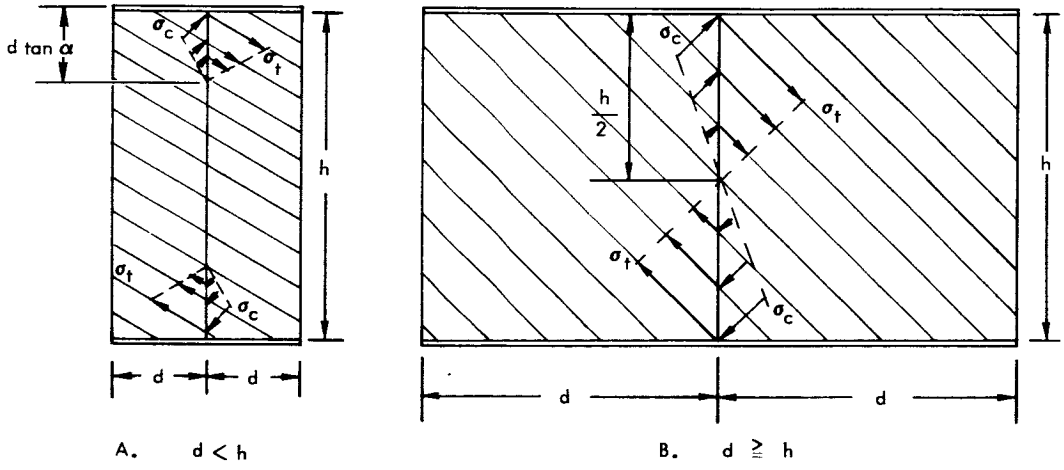

Figure 60. Net Diagonal Forces for d<h and d≥h

The consideration that the web adds restraint to the deflection behavior of the upright can be considered as an elastic foundation effect. The elastic foundation modulus β has the units of force per square length. The reaction to the upright at any cross section of the upright is proportional to the deflection at that section.

The upright boundary is assumed to be simple support since experimental evidence for vertically loaded uprights more closely approach this boundary rather than fixed or partially fixed. Figure 61 shows (Reference 33) comparison between simple supports, fixed supports, experimental results.

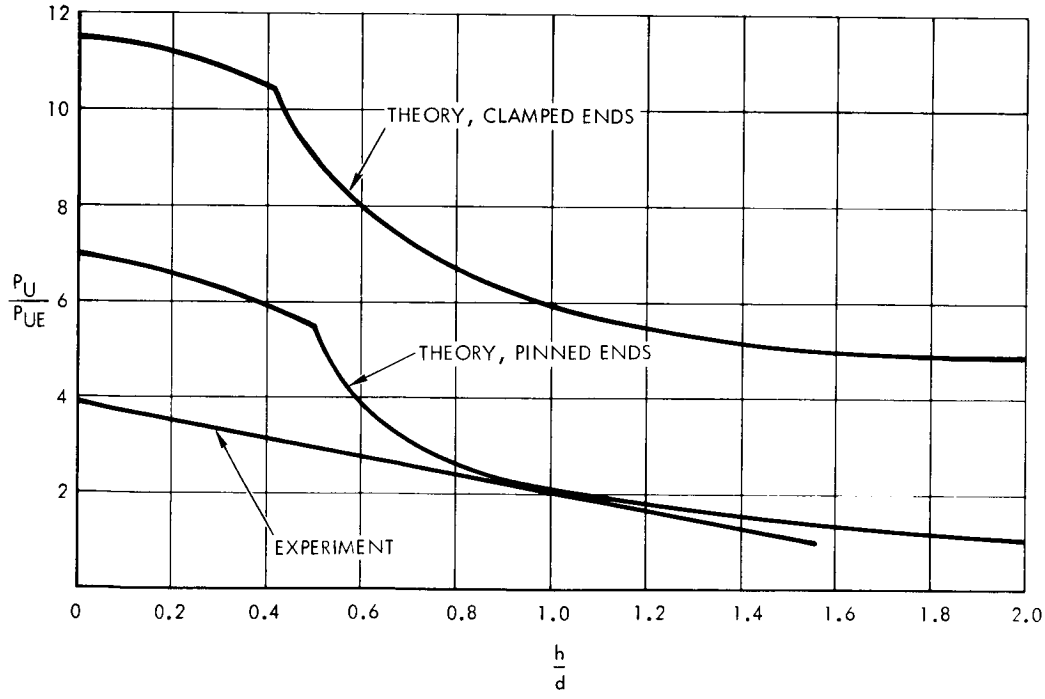

Figure 61. Comparison Between Theory and Experiment for Buckling of Upright

The deflection (Figure 62) at any section along the upright in the direction of the lateral load (z-direction) is

$$z = \frac{2h}{P_{cr}\pi^2}\left[\frac{\frac{q_{oz}h}{2} + \left(Q_1 \sin\frac{\pi C_1}{h} + Q_2 \sin\frac{\pi C_2}{h} + \ldots + Q_i \sin\frac{\pi C_i}{h}\right)}{1 - \frac{P}{P_{cr}} - \frac{F_o h}{4P_{cr}}\left(\frac{2}{\pi 2}\right)\left(\frac{\pi^2}{3} - 1\right)}\right] \sin\frac{\pi x}{h} \qquad (3\text{-}15)$$

where

$$P_{cr} = \frac{\pi^2 EI}{L_e^2}$$

h = upright free length, in.

E = modulus of elasticity of upright material, psi

I = cross sectional moment of inertia of upright, in^4.

and L_e is the effective length of the upright determined empirically as in Reference 30. See Appendix B.

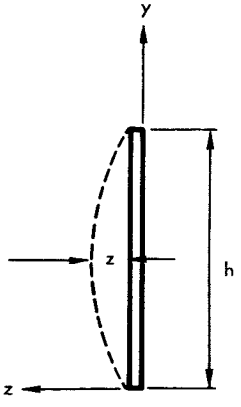

Figure 62. Lateral Deflection of Upright

$$L_e = \frac{h}{\sqrt{1 + k^2(3 - 2\frac{d}{h})}} \qquad (3\text{-}16)$$

for $d < 1.5\,h$ and for $d > 1.5\,h$, $L_e = h$ where d is the upright spacing in inches and k is the empirical constant defined by

$$k = \tanh\left(0.5 \log \frac{\tau_o}{\tau_{cr}}\right)$$

Whenever

$$P + \frac{F_o h}{4}\left(\frac{2}{\pi^2}\right)\left(\frac{\pi^2}{3} - 1\right)$$

is less than P_{cr} there is a finite deflection. The deflection can readily be computed for any P/P_{cr} and $F_o h/4$ by using Figure 63. The curves in Figure 63 were determined by defining the amplification factor, A_{sym} as follows:

for d>h:

$$\text{Amplification factor} = A_{sym} = \frac{1}{1 - \frac{P}{P_{cr}} - \frac{F_o h}{4P_{cr}}\left(\frac{2}{\pi^2}\right)\left(\frac{\pi^2}{3} - 1\right)} \qquad (3\text{-}17)$$

for d< h

$$A_{sym} = \frac{1}{1 - \frac{P}{P_{cr}}}$$

where P accounts for F_o at the ends of the upright to assure a conservative design.

The deflection of the upright can now be simply expressed as

$$z = \frac{2hA_{sym}}{P_{cr}\pi^2}\left[\frac{q_o z h}{2} + \sum_{i=1}^{N} Q_i \sin\frac{\pi C_i}{h}\right]\sin\frac{\pi x}{h} \qquad (3\text{-}18)$$

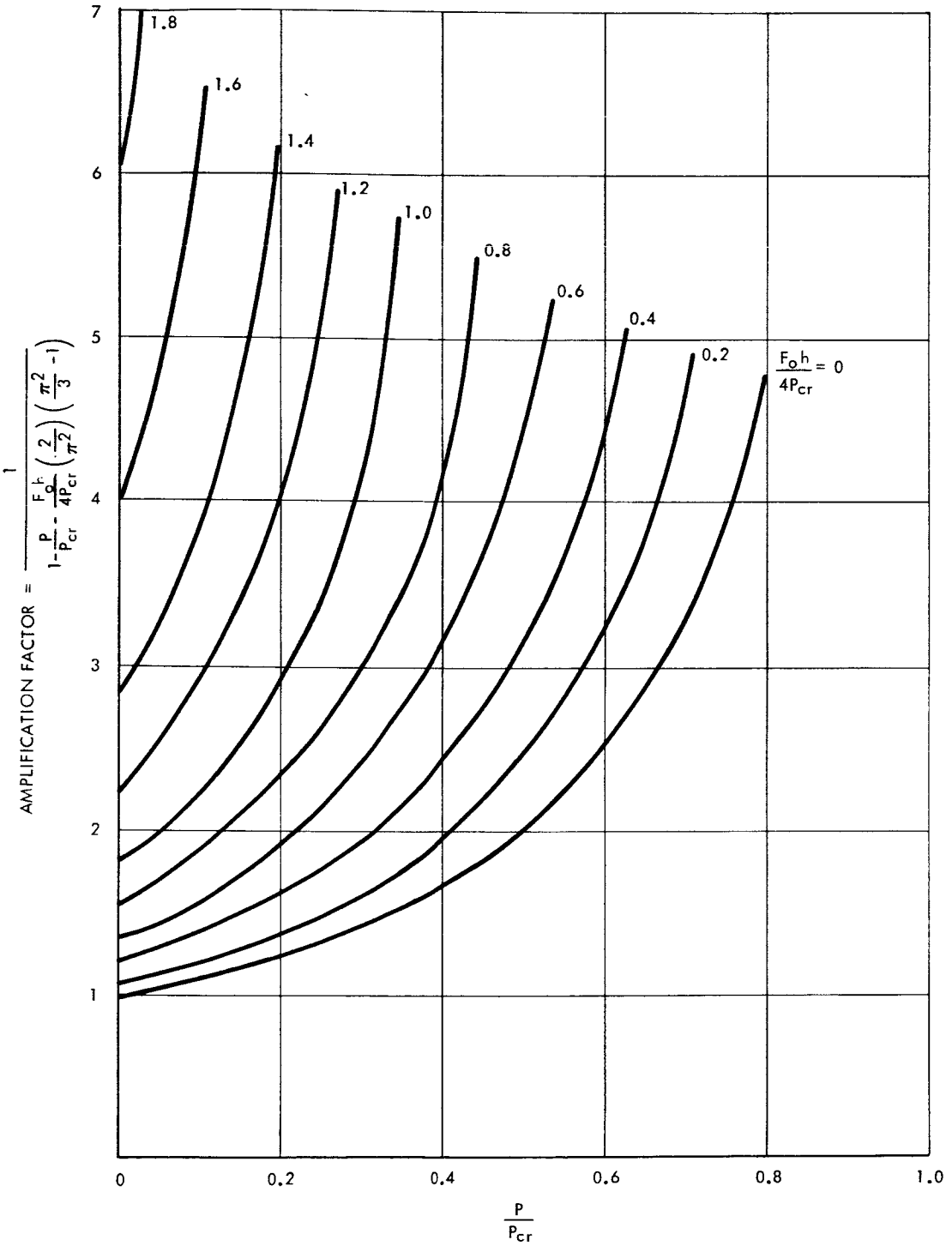

Figure 63. Amplification Factor for Symmetrical Deflection

The corresponding slope and bending stress at any section of the upright can be determined from

$$\theta = \frac{2A_{sym}}{P_{cr}\pi^2}\left[\frac{q_{oz}h}{2} + \sum_{i=1}^{N} Q_i \sin\frac{\pi C_i}{h}\right]\cos\frac{\pi x}{h} \qquad (3\text{-}19)$$

and

$$\sigma_{bend_y} = \frac{2EI_y A_{sym}}{P_{cr} h Z_y}\left[\frac{q_{oz}h}{2} + \sum_{i=1}^{N} Q_i \sin\frac{\pi C_i}{h}\right]\sin\frac{\pi x}{h} \qquad (3\text{-}20)$$

where

$$Z_y = \frac{I_y}{c}$$

is the sectonal modulus. The maximum bending stress occurs at the mid-height of the upright, i.e., $x = h/2$ such that $\sin \pi h/2h = 1$ in the a above equation.

To the bending stress σ_{bend} we add compressive stresses due to σ_c and σ_t (compressive and tensile stresses in the web) of

$$\sigma_{comp} = \frac{P}{A} \qquad (3\text{-}21)$$

where

$$A = A_U + 0.5\, t_w d\,(1\text{-}k)$$

for $d < h$ (Figure 60, diagram A)

$$P = \frac{\sigma_t t_w d \sin\alpha}{2} + \frac{\sigma_c t_w d\cos\alpha}{2} + \frac{\sigma_t t_w d\tan\alpha\,\sin\alpha}{2} + \frac{\sigma_c t_w d\tan\alpha\cos\alpha}{2}$$

or

$$P = \frac{\sigma_t t_w d \sin\alpha\,(1+\tan\alpha)}{2} + \frac{\sigma_c t_w d\cos\alpha(1+\tan\alpha)}{2}$$

for d>h (Figure 60, diagram B)

$$P = \frac{\sigma_t t_w d \sin\alpha}{2} + \frac{\sigma_c t_w d \cos\alpha}{2} + \frac{\sigma_t t_w \frac{h}{2} \sin\alpha}{2} + \frac{\sigma_c t_w \frac{h}{2} \cos\alpha}{2}$$

or

$$P = \frac{\sigma_t t_w \sin\alpha}{2}(d + \frac{h}{2}) + \frac{\sigma_c t_w \cos\alpha}{2}(d + \frac{h}{2})$$

The total stress in the upright due to out-of-plane deflection becomes

$$\sigma_y = \sigma_{bend_y} + \sigma_{comp} \qquad (3\text{-}22)$$

Whenever σ_y is greater than the material allowable properties, then material failure will exist in the upright such that large lateral deformation will exist. In addition to σ_y, there exists some tendency to have a bending stress σ_z. The in-plane deflection y caused by the lateral pressure loading p and vertical loading V (Figure 64) can be determined from

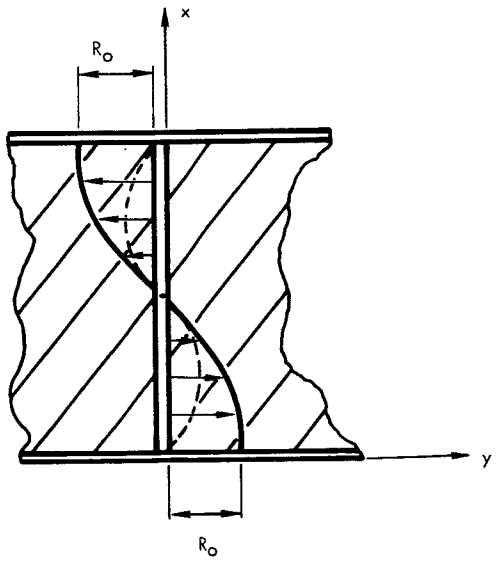

Figure 64. Net Horizontal Component of Diagonal Tension Forces

where

$$y = \frac{h A_{Anti}}{8\pi^2 P_{cr}} \left[\frac{2 R_o h}{3\pi}\right] \sin \frac{2\pi x}{h} \qquad (3\text{-}23)$$

for $d < h$

$$A_{Anti} = \frac{1}{1 - \frac{P}{4 P_{cr}}}$$

for $d < h$

$$A_{Anti} = \frac{1}{1 - \frac{P}{4 P_{cr}} - \frac{F_o h}{4 P_{cr}} \left(\frac{1}{8\pi^2}\right)\left(\frac{4\pi^2}{3} - 1\right)}$$

The bending stress in the upright is

$$\sigma_{bend_z} = \frac{EI_z A_{Anti}}{2h P_{cr} Z_z} \left[\frac{2}{3\pi} R_o h\right] \sin \frac{2\pi x}{h} \qquad (3\text{-}24)$$

and to this the compressive stress due to σ_c and σ_t is added, i.e., Equation 3-21.

The total upright stress due to in-plane deflection of upright is

$$\sigma_z = \sigma_{bend} + \sigma_{comp} \qquad (3\text{-}25)$$

The stress can be readily computed with the aid of Figure 65.

Single Uprights

Single uprights exist when all of the uprights are positioned only on one side of the web. For this case an eccentric load on the upright due to compressive force P and F_o is obtained. The deflection caused by the eccentricity can be accounted for by making use of the theory of superposition. Thus, it is known that the deflection due to eccentric loading is

$$M = \left(P + \frac{F_o h}{2}\right) e$$

where e is the eccentricity, in.

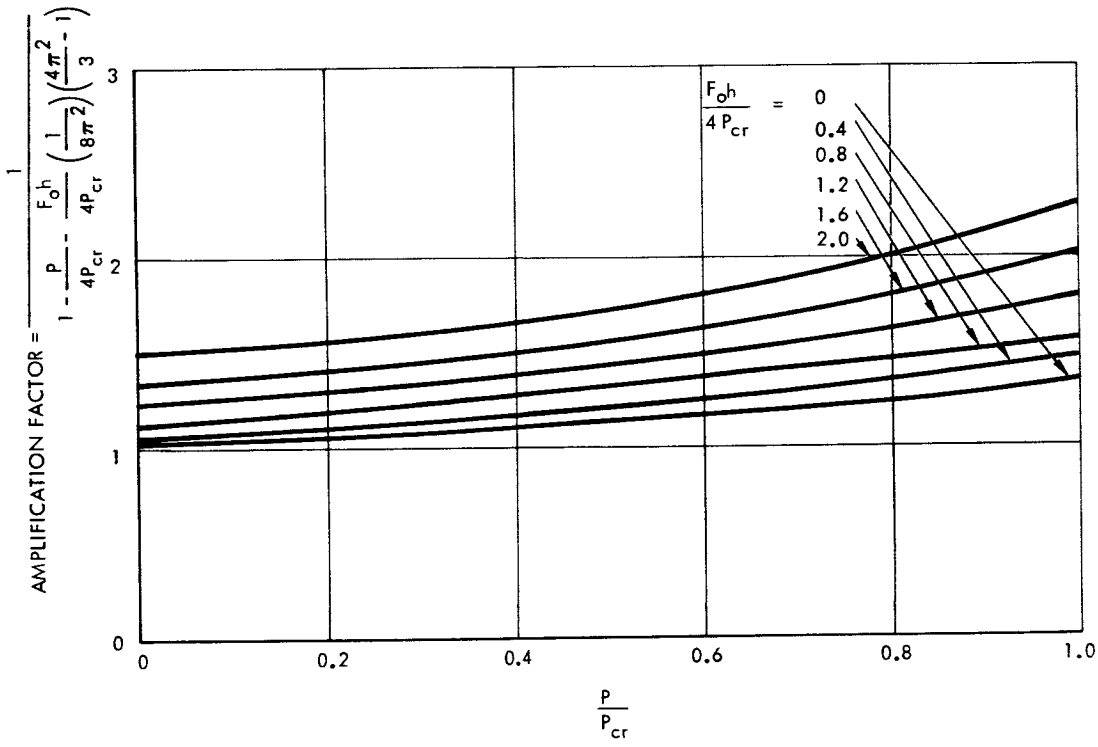

Figure 65. Amplification Factor for Antisymmetrical Deflection

For a simple beam-column (Reference 34) the deflection is

$$z = \frac{4 M h^2}{\pi^3 EI} \sum_{n=1,3,5}^{\infty} \frac{1}{n^2(n^2 - \alpha)} \sin \frac{n\pi x}{h} \qquad (3\text{-}26)$$

where

$$\alpha = \frac{P}{P_{cr}}$$

Consider now the case for which web restraint exists. Equation 3-26 is modified and web restraint is accounted for and is added to Equation 3-18 by applying the principle of superposition. Thus, the deflection for single upright case becomes

$$z = \frac{2h A_{sym}}{P_{cr} \pi^2} \left[\frac{q_{oz} h}{2} + \frac{2M\pi}{h} + \sum_{i=1}^{N} Q_i \sin \frac{\pi C_i}{h} \right] \sin \frac{\pi x}{h} \qquad (3\text{-}27)$$

The maximum stress occurs at midheight, $x = h/2$ or $\sin \pi x/h = 1$. The slope and stresses for single upright becomes, respectively

$$\theta = \frac{2 A_{sym}}{P_{cr} \pi} \left[\frac{q_{oz} h}{2} + \frac{2 M\pi}{h} + \sum_{i=1}^{N} Q_i \sin \frac{\pi C_i}{h} \right] \cos \frac{\pi x}{h} \qquad (3\text{-}28)$$

and

$$\sigma_{bend} = \frac{2EI_y A_{sym}}{Z_s P_{cr} h} \left[\frac{q_{oz} h}{2} + \frac{2M\pi}{h} + \sum_{i=1}^{N} Q_i \sin \frac{\pi C_i}{h} \right] \sin \frac{\pi x}{h} \qquad (3\text{-}29)$$

where Z_s is the section modulus for single uprights.

In addition the bending stress, there exists a compression stress due to compressive loads P and F_o and the local stresses due to local effects. Thus, the combined stress about the y axis is

$$\sigma_{y_{single}} = \sigma_{bend_{single}} + \sigma_{comp_{single}} + \sigma_{local_{single}} \qquad (3\text{-}30)$$

where

$$\sigma_{comp_{single}} \quad \text{and} \quad \sigma_{local_{single}}$$

are given by Equations 3-21 and 3-23 and A(area) in the equations to be used is for single upright area. Equation 3-30 is for symmetrical bending about y axis. For antisymmetric bending existing due to diagonal tension being formed, the stress is given by Equation 3-25 with I_z and areas taken for single uprights.

Local Stresses Due to Influence of Diagonal Web Folds On the Bending Stresses of Uprights

The influence of the diagonal web folds on the buckling stress of upright (Figure 66) can be studied by considering that the diagonal tension folds produces local bending due to the distributed shear stress induced into the upright by the web system. The distributed load can be considered

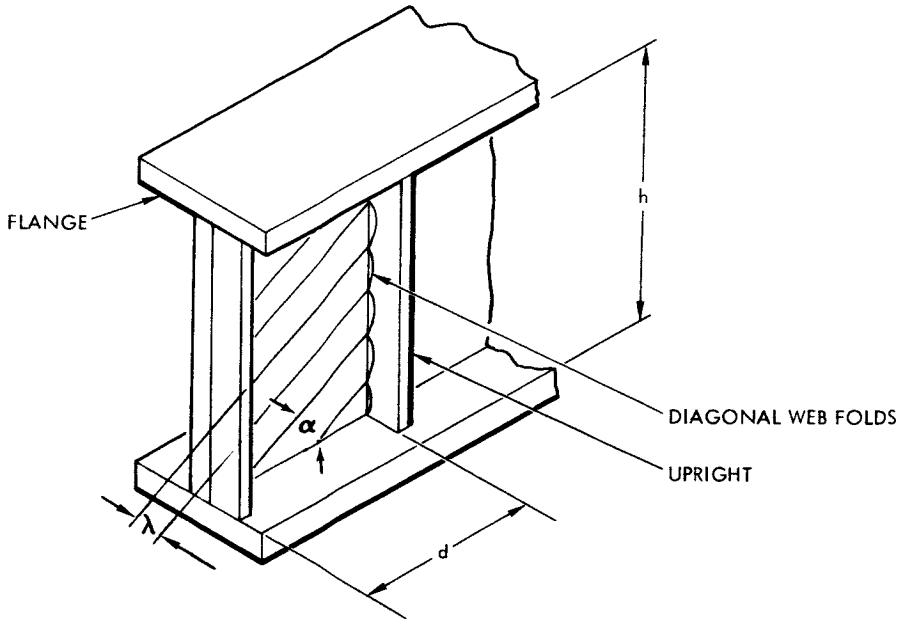

Figure 66. Buckled Web

(for design purposes) as a sinusoidal distribution since the web buckled folds resemble a sinusoidal distribution. By considering only one-half wave lengths λ_f as the length and the upright as a beam-column subjected to sinusoidal loading (Reference 31),

$$M_m = \frac{L^2 Q_{xm}}{\pi^2 - \frac{L^2}{j^2}} + \frac{M_o}{\cos \frac{L}{2j}} \qquad (3\text{-}31)$$

where

L = length

M_o = bending moment applied at ends (due to eccentric load)

I = moment of inertia of upright

P = upright load

$$j = \sqrt{\frac{EI}{P}}$$

Q_{xm} = maximum load per inch of sinusoidal distribution

The bending moment causes a bending stress of

$$\sigma_{vb} = \frac{\frac{t_w L^2 Q_{xm}/t_w}{ZE}}{\pi^2 - \left(\frac{L}{\rho_s}\right)^2 \frac{\sigma_v}{E}} + \frac{\frac{A_v z \sigma_v}{ZE}}{\cos \frac{1}{2}\sqrt{\left(\frac{L}{\rho_s}\right)^2 \left(\frac{\sigma_v}{E}\right)}} \qquad (3\text{-}32)$$

where

σ_{vb} = stress due to bending moment

t_w = web thickness

Z = section modulus

ρ_s = radius of gyration = $\sqrt{I/A}$

$M_o = \sigma_v A_v z$

$$\frac{L}{j} = \sqrt{\left(\frac{L}{\rho_s}\right)^2 \left(\frac{\sigma_v}{E}\right)}$$

A = cross-sectional area of upright

z = eccentricity of the axis of the upright with respect to middle plane of the web.

$$L = h \sqrt{\left(\frac{d}{h}\right)\left(\frac{1}{\zeta}\right)}$$

$$\zeta = \frac{A}{\lambda^2} \cos^2 \alpha$$

λ = distance between web fold crest

α = angle of diagonal folds relative to flange

When the load is acting through the center-line, i.e., symmetric stiffeners, $z = o$ and

$$\sigma_{vb} = \frac{\frac{Et_w L^2}{z} \frac{Q_{xm/tw}}{E}}{\pi^2 - \left(\frac{L}{\rho_s}\right)^2 \left(\frac{\sigma_v}{E}\right)} \qquad (3\text{-}33)$$

STABILITY CONSIDERATION FOR UPRIGHTS

The stability criterion for the upright can be categorized into four classes: upright buckling, including effective sheet behavior; upright bowing, including effective sheet behavior; torsional stability; and local buckling phenomena. To ensure that stability conditions are satisfied, all of the various buckling criteria should be investigated.

Upright Buckling Including Effective Web Behavior

Upright buckling takes place as a "snap" or bifurcation phenomenon when the axial compression loads are equal or greater than P_{cr}, i.e.

$$P + \frac{F_o h}{4}\left(\frac{2}{\pi^2}\right)\left(\frac{\pi^2}{3} - 1\right) \geq P_{cr} \qquad (3\text{-}34)$$

where

$$P_{cr} = \frac{\pi^2 EI}{L_e^2}$$

Equation 3-34 is for the symmetric buckle shape. For antisymmetric buckle shape, the buckling criterion is

$$\frac{P}{4} + \frac{F_o h}{4}\left(\frac{1}{8\pi^2}\right)\left(\frac{4\pi^2}{3} - 1\right) \geq P_{cr} \qquad (3\text{-}35)$$

Upright Bowing Including Effective Web Behavior

When upright bowing exists due to combinations of lateral and vertical loadings, then the stress level due to bending and compression should not exceed the σ_{design} level. Generally σ_{design} is the 0.2% yield point of the upright material with some additional safety factor. The stress σ criteria then is expressed as

$$\sigma < \sigma_{design}$$

where

$$\sigma = \sigma_{bending} + \sigma_{comp} + \sigma_{local}$$

where $\sigma_{bending}$, σ_{comp}, and σ_{local} are given by Equations 3-20, 3-21, and 3-32 respectively, for symmetrical bowing shape. For antisymmetrical bowing shape $\sigma_{bending}$, σ_{comp} and σ_{local} are given by Equations 3-21, 3-24 and 3-32 respectively. Thus, for bowing in two degrees of freedom, bending about y axis and z axis of the upright must be checked. Furthermore, the stability type of problem existing here is that due to excessive deflection without additional load once the stress level in the upright approaches the yield point of the upright material.

Torsional Stability

For partial-tension-field beams, the web adds restraint to the twisting of uprights. The in-plane web restraint is the largest restraint that the web gives to the uprights. Hence, the most typical rotation of uprights is that in which the rotation takes place in the plane of the web. The differential equation describing the behavior of columns attached to a sheet were developed by Goodier and the results are presented in Reference 9).

By making use of the bending moments in the upright as

$$M_y = EI_y \frac{d^2w}{dx^2} + EI_{yz} \frac{d^2v}{dx^2} \tag{3-36}$$

$$M_z = EI_z \frac{d^2v}{dx^2} + EI_{yz} \frac{d^2w}{dx^2} \tag{3-37}$$

the differential equations become (Reference 9)

$$EI_y \frac{d^4w}{dx^4} + P\frac{d^2w}{dx^2} - EI_{yz}(z_o - h_z)\frac{d^4\phi}{dx^4} - Py_o \frac{d^2\phi}{dx^2} = 0 \tag{3-38}$$

and

$$\left[C_1 + EI_z (z_o - h_z)^2\right]\frac{d^4\phi}{dx^4} - \left(C - \frac{I_o}{A} P + P z_o^2 - Ph_z^2\right)\frac{d^2\phi}{dx^2}$$

$$- EI_{yz} (z_o - h_z)\frac{d^4w}{dx^4} - Py_o \frac{d^2w}{dx^2} = 0 \tag{3-39}$$

where $C = GJ$ the torsional rigidity and $C_1 = EC_w$ the warping rigidity. The other dimensions are defined in Figure 67.

For partial-tension-field beams, the uprights can be considered as simple supports, since test results show that the simple support system

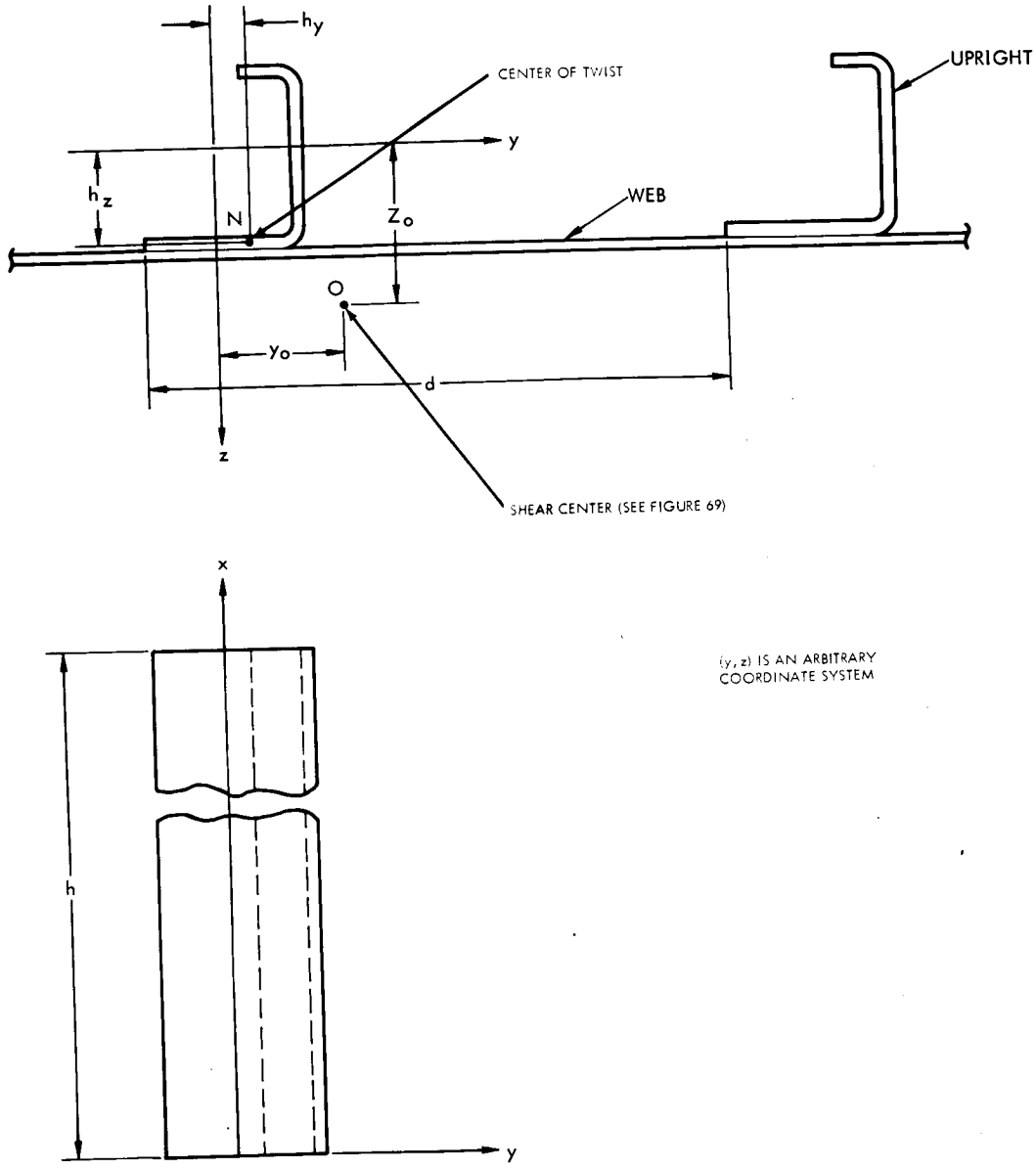

Figure 67. Torsional Stability

more closely approach test results than fixed ends. Thus, the solution takes the form

$$w = A_2 \sin \frac{\pi x}{h} \tag{3-40}$$

$$\phi = A_3 \sin \frac{\pi x}{h} \tag{3-41}$$

since these functions satisfy the boundary conditions for simple support. Upon substituting Equations 3-40 and 3-41 into the differential equations

$$\left(EI_y \frac{\pi^2}{h^2} - P\right) A_2 - \left[EI_{yz} \left(z_o - h_z\right)\frac{\pi^2}{h^2} - Py_o\right] A_3 = 0 \tag{3-42}$$

$$\left[-EI_{yz} \left(z_o - h_z\right)\frac{\pi^2}{h^2} + Py_o\right] A_2$$

$$+ \left[C_1 \frac{\pi^2}{h^2} + EI_z \left(z_o - h_z\right)^2 \frac{\pi^2}{h^2} + C - \frac{I_o}{A} P + Pz_o^2 - Ph_z^2\right] A_3 = 0$$

For nontrivial solution, the coefficients of A_2 and A_3 are not equal to zero and the determinant is made equal to zero to determine the critical buckling load.

Many of the upright cross sections in partial-tension-field beams are generally symmetrical about some axis. Consider, for example, the I, channel and T sections for uprights. For symmetry we have $I_{yz} = 0$ and $y_o = 0$ (see Figure 68).

The critical loads become

$$\left(EI_y \frac{\pi^2}{h^2} - P\right) A_2 = 0 \tag{3-43}$$

$$\left[C_1 \frac{\pi^2}{h^2} + EI_z \left(z_o - h_z\right)^2 \frac{\pi^2}{h^2} + C - \frac{I_o P}{A} + P z_o^2 - Ph_z^2\right] A_3 = 0 \tag{3-44}$$

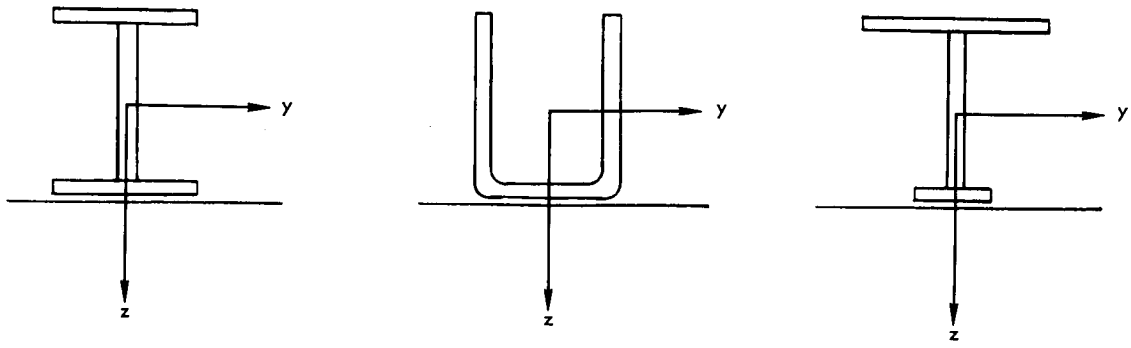

Figure 68. Symmetrical Cross-Sectional Uprights

Equation 3-43 gives the Euler-type buckling in the plane of symmetry and the value of I_y, including some effective web sheet, gives Equation 3-43 as

$$P_{cr} = \frac{\pi^2 E I_y}{L_e^2} \tag{3-45}$$

where

$$L_e = \frac{h}{\sqrt{1 + k^2\left(3 - 2\frac{d}{h}\right)}} \tag{3-46}$$

for $d<1.5h$ and for $d>1.5h$, $L_e = h$ Equation 3-44 gives the torsional buckling criteria for which the axis of rotation lies in the plane of the web sheet as (Reference 9).

$$P_{cr} = \frac{C_1\left(\frac{\pi^2}{h^2}\right) + EI_z\left(z_o - h_z\right)^2 \frac{\pi^2}{h^2} + C}{\frac{I_o}{A} - z_o^2 + h_z^2} \qquad (3\text{-}47)$$

The section properties C_w and J needed to determine the warping rigidity and torsional rigidity as shown in Figure 69 (from Reference 9).

Local Buckling Phenomena

Whenever the outstanding leg of an upright is relatively thin (same order as the web), local buckling generally takes place. To ensure that local buckling does not take place, the empirical crippling criteria (Reference 1) can be used.

$$\sigma_o = CK^{2/3}\left(\frac{t_u}{t_w}\right)^{1/3}, \text{ ksi} \qquad (3\text{-}48)$$

where

C = 21 for 2024-T3 double uprights

C = 26 for 7075-T6 double uprights

C = 26 for 2024-T3 single uprights

C = 32.5 for 7075-T6 single uprights

For closed uprights like the hat section, it is suggested that Equations 1-3 or 1-4 of Section 1 be used. Use Equation 1-3 when investigating for $A_U/t_w d \leq 0.2$ while Equation 1-4 should be investigated for $A_U/t_w d \geq 0.2$.

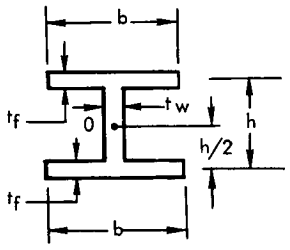

$$J = \frac{2bt_f^3 + ht_w^3}{3}$$

$$C_W = \frac{t_f h^2 b^3}{24}$$

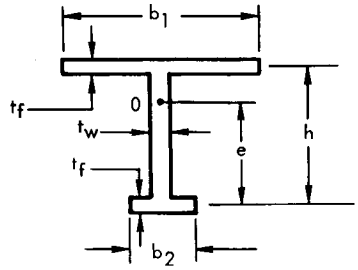

$$e = h\,\frac{b_1^3}{b_1^3 + b_2^3}$$

$$J = \frac{(b_1 + b_2)\,t_f^3 + ht_w^3}{3}$$

$$C_W = \frac{t_f h^2}{12} \cdot \frac{b_1^3 b_2^3}{b_1^3 + b_2^3}$$

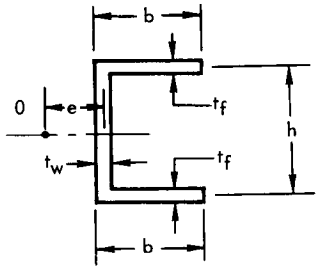

$$e = \frac{3b^2 t_f}{6bt_f + ht_w}$$

$$J = \frac{2bt_f^3 + ht_w^3}{3}$$

$$C_w = \frac{t_f b^3 h^2}{12} \cdot \frac{3bt_f + 2ht_w}{6bt_f + ht_w}$$

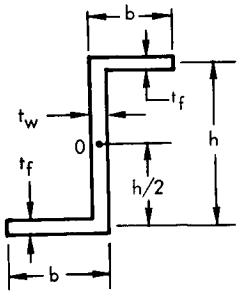

$$J = \frac{2bt_f^3 + ht_w^3}{3}$$

$$C_w = \frac{b^3 h^2}{12(2b + h)^2}\left[2t_f(b^2 + bh + h^2) + 3t_w bh\right]$$

O = SHEAR CENTER

J = TORSIONAL CONSTANT

C_W = WARPING CONSTANT

Figure 69. Section Properties

STRENGTH ANALYSIS OF FLANGES

The flange is generally the stiffest member of a partial-tension-field beam. The strength analysis of the flange can be approached from the elementary strength analysis of beams subjected to lateral and vertical loads. By considering the flange as a continuous beam on elastic supports (uprights), the bending moment in the flange at the upright can be obtained by adding $qd^2/12$ to that bending moment expressed by Reference 30 such as that

$$M_{max} = C_3 \frac{Sd^2 \tan\alpha}{12h} + \frac{qd^2}{12}$$

where the first term is that due to vertical shear load; and the second term is that due to lateral pressure causing tension in the web. The buckling stress in the upright is then

$$\sigma = \pm \frac{M_{max} c}{I_{FL}}$$

where

c = distance from neutral axis to outer fiber of flange, in.

I_{FL} = cross sectional moment of inertia of the flange, in^4

S = shear force in bay under consideration

In addition to the bending stress in the flange there is a compressive stress in the flange of Reference 1.

$$\sigma_c = \frac{k \tau h t_w \cot\alpha}{2A_{FL} + 0.5(J-K)}$$

where

τ = is the shear in the panel under consideration

A_{FL} = is the flange cross section.

The stresses due to bending and compression must be less than the design allowable.

STABILITY CONSIDERATION FOR FLANGES

The general stability of the partial-tension-field beam should be checked when subjected to any vertical loading or any axial compressive loading that may induce compressive stresses in the flange member. The type of instability involved is one that the beam deflects out of the plane of the web. The method of determining the allowable flexural compressive stress is Reference 35.

$$\sigma = 39 \times 10^6 \left(I_{yy} \frac{d}{SL^2} \right) \sqrt{1 + 0.078 \frac{JL^2}{I_{yy} d^2}}$$

for the loading shown in Figure 70.

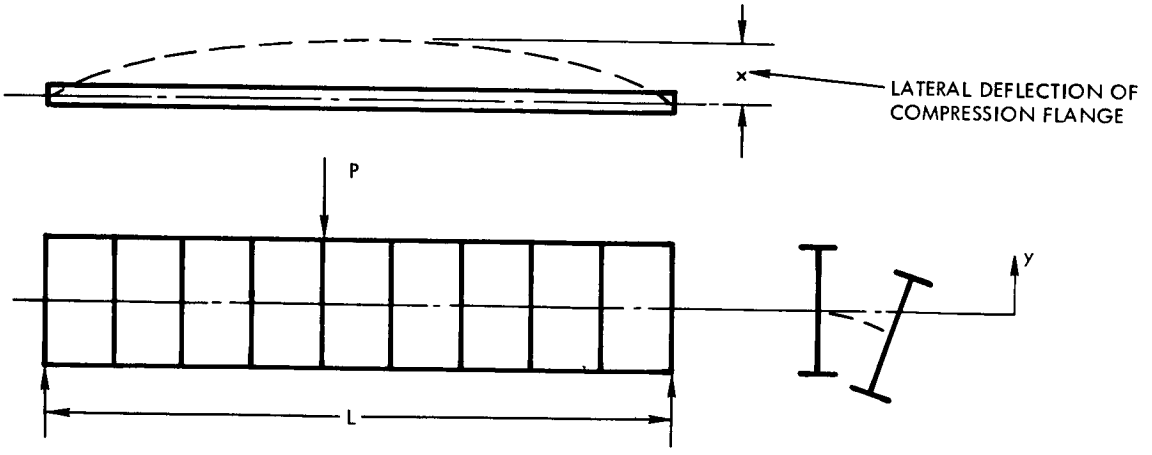

Figure 70. Determination of the Allowable Flexural Compressive Stress

The simplified formula to predict lateral stability that neglects the effect of loading is given by Reference 36. Such simplifications are in common use and are presented as

$$\sigma_c = \frac{102,000}{\left(\frac{KL}{r} \right)^2}$$

for

$$\frac{KL}{r} > C$$

and

$$\sigma_c = B - D\frac{KL}{r}$$

for

$$\frac{KL}{r} \leq C$$

where B, C, and D are defined by the mechanical properties shown in Figure 71 and can be obtained from Figures 20 and 21 for 7075-T6 as a typical aluminum alloy.

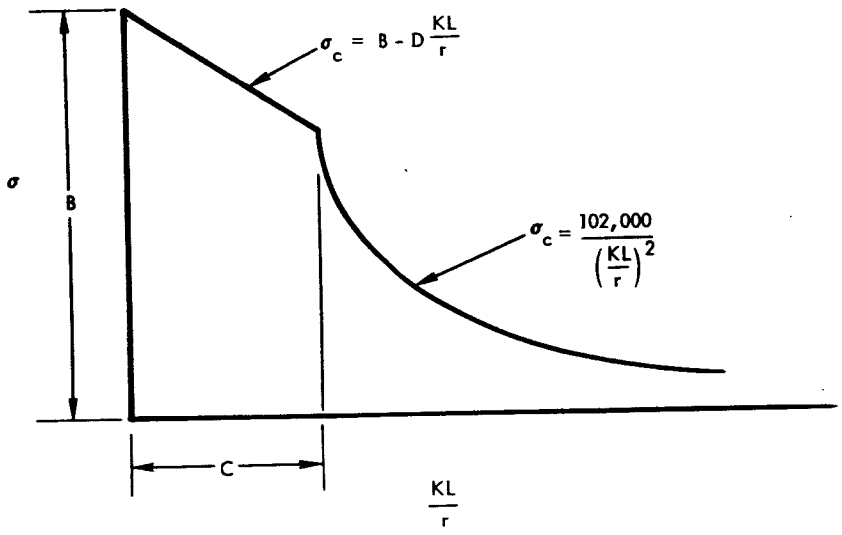

Figure 71. Column Strength Curve

The numerical values for K are defined as follows:

K = 0.5 fixed ends

K = 0.7 one end fixed and one end pinned

K = 1.0 pinned ends

K = 2.0 one end fixed and one end free

The values for r (radius of gyration) to be used is as follows:

(a) Symmetrical I and channel beams and girders, supported at ends

$$r^2 = \frac{\sqrt{Iy}}{S_c}\sqrt{C_3 + 0.038J\,(KL)^2}$$

(b) Cantilever I sections and channels loaded at free end

$$r^2 = 1.28\,\frac{\sqrt{Iy}}{S_c}\sqrt{C_s + 0.038J\,(KL)^2}$$

(c) Cantilever I sections and channels loaded uniformily along length of beam

$$r^2 = 2.05\,\frac{\sqrt{Iy}}{S_c}\sqrt{C_s + 0.038J\,(KL)^2}$$

where

I_y = moment of inertia, in.^{4}

S_c = section modulus for beam about axis normal to web, in.^{3}

C_s = torsion warping constant defined by Figure 69 (defined as C_W in Figure 69), in.^{6}

J = torsional constant, in.^{4}

L = lateral unsupported length, in.

SUMMARY AND CONCLUSIONS

The structural behavior of uprights and flanges of the partial-tension-field beam subjected to combined lateral pressure and vertical load is presented. Formulas and graphical aids have been included in determining the stresses and stability of the uprights and flanges. Accuracy of the basic assumptions has been included. Empirical effect has been included in the analysis by taking into account the behavior of diagonal web folds as bracing

effect for the upright for partial-tension-field beams. The equations can readily be applied for pure diagonal-tension-field beam by letting the diagonal tension factor be equal to unity. Both single- and double-upright arrangements have been considered.

The analysis of the flange is based upon the application of elementary strength analysis when considering the effect of lateral loads. The analysis of partial-tension-field beams subjected to vertical loading has been analyzed similar to the earlier researchers.

The energy method is applied to formulate the equations describing the behavior of the uprights. The total energy of the system consisted of the strain energy of the upright bending, strain energy of the web system, potential energy of the in-plane forces, and the potential energy of lateral loads. The arbitrary deflection coefficients are determined from application of the stationary potential. Both symmetric and antisymmetric deflections were considered. The bending stress was obtained from the deflection function. The compressive stress was then added to the bending stress to determine the total stress in the upright.

The buckling criteria for the upright was determined by letting the denominator of the deflection function approach zero. Empirical effect on the stability of uprights was considered by letting the elastic restraint of the upright-web system be represented by the critical load as determined from a previously published test. The symmetrical buckling mode has been defined as one that gives critical load when the upright deflects out of the plane of the web. For antisymmetric buckling mode, the level of buckling was found to be approximately four times that of the symmetric mode. Here, antisymmetric buckling is one that considers an upright to buckle in two half waves in the plane of the web system.

Other buckling phenomena included the determination of forced crippling, crippling, and torsional buckling criteria.

IV. CURVED BEAMS

INTRODUCTION

The cases for straight beams which were considered in the first three sections are special or limiting to curved beams. The radius of curvature, R, approaches infinity for straight beams.

In this section, a method of analysis is developed for analyzing curved partial-tension-field beams. As in the case of straight beams, vertical loading and lateral pressure are the loadings considered. The analysis procedure is general. Curved-beam analysis methods closely follow those developed for straight beams, though some alterations are made necessary by geometrical load- and stress-distribution variations brought about by beam curvature.

Most of the straight-beam nomenclature is directly applicable to curved beams. Panel dimensions, h and d, and the diagonal tension angle, α, are defined in Figure 72. The basic assumptions used for straight beams are also used for curved beams, i.e., heavy flanges, relatively heavy uprights, and thin webs.

A new consideration is the treatment of curved beams with finite values or $R/t \geq 1000$. The beam radius of curvature R is finite for a curved beam.

It is assumed that the analyst is familiar with structural analysis of curved beams and that, for any statically determinate or indeterminate beam, he can determine (1) bending moment, (2) torsional moment, and (3) shear at any section of the curved beam. Axial loads on the beam are considered in the analysis by assuming that all of the axial load is carried in the flanges of the beam.

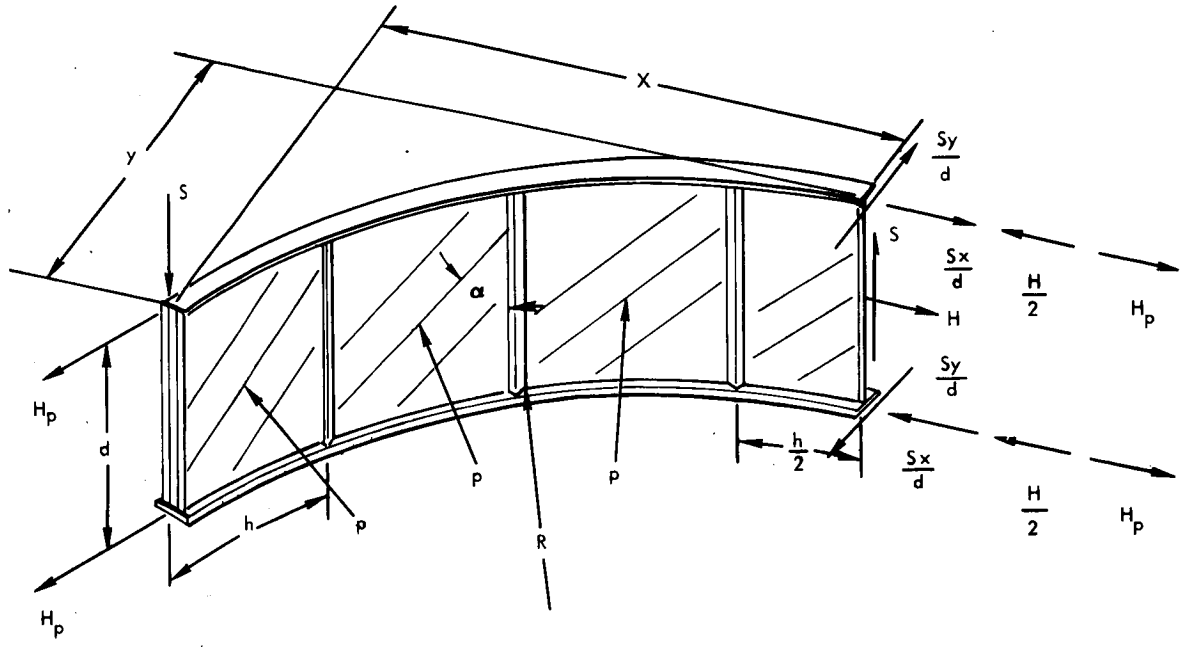

A. GENERAL CONFIGURATION

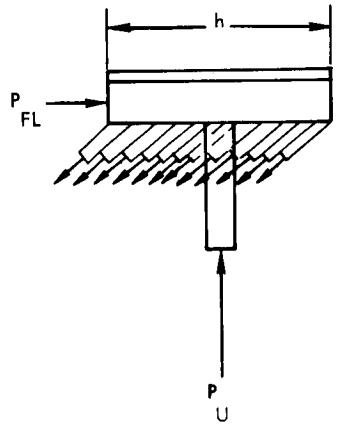

B. INTERMEDIATE UPRIGHT

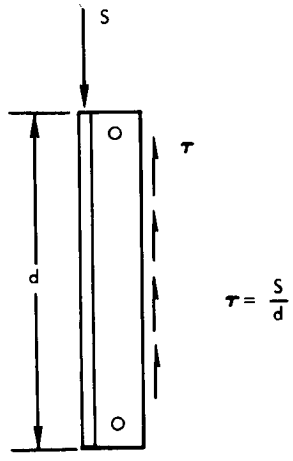

C. LOADED UPRIGHT

Figure 72. Curved Beam Equilibrium

CURVED-BEAM AND LOADING CONFIGURATIONS CONSIDERED

In this study, beams under consideration are limited to those having beam height (dimension d in Figure 72) relatively small compared to length or circumferential dimension. Two flanges, one upper and one lower, are connected by vertical uprights that separate the web panels.

A beam of this type will normally be supported laterally at the ends and at intermediate points along the flanges. Lateral support could be furnished by crossbeams or by bulkheads. Pressure-tight bulkheads may introduce axial-stress components in the web and uprights when the structure is subjected to pressure loading; however, this effect will not be considered.

Curved beams with two loading conditions (vertical and lateral pressure), and combinations of these, are investigated in this study. The two types of loading are as follows:

1. Vertical beam loading includes any vertical (in plane of the web) loading applied to the flanges. This loading may be in the form of concentrated loads or, may be applied as distributed loading along the flanges. The beam flanges are considered to be relatively stiff, so that all vertical loadings applied to them will be carried over to adjacent uprights. Due to beam curvature, loading eccentricities will set up a torsional moment in the beam cross section. This torsion will be counteracted by the flanges.

2. Lateral pressure loading will be applied primarily to the web panels.

Two phases of loading will be considered, (1) prebuckling, and (2) postbuckling. For the prebuckling phase, the stress distributions in webs, web-attachment joints, flanges, and uprights are straightforward. The occurrence of web buckling will be predicted under combined loading. After this nonlinear perturbation, postbuckling development of diagonal tension will be investigated during load build-up to failure.

The modes of failure covered are as follows:

Web material ruptured in tension, including rivet or fastening failure at web connections to flange or upright

Upright failure by column buckling, bending, or forced crippling

Flange failure by the same mechanisms as the uprights

Due to curvature, structural-system analysis is more complicated in the curved-beam than in the straight-beam case. A three-dimensional rather than a two-dimensional deflection system results from the curvature. As seen in Figure 72, the eccentricity of loading produces overall torsion in the beam. This torsional moment is carried by the forces labeled Sy/d applied to the flanges. This is in addition to the beam bending and shear effects produced in straight beams. As in the case of the straight beam, loads will be assumed to be carried as follows:

Beam bending will be resisted by flanges only.

Shear load will be supported by webs only.

Beam torsion will be reacted by the flanges only.

CURVED VERSUS STRAIGHT BEAM COMPARISON

Curvature makes it possible for the web to support a higher pre-buckling shear load than the flat web panels of the straight beam. In general, the higher the curvature, the more load may be carried; as increased curvature, tends to stabilize the web. This curvature effect delays buckling of the web under shear loading. Buckling may also be delayed by internal lateral pressure. Conversely, external lateral pressure will tend to decrease the buckling shear load.

Above the buckling shear load, a thin curved web will tend to deflect toward a flat panel configuration. It is expected that this phenomenon would be accompanied by a marked, incremental, vertical beam deflection as the curved diagonal-tension panel elements straighten out. In the postbuckling phase, the curved beam web panel (buckled into a flat configuration) should react to either internal or external lateral pressure loading in a manner roughly parallel to the straight beam web-panel behavior. Diagonal-tension stresses (in diagonal catenaries) will continue to build up with vertical and/or pressure loading until the web ruptures.

External pressure will tend to reverse web-panel curvature and, depending on the panel-aspect ratio, the loads will be carried to the uprights and flanges by catenaries with reversed curvature. If the panel is narrow, the more closely spaced edge members of the panel will support the majority of the load.

The uprights will support essentially the same types and components of loading as for the straight-beam case. One additional component will be the radial load caused by web-sheet loads acting at panel-intersection angles, brought about by the postbuckled polygon shape (Figure 73, diagram C). This shape results from the web panels buckling into approximately flat-sheet elements between uprights.

The main differences in flange loading between the straight- and curved-beam configurations will be caused by the beam torsion introduced by the loading, (Figure 72). Also, lateral pressure loading will produce axial loads in the curved flanges; while in straight beams, the primary loads in the flange will be lateral and vertical bending only.

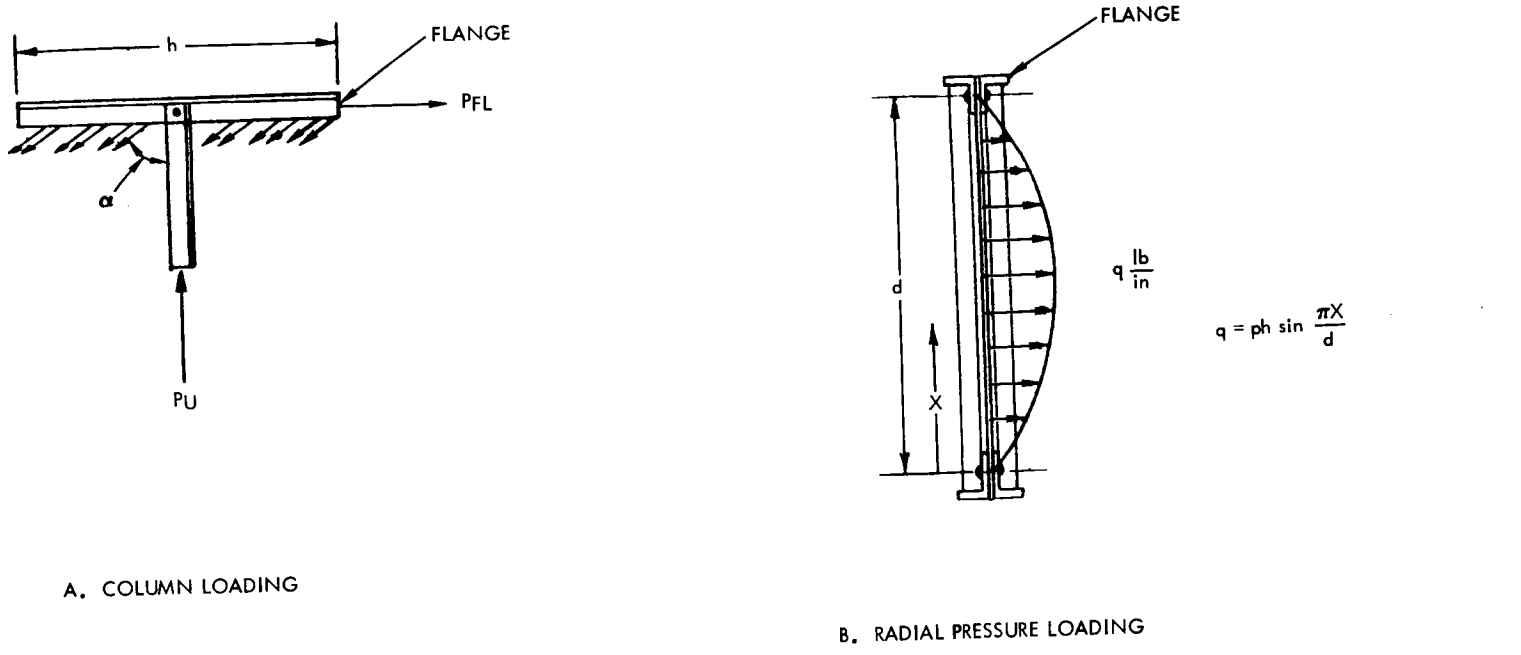

Figure 73. Curved Beam Upright Loading

CURVED WEBS

The thin sheet serving as web in semitension field beams will sustain only a limited amount of shear and/or compressive stress without buckling. Added loading with internal lateral pressure will cause a postponement of buckling until higher shear loads are applied. Conversely, external pressure reduces the amount of shear the web is able to withstand at buckling.

Two phases of web loading may be defined (1) prebuckling, and (2) post-buckling; these are separated by the web buckling phenomenon. The two phases will be considered first for beam vertical loading only, then lateral pressure loading only, and finally for combined loading with various loading sequences.

VERTICAL LOADING

This loading may be a concentrated vertical load, such as S in Figure 72, or any distributed vertical loading along the flange. It will be assumed that all loading between uprights will be transferred to adjacent uprights by relatively stiff flanges. If the loaded flanges were not stiff, the loading would still be transferred to adjacent uprights, but the flange deflection under load would cause a change in stress distribution in the web. The web cannot support significant in-plane compressive stresses, but panel boundary or edge movement would affect web stress distribution.

Prebuckling Stage

Under beam vertical loading, the web panel will be required to support only shear loading. If the joints between the uprights and flanges are pinned, web shear stress in the loading configuration of Figure 72, diagram A.

$$\tau = \frac{S}{dt} \tag{4-1}$$

For the thin web sheet considered,

$$\left|\tau\right| = \left|\sigma_t\right| = \left|\sigma_c\right| \tag{4-2}$$

where σ_t and σ_c are oriented in diagonal directions.

Mohr's circle demonstrates this stress condition in Figure 1. As vertical beam loading increases, web-shear stress, τ, the principal tensile stress, σ_t, at 45 degrees, and the principal compressive stress, σ_c, in the orthogonal direction, all increase in proportion, until the buckling load is reached.

Web-Buckling Phenomenon

At buckling, a radical redistribution of stress occurs and a new mathematical model is required. Mohr's circle no longer portrays the stress system. As in the case for straight beams in Section I, (Reference 30, Part I) furnishes a direct approach to predicting the buckling shear, τ_{cr}.

$$\tau_{cr} = k_s \frac{\pi^2 E h^2}{12 R^2 Z^2} \qquad (4\text{-}3)$$

where k_s is found from Figures 74 and 75, and

$$Z = \frac{h^2}{R_t} \sqrt{1 - \mu^2}.$$

These curves are based on simple-support edge conditions. For the relatively thin webs used in diagonal-tension-web beams, the effects of edge restraint die out rather quickly away from the edge due to low sheet bending stiffness. On this basis, these curves are applicable to curved webs with any degree of edge restraint up to the limit of fixed or "built-in" panel edges.

An alternate theoretical approach from a more recent work by a Russian author, V. A. Marjin (Reference 37), is presented. The buckling parameters of curved plates, using both small and large deflection theory, are portrayed in Figures 76 and 77. The variation between the two approaches is readily apparent by comparing curves of the two graphs. Some "thin" web configurations may be best handled as shown in Figure 76; while the "very thin" web should conform more closely to the curves of Figure 77.

The Kuhn approach (Reference 1) is based primarily on empirical data. Having available the above-mentioned methods for determination of the critical shear in the curved web, the analyst may choose one of them which appears most appropriate to the specific configuration being analyzed.

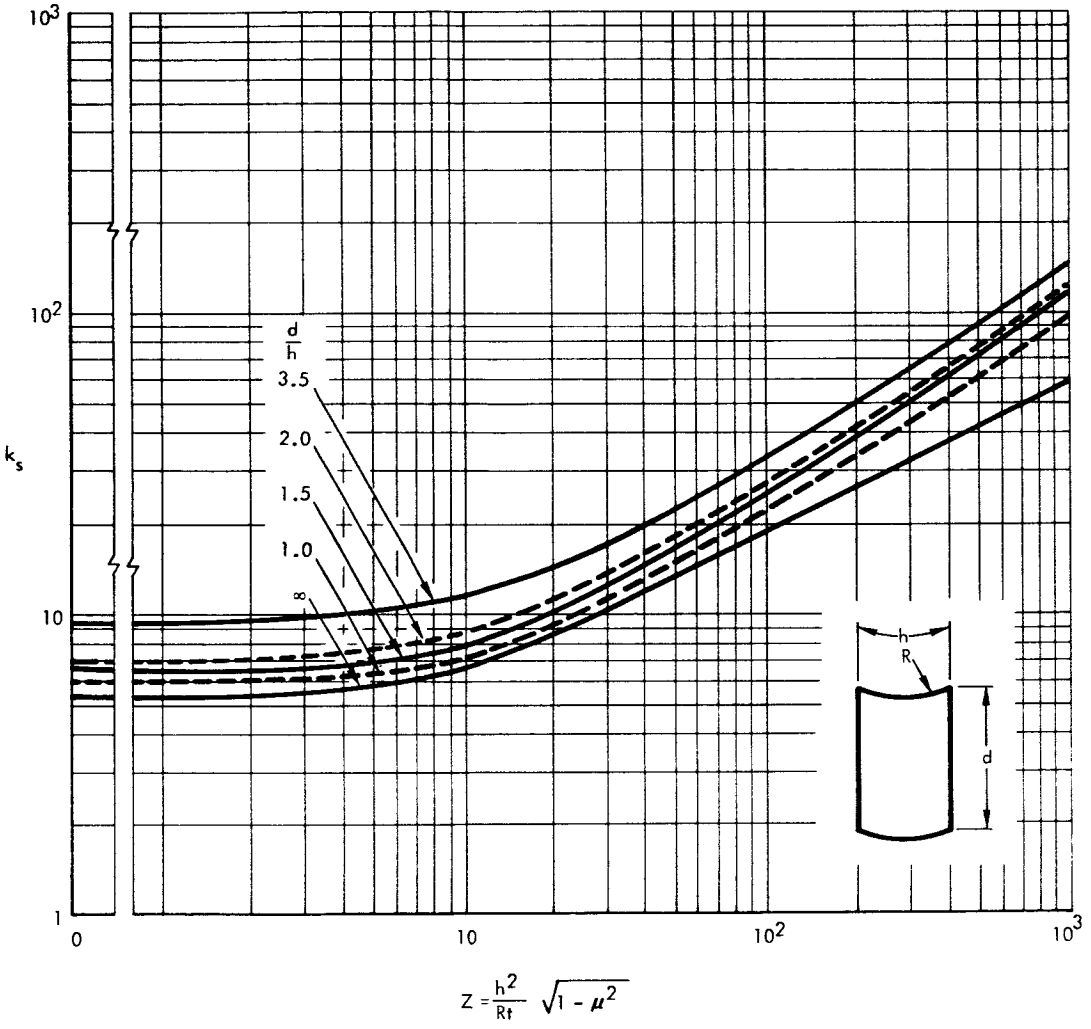

PLATES LONG AXIALLY ($d \geq h$). $\tau_{cr,\ ELASTIC} = k_S \frac{\pi^2 E h^2}{12R^2Z^2}$

Figure 74. Critical Shear-Stress Coefficients for Simply Supported Curved Plates, Plates Long Axially

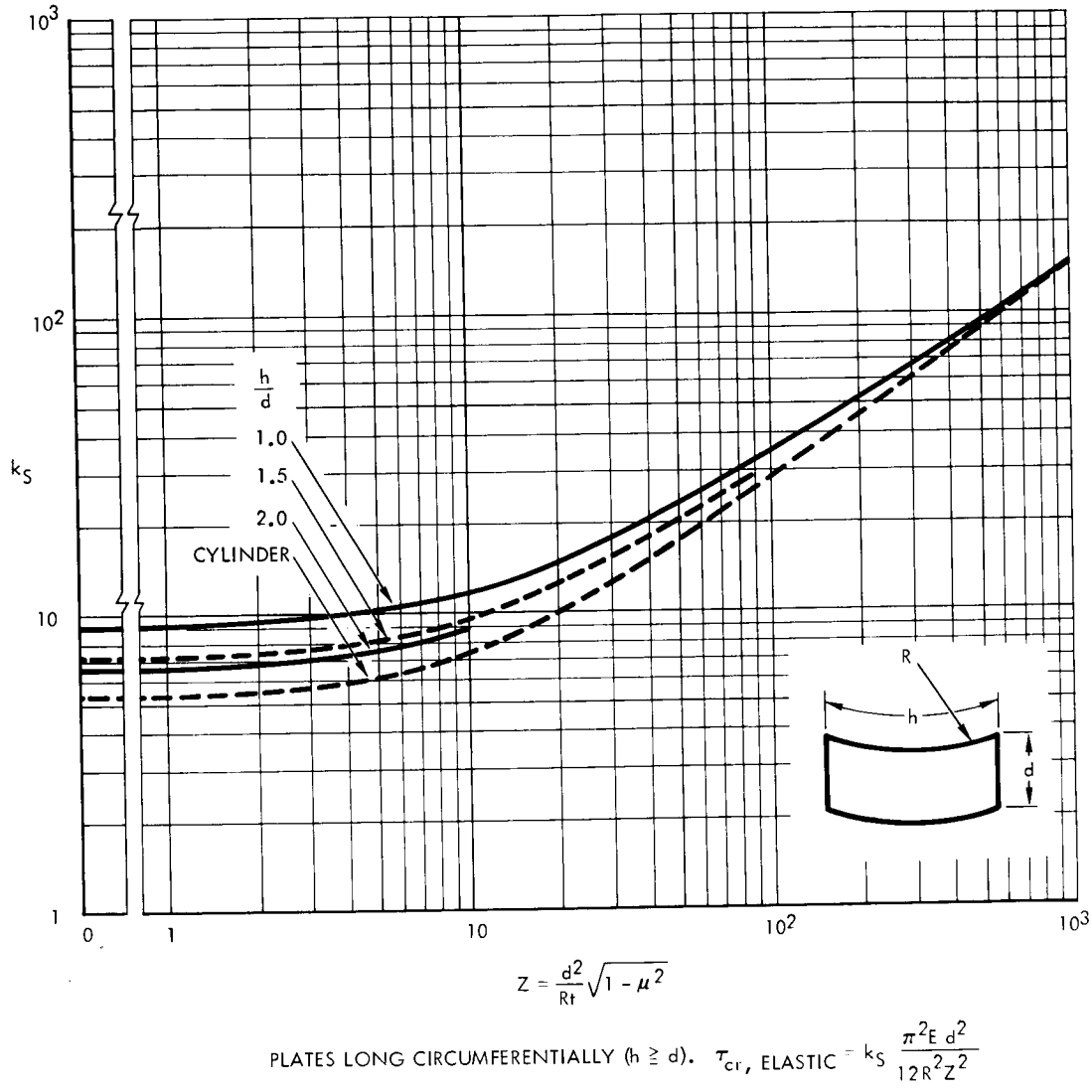

PLATES LONG CIRCUMFERENTIALLY ($h \geq d$). $\tau_{cr,\ ELASTIC} = k_S \frac{\pi^2 E\, d^2}{12R^2Z^2}$

Figure 75. Critical Shear-Stress Coefficients for Simply Supported Curved Plates, Plates Long Circumferentially

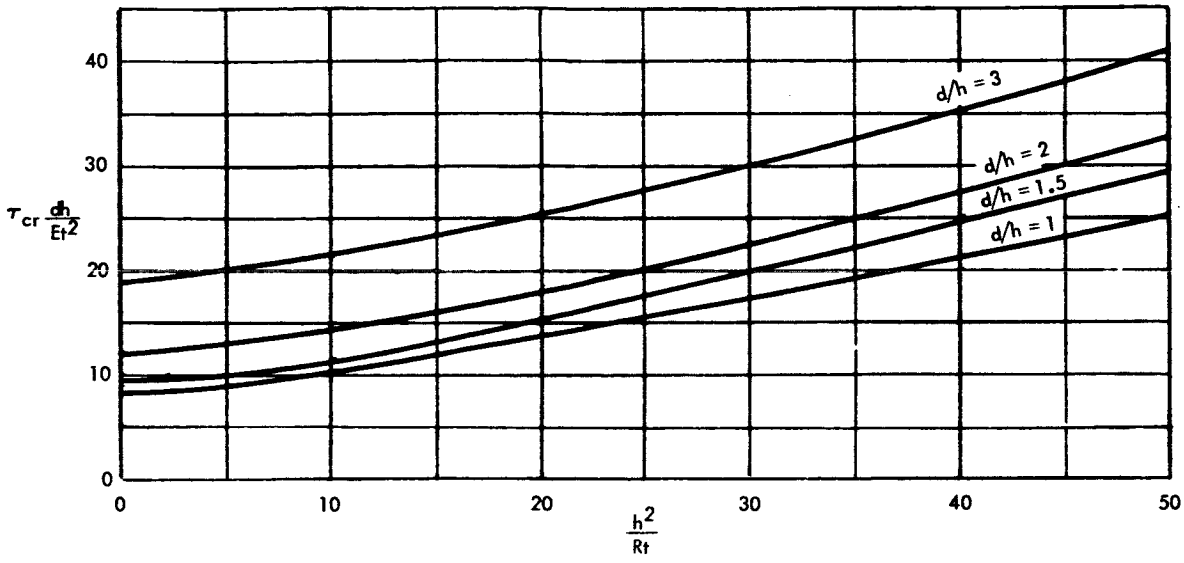

Figure 76. Curved-Web Critical Buckling, "Small Deflection" Theory

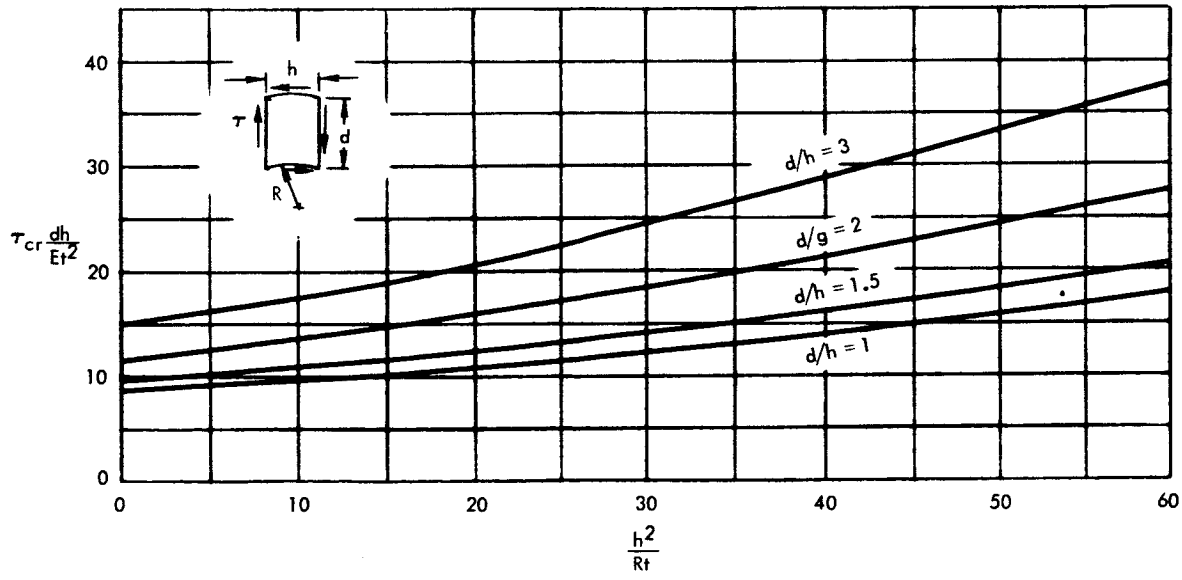

Figure 77. Curved-Web Critical Buckling, "Large Deflection" Theory

Postbuckling Stage

In curved semitension-field beams with usual geometric proportions, the web will tend to buckle into flat panels between the uprights. This results in a polygon shaped section (Figure 73, diagram C). Tension in the thin-web diagonal-tension elements tends to pull the web into a flat panel, and diagonal buckle waves across the panel tend to stiffen the panel as sheet material moves out of the neutral plane of the sheet. As the wave crests move out of the neutral plane, higher bending moment of inertia in the direction of the ridges is produced in the sheet.

As the diagonal section of the curved sheet buckles, it tends to move into the plane of the chord ($\overline{Ch}_2$ of Figure 78). The lengthening of the chordal distance is accompanied by relatively high panel-shear deformation. As the panel frame distorts into parallelogram shape, high tensile stresses at angle α will be set up in the larger opposite corners of the panel (upper left and lower right corners in Figure 78) because of "gusset" effects.

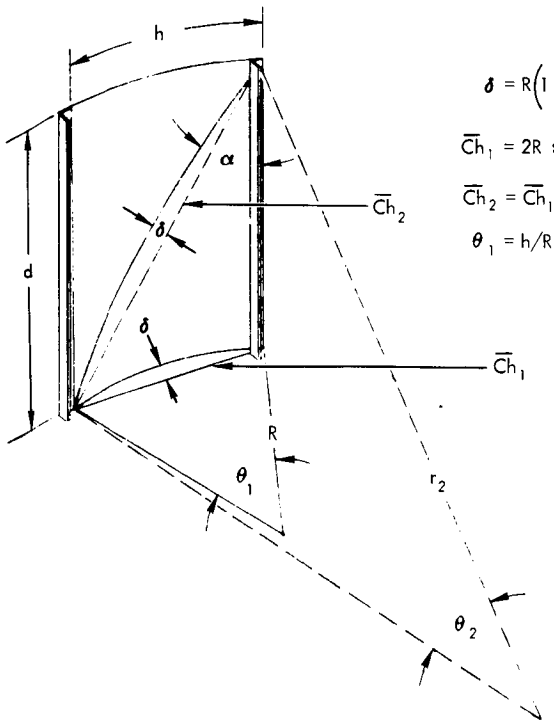

Figure 78. Geometric Relationships of Diagonal Tension Strips

The flat panel buckled configuration will be somewhat modified near the flanges, as the flanges will be stiff enough to restrain sheet edge shape in these areas to the original lateral curvature. The edge-curvature effect decreases as R/t increases from the lower limit of 1000, and as the sheet becomes thinner, therefore decreasing sheet-bending-stiffness effects.

From the geometry in Figure 78, the change in chord length may be computed to be

$$\Delta\overline{Ch}_2 = \frac{R \sin \frac{h}{2R}}{\sin \alpha} \left(\frac{\theta_2}{\sin \frac{\theta_2}{2}} - 2 \right) \tag{4-4}$$

where

$$\theta_2 = \cos^{-1} \left[2 \left(\frac{1-K_1^2}{1+K_1^2} \right)^2 - 1 \right] \tag{4-5}$$

and

$$K_1 = \frac{\left(1 - \cos \frac{h}{2R}\right) \sin \alpha}{\sin \frac{h}{2R}} \tag{4-6}$$

This derivation is based on the assumption that the shape of the curved cylindrical section at angle α approximates a circular arc which is defined by chord $\overline{CH}_2$ and δ. Also the assumption is made that α may be measured by the angle between the chords. This approximation becomes less valid at large ratios of h/R. The center dimension, δ, is equal to the center distance between $\overline{Ch}_1$ and the associated arc of the curved web panel (Figure 78). A curve defining the relationship between θ_2 and h/R is shown in Figure 79.

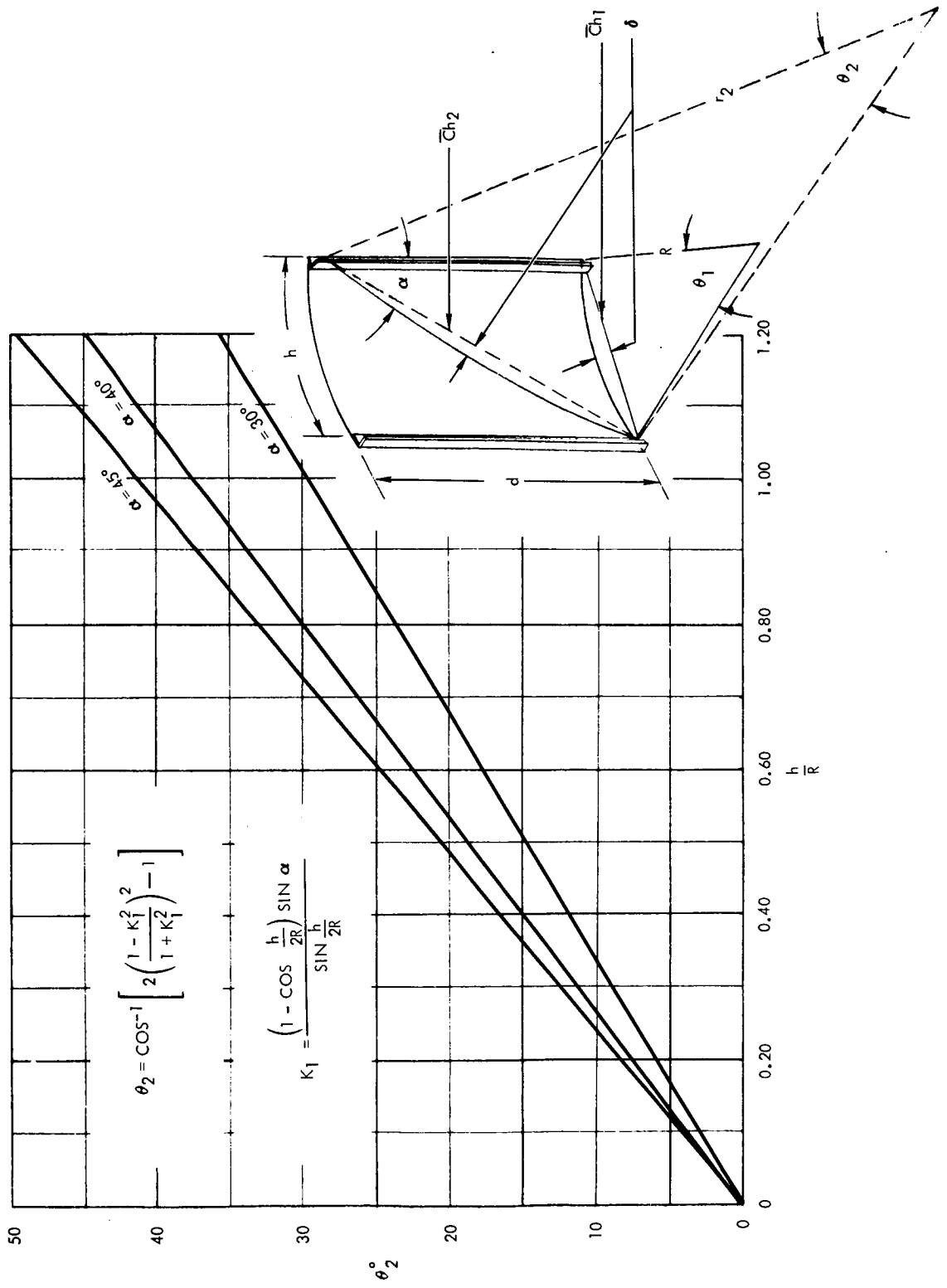

Figure 79. Diagonal Tension Strip Parameters

For reference, the radius, r_2, may be defined by

$$r_2 = \frac{\delta\left(1 + \frac{4\delta^2}{\overline{Ch}_2^2}\right)}{2\left(\frac{4\delta^2}{\overline{Ch}_2^2}\right)} = \frac{\overline{Ch}_2^2 + 4\delta^2}{8\delta}$$

$$= \frac{\left(\frac{\overline{Ch}_1}{\sin\alpha}\right)^2 + 4\left[R\left(1 - \cos\frac{\theta_1}{2}\right)\right]^2}{8R\left(1 - \cos\frac{\theta_1}{2}\right)}$$

$$= \frac{R\frac{\sin^2\frac{\theta_1}{2}}{\sin^2\alpha} + R\left(1 - \cos\frac{\theta_1}{2}\right)^2}{2\left(1 - \cos\frac{\theta_1}{2}\right)} \qquad (4-7)$$

The beam is assumed to deflect sufficiently that the buckled-flat-panel $\Delta\,\overline{Ch_2}$ strains are absorbed, and the loading maintains its original value as it moves during beam deflection. Under these conditions, the opposite larger corners of the panel will show higher-than-average stresses due to the gusset effect. As a result, the upright will tend to deflect in a modified S shape. The definition of these stresses appears to be a complex task, and it is probably not very significant in the overall analysis. On this basis, they will be disregarded in this study.

The lateral angle between buckled, adjacent flat panels of the curved beam will have some effect on the web stresses. However, in this configuration, the stiff uprights will minimize the effect, and for the present analysis, web in-plane stresses are computed by essentially the same methods as for straight beams (simple-support edge conditions).

The development of the stress system under increasing loading as explained in Section I is applicable. The compressive stress, σ_c, which is perpendicular to the diagonal-tension elements, will maintain

approximately the same value as at web buckling during additional load application. The value of σ_c from Kuhn (Reference 1) is

$$\sigma_c = -\tau_o (1-k) \sin 2\alpha \tag{4-8}$$

The trigonometric factor is applied, because of the difference between the 45-degree pure-shear-induced principal stresses, and the angle, α, of the diagonal tension elements. A shear stress component is built up as α varies from 45 degrees. At α = 30 degrees, the shear component is about 25 percent of the compressive stress component.

The tensile stress along the diagonal tension elements at the angle α. may be calculated from

$$\sigma_t = \frac{2k\tau_o}{\sin 2\alpha} + \tau_o (1-k) \sin 2\alpha \tag{4-9}$$

where τ_o = S/dt for the loading in Figure 72. The discussion of the last paragraph relative to the trigonometric factor applies also to the trigonometric factor in the second term of Equation 4-9.

The value of k, the diagonal tension factor, is found from the following equation (Reference 30, Part 1).

$$k = \tanh \left[\left(0.5 + 300 \frac{td}{Rh} \right) \log \frac{\tau_o}{\tau_{cr}} \right] \tag{4-10}$$

This equation may be solved with the aid of Figure 80.

The value of α_{PDT}, the angle of pure diagonal tension, may be found from Figure 81. The structural geometric and loading configurations must be known, along with Young's Modulus of the web material.

The diagonal tension angle, α, for less than fully developed diagonal tension, is a function of k, the diagonal-tension factor. A curve of empirical data from Reference 30, Part I, is shown in Figure 81C. This shows the relation of α/α_{PDT} to k. Reference 30, Part I states that the value of α found from this curve should be within 2 or 3 degrees of the final computed value, using the iterative procedure prescribed in that report.

These stress formulas may be applied up to ultimate loading. Web loading is limited by the attainment of ultimate tensile stress in the sheet. The ultimate stress will often occur at the web attachment joint to the

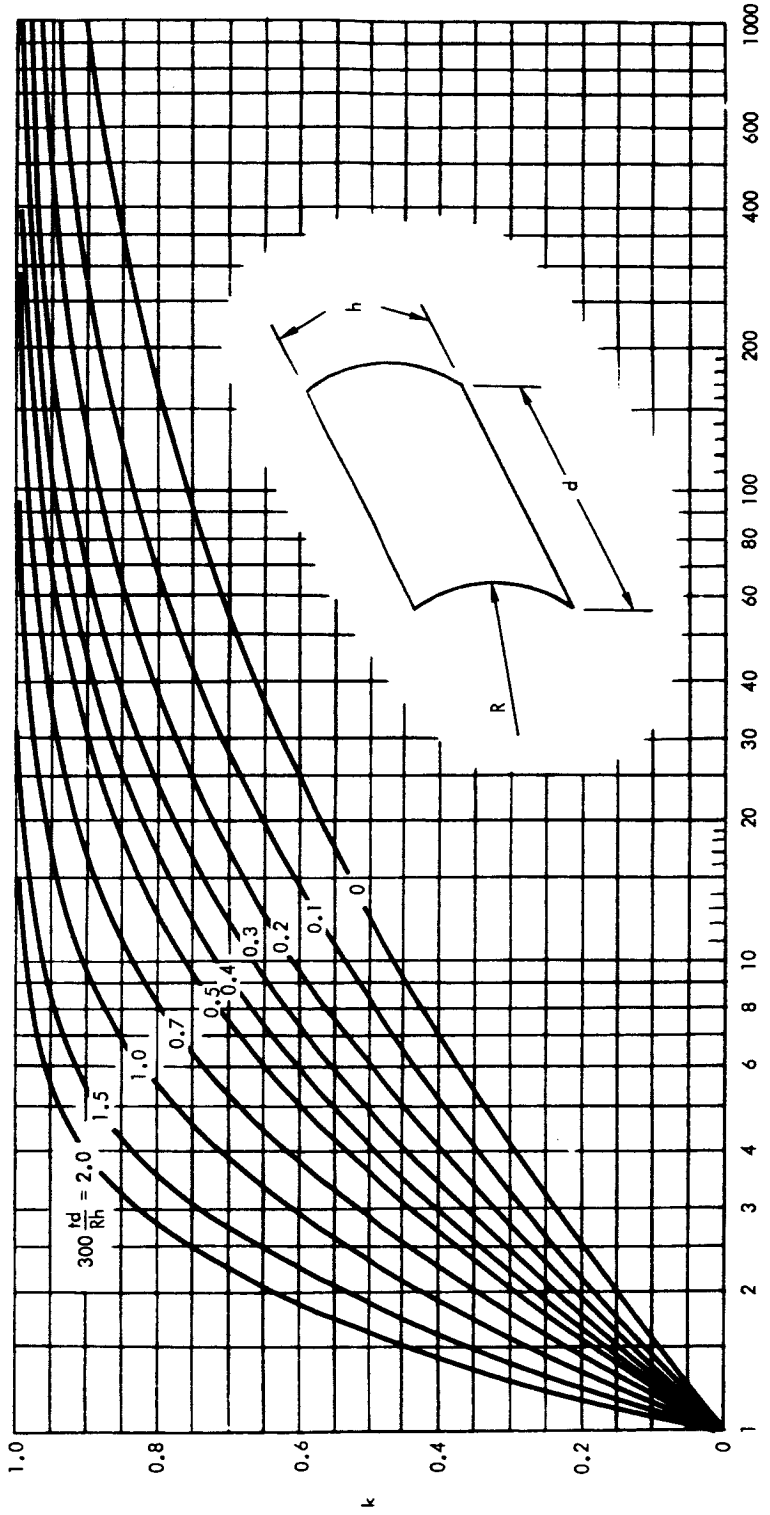

Figure 80. Diagonal Tension Factor, k

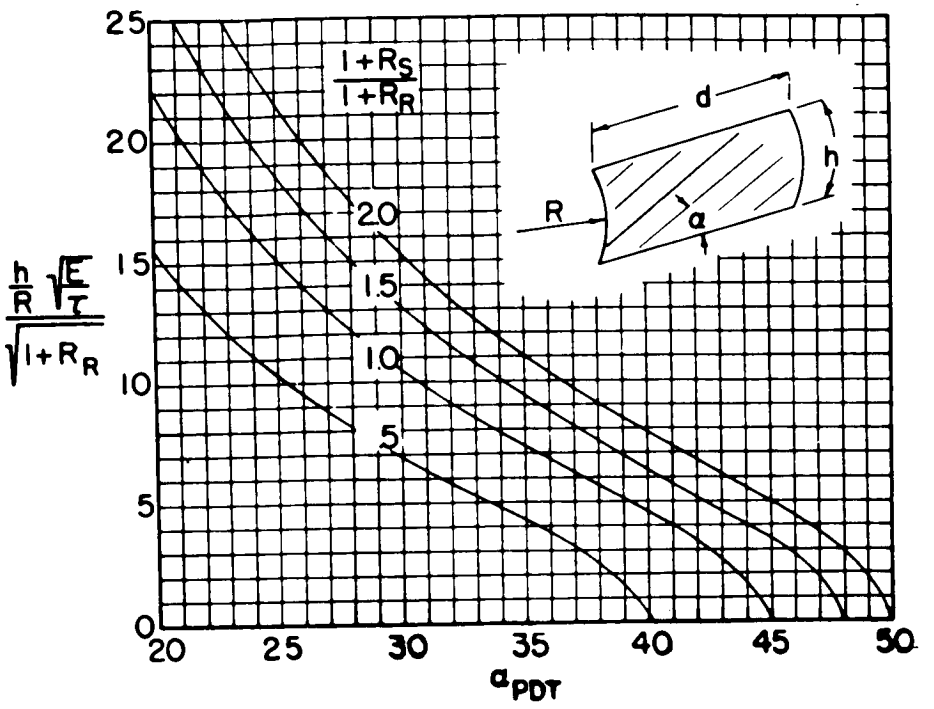

(A)

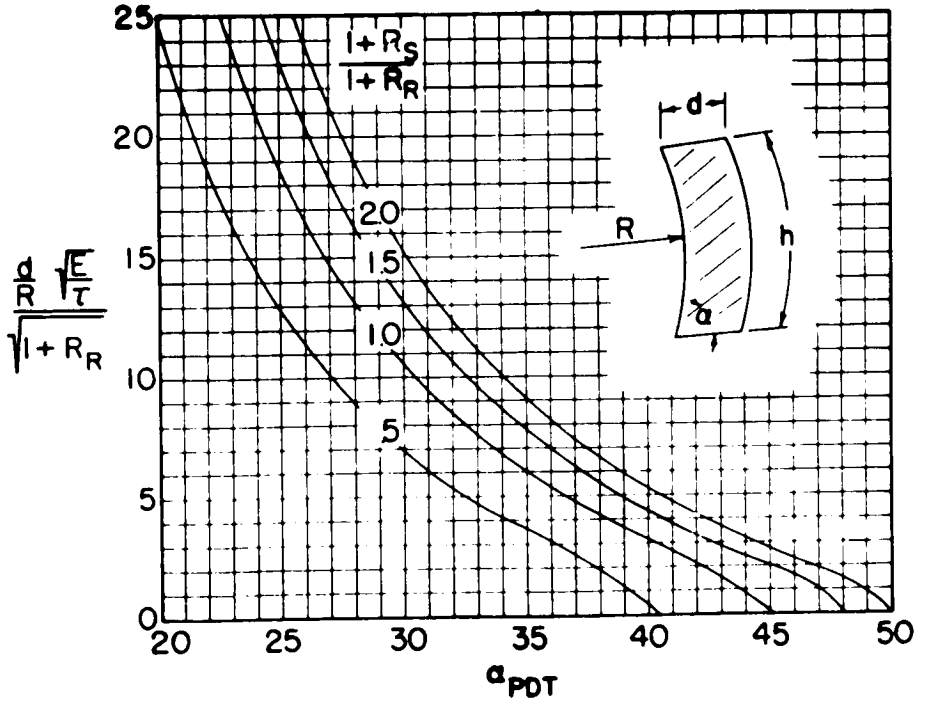

(B)

Figure 81. Angle of Pure Diagonal Tension (Sheet 1 of 2)

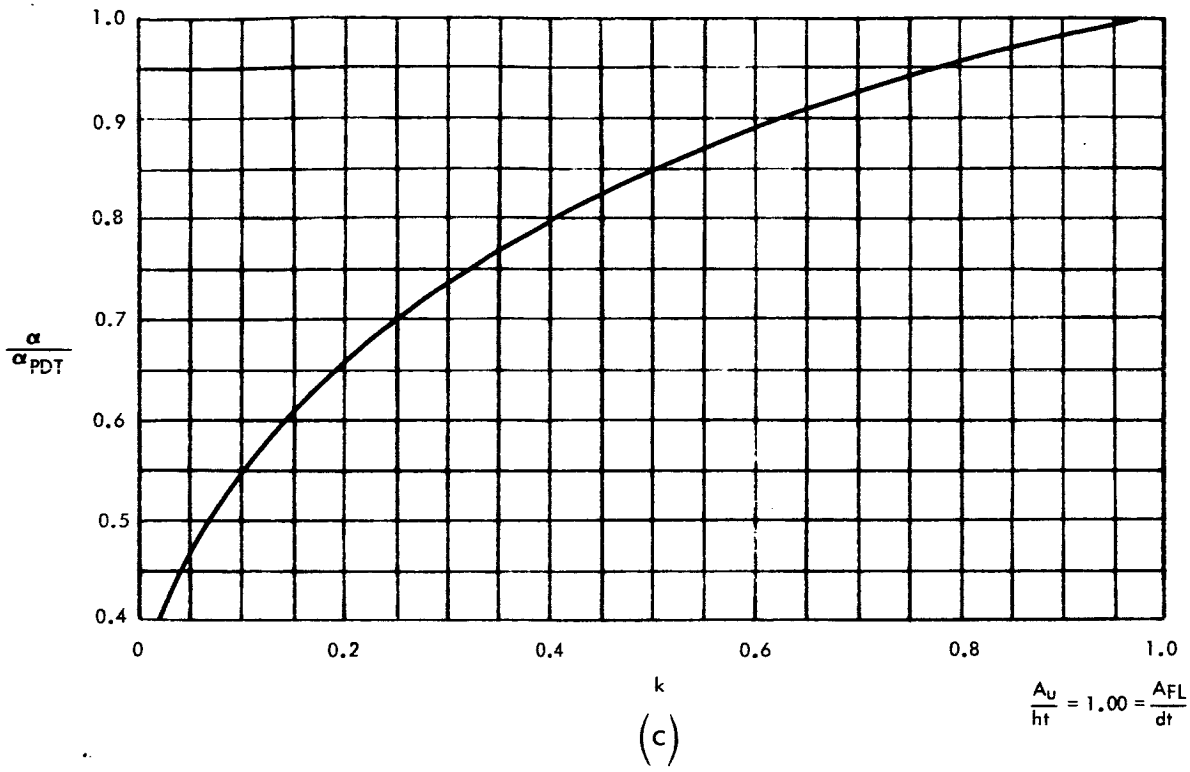

Figure 81. Angle of Pure Diagonal Tension (Sheet 2 of 2)

uprights or flanges. This is due to the stress concentrations normally associated with structural joints.

The ultimate shear stress in the curved web, τ_{all}, may be calculated from the empirical equation of Reference 1.

$$\tau_{all} = \tau^{*}_{all} (0.65 + \Delta) \qquad (4\text{-}11)$$

where the flat web value, τ^{*}_{all} for 2024-T3 or 7075-T6 aluminum alloy is found from Figure 82, and Δ is calculated from the empirical expression

$$\Delta = 0.3 \tanh \frac{A_{FL}}{dt} + 0.1 \tanh \frac{A_U}{ht} \qquad (4\text{-}12)$$

The correction factor, Δ, for curved webs may be read from Figure 83.

It is noted that τ_{all} can exceed τ^{*}_{all} because the quantity Δ can exceed the value 0.35 if the flanges and uprights are heavy. The explanation lies in the fact that a grid system of uprights and flanges can absorb some shear; the effect is analogous to the portal-frame effect in plane-web systems.

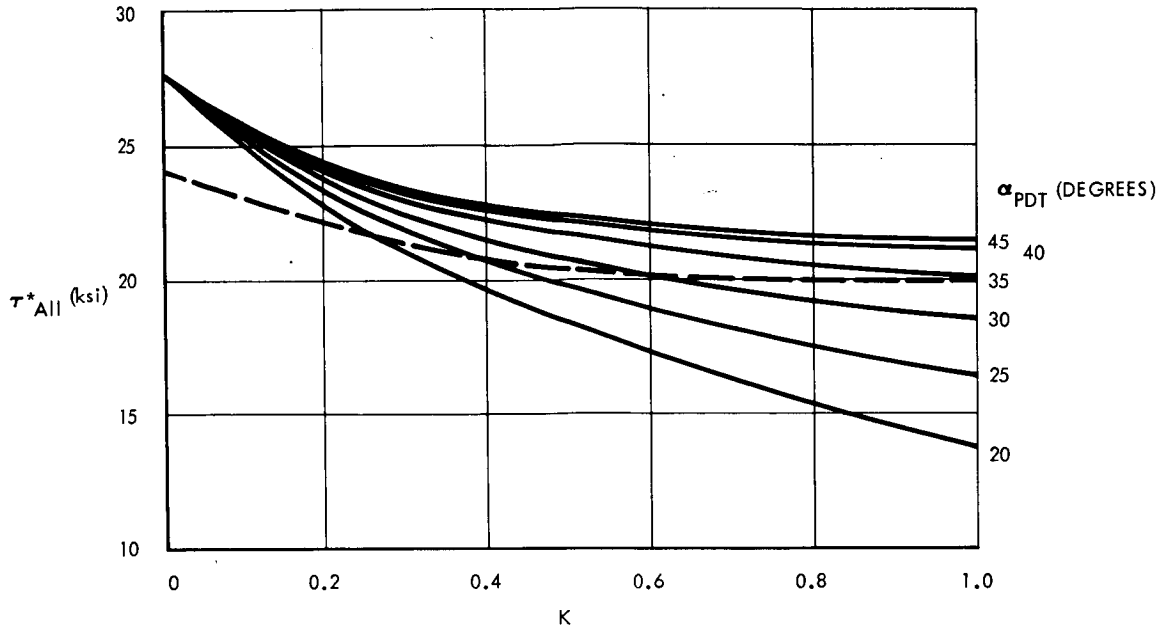

A 24S-T3 ALUMINUM ALLOY. σ_{tu} = 62 ksi.
DASHED LINE IS ALLOWABLE YIELD STRESS.

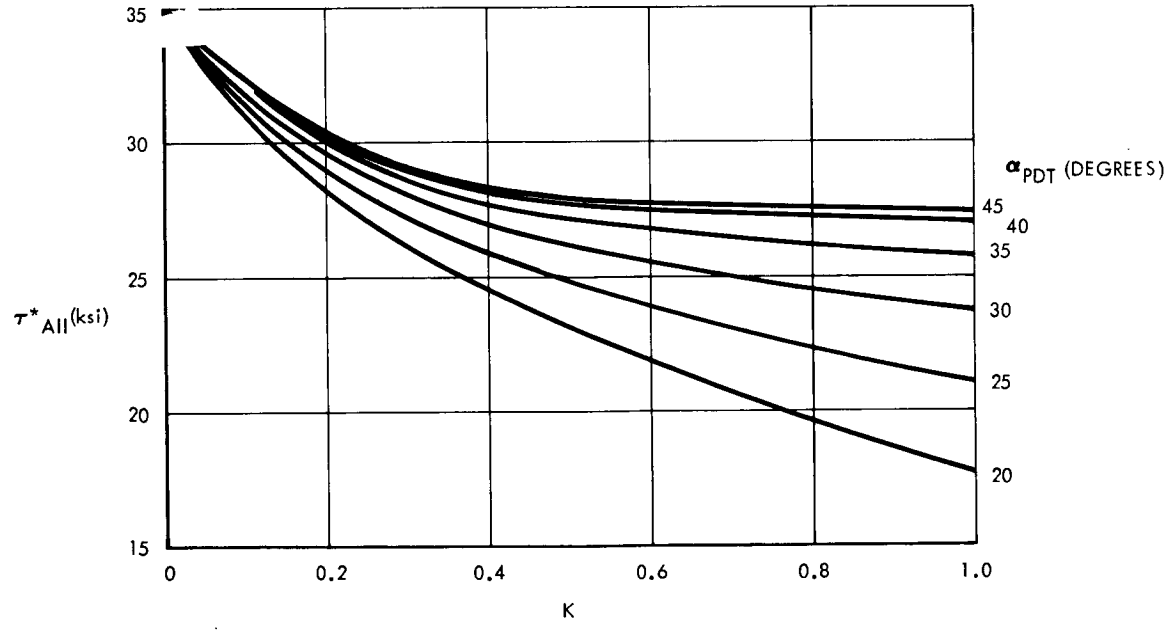

B ALCLAD 75S-T6 ALUMINUM ALLOY. σ_{tu} = 72 ksi.

Figure 82. Basic Allowable Values of τ_{max}

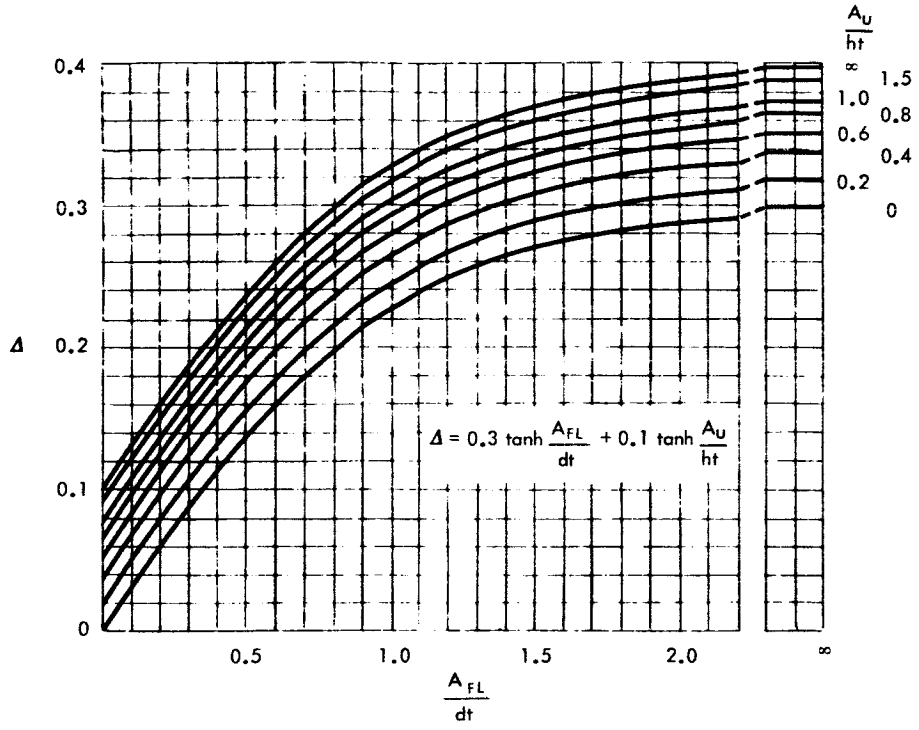

Figure 83. Correction for Allowable Ultimate Shear Stress in Curved Webs

The value of τ^*_{all} found in Figure 82 should be adjusted according to the ultimate-stress values of the particular materials used. The data of the figure is based on stress values noted in the title. The value of τ^*_{all} then should be modified by multiplying the graph value by the ratio of actual ultimate stress to the value noted in the applicable part of Figure 82.

The empirical value of τ^*_{all}, the basic allowable, may be modified according to Reference 1 by the following consideration relative to flange-web and upright-web joints:

1. Joint bolts just snug, heavy washers under bolt heads, or web sheet between flange angles: use basic allowable.

2. Bolts just snug, bolt heads bearing directly on sheet: reduce basic allowable 10 percent.

3. Rivets tight: increase basic allowable 10 percent.

4. Rivets assumed loosened in service: use basic allowable.

These rules hold if allowable bearing stresses of the rivets or bolts on the sheet are not exceeded. Also, they are not applicable to countersunk rivets.

LATERAL LOADING - INTERNAL PRESSURE

Internal lateral loading will be defined as uniformly distributed pressure loading acting in the radial direction from the center of curvature. The curved web will be considered to be of cylindrical shape. In general, the web is a "thin" or "very thin" curved plate, simply supported on all four sides by uprights and flanges.

This static system is different from the usual cylinder, which has known membrane loads, (pr and pr/2), due to either internal or external pressure. Boundary conditions make the curved plate work differently from a cylinder. Due to pressurization, the curvature will change, and in the direction parallel with uprights, curvature will be introduced. Therefore, we have a surface with double curvature.

Figure 84 illustrates deformations of both a long cylinder and a simply supported cuved plate. The difference of the resulting surface is evident. The cylinder will be deformed into a similar cylindrical surface (if observation is made at a significant distance from the bulkheads), but the curved cylindrical web will be deformed into a new surface of double curvature. Consequently it is not desirable to use formulas for the determination of stresses based on pressurized cylinders.

Unfortunately, it is not a simple problem to derive the formulas for such curved plates. There appears to be no coverage in the literature on this subject.

Of some significance for this work is the "very thin" curved plate analysis. A search of the literature discloses the work of Föppl (Reference 22), who solved the case of "very thin" rectangular plates (without curvature), simply supported on all four sides, under normal loading. This method is presented in Section II and is applied to rectangular webs without curvature. The flat web case, however, can be regarded as a special case ($R = \infty$) of a curved plate.

Here an attempt is made to devise a method for the determination of approximate stresses and deformations in curved, simply supported, "very thin" sheets. Advantage will be taken of the theory of catenaries and the Marcus theory for analyzing rectangular plates.

The theory of Marcus is unique and simple. He considers two mutually perpendicular fibers of the plate, located parallel to the sides and passing thru the center of the plate. He applied his method to "thin plates." The total lateral-pressure loading, p, is separated by Marcus into two unknown components, p_a and p_b; where p_a is the partial loading applicable to the strip in the "a" direction and p_b the partial loading applicable to the strip in

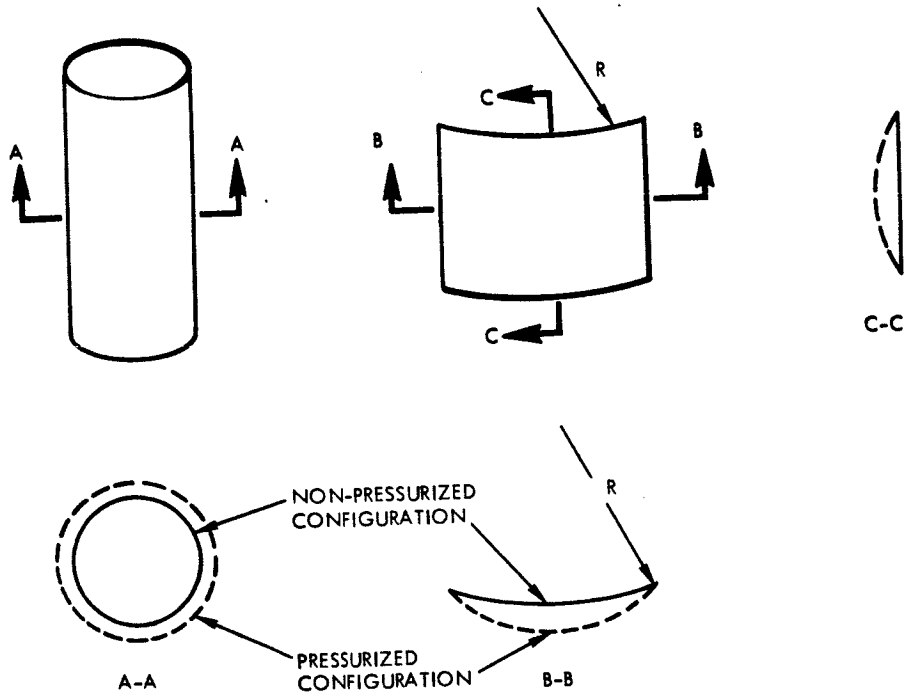

Figure 84. Comparison of Deformations Due to Internal Pressure, Cylinders, and Curved Simply Supported Sheets

the "b" direction. The equation $p = p_a + p_b$ holds. Then he determined the deflections of both strips in terms of p_a and p_b, and equated the two expressions. From this equation, in combination with the equation $p = p_a + p_b$, he was able to determine p_a and p_b. This leads to the coefficients η_i $(i = a, b)$ such that:

$$p_a = \eta_a p \tag{4-13}$$

$$p_b = \eta_b p \tag{4-14}$$

Having p_a and p_b, Marcus treated each strip as a beam in the usual manner to find the stresses and deflections. This method gives good agreement with test results and other theories of plates which could be checked.

We can use the same approach here for curved, simply supported, "very thin" webs, loaded laterally with internal pressure. The only difference will be in the configuration of the selected strips. Figure 85 shows two central strips under partial loadings p_a and p_b. Each strip, however, will be represented not as a beam but as a catenary. Axial extensibility and membrane-type of stresses will be considered.

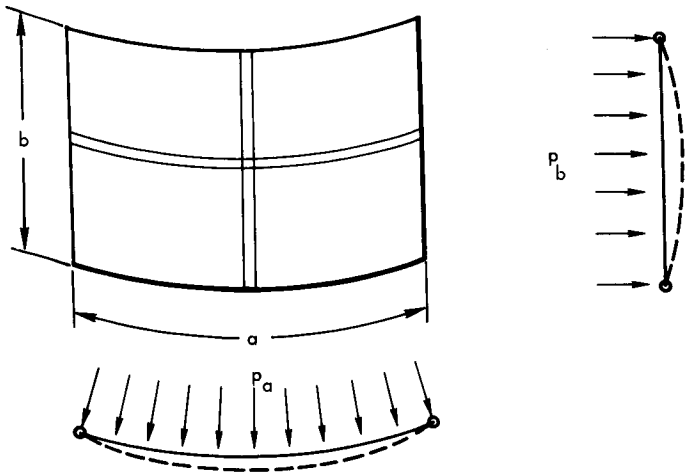

Figure 85. Curved "Very Thin" Plate, Simply Supported on All Four Sides

In the b direction, the catenary will be without initial deflection and will be loaded with the normal pressure loading p_b. In the a direction, the catenary will be loaded radially with the partial loading p_a and will be initially of circular shape. Dotted lines show the assumed deflections due to the loadings p_a and p_b. The deflection may be determined for each catenary. The extensibility of the material must be considered. Central deflections can be equalized, and this leads to the determination of p_a and p_b. Then, using the usual approach, the tensile stress in each catenary may be specified.

The derivation is rather simple, but proof will not be presented for justification of this approach, as there is no other existing procedure for comparison.

However, we can make a comparison for the special case of a rectangular flat membrane ($R = \infty$) using Föppl's procedure.

Square Plate

For a square plate, $a = b$, $p_a = p_b = 0.5\ p$. The tension in the catenary of unit width is given as:

$$H = 0.347 \sqrt[3]{AE\ p_a^{\ 2} a^2} \qquad (4\text{-}15)$$

Deflection:

$y = \frac{M}{H}$, where M = the moment in the middle of the span of the catenary.

$$M = \frac{p_a a^2}{8} \tag{4-16}$$

$$y = \frac{p_a a^2}{(8)0.347\sqrt[3]{AE\, p_a^2 a^2}} = \frac{p_a a^2}{2.78\sqrt[3]{AE\, p_a^2 a^2}} \tag{4-17}$$

Rectangular Plate

The system is shown in Figure 86 .

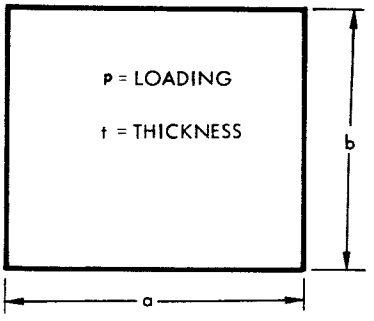

Figure 86. Rectangular Plate

$$p_a + p_b = p \tag{4-18}$$

$$M_a = \frac{p_a a^2}{8} \tag{4-19}$$

$$M_b = \frac{p_b b^2}{8} \tag{4-20}$$

Deflections:

$$y_a = \frac{M_a}{H_a} = \frac{p_a a^2}{8H_a} \tag{4-21}$$

$$y_b = \frac{M_b}{H_b} = \frac{p_b b^2}{8H_b} \tag{4-22}$$

where H_a and H_b are internal tensions in a and b directions. From the developed catenary theory, these values are found to be:

$$H_a = 0.347 \sqrt[3]{AE\, p_a^2 a^2} \tag{4-23}$$

$$H_b = 0.347 \sqrt[3]{AE\, p_b^2 b^2} \tag{4-24}$$

Deflections of both catenaries must be equal.

$$y_a = y_b \tag{4-25}$$

$$\frac{p_a a^2}{(0.347)\, 8 \sqrt[3]{AE\, p_a^2 a^2}} = \frac{p_b b^2}{(0.347)\, 8 \sqrt[3]{AE\, p_b^2 b^2}} \tag{4-26}$$

If Equation 4-18 is considered together with Equation 4-26, it will lead to the following results:

$$p_a = \eta_a p \text{ and } p_b = \eta_b p \tag{4-27}$$

where

$$\eta_a = \frac{b^4}{a^4+b^4} \text{ and } \eta_b = \frac{a^4}{a^4+b^4} \tag{4-28}$$

These results are the same as for a "thin plate" determined by Marcus, except that, in this case, p_a and p_b apply to the catenaries.

To demonstrate ranges of representative values for η_a and η_b, Table 3 was prepared for a range of panel aspect ratios.

Table 3. Representative Values of η_a and η_b for a Range of Panel Aspect Ratios

Panel Aspect Ratios, a/b											
a/b	1	1.1	1.2	1.3	1.4	1.5	1.6	1.7	1.8	1.9	2.0
η_a	0.5	0.408	0.325	0.260	0.220	0.165	0.133	0.108	0.088	0.070	0.059
η_b	0.5	0.592	0.675	0.740	0.798	0.835	0.867	0.892	0.912	0.930	0.941

Then:

$$H_a = 0.347\sqrt[3]{AE\,p_a^2 a^2} \text{ and } H_b = 0.347\sqrt[3]{AE\,p_b^2 b^2} \qquad (4\text{-}29)$$

The tensile stresses are:

$$\sigma_a = H_a/A \text{ and } \sigma_b = H_b/A \qquad (4\text{-}30)$$

Deflection:

$$y = \frac{p_a a^2}{8H_a} = \frac{p_b b^2}{8H_b} \qquad (4\text{-}31)$$

Results of the above derivation are compared with Föppl's theory for several(50) examples (Figure 87). The ratios of the sides of the flat plates are chosed between 0.75 to 1.50.

Figure 30 shows the comparison of the Föppl theory with test results. We can see that the Föppl theory leads to results which are about 20 percent higher for pressure loading from 0 to 20 psi.

The results obtained with the catenary method are lower than Föppl's results and correspondingly closer to the test results. Comparison (Föppl's theory versus catenary approach) graphs for deflection and stresses σ_a and σ_b are given in Figure 87. This comparison gives us some confidence that the approach leads to reasonable results. After this conclusion, we proceed to the curved "very thin" plate.

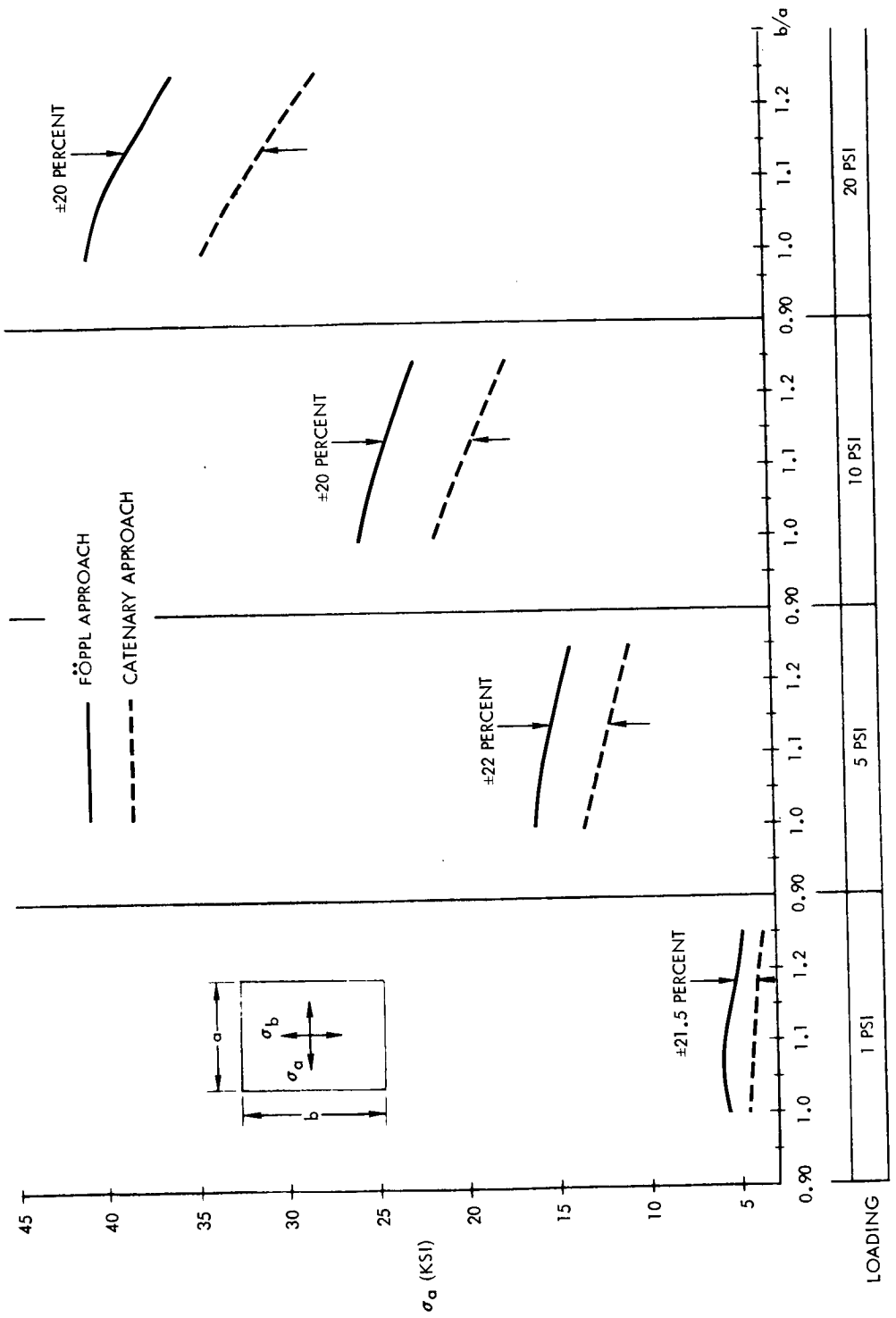

Figure 87. Comparison of Results: Föppl Versus Catenary Theories (Sheet 1 of 3)

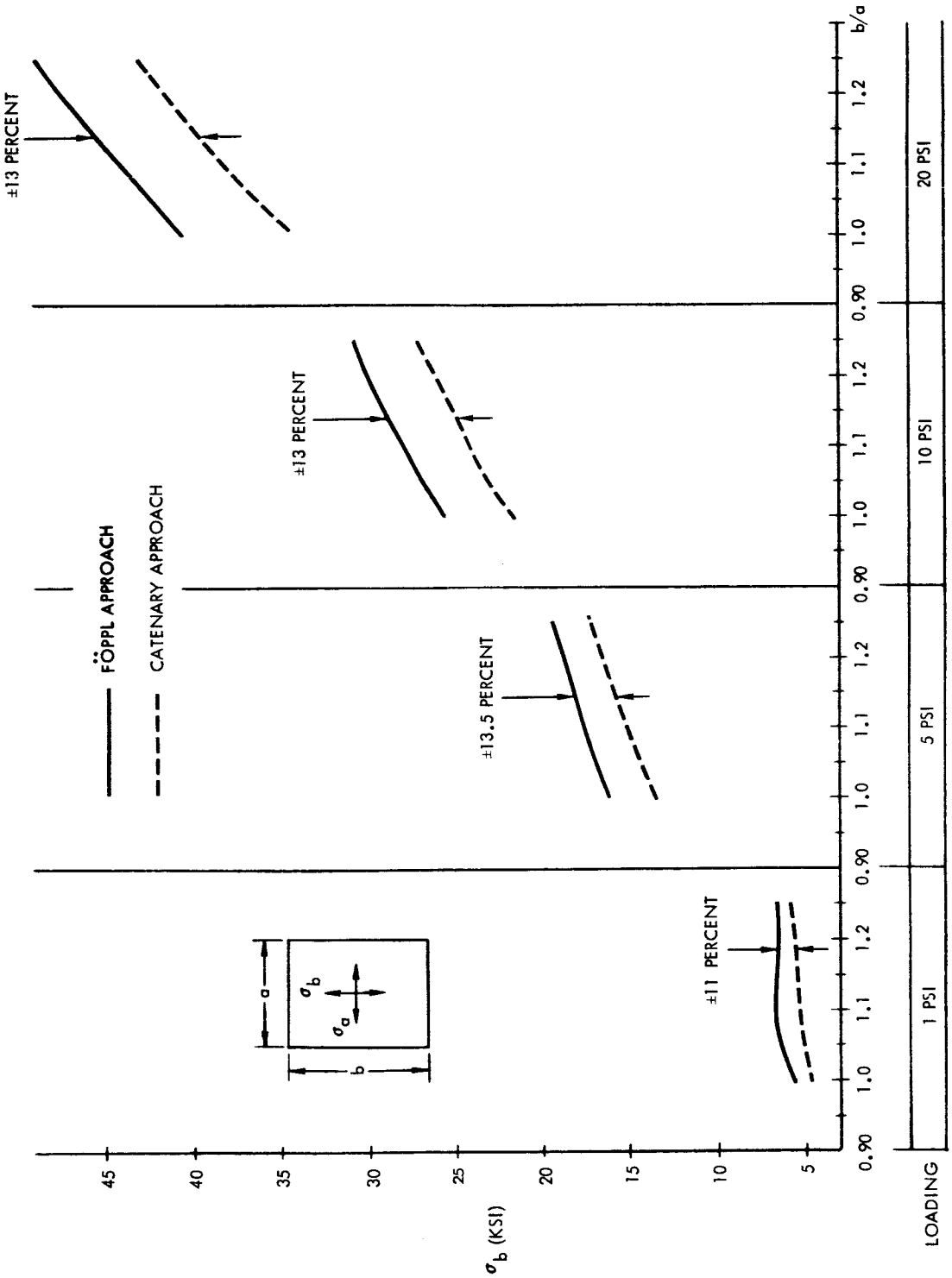

Figure 87. Comparison of Results: Föppl Versus Catenary Theories
(Sheet 2 of 3)

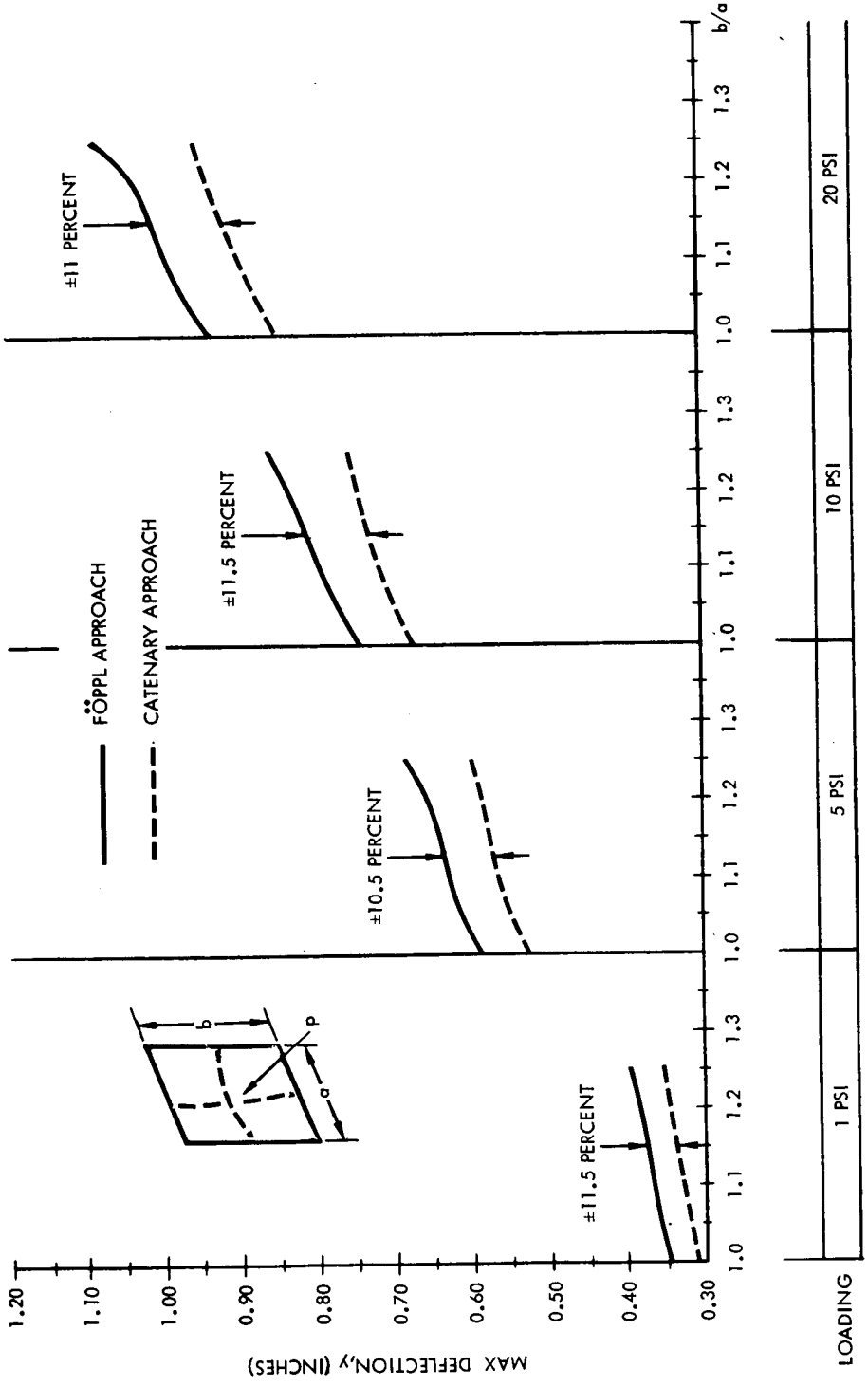

Figure 87. Comparison of Results: Föppl Versus Catenary Theories
(Sheet 3 of 3)

Curved Plate

Reference is made to Figure 85 and the corresponding discussion given with this figure. For the strip in the b direction, we have the formula for deflection. For the a direction, such a formula may be derived. In connection with Figure 88, the following nomenclature is used:

S = initial length of catenary

h = initial deflection of the catenary

p = loading on catenary

ℓ = span between the supports

R = radius

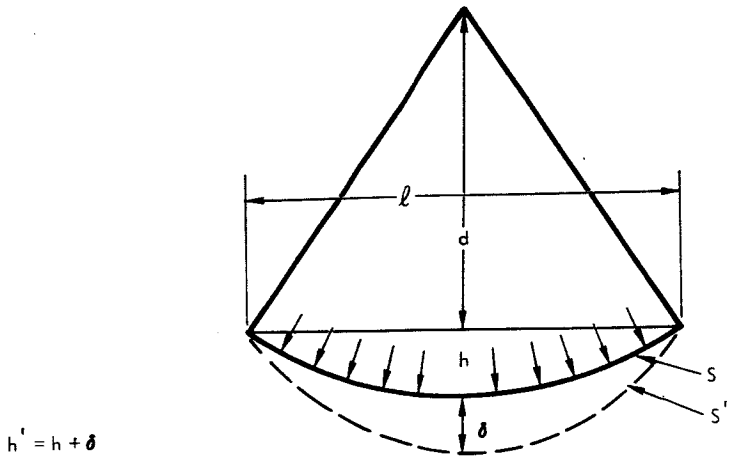

Figure 88. Catenary Loaded Radially

Due to the loading, p, the catenary will deflect an additional distance, δ, and initial length S will be increased by ΔS.

$$\Delta S = \frac{pRS}{EA}, \quad S' = S + \Delta S \tag{4-32}$$

The value of h will be increased to h'. The following geometric relation is known between S', h', and ℓ:

$$S' = \sqrt{\ell^2 + \frac{16}{3} h'^2} \tag{4-33}$$

From this formula, h' can be determined:

$$h' = 0.433\sqrt{(S')^2 - \ell^2} \tag{4-34}$$

Actual deflection is:

$$\delta = h' - h \tag{4-35}$$

where h = R - d

$$d = \frac{1}{2}\sqrt{4R^2 - \ell^2} \tag{4-36}$$

Finally:

$$\delta = 0.433\sqrt{\left(S + \frac{pRS}{EA}\right)^2 - \ell^2} + \frac{1}{2}\sqrt{4R^2 - \ell^2} - R \tag{4-37}$$

The shorter radius, r<R, corresponds to the deflected shape and must be determined in order to find stresses in the deformed catenary. Figure 89 shows the relation of deformed catenary shape with respect to undeformed.

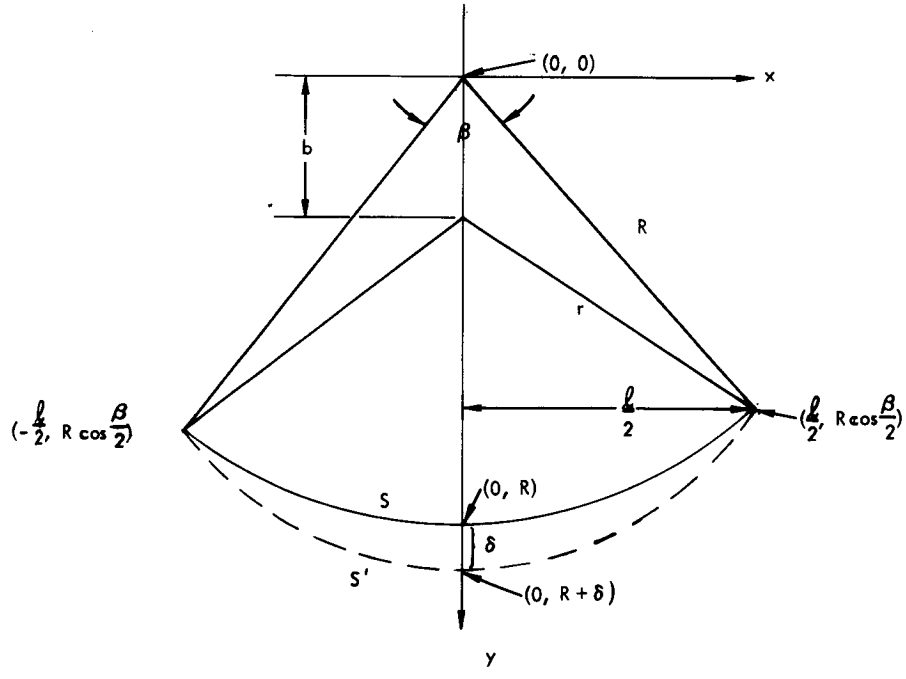

Figure 89. Relationship Between the Deformed and the Undeformed Catenary

The equation of the deformed shape is assumed to be:

$$x^2 + (y - b)^2 = r^2 \tag{4-38}$$

Also $r = R + \delta - b$

Designate $R + \delta = u$.

The coordinates of the point $\left(\frac{\ell}{2},\ R \cos\frac{\beta}{2}\right)$ can now be used in connection with the Equation 4-38.

$$\left(\frac{\ell}{2}\right)^2 + \left(R \cos\frac{\beta}{2} - b\right)^2 = r^2 = (u - b)^2 \tag{4-39}$$

From this equation can be determined:

$$b = \frac{u^2 - R^2 \cos^2\frac{\beta}{2} - \frac{\ell^2}{4}}{2\left(u - R \cos\frac{\beta}{2}\right)} \tag{4-40}$$

Consequently

$$r = u - \frac{u^2 - R^2 \cos^2\frac{\beta}{2} - \frac{\ell^2}{4}}{2\left(u - R \cos\frac{\beta}{2}\right)}, \quad \beta^\circ = 180^\circ \frac{S}{\pi R} \tag{4-41}$$

The new tension in the catenary will be:

$$H = pr \text{ or } \sigma = \frac{H}{A} \tag{4-42}$$

The solution of the problem can now be attempted. Assume the internal pressure to be p. The unknown loading which is prescribed for b direction is p_b. The unknown loading which is defined for a direction is p_a. Then the maximum deflection for the central strip in the b direction is:

$$y_b = \frac{p_b b^2}{2.78 \sqrt[3]{AE\, p_b^2 b^2}} \tag{4-43}$$

Maximum deflection of strip a:

$$y_a = 0.433\sqrt{\left(a + \frac{p_a R a}{EA}\right)^2 - \ell^2} + \frac{1}{2}\sqrt{4R^2 - \ell^2} - R \qquad (4\text{-}44)$$

where a = s.
Necessary condition, $y_b = y_a$

$$\frac{p_b b^2}{2.78\sqrt[3]{AE\, p_b^2 b^2}} = 0.433\sqrt{\left(a + \frac{p_a R a}{EA}\right)^2 - \ell^2} + \frac{1}{2}\sqrt{4R^2 - \ell^2} - R \qquad (4\text{-}45)$$

Also $p_a = p - p_b$

This leads to:

$$\frac{p_b b^2}{2.78\sqrt[3]{AE\, p_b^2 b^2}} - 0.433\sqrt{\left[a + \frac{(p-p_b) R a}{EA}\right]^2 - \ell^2} = \frac{1}{2}\sqrt{4R^2 - \ell^2} - R \qquad (4\text{-}46)$$

where

$$b = 2R \sin\frac{\beta^\circ}{2}$$

$$\beta^\circ = 180^\circ \frac{a}{\pi R}$$

Equation 4-46, however, is not easily solved, because of the large numbers and small differences involved. Consequently, it would be difficult to obtain with the slide rule a solution as a result of trial and error process. For this purpose, however, a FORTRAN program is added in the appendix which automatically leads to the required solution.

The input:

a = length of curved side, in.

b = length of straight side, in.

R = radius of curvature, in.

E = Young's modulus, psi.

t = thickness, in.

p = total loading, lb.

The output will be:

p_b = partial loading assigned to b direction

From the above equation, p_b can be determined. Having $p_b = \eta_b p$, we can perform calculation of both catenaries:

$$y_b = \frac{p_b b^2}{2.78 \sqrt[3]{AE\, p_b^2 b^2}} \tag{4-47}$$

$$H_b = 0.347 \sqrt[3]{AE\, p_b^2 b^2} \tag{4-48}$$

$$H_a = p_a \left[u - \frac{u^2 - R^2 \cos^2 \frac{\beta}{2} - \frac{\ell^2}{4}}{2\left(u - R \cos \frac{\beta}{2}\right.} \right] \tag{4-49}$$

where

$$\beta^\circ = 180^\circ \frac{S}{\pi R}$$

$$u = R + \delta$$

$$p_a = p - p_b$$

Finally

$$\sigma_b = \frac{H_b}{A}, \quad \sigma_a = \frac{H_a}{A} \tag{4-50}$$

This state of stress is shown in Figure 90 and represents the membrane stresses due to internal pressurization at the middle-point of the plate, in the prebuckling stage. There is no theory nor test results at this time with which we can compare the derived approach. However, since this approach was satisfactory for the special case at $R = \infty$, we will assume that the results also are satisfactory for $R \neq \infty$.

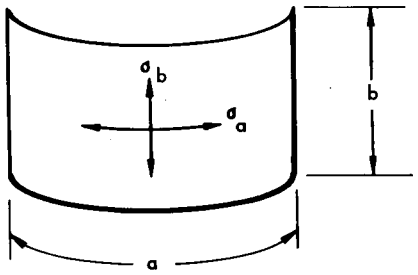

Figure 90. Stresses in Prebuckled Web Due to Internal Pressure

LATERAL LOADING - EXTERNAL PRESSURE

Under external lateral-pressure loading on the curved panel, it will be assumed that lateral loading is acting in the inward radial direction toward the center of curvature. Only uniformly distributed loading will be considered.

It can be noted that this problem is different from the previous problem because the strip through the center of the web panel, oriented parallel with the flanges, is curved and obviously stressed in compression. The orthogonal strip, which is parallel to the uprights, is still stressed in tension and does not differ from the previous case for internal pressure.

The preceding discussion also applies here: The curved plate cannot be treated exactly as a cylinder.

Prebuckling stage

Assuming that the modulii of elasticity for tension and compression are approximately equal, we may conclude that the behavior of the plate will be similar to the previous case. Consequently, in the prebuckling stage we will assume the same distribution coefficients η_i as in the case of internal pressurization. The only difference will be that the curved strip will be stressed in compression, but the orthogonal straight strip, as before, will be stressed in tension. Consequently, Equation 4-46 will apply for determination of the partial loadings, p_a and p_b. The stresses will be numerically equal to the previously established stresses, except for the curved strip, where the stress will be compression (negative sign):

$$\sigma_a = -\frac{H_a}{A} \quad , \quad \sigma_b = +\frac{H_a}{A} \tag{4-51}$$

Buckling

The critical external pressure which will cause buckling of a cylindrical surface can be assumed, with reasonable accuracy, to be approximately equal to that critical external pressure, derived by von Mises (Reference 38), which is:

$$p^{\circ}_{cr} = \frac{2E\,h}{a\,(n^2-1)\left[1+\left(\frac{n\ell}{\pi a}\right)^2\right]^2} + \frac{2Em^2}{3\left(m^2-1\right)}\left[n^2-1+\frac{2n^2-\frac{m+1}{m}}{1+\left(\frac{n\ell}{\pi a}\right)^2}\right]\frac{h^3}{a^3} \tag{4-52}$$

This formula is not very practical because of complexity and the number of required algebraic manipulations. Since usage of this formula appears impractical, no further usage will be made of it at present. Instead, a much simpler formula (4-53) can be recommended. It results in solutions in good agreement with the above formula of von Mises.

$$p^{\circ}_{cr} = \frac{-2\pi}{3\sqrt{6}\left(1-\mu^2\right)} 3/4 \frac{Et^2}{dR}\sqrt{\frac{t}{R}} \qquad (4\text{-}53)$$

where

p°_{cr} = critical external pressurization, psi

μ = Poisson's ratio

E = modulus of elasticity, psi

t = thickness of the wall, in.

d = length of upright, in.

R = radius of curvature, in.

with $\mu = 0.3$, the equation reduces to:

$$p^{\circ}_{cr} = -0.92 \frac{Et^2}{dR}\sqrt{\frac{t}{R}} \qquad (4\text{-}54)$$

Up to this level, stresses in the web are still determinable by the method described for the prebuckling stage.

Postbuckling Stage

After buckling occurs, complete collapse of the sheet does not occur, but the model will be changed. When panels buckle, which are relatively long in the curved (or circumferential) direction, the strips oriented longitudinally (or in the direction of the uprights) will support most of the pressure loading. The relatively longer curved lateral strips are much more flexible due to both added length and curvature.

In the case of the web panel short in the circumferential direction and long in the longitudinal direction, the short curved elements will buckle into reversed curvature and support most of the external pressure load by tension in the elements.

In the usual practical case, these two extremes will seldom occur. There will be some distribution of loading between the orthogonal strips depending on such parameters as web panel aspect ratio, curvature, R/t, etc.

Consequently, depending on the ratio of the sides of the curved sheet, a/b, two possibilities exist. One possibility holds that the ratio of sides of the plate is such that the strip, b, cannot develop a deflection of the magnitude to permit the strip, a, to take the new (reversed) shape of catenary, which is stressed in tension. In this case, the whole loading, after buckling occurs, will be carried by the set of strips in the b direction, and will be carried exclusively to the flanges. In the absence of a more accurate study of this local phenomenon, it is assumed that the total loading will be taken by strips b and transferred to the flanges, and the distribution will follow a triangular or trapezoidal shape. The other possibility is that the new interaction of two catenaries may be calculated in the manner given for internal-pressure lateral loading of curved webs.

COMBINED VERTICAL AND LATERAL LOADING

Separate applications of vertical and lateral pressure loadings have been previously discussed. In this section, the interaction effects due to combined simultaneous loading will be studied. Simultaneous loadings primarily affect the web.

Superimposition

In the prebuckling stage, stresses throughout the beam will be well below yield stresses. Thus, stresses caused by vertical loading and lateral pressure may be superimposed by algebraic addition for all elements of the beam.

This approximation should be fairly good. Thin plate deflections are usually not linear, but deviations from linearity in the case of aluminum (Reference 19, page 291) for relatively low loading are not significant (Figure 30). Since web stresses are caused by both vertical and pressure loadings, it seems reasonable to superimpose these stresses. The procedure may be applied in the same manner as for flat webs, as described in Section III. Compressive web stress in the diagonal direction may be found from

$$\sigma_I = \sigma_c + {}_H\sigma_l \qquad (4\text{-}55)$$

where σ_c is the compressive stress due to vertical loading

$$\left(|\sigma_c| = |\sigma_t| = |\tau|\right),$$

and ${}_1\sigma_H$ results from lateral pressure loading. For example, assume that horizontal and vertical stresses are σ_a and σ_b respectively, found by the procedure for lateral loading - external pressure.

$$ {}_H\sigma_1 = \sigma_a \operatorname{Cos}^2 \alpha + \sigma_b \operatorname{Sin}^2 \alpha \qquad (4\text{-}56) $$

For α = 45 degrees, Equation 4-56 will be

$$ {}_H\sigma_1 \approx 0.5\,\sigma_a + 0.5\,\sigma_b = \frac{\sigma_a + \sigma_b}{2} \qquad (4\text{-}57) $$

Similarly, tensile stress in the diagonal direction, σ_{II} may be defined by

$$ \sigma_{II} = \sigma_t + {}_H\sigma_2 \qquad (4\text{-}58) $$

where σ_t is the tensile stress due to vertical loading, and ${}_2\sigma_H$ is the stress in the same direction (45 degrees) due to lateral pressure loadings, determined in a similar fashion to ${}_1\sigma_H$, using the same formulas but using the complementary angle.

The web-buckling phenomenon divides the prebuckling and postbuckling phases. Figure 91 illustrates σ_I versus τ for superimposed vertical and lateral pressure loading, showing the effects of internal and external pressure on buckling. The prediction of web buckling under combined loading may be made with an interaction formula from Reference 39, (Equation 4-59 in the following postbuckling discussion). At buckling, the analytical structural model changes to a set of catenaries as in the noncurved web case. The presence of internal pressure will postpone web buckling, while external pressure will decrease web stability and therefore hasten buckling. The external lateral pressure case involves a more complex buckling system due to the additional "snap-through" buckling caused by the direction of the pressure. This buckling phenomenon is shown in Figure 91, diagram B as the first perturbation as τ increases.

There are two possible buckling sequences for the combined-loading, external-pressure case. In one case (Figure 91, diagram B), the curved web snap-through due to pressure will occur before critical shear load τ'_{cr} is reached. After snap-through, the curved web has reversed curvature. After this happens, the curved web will become a web stressed in tension and will follow the usual path, until τ^* occurs. Then the shear load will tend to pull the web panel into a flat configuration, while lateral pressure will be taken by set of prestressed catenaries.

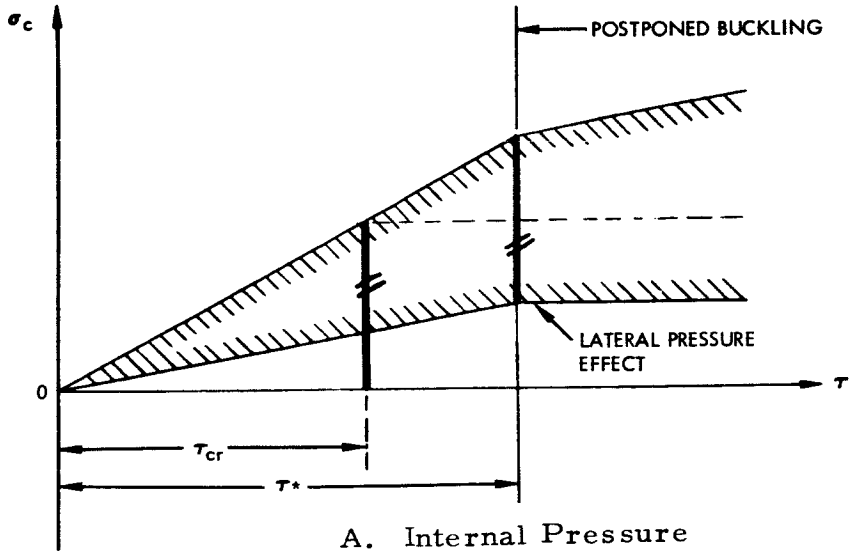

A. Internal Pressure

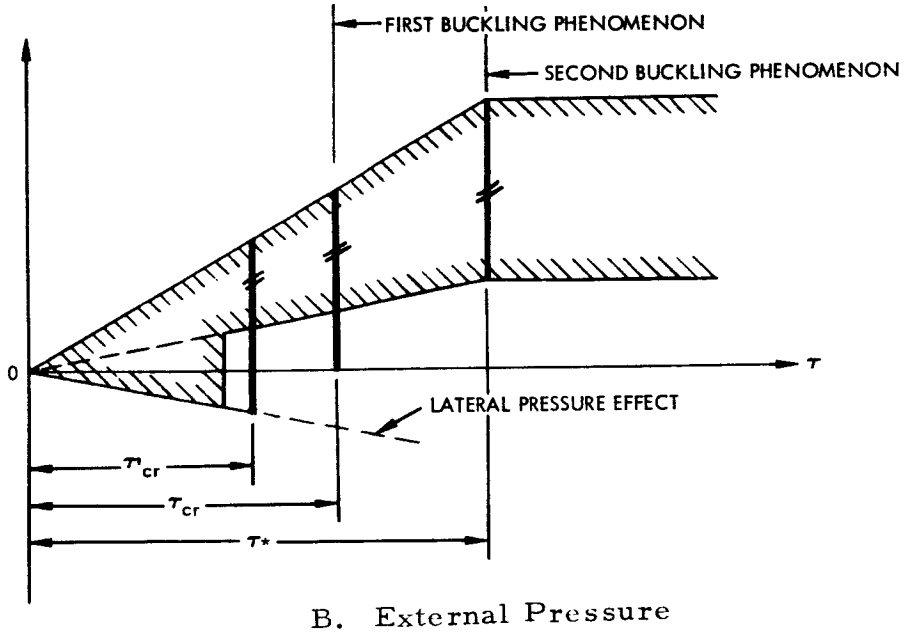

B. External Pressure

Figure 91. Effect of Pressure on Curved Web Shear Buckling
(Sheet 1 of 2)

In the second case (Figure 91, diagram C), shear buckling, τ'_{cr}, into diagonal-tension elements occurs prior to the pressure load causing snap-through or pressure buckling. At the time of buckling, the web tends

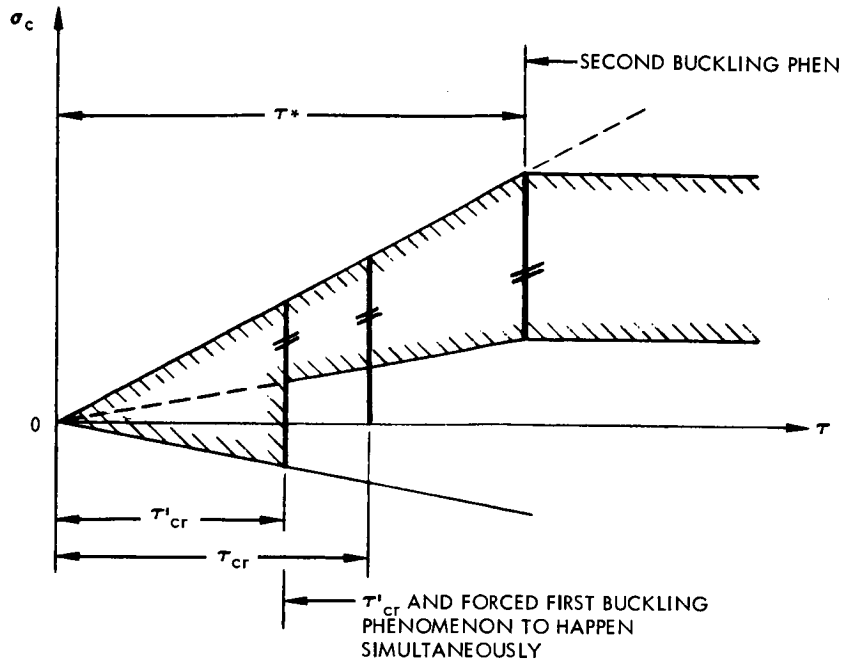

C. Shear Buckle Before "Snap Through"

Figure 91. Effect of Pressure on Curved Web Shear Buckling (Sheet 2 of 2)

to pull into a flat plane, and external pressure then tends to induce reverse curvature in the buckled plate. Pressure buckling or snap-through occurs simultaneously with the diagonal-tension buckle. It is expected that a relatively large shear deflection will occur at web buckling due to the curved diagonal tension elements straightening out.

In both cases, as can be seen from Figure 91 the behavior of externally pressurized webs after snap-through occurs is similar to the behavior of internally pressurized webs. The change of curvature makes the web internally pressurized. If the horizontal dimension is larger than the vertical dimension, snap-through buckling may not occur at all.

For the postbuckling regime, the structural model of the web changes to diagonal-tension elements. Lateral pressure is assumed to raise the tensile stress in these elements (because the whole load will be taken by tensile elements in one direction) without affecting the orthogonal compressive stresses.

Determination of Final Critical Buckling Combination

Combined-loading buckling may be predicted through the use of the following equation (References 37 and 38):

$$\left(\frac{\tau^*}{\tau_{cr}}\right)^2 + \frac{p}{p^\circ_{cr}} = 1 \qquad (4\text{-}59)$$

where τ_{cr} is found as explained in this Section (See Web-Buckling Phenomenon) and p is the applied lateral pressure with a positive sign for internal pressure and negative sign for external pressure.

The value of p°_{cr} (an external pressure with negative sign value) remains to be found to enable use of the equation to predict τ^{*}. A method of calculating p°_{cr} is described under Lateral Loading - External Pressure. The derivation of the method is based on lateral pressure only, with no longitudinal load. A pressurized cylinder may have longitudinal shell stresses due to pressure on the bulkheads. In this study, however, no effort is made to define these effects. It is assumed that the curved beams under study have no pressure-induced stress components in the axial (vertical) direction.

It may be noted that Equation 4-59 permits the determination of critical stresses without the necessity of using superimposition, as described in Section II and used for straight beams. This simplifies the combined-loading analysis procedure considerably.

Postbuckling Stage

As in the case of the straight beam, it will be assumed that the compressive stress in the web increases with shear loading up to the buckling load, and then stays approximately constant (the increase is small) as the diagonal-tension elements are stressed with higher loading (Figure 42). The principal compressive stress in this case increases slowly under postbuckling conditions. Equation 4-8 defines the contribution of vertical loading. The contribution of the lateral loading will be ${}_{H}\sigma_{1}^{*}$. Finally, the compressive stress will be

$$\sigma_{I} = -\tau_{o}(1-k^{*}) \sin 2\alpha + {}_{H}\sigma_{1}^{*} \qquad (4\text{-}60)$$

where k^{*} is a function of τ_{o} / τ_{cr} obtainable from Figure 80.

The tensile stress due to vertical loading is:

$$\sigma_{II}^{1} = \tau_{o} (1-k^{*}) + \frac{k^{*} \tau_{o}}{\sin 2\alpha} + {}_{H}\sigma_{2}^{*} \qquad (4\text{-}61)$$

where τ_{o} is a fictitious shear due to total vertical loading, if buckling were prevented; $\tau_{o} = P/dt$, where d is the height of the web. The tension stress in the diagonal element consists of two components, one due to applied shear load on the web panel, and another due to lateral pressure. The contribution

due to lateral loading which carries over from the prebuckling stage is ${}_H\sigma_2^*$. The stress ${}_H\sigma_2^*$ results from that part of the lateral pressure loading applied up to buckling, p'. The remainder of the lateral loading is caused by pressure component

$$p'' = p - p' \tag{4-62}$$

This load is reacted by the diagonal strips of the postbuckled model. Consequently, each catenary will be:

1. Loaded with p'' while initially prestressed with $\sigma_{II}' = \sigma_t + {}_H\sigma_2^*$
2. Deflected an amount, y, due to lateral pressure loading, p'

In Section III, methods of analyzing the catenaries are defined, direct formulas are given, and FORTRAN solutions are provided for more complex problems. The results in either case will include the required tensile stress, σ_{II} ($\sigma_{II} = H/A$), and the deflection, y.

The resulting stress, σ_{II}, must be less then the ultimate stress, σ_{tu}, where σ_{tu} includes stress concentration effects of web-upright and web-flange attachments.

SEQUENCE OF LOADING APPLICATION

A study of the interaction between vertical and lateral pressure loading leads to the fundamental conclusion that, due to the presence of lateral loading, the buckling of flat web may be postponed until higher shear loads are applied.

When combined loading reaches the buckling level, the structural analytical model changes, and loading beyond this level will be taken by a different structural model. The new model is represented by a diagonal set of catenaries.

Before buckling occurs, the loads are resisted by plate-action, which is a two-dimensional system. The plate resists the loading by in-plane two-directional stresses and, due to the loading, is stressed and strained in shear. After buckling occurs, the system immediately changes into a one-dimensional system, a set of catenaries, which then continues to take the rest of the loading (small additional compression in the postbuckling stage due to vertical loading is not significant). Generally, the catenaries are more flexible than the plate, as they are stressed in only one direction. Lateral deflections will therefore be larger.

Consequently, the following conclusion can be made: after buckling occurs, compression (in the diagonal direction) will not continue to increase significantly (Wagner even recommends that this increase be disregarded). The tension (in the diagonal direction) will continue to increase, faster than in the prebuckling stage. Deflection due to the lateral loading also will increase faster, because the system is one-dimensional.

This leads to the conclusion that the rate of increase of stresses and deformations will be generally changed at the buckling level. The total loading at the buckling level may be divided into two components: the first part resisted by plate-shearing stress (prebuckling stage) and the second part resisted by catenary action (postbuckling stage).

It has been demonstrated that the amount of lateral loading influences the buckling level. With additional internal pressure, the buckling shear level will be raised. Buckling will occur later, and consequently less load remains to be taken by the catenary system.

OUTLINE OF CURVED WEB ANALYSIS PROCEDURE

The procedures discussed in this section follow the approach that was taken for the analysis of straight beams. The first procedure discussed is the analysis of curved beams which assumes that the prebuckling principal compression stresses are "frozen" for the analysis of postbuckling behavior. This procedure is presented as background information.

The recommended procedure is not dependent on the assumption of frozen stresses for the lateral-pressure loadings. It is assumed that all of the postbuckling pressure loads are taken by the catenaries. The analysis depends only on the final shears and pressures. The law of conservation of energy vigorously holds for the nonlinear analysis.

First Procedure

Assume a partial-tension-field beam system loaded with vertical loading, g_o, and internal pressure loading, p_o. The beam geometric data, material properties, and static load systems are known. In any section of the beam, we can determine bending moment, torsional moment, and shear. Only shear will be required for web analysis.

1. The first step will be to determine the following:

$$\tau_{cr} = K_s \frac{\pi^2 E h^2}{12 R^2 Z^2} \quad \text{(Equation 4-3)}$$

$$p^o_{cr} = -0.92 \frac{E t^2}{dR} \sqrt{\frac{t}{R}} \qquad (4\text{-}63)$$

$$\left| \tau_o \right| = \left| \frac{S}{dt} \right| = \left| \sigma_c \right| = \left| \sigma_t \right|$$

Now it is possible to determine whether the web are in the prebuckling or the postbuckling stage. The critical combination (τ^*, p^*) is selected under which we prefer to have the web buckled. Initial application of internal pressure, p, postpones buckling. So, one way to determine buckling phase would be to enter into the interaction equation the whole p_o or any $p^* \leq p_o$ at which we would prefer to have the web buckled (See Equation 4-59)

$$\left(\frac{\tau^*}{\tau_{cr}} \right)^2 + \frac{p^*}{p^o_{cr}} = 1 \qquad (4\text{-}64)$$

From this equation τ^* will be determined.

If $\tau^* < \tau_o$, the web is in the postbuckling range.

If $\tau^* \geq \tau_o$, the web is in the prebuckling range.

It may be that we want to have the web buckled at certain $\tau^* < \tau_o$. From the interaction equation, we can determine the corresponding p^*.

If $p^* < p_o$, the web is in the postbuckling range.

If $p^* \geq p_o$, the web is in the prebuckling range.

Consequently, both methods give the critical combination (τ^*, p^*) under which the web buckles, and the change in the system occurs.

If the prebuckling stage governs, then, from Equation 4-46, p_b will be determined.

Then, determine:

H_b using Equation 4-48

H_a using Equation 4-49

σ_a using Equation 4-50

σ_b using Equation 4-50

Finally, determine ${}_H\sigma_1$ and ${}_H\sigma_2$ with Equation 4-56. The lateral deflection then is given by

$$\delta = \frac{p_b b^2}{2.78 \sqrt[3]{AEp_b^2 b^2}} \tag{4-64}$$

The compression stress in diagonal direction is given by

$$\sigma_I = \sigma_c + {}_H\sigma_1 \tag{4-65}$$

The tension stress is given by

$$\sigma_{II} = \sigma_t + {}_H\sigma_2 \tag{4-66}$$

Thus, the state of stress in the web is determined by (σ_a, σ_b, τ_o).

If, however, the postbuckling range governs, then the following method leads to the required results.

Using p^* in connection with Equation 4-46, determine p_b^* and p_a^*. Then determine

H_b^* using Equation 4-48

H_a^* using Equation 4-49.

$\left.\begin{matrix}\sigma_a^* \\ \sigma_b^*\end{matrix}\right\}$ using Equation 4-50.

Now, using Equation 4-56, the "frozen stresses" can be determined.

$$H\sigma_1^* \text{ and } H\sigma_2^*$$

Then we are dealing with the changed model which is not curved any more but is a set of pretensioned catenaries.

τ_o/τ_{cr} leads to determination of k^* with Figure 80 and the graph in Figure 81 leads to determination of angle α_{PDT}, which will be modified.

The final compression stress then is determined with the formula

$$\sigma_I = -\tau_o (1-k^*) \sin 2\alpha + {}_H\sigma_1^* \qquad (4\text{-}67)$$

The tension component σ_{II} is determined with the FORTRAN program or with the corresponding formula for the pretensioned catenary. The length of this catenary is slightly increased due to straightening effect, as described in this Section under "Postbuckling Stage." The prestressing is $H_o = \sigma_{II} \times 1 \times t$

where

$$\sigma_{II}' = \frac{2k^* \tau_o}{\sin 2\alpha} + \tau_o (1-k^*) \sin 2\alpha + {}_H\sigma_2^* \qquad (4\text{-}68)$$

The initial deflection is

$$\delta^* = \frac{p_b^* b^2}{2.78 \sqrt[3]{AEp_b^{*2} b^2}} \qquad (4\text{-}69)$$

The output of the program is

Tension Stress, σ_{II}, (actually $H = \sigma_{II} A$)

Final lateral deflection, y.

A "flow-diagram" (Figure 92) illustrates the method.

This concludes the determination of stresses and deflections in the web of a curved beam, which is loaded simultaneously with vertical loads and lateral pressure. The resulting solution is unique and independent of the path of loading. If the results are found to be dependent on the sequence of loading, it is because of the assumption of "frozen" stresses.

The analysis will not be very different if external pressure instead of internal pressure is involved.

Some modifications are required as shown in the section on Lateral Loading - External Pressure, page 167.

Recommended Procedure

In Section III, it was stated it may be necessary to revise the assumption of the frozen state of stresses that remains after the buckling occurs. The same philosophy can be applied here too.

The governing principle now is that after final buckling occurs, the whole lateral loading will be taken by the set of the catenaries. Then the system will be perfectly conservative, and the results will not depend on the path. It will also eliminate the necessity for determination of the critical combination (τ^*, p^*).

The revised procedure then will be outlined as follows:

a. Determine as before

τ_{cr} using Equation 4-3

p^o_{cr} using Equation 4-54

$\left|\tau_o\right| = \left|\frac{S}{dt}\right| = \left|\sigma_c\right| = \left|\sigma_t\right|$, using Equation 4-1

b. As before, determine if the web is in a prebuckling or postbuckling range. Prebuckling range may be extended by application of more lateral loading. Consequently, any $p^* \leq p_o$ can be selected under which it is desirable to get the web buckled. This selected value of p* will be entered into the equation of interaction:

$$\left(\frac{\tau^*}{\tau_{cr}}\right)^2 + \frac{p^*}{p_{cr}^o} = 1 \qquad \text{(Equation 4-59)}$$

From this equation τ^* will be determined. If $\tau^* < \tau_o$ is obtained, the web is in the postbuckling range. If $\tau^* \geq \tau_o$ is obtained, the web is in the prebuckling range.

c. If in the prebuckling range, determine the loading p_b and p_a using Equation 4-46. Then find:

H_b using Equation 4-48

H_a using Equation 4-49.

σ_b and σ_a using Equation 4-50

Now the state of the stresses is given by

$$(\sigma_b, \sigma_a, \tau_o)$$

and the horizontal deflection

$$\delta = \frac{p_b b^2}{2.78 \sqrt[3]{AEp_b^2 b^2}} \qquad \text{(Equation 4-64)}$$

d. If in the postbuckling stage, proceed as follows: determine ratio τ_o/τ_{cr} and find the corresponding k using Figure 80. Then, with Figure 81 determine α_{PDT}. This value should be slightly modified, considering curvature.

Then, the final compressive stress is $\sigma_I = -\tau_o (1-k) \sin 2\alpha$ (in diagonal direction). The tension stress is determined from the FORTRAN

program or corresponding formulas. The input will be:

Prestressing $H_o = \sigma'_{II} \times l \times t$

where

$$\sigma'_{II} = \frac{2k\tau_o}{\sin 2\alpha} + \tau_o (1-k) \sin 2\alpha \qquad \text{(Equation 4-9)}$$

Initial deflection $\delta = o$

Loading on catenary is total p_o.

The length of catenary shall be diagonal length in accordance with the angle α and modified due to straightening of the fiber as is shown in the beginning of this section.

The output will be:

$H = \sigma_{II} A \rightarrow$ final tensional stress in diagonal direction

y = lateral deflection

For better illustration of this procedure a flow diagram is included.

SUMMARY

First Procedure

The first step will be to determine τ_{cr} (Equation 4-3) and p°_{cr} (Equation 4-54).

Then $\left|\tau_o\right| = \left|\frac{S}{dt}\right| = \left|\sigma_c\right| = \left|\sigma_t\right|$ Equation 4-1.

Substitute $p_o = p^*$ in Equation 4-59

$$\left(\frac{\tau^*}{\tau_{cr}}\right)^2 + \frac{p^*}{p^{\circ}_{cr}} = 1$$

To calculate the associated τ^*.

If $\tau^* < \tau_o$, the web is in the postbuckling range.

If $\tau^* \geq \tau_o$, the web is in the prebuckling range.

Alternately, substitute $\tau_o = \tau^*$ and determine the associated p^*.

If $p^* < p_o$, the web is in the postbuckling range.

If $p^* \geq p_o$, the web is in the prebuckling range.

For prebuckling phase, calculate

p_b	Equation 4-46
H_b	Equation 4-48
H_a	Equation 4-49
σ_a, σ_b	Equation 4-50
${}_1\sigma_h$, ${}_2\sigma_h$	Equation 4-56

$$\delta = \frac{p_b b^2}{2.78 \sqrt[3]{AE\, p_b^2\, b^2}}$$

$$\sigma_I = \sigma_c + {}_H\sigma_1$$

$$\sigma_{II} = \sigma_t + {}_H\sigma_2$$

For the postbuckling phase, calculate

p_b^* and p_a^*	Equation 4-46
H_b^*	Equation 4-48
H_a^*	Equation 4-49
σ_a^*, σ_b^*	Equation 4-50
${}_H\sigma_1$, ${}_H\sigma_2$	Equation 4-56
k^*	Equation 4-10
α_{PDT}, α	Figure 81

$$\sigma_I = -\tau_o (1-k^*) \sin 2\alpha + {}_H\sigma_1^*$$

The tension stress σ_{II} will be determined with the aid of the FORTRAN program for analyzing catenaries:

$$\sigma_{II}' = \frac{2k^* \tau_o}{\sin 2\alpha} + \tau_o (1-k^*) \sin 2\alpha + {}_H\sigma_2^*$$

$$H_o = \sigma_{II}' \times 1'' \times t''$$

Initial deflection,

$$\delta^* = \frac{p_b^* b^2}{2.78 \sqrt[3]{AE\, (p_b^*)^2\, b^2}}$$

FORTRAN program output will be the tension stress σ_{II} (actually $H = \sigma_{II}A$) and deflection y (see flow diagram, Figure 92).

Recommended Procedure

The analytical procedure follows:

Determine

τ_{cr} Equation 4-3

p°_{cr} Equation 4-54

$|\tau_o| = \left|\frac{S}{td}\right| = |\sigma_c| = |\sigma_t|$ Equation 4-1

Define buckling phase, pre-or postbuckling. As in the procedure, internal pressure increases buckling load. (See Equation 4-59.)

$$\left(\frac{\tau^*}{\tau_{cr}}\right)^2 + \frac{p^*}{p^{\circ}_{cr}} = 1$$

If p_o is substituted for p^*, an associated τ^* is found.

If $\tau^* < \tau_o$, the web is in the postbuckling phase.

If $\tau^* \geq \tau_o$, the web is in the prebuckling phase.

If in the prebuckling range of loading, determine p_a and p_b using Equation 4-46.

Then find:

H_b Equation 4-48

H_a Equation 4-49

σ_a and σ_b Equation 4-50

The state of stress in the web is defined by σ_a, σ_b, and τ_o, and maximum lateral deflection is

CURVED BEAM PARAMETERS

1. Geometry

A_{FL}	d
A_u	h
R	t

2. Material Properties

E	σ_{ty}
μ	σ_{tu}

3. Loading
   - Vertical , g_o
   - Lateral , p_o

4. Derived Loads
   - Bending moment , M_B
   - Torsional moment , M_T
   - Web shear , τ_o

BUCKLING CRITERIA TO DEFINE

1. Compute :

$$\tau_{cr} = k_s \frac{\pi^2 E h^2}{12 R^2 Z^2}$$

$$p^o_{cr} = -0.92 \frac{Et^2}{Rd}\sqrt{\frac{t}{R}}$$

2. Substitute above values and p =

a) $\left(\frac{\tau^*}{\tau_{cr}}\right)^2 + \frac{p_o}{p^o_{cr}} = 1$

If $\tau^* < \tau_o$, web is in prebucklin

If $\tau^* \geq \tau_o$, web is in postbucklin

OR

b) Substitute $\tau = \tau^*$ in equation

If $p > p_o$, web is in prebuckli

If $p \leq p_o$, web is in postbuckli

BUCKLED STAGE

DETERMINE "FROZEN" COMPONENT

$$\frac{p^*_b b^2}{2.78\sqrt[3]{AE\, p^{*2}_b b^2}} - 0.433\sqrt{\left[a + \frac{(p^* - p^*_b)Ra}{AE}\right]^2 - \ell^2} = \frac{1}{2}\sqrt{4R^2 - \ell^2} - R$$

Find $H^*_b = 0.347\sqrt{AE\, p^{*2}_b b^2}$

$$H^*_a = p^*_a\left[u - \frac{u^2 - R^2\cos^2\frac{\beta}{2} - \frac{\ell^2}{4}}{2\left(u - R\cos\frac{\beta}{2}\right)}\right]$$

$$p^*_a = p^* - p^*_b$$

where $\beta^\circ = 180\frac{S}{\pi R}$

$u = R + \delta^*$

$$\delta^* = \frac{p^*_b b^2}{2.78\sqrt{AE\, p^*_b b^2}}$$

$$\sigma^*_b = \frac{H^*_b}{A}$$

$$\sigma^*_a = \frac{H^*_a}{A}$$

$${}_1\sigma^*_H = \sigma^*_a\cos^2\alpha + \sigma^*_b\sin^2\alpha$$

$${}_2\sigma^*_H = \sigma^*_a\cos^2\left(\frac{\pi}{4} - \alpha\right) + \sigma^*_b\sin^2\left(\frac{\pi}{4} - \alpha\right)$$

1850

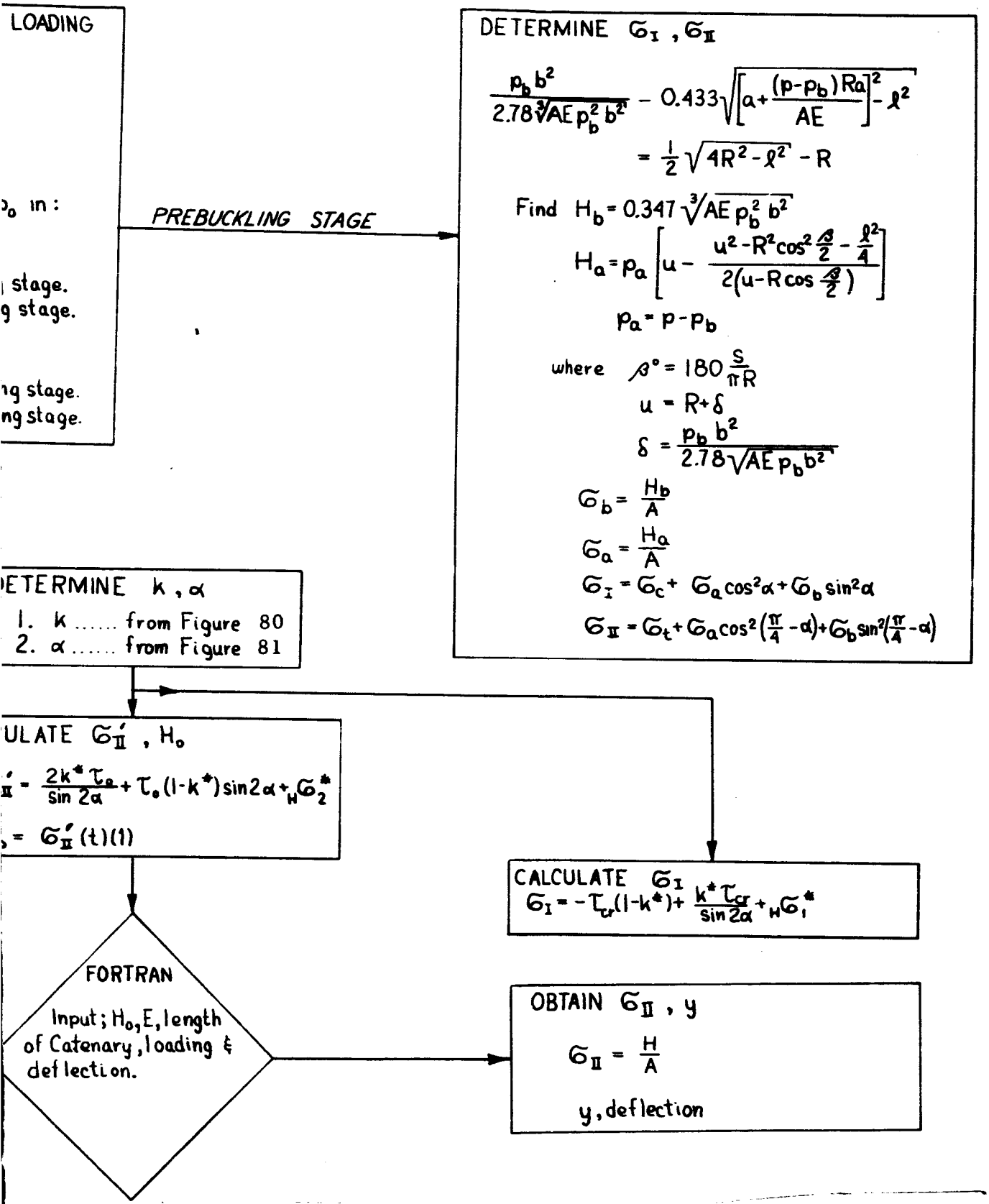

Figure 92. Curved Web Analysis Flow Diagram With "Frozen Compressive Stress" Considered (Background)

$$\delta = \frac{p_b b^2}{2.78 \sqrt[3]{AE p_b^2 b^2}}$$

If in the postbuckling range, determine

k Figure 80

α_{PDT}, α Figure 81

$\sigma_I = - \tau_o (1-k) \sin 2\alpha$ (Diagonal Compression)

σ_{II} obtainable by FORTRAN Program or formulas:

(1) $$\sigma'_{II} = \frac{2k \tau_o}{\sin 2\alpha} + \tau_o (1-k) \sin 2\alpha$$

(2) $$H_o = \sigma'_{II} \times 1'' \times t$$

(3) Initial deflection, $\delta = 0$, loading, p_o, and initial length of catenary, $\theta_2 r_2$ from Equations 4-5, 4-7.

(4) Output of program or formulas is; σ_{II} = final tension stress in catenary; y = maximum lateral deflection

A flow diagram summarizes this procedure (Figure 93).

CURVED BEAM PARAMETERS

1. Geometry

A_{FL}	d
A_U	h
R	t

2. Material Properties

E	σ_{ty}
μ	σ_{tu}

3. Loading
   - Vertical , g_o
   - Lateral , p_o

4. Derived Loads
   - Bending moment , M_B
   - Torsional moment , M_T
   - Web shear , τ_o

BUCKLING CRITERIA TO DEFINE LOADING

1. Compute :

$$\tau_{cr} = k_s \frac{\pi^2 E h^2}{12 R^2 Z^2}$$

$$p^o_{cr} = -0.92 \frac{Et^2}{Rd} \sqrt{\frac{t}{R}}$$

2. Substitute above values and $p = p_o$ into:

a) $$\left(\frac{\tau^*}{\tau_{cr}}\right)^2 + \frac{p_o}{p^o_{cr}} = 1$$

If $\tau^* < \tau_o$, web is in prebuckling stage.
If $\tau^* \geq \tau_o$, web is in postbuckling stage.

OR

b) Substitute $\tau = \tau^*$ in equation

If $p > p_o$, web is in prebuckling stage.
If $p \leq p_o$, web is in postbuckling stage.

1890

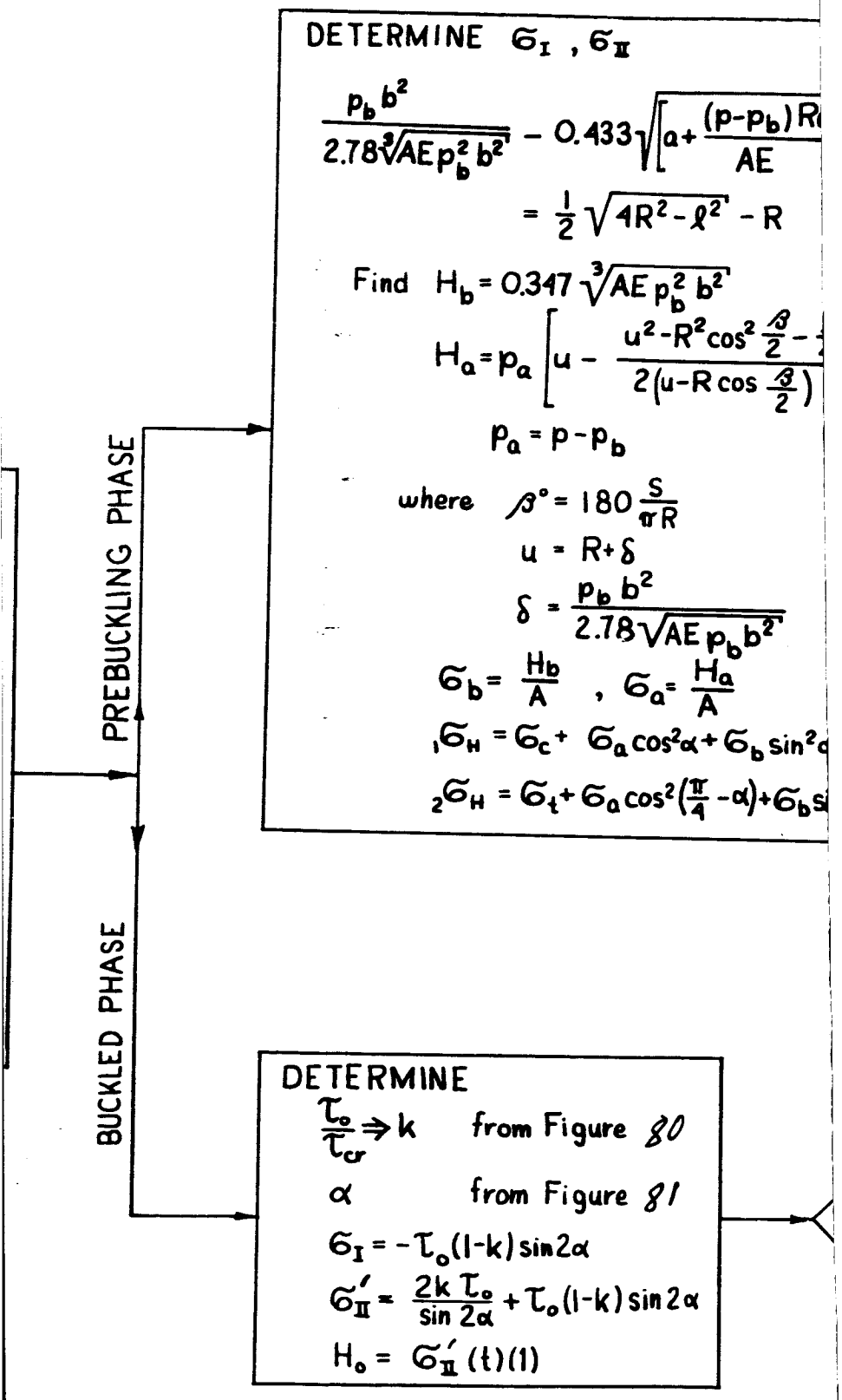
DETERMINE σ_I , σ_{II}
$\frac{p_b b^2}{2.78\sqrt[3]{AE p_b^2 b^2}} - 0.433\sqrt{\left[a + \frac{(p-p_b)R}{AE}\right.}$
$= \frac{1}{2}\sqrt{4R^2 - \ell^2} - R$
Find $H_b = 0.347\sqrt[3]{AE p_b^2 b^2}$
$H_a = p_a\left[u - \frac{u^2 - R^2\cos^2\frac{\beta}{2} -}{2(u - R\cos\frac{\beta}{2})}\right.$
$p_a = p - p_b$
where $\beta^\circ = 180\frac{S}{\pi R}$
$u = R + \delta$
$\delta = \frac{p_b b^2}{2.78\sqrt{AE p_b b^2}}$
$\sigma_b = \frac{H_b}{A}$, $\sigma_a = \frac{H_a}{A}$
$_1\sigma_H = \sigma_c + \sigma_a\cos^2\alpha + \sigma_b\sin^2$
$_2\sigma_H = \sigma_t + \sigma_a\cos^2(\frac{\pi}{4} - \alpha) + \sigma_b$
PREBUCKLING PHASE
BUCKLED PHASE
DETERMINE
$\frac{\tau_o}{\tau_{cr}} \Rightarrow k$ from Figure 80
α from Figure 81
$\sigma_I = -\tau_o(1-k)\sin 2\alpha$
$\sigma_{II}' = \frac{2k\tau_o}{\sin 2\alpha} + \tau_o(1-k)\sin 2\alpha$
$H_o = \sigma_{II}'(t)(1)$

Figure 93.

$\left.\right]^2 - \ell^2$

$\left.\right]$

$m^2\left(\frac{\pi}{4}-\alpha\right)$

$\sigma_I = -\sigma_c + {}_H\sigma_1$

$\sigma_{II} = \sigma_t + {}_H\sigma_2$

Enter FORTRAN program with prestressing H_o, $\delta = 0$, loading p_o, diagonal length of Catenary, and Area A = t×1

OBTAIN σ_{II}, y

$\sigma_{II} = \frac{H}{A}$

y, deflection.

Recommended Procedure for Curved Web Analysis

UPRIGHTS AND FLANGES

STRUCTURAL ANALYSIS OF UPRIGHTS

The stress analysis and stability consideration of the uprights for curved partial-tension-field beams are identical to that of straight beams with the addition of the component of web forces acting out of the flat-plane web system (Figure 73). The method of analysis developed in Appendix A for the upright is general, and the out-of-plane components have been accounted for. The analysis of the upright reduces to that of Kuhn, with the values for p_{cr} in A_{sym} and $A_{antisym}$ slightly modified:

$$A_{sym} = \frac{1}{1 - \frac{P}{P_{cr}} - \frac{F_o d}{4p_{cr}}\left(\frac{2}{\pi^2}\right)\left(\frac{\pi^2}{3} - 1\right)} \tag{4-70}$$

where the critical axial upright load becomes

$$P_{cr} = \frac{\pi^2 EI}{L_e^2} \tag{4-71}$$

where

$$L_e = \frac{d}{\sqrt{1 + k^{*2}\left(3 - \frac{2h}{d}\right)}} \tag{4-72}$$

Note: Valid for $h<1.5d$; for $h>1.5d$, $L_e = d$.

$$k^* = \tanh\left[\left(0.5 + 300\frac{td}{Rh}\right)\log\frac{\tau_o}{\tau^*_{cr}}\right] \tag{4-73}$$

With

1. If $d<h$, replace d/h by h/d.
2. If h/d (or d/h) is larger than 2, use 2 (Figure 94).

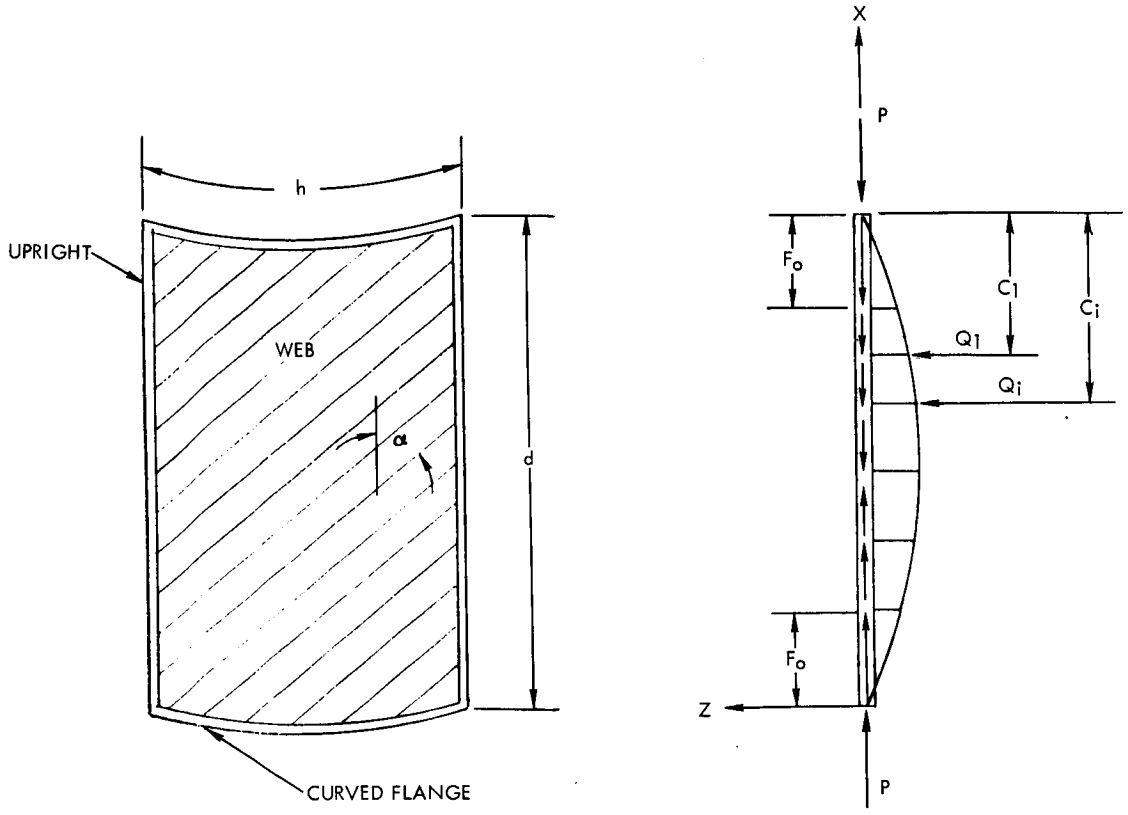

Figure 94. Symmetric Mode

For antisymmetrical deflection shape

$$A_{antisym} = \frac{1}{1 - \frac{P}{4P_{cr}} - \frac{F_o d}{4P_{cr}}\left(\frac{1}{8\pi^2}\right)\left(\frac{4\pi^2}{3} - 1\right)} \qquad (4\text{-}74)$$

The bending stresses due to lateral load can be expressed as

$$\sigma_{\substack{bend \\ sym}} = \frac{2EI_y A_{sym}}{P_{cr} d Z_y}\left[\frac{q_{oz} d}{2} + \sum_{i=1}^{N} Q_n \sin\frac{\pi C_i}{h}\right] \qquad (4\text{-}75)$$

$$\sigma_{\substack{bend \\ antisym}} = \frac{EI_z A_{antisym}}{2dP_{cr} Z_z}\left[\frac{2}{3\pi} q_{oy} d\right] \qquad (4\text{-}76)$$

To this bending stress, add the compressive stress as defined in Reference 1 ,

$$\sigma_C = \frac{k^* \cot \alpha}{\frac{A_u}{ht} + 0.5\,(1-k^*)} \qquad (4\text{-}77)$$

where A_u is the area of upright (Figure 95).

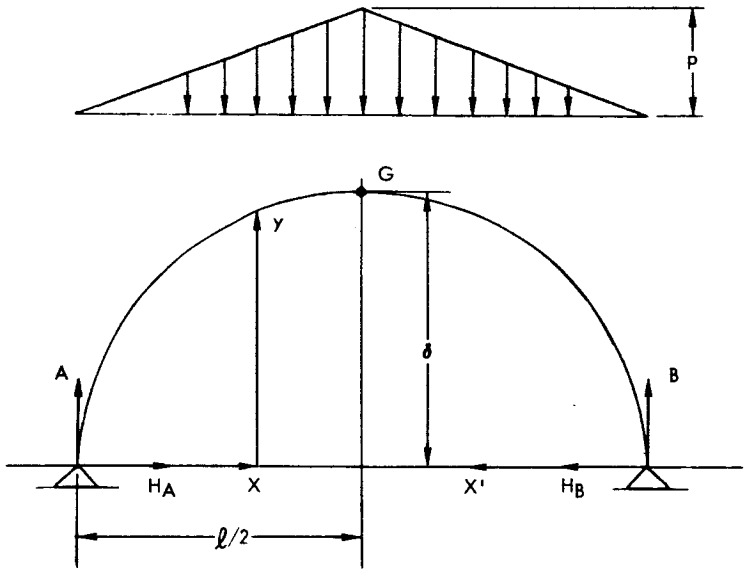

Figure 95. Antisymmetric Mode

To assure structural integrity of the uprights, the bending plus compressive stresses as determined from Equations 4-75 and 4-77 for out-of-plane upright deflection and from Equations 4-76 and 4-77 for tangent-in-plane of web should be less than the design allowable. Furthermore, the stability criteria as determined from Equations 4-71 through 4-73, inclusive, must not be violated. For local stability criteria, the crippling is determined from Equation 3-35 in Section III and from Equations 1-3 or 1-4 of Section I.

STRENGTH ANALYSIS OF FLANGES

The load acting on the flange (ring) due to lateral pressure is shown in Figure 96.

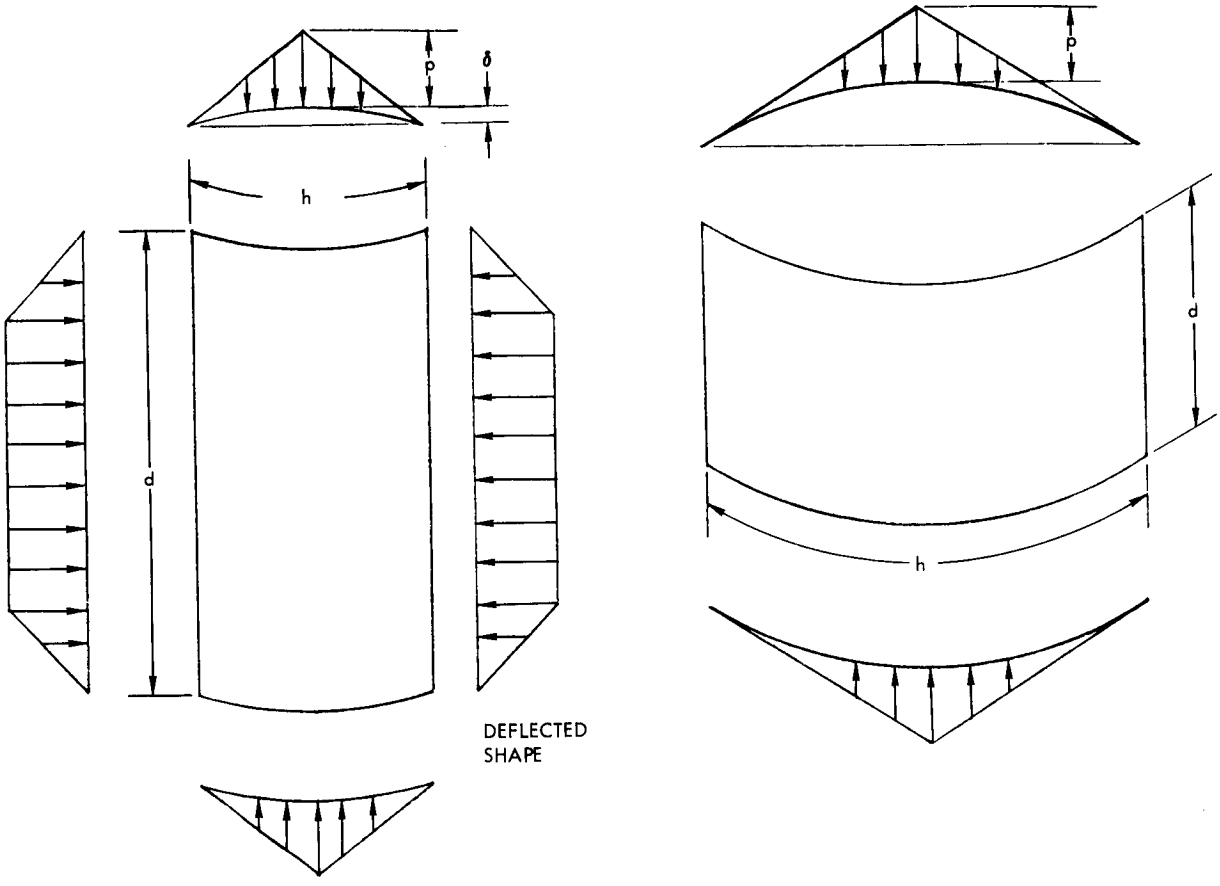

Figure 96. Flange Load Distribution

In this study, webs with $R/_t \geq 1000$ are being investigated. It is still conceivable to have a relatively small radius. Considering the flange portion for one panel, the reactions and bending moments are given in Figure 97. See Reference 16. Making use of the elementary beam theory, determine the bending stress σ_{bend} due to lateral pressure on the curved beam as

$$\sigma_{bend} = \frac{\pm Mc}{I} \qquad (4\text{-}78)$$

where

c = distance from neutral axis to outer fiber, in.

I = cross-sectional moment of inertia about bending cross section, $in.^4$

To this bending stress add the compressive stress in the flange due to diagonal tension (Reference 1) expressed as

$$\sigma_{C_{FL}} = \frac{k_T \tan \alpha}{\frac{A_{FL}}{dt} + 0.5(1 - k^*)} \tag{4-79}$$

where d and α are defined in Figure 94, and t is web thickness.

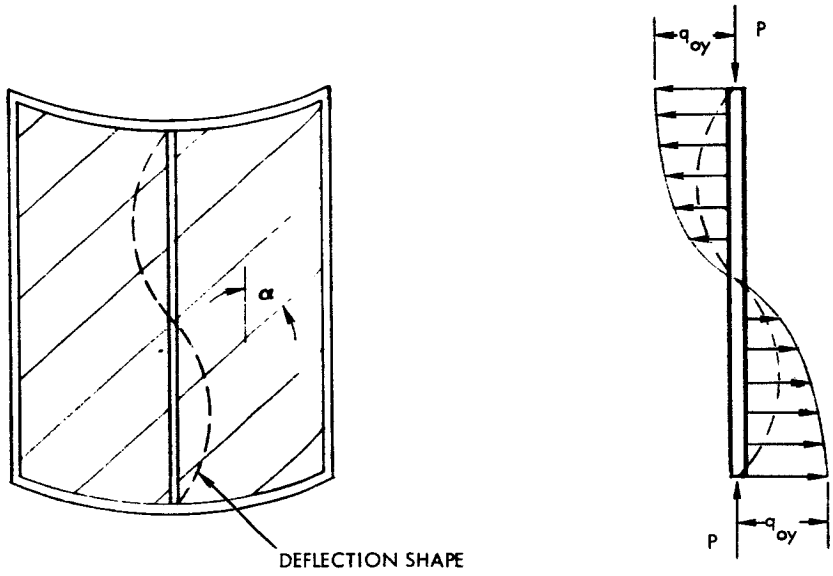

Figure 97. Curved Flange Under Triangular Loading

$$A = B = \frac{p\ell}{4}$$

$$H = \frac{p\ell^2}{12\delta} \tag{4-80}$$

$$M_{x_{A \text{ to } G}} = \frac{p\ell^2}{12}\left[3\left(\frac{x}{\ell}\right) - 4\left(\frac{x}{\ell}\right)^3 - \frac{y}{\delta}\right] \tag{4-81}$$

$$M_{x_{B \text{ to } G}} = \frac{p\ell^2}{12}\left[3\left(\frac{x'}{\ell}\right) - 4\left(\frac{x'}{\ell}\right)^3 - \frac{y}{\delta}\right] \tag{4-82}$$

SUMMARY AND CONCLUSIONS

In this section a systematic procedure was presented for analysis of curved, partial-tension-field beams. Curved-beam analysis follows the straight beam procedures closely in the areas of flange and upright. Additional torsion and axial loads occur in the flange due to beam curvature, and a radial loading component is applied to uprights due to the postbuckling polygon shape of the curved web. These loads are accounted for in the equations developed for straight-beam analysis.

For the webs, new curves of buckling coefficients are provided. Also, the direction of lateral pressure (internal or external) will affect web buckling. After buckling, the catenary model will apply as in the case of the flat webs covered in Section III.

The sequence of a curved-beam analysis is summarized in the flow diagram of Figures 92 and 93.

None of the proposed methods were verified with test results. The case of external pressure requires more development and justification by a test program. Thus, the procedures as outlined in this chapter should be verified by a test program.

OVERALL CONCLUSIONS AND RECOMMENDATIONS

A reasonable procedure has been developed for the analysis of straight and curved partial-tension-field beams under combined vertical and lateral pressure loading. The procedure is based on extensions of existing empirical and analytical data and procedures. Little test data are available which is applicable to this particular combined loading configuration. Therefore, the procedures should be used with caution until confirming test data become available.

The work performed under this contract is a step, or contribution to development of more general partical tension field webs theory which will be applicable to partial tension field behavior of stiffened cylindrical shell structures of boosters and other aerospace vehicles. The procedure is currently restricted to beams loaded vertically and laterally. Use was made of computer programs in order to simplify certain steps of the analysis. It is possible to rewrite the entire procedure for digital computer solution. This would make the whole procedure automatic.

In addition to the actual program of study the state-of-the-art documented in domestic and foreign literature was reviewed in Section I. The following additional areas of study are recommended:

GENERAL TEST PROGRAM

Of first importance is a general test program to check the validity of the assumptions made in developing the procedures of this study. Interaction effects of the two types of loading under various combinations of loading and for various structural geometries are of primary interest.

The effect on k, the diagonal tension factor, of various combinations of loading can be investigated to provide further understanding of the diagonal tension phenomenon. This factor is probably affected by combinations of loading as well as geometric factors.

APPLICATION TO CURVED BEAMS

The above general program should be applied separately to curved beams. Concurrent analytical effort and testing is desirable due to the mutual support required on each area by the other. Analytical predictions require validation by test programs.

BIAXIAL COMPRESSION IN WEBS

Under certain loading conditions, particularly with flexible flanges or uprights, biaxial compression exists in the webs. It appears that no work has been done in this area.

DEEP OR "HIGH" PARTIAL-TENSION-FIELD BEAMS

Unusual geometry such as a very deep beam changes the web boundary conditions sufficiently that further study is required to define stress distributions.

Intrapanel auxiliary uprights and flanges provide a parametric approach to designing optimum beams. Uprights or flanges may be either continuous or discontinuous.

All combinations of loading require analytical investigation with concurrent tests performed to check assumptions used in the development and validity of the final equations.

The deep, curved-beam configuration differs sufficiently from the straight beam that a separate analysis and test program is justified. Included in this area is the investigation of curved beams as elements of cylinders and conical sections. Longitudinal stresses induced by pressure against the ends of a closed cylinder (bulkhead effect) require investigation.

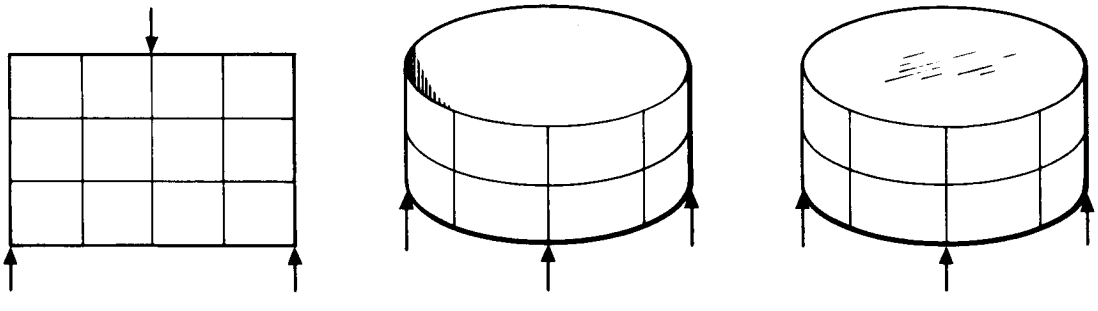

a. Deep or "High" Beam

b. Unpressurized Liquid Tank

c. Pressurized Cylinder

PLASTIC BEHAVIOR

At high web loadings, where tension-field beams are most efficient structurally, the material will usually be well within the plasticity range. The effect of combined loading should be investigated. Considering the state of the art in plasticity, this program should have most of the emphasis placed on strain instrumentation and testing.

FORCED-CRIPPLING OF STIFFENERS

Flange and upright considerations are of fundamental importance in optimum weight beam analyses. Forced crippling appears to be the most important failure mode. Unfortunately, a forced-crippling theory is not generally established. A comprehensive study of forced crippling of stiffeners attached to buckled sheets should result in lighter weight structures.

LOAD CARRYING FRAMES IN BUCKLED WEBS

It is expected that further study in this area should yield better analysis techniques and lighter structures.

APPENDIX A

DERIVATION

The upright (Figure 57) can be analyzed as a beam column with the Fourier series method of analysis. Normally, the external forces acting on the upright are conservative. The principle of stationary potential energy can be applied to establish the coefficients in the Fourier series for the deflection of the upright. The condition for termwise differentiation of the Fourier series must not be violated. The deflection function then can be expressed as

$$y = \sum_{n=1}^{\infty} b_n \sin \frac{n\pi x}{h} \tag{A1}$$

where

b_n = any arbitrary coefficient

n = an integer

h = the upright height, inches

For a simple support system, the boundary conditions are defined by

$$y = 0 \text{ at } \begin{cases} x = o \\ x = h \end{cases}$$

$$EI \frac{d^2y}{dx^2} = 0 \text{ at } \begin{cases} x = o \\ x = h \end{cases} \tag{A2}$$

where

E = modulus of elasticity of upright material, psi

I = cross-sectional moment of inertia of upright, inches^4

The deflection function expressed by Equation A1 is shown to be termwise differentiable in Reference 40. The first and second derivatives of y with respect to x are

$$\frac{dy}{dx} = \frac{\pi}{h} \sum_{n=1}^{\infty} n\, b_n \cos \frac{n\pi x}{h}$$

$$\frac{d^2y}{dx^2} = \frac{-\pi^2}{h^2} \sum_{n=1}^{\infty} n^2\, b_n \sin \frac{n\pi x}{h} \tag{A3}$$

The expressions for the strain energy of bending, potential energy of the inplane force p, the potential energy of the lateral loads Q_1, Q_2, . . . , and the potential energy of the distributed load q(x) can be obtained directly from Reference 41. The strain energy of the elastic foundation effect and the potential energy of the axial effect can be obtained from Reference 9.

From Reference 41 the strain energy of bending is

$$U_B = \frac{1}{2} \int_o^h EI \left(\frac{d^2y}{dx^2}\right)^2 dx \tag{A4}$$

or for constant cross-sectional area and material

$$U_B = \frac{EI}{2} \int_o^h \left[\frac{-\pi^2}{h^2} \sum_{n=1}^{\infty} n^2\, b_n \sin \frac{n\pi x}{h}\right]^2 dx$$

or by expanding the equation and upon integration

$$U_B = \frac{\pi^4\, EI}{4h^3} \sum_{n=1}^{\infty} n^4\, b_n^2 \tag{A5}$$

Since the integrals of the cross products resulting from squaring the series cancel because of the relationships:

for $m \neq n$

$$\int_o^h \sin \frac{m\pi x}{h} \sin \frac{n\pi x}{h}\, dx = \int_o^h \cos \frac{m\pi x}{h} \cos \frac{n\pi x}{h}\, dx = 0$$

for m = n

$$\int_o^h \sin\frac{m\pi x}{h}\sin\frac{n\pi x}{h}\,dx = \int_o^h \cos\frac{m\pi x}{h}\cos\frac{n\pi x}{h}\,dx = \frac{h}{2}$$

where m and n are any positive integers.

The strain energy of the web system can be determined by considering the web system giving elastic restraint having β as the equivalent modulus of foundation. The reaction of the web at any cross section of the upright is then proportional to the deflection at that section. The lateral reaction of an element dx of the upright is $\beta y\,dx$. Hence, the energy of the elastic restraint for the element dx is $\frac{\beta y^2}{2}dx$. The total strain energy U_E of the elastic restraint can be obtained by integrating over the entire length of upright. Hence,

$$U_E = \frac{\beta}{2}\int_o^h y^2\,dx \tag{A6}$$

From Equations A1 and A6

$$U_E = \frac{\beta}{2}\int_o^h \left[\Sigma\, b_n \sin\frac{n\pi x}{h}\right]^2 dx$$

or

$$U_E = \frac{\beta h}{4}\sum_{n=1}^{\infty} b_n^2 \tag{A7}$$

The potential energy of the axial load is

$$\Omega_P = -P\Delta h \tag{A8}$$

where $\Delta h = h - h_1$. By assuming that the upright bends without any change of the center line length, Reference 41 indicates

$$h_1 = \int_o^h \frac{dx}{ds}\,ds$$

or

$$\Delta h = \frac{1}{2}\int_o^h \left(\frac{dy}{dx}\right)^2 dx \qquad (A9)$$

The potential energy of the axial load becomes

$$\Omega_P = -\frac{P}{2}\int_o^h \left(\frac{\pi}{h}\sum_{n=1}^{\infty} n\, b_n \cos\frac{n\pi x}{h}\right)^2 dx$$

or

$$\Omega_P = -\frac{\pi^2 P}{4h}\sum_{n=1}^{\infty} n^2\, b_n^2 \qquad (A10)$$

From Reference 9, the potential energy of the distributed axial compression load due to the tension in the diagonal web fold is

$$\Omega_{F_o} = -\frac{F_o}{2}\left[\sum_{n=1}^{\infty} b_n^2\left(\frac{n^2\pi^2}{12} - \frac{1}{4}\right) - 4\sum_{n=1}^{\infty}\sum_{m=1}^{\infty} b_n\, b_m \frac{nm\,(m^2+n^2)}{(m^2-n^2)^2}\right] \qquad (A11)$$

where

$(m + n)$ = an even integer

$m \neq n$

F_o = maximum distributed force due to net diagonal tension force (Figure 98)

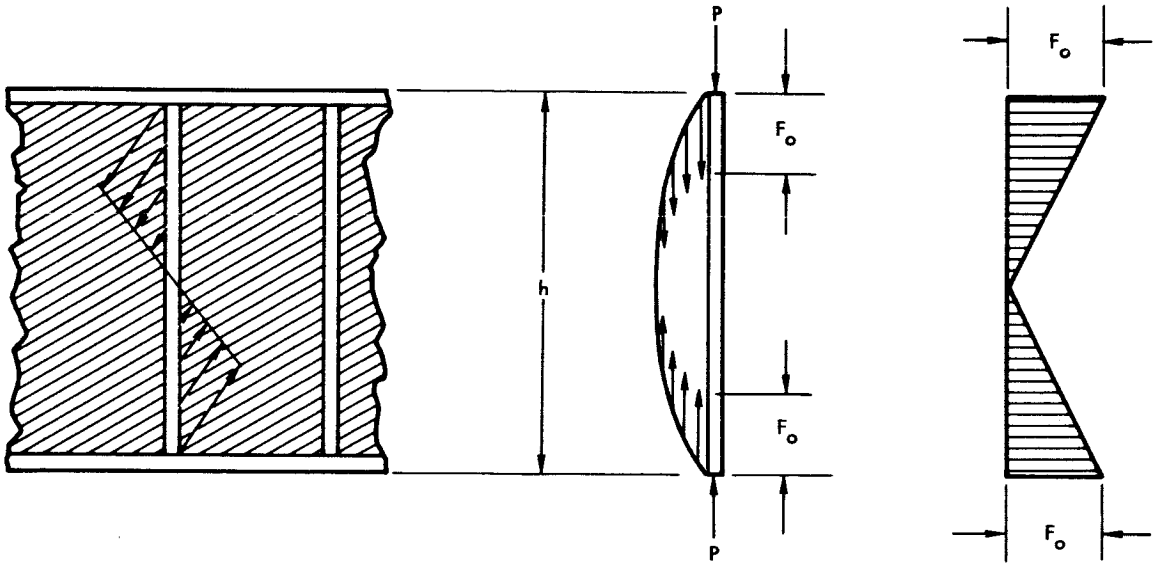

Figure 98. In-plane Net Diagonal Tension Force

The application of Reference 41 to the upright for the potential energy due to lateral loads Q_1, Q_2, Q_3, . . . and that due to some distributed load q(x) are, respectively

$$\Omega_{Q_n} = - Q_1 \sum_{n=1}^{\infty} b_n \sin\frac{n\pi C_1}{h} - Q_2 \sum_{n=1}^{\infty} b_n \sin\frac{n\pi C_2}{h} \qquad \text{(A12)}$$

$$- Q_3 \sum_{n=1}^{\infty} b_n \sin\frac{n\pi C_3}{h} - \ldots$$

and

$$\Omega_{q(x)} = - \sum_{n=1}^{\infty} b_n \int_o^h q(x) \sin\frac{n\pi x}{h} dx \qquad \text{(A13)}$$

The summation of each of the energy system gives the total potential Π as

$$\Pi = U_B + U_E + \Omega_P + \Omega_{F_o} + \Omega_{Q_n} + \Omega_{q(x)} \qquad \text{(A14)}$$

or

$$\Pi = \frac{\pi^4 EI}{4h^3} \sum_{n=1}^{\infty} n^4 b_n^2 + \frac{\beta h}{4} \sum_{n=1}^{\infty} b_n^2 - \frac{\pi^2 P}{4h} \sum_{n=1}^{\infty} n^2 b_n^2$$

$$- \frac{F_o}{2} \left[\sum_{n=1}^{\infty} b_n^2 \left(\frac{n^2\pi^2}{12} - \frac{1}{4} \right) - 4 \sum_{n=1}^{\infty} \sum_{m=1}^{\infty} b_n b_m \frac{nm\,(m^2 + n^2)}{(m^2 - n^2)^2} \right]$$

$$+ \left[- Q_1 \sum_{n=1}^{\infty} b_n \sin \frac{n\pi C_1}{h} - Q_2 \sum_{n=1}^{\infty} b_n \sin \frac{n\pi C_2}{h} - \cdots \right]$$

$$- \sum_{n=1}^{\infty} b_n \int_o^h q(x) \sin \frac{n\pi x}{h}\, dx \qquad \text{(A15)}$$

The coefficient b_n can be obtained by the condition of stationary potential energy. Hence, from $\frac{\partial \Pi}{\partial b_i} = 0$ we have

$$\frac{\pi^4 EI}{2h^3} n^4 b_n + \frac{\beta h}{2} b_n - \frac{\pi^2 P\, n^2}{2\ h} b_n - F_o\, b_n \left(\frac{n^2\pi^2}{12} - \frac{1}{4} \right)$$

$$+ 2 F_o \sum_{m=1}^{\infty} b_m \frac{nm\,(m^2 + n^2)}{(m^2 - n^2)^2} - \left(Q_1 \sin \frac{n\pi C_1}{h} + Q_2 \sin \frac{n\pi C_2}{h} \right.$$

$$\left. + Q_3 \sin \frac{n\pi C_3}{h} + \cdots \right) - \int_o^h q(x) \sin \frac{n\pi x}{h}\, dx = 0 \qquad \text{(A16)}$$

Solving for b_n

$$b_n = \frac{\left[\int_o^h q(x) \sin\frac{n\pi x}{h}\,dx + \left(Q_1 \sin\frac{n\pi C_1}{h} + Q_2 \sin\frac{n\pi C_2}{h} + \ldots\right) - 2F_o \sum_{m=1}^{\infty} b_m \frac{nm(m^2+n^2)}{(m^2-n^2)^2}\right]}{\frac{\pi^4 EI}{2h^3}n^4 - \frac{\pi^2 Pn^2}{2h} + \frac{\beta h}{2} - \frac{F_o}{4}\left(\frac{n^2\pi^2}{3} - 1\right)} \qquad (A17)$$

The summation in Equation A17 indicates that two groups of equations exist since (m + n) is an even integer and m is not equal to n. One group has m as an odd integer, e.g., n = 1.

$$b_1 = \frac{\left\{\int_o^h q(x) \sin\frac{\pi x}{h}\,dx + \left(Q_1 \sin\frac{\pi C_1}{h} + Q_2 \sin\frac{\pi C_2}{h} + \ldots\right) - 2F_o\left[\frac{3(10)}{(8)^2}b_3 + \frac{5(26)}{(24)^2}b_5 + \frac{7(50)}{(48)^2}b_7 + \ldots\right]\right\}}{\frac{\pi^4 EI}{2h^3}(1)^4 - \frac{\pi^2 P}{2h}(1)^2 + \frac{\beta h}{2} - \frac{F_o}{4}\left[\frac{(1)^2\pi^2}{3} - 1\right]} \qquad (A18a)$$

Similarly n = 3 and m is an odd integer

$$b_3 = \frac{\left\{\int_o^h q(x) \sin\frac{3\pi x}{h}dx + \left(Q_1 \sin\frac{3\pi C_1}{h} + Q_2 \sin\frac{3\pi C_2}{h} + \ldots\right) - 2F_o\left[b_1\frac{3(10)}{(8)^2} + b_5\frac{15(34)}{(16)^2} + b_7\frac{(21)(58)}{(40)^2} + \ldots\right]\right\}}{\frac{\pi^4 EI}{2h^3}(3)^4 - \frac{\pi^2 P(3)^2}{2h} + \frac{\beta h}{2} - \frac{F_o}{4}\left(\frac{(3)^2\pi^2}{3} - 1\right)} \qquad (A18b)$$

The second group consists of m as an even integer and not equal to n with (n + m) as an even integer. Hence, for n = 2 and m as an even integer

$$b_2 = \frac{\left\{ \int_o^h q(x) \sin\frac{2\pi x}{h}dx + \left(Q_1 \sin\frac{2\pi C_1}{h} + Q_2 \sin\frac{2\pi C_2}{h} + \ldots\right) - 2F_o\left[b_4\frac{(8)(20)}{(12)^2} + b_6\frac{(12)(40)}{(32)^2} + b_8\frac{(16)(68)}{(60)^2} + \ldots\right]\right\}}{\frac{\pi^4 EI}{2h^3}(2)^4 - \frac{\pi^2 P(2)^2}{2h} + \frac{\beta h}{2} - \frac{F_o}{4}\left[\frac{(2)^2\pi^2}{3} - 1\right]} \qquad \text{(A19a)}$$

and similarly for n = 4 and m as an even integer

$$b_4 = \frac{\left\{ \int_o^h q(x) \sin\frac{4\pi x}{h}dx + \left(Q_1 \sin\frac{4\pi C_1}{h} + Q_2 \sin\frac{4\pi C_2}{h} + \ldots\right) - 2F_o\left[b_2\frac{8(20)}{(12)^2} + b_6\frac{24(52)}{(20)^2} + \ldots\right]\right\}}{\frac{\pi^4 EI}{2h^3}(4)^4 - \frac{\pi^2 P(4)^2}{2h} + \frac{\beta h}{2} - \frac{F_o}{4}\left(\frac{(4)^2\pi^2}{3} - 1\right)} \qquad \text{(A19b)}$$

For a nontrivial solution b_n is not equal to zero. Thus, two systems of equations describe the buckled upright: Equation A18 for the symmetrical shape and Equation A19 for the antisymmetrical shape.

For the symmetrical mode, the deflection goes to infinity when the denominator goes to zero. Hence, the symmetrical buckling criteria for the upright becomes

$$\frac{\pi^4 EI}{2h^3}n^4 - \frac{\pi^2 Pn^2}{2h} + \frac{\beta h}{2} - \frac{F_o}{4}\left(\frac{n^2\pi^2}{3} - 1\right) = 0$$

or

$$P + \frac{F_o h}{4}\left(\frac{2}{\pi^2}\right)\left(\frac{\pi^2}{3} - \frac{1}{n^2}\right) = \frac{\pi^2 EIn^2}{h^2} + \frac{h^2\beta}{\pi^2 n^2} \qquad \text{(A20)}$$

The left-hand side of Equation A20 represents the loading function on the upright and the right-hand side represents the elastic restraint of the upright-web system. For a vertical loaded beam, Kuhn showed that P_{cr} is given by

$$P_{cr} = \frac{\pi^2 EI}{L_e^2} \tag{A21}$$

where L_e is the effective upright length determined empirically as

$$L_e = \frac{h}{\sqrt{1 + k^2 \left(3 - 2\frac{d}{h}\right)}} \tag{A22}$$

The critical buckling load in Equation A20 can now be expressed as

$$P_{cr} = \frac{\pi^2 EI\, n^2}{h^2} + \frac{h^2}{\pi^2}\frac{\beta}{n^2} \tag{A23}$$

which indicates that an empirical β effect can be determined. Hence, the governing equation used was for symmetrical buckling and that the buckling occurs out of the plane (in the direction of the lateral load for lateral-vertical, loaded-tension-field beams). Such a case exists when the lateral load and/or vertical load is acting on the upright as shown in Figure 57.

Equation A23 shows the buckling takes place in the upright when

$$P + \frac{F_o h}{4}\left(\frac{2}{\pi^2}\right)\left(\frac{\pi^2}{3} - \frac{1}{n^2}\right) \geq P_{cr} \tag{A24}$$

Whenever the load acting on the upright is less than P_{cr}, then the upright deflection in the direction of the lateral load is as follows:

$$z = \frac{2h}{P_{cr}\,\pi^2}\left[\frac{\int_o^h q(x)\sin\frac{\pi x}{h}\,dx + \sum_{i=1}^{N} Q_i \sin\frac{\pi C_i}{h}}{1 - \frac{P}{P_{cr}} - \frac{F_o h}{4P_{cr}}\left(\frac{2}{\pi^2}\right)\left(\frac{\pi^2}{3} - 1\right)}\right]\sin\frac{\pi x}{h} \tag{A25}$$

The maximum deflection occurs at the mid-height, i.e., $x = \frac{h}{2}$ such that $\sin \frac{\pi h}{2h} = 1$. Hence

$$z_{max} = \frac{2h}{P_{cr}\pi^2} \frac{\int_o^h q(x) \sin \frac{\pi x}{h} dx + \sum_{i=1}^{N} Q_i \sin \frac{\pi C_i}{h}}{1 - \frac{P}{P_{cr}} - \frac{F_o h}{4P_{cr}} \left(\frac{2}{\pi^2}\right) \left(\frac{\pi^2}{3} - 1\right)} \qquad \text{(A26)}$$

Equation A26 was derived by only considering the first term in the deflection function, i.e., b_1. The accuracy of this approximation is indicated for loading condition shown in Figure 54 by considering only one term. From Equations A18a and A18b two equations with two unknown coefficients b_1 and b_3. Consider the case for which no distributed axial compression F_o exist. Then from Equation A17

$$b_n = \frac{\int_o^h q(x) \sin \frac{n\pi x}{h} dx + \sum_{i=1}^{N} Q_i \sin \frac{n\pi C_i}{h}}{n^2 \left(n^2 - \frac{P}{P_{cr}}\right)}$$

and

$$z_{max} = \frac{2h}{P_{cr}\pi^2} \sum_{n=1}^{\infty} \frac{\int_o^h q(x) \sin \frac{n\pi x}{h} dx + \sum_{i=1}^{N} Q_i \sin \frac{n\pi C_i}{h}}{n^2 \left(n^2 - \frac{P}{P_{cr}}\right)}$$

where $x = \frac{h}{2}$

Note that for n even there is no contribution towards the deflection since $\sin \frac{n\pi}{2} = 0$ for n even.

The maximum deflection in the direction of the lateral load is

$$z_{max} = \frac{2h}{\pi^2 P_{cr}} \left[\frac{\int_o^h q(x) \sin\frac{\pi x}{h} dx + \sum_{i=1}^{N} Q_i \sin\frac{\pi C_i}{h}}{1 - \frac{P}{P_{cr}}} \right.$$

$$+ \frac{\int_o^h q(x) \sin\frac{3\pi x}{h} dx + \sum_{i=1}^{N} Q_i \sin\frac{3\pi C_i}{h}}{9\left(9 - \frac{P}{P_{cr}}\right)}$$

$$+ \frac{\int_o^h q(x) \sin\frac{5\pi x}{h} dx + \sum_{i=1}^{N} Q_i \sin\frac{5\pi C_i}{h}}{25\left(25 - \frac{P}{P_{cr}}\right)}$$

$$\left. + \ldots \right]$$

For a particular case, as an example,

$$q(x) = q_{oz} \sin\frac{\pi x}{h}$$

or

$$\int_o^h q_{oz} \sin\frac{\pi x}{h} \sin\frac{n\pi x}{h} dx = \frac{h}{2} \text{ for } n = 1$$

$$= 0 \text{ for } n \neq 1$$

and

$$Q_i \sin\frac{\pi C_i}{h} = \frac{h q_{oz}}{2} \sin\frac{\pi}{2} = \frac{q_{oz} h}{2}$$

and

$$z_{max} = \frac{2h^2 q_{oz}}{\pi^2 P_{cr}} \sum_{n=1}^{\infty} \frac{\sin\frac{n\pi}{2}}{n^2\left(n^2 - \frac{P}{P_{cr}}\right)}$$

The relative accuracy of a one-term approximation for $\frac{P}{P_{cr}}$ is as follows:

$\frac{P}{P_{cr}}$	0	0.2	0.4	0.6	0.6	1.0
$\frac{z\pi^2 P_{cr}}{2h^2 q_{oz}} \sum_{n=1}^{\infty} \frac{\sin \frac{n\pi}{2}}{n^2 \left(n^2 - \frac{P}{P_{cr}}\right)}$	0.987	1.237	1.653	2.487	9.986	∞
$\frac{z\pi^2 P_{cr}}{2h^2 q_{oz}}$, n=1 only	1.00	1.250	1.667	2.500	10.00	∞

To study the error associated with the effect of the distributed axial compression force F_o, refer to Timoshenko's case (Reference 9) for which lateral loads are not existing. Reference 9 shows that for F_o only, the critical loads with the relative accuracy of a one-term approximation for $\left(\frac{F_o h}{4}\right)_{cr}$ are as follows:

Coefficients	$\left(\frac{F_o h}{4}\right)_{cr}$	Error
b_1	2.15	4%
b_1 and b_3	2.06	<1%
b_1, b_3, b_5	2.06	<1%

For q(x) to be approximated by $q_{oz} \sin \frac{\pi x}{h}$ as the lateral load due to lateral pressure p acting on the tension field beam:

$$\int_o^h q(x) \sin \frac{\pi x}{h} dx = q_{oz} \int_o^h \sin^2 \frac{\pi x}{h} dx = \frac{h q_{oz}}{2}$$

Thus, the deflection at any section along the upright is

$$z = \frac{2h}{P_{cr}\pi^2} \left[\frac{\frac{q_{oz}h}{2} + \sum_{i=1}^{N} Q_i \sin \frac{\pi C_i}{h}}{1 - \frac{P}{P_{cr}} - \left(\frac{F_o h}{4P_{cr}}\right) \frac{2}{\pi^2} \left(\frac{\pi^2}{3} - 1\right)} \right] \sin \frac{\pi x}{h}$$

and the deflection is positive in the direction of the load. The slope of the upright at any section θ becomes

$$\theta = \frac{dz}{dx} = \frac{2}{\pi P_{cr}} \left[\frac{\frac{q_{oz}h}{2} + \sum_{i=1}^{N} Q_i \sin \frac{\pi C_i}{h}}{1 - \frac{P}{P_{cr}} - \left(\frac{F_o h}{4P_{cr}}\right) \frac{2}{\pi^2} \left(\frac{\pi^2}{3} - 1\right)} \right] \cos \frac{\pi x}{h}$$

The bending moment at any section becomes

$$M_y = -EI_y \frac{d^2 z}{dx^2} = \frac{-2EI_y}{P_{cr} h} \left[\frac{\frac{q_{oz}h}{2} + \sum_{i=1}^{N} Q_i \sin \frac{\pi C_i}{h}}{1 - \frac{P}{P_{cr}} - \left(\frac{F_o h}{4P_{cr}}\right) \frac{2}{\pi^2} \left(\frac{\pi^2}{3} - 1\right)} \right] \sin \frac{\pi x}{h}$$

The maximum bending stress then becomes

$$\sigma_{y\ bend} = \frac{2EI_y}{P_{cr} h Z} \left[\frac{\frac{q_{oz}h}{2} + \sum_{i=1}^{N} Q_i \sin \frac{\pi C_i}{h}}{1 - \frac{P}{P_{cr}} - \frac{F_o h}{4P_{cr}} \left(\frac{2}{\pi^2}\right) \left(\frac{\pi^2}{3} - 1\right)} \right] \sin \frac{\pi x}{h}$$

where $Z = \frac{I_y}{c}$ section modulus. The maximum bending stress occurs at $X = \frac{h}{2}$ such that $\sin \frac{\pi h}{2h} = 1$. To this we add compressive stress of $\sigma_{comp} = \frac{P}{A} + \frac{F_o h}{2A}$ and local stress of σ_{local} such that the stresses become

$$\sigma_y = \sigma_{y\ bend} + \sigma_{comp} + \sigma_{local}$$

For stability consideration, note that when the denominator of the deflection function goes to zero the deflection approaches infinity. Thus, when

$$1 - \frac{P}{P_{cr}} - \frac{F_o h}{4P_{cr}} \left(\frac{2}{\pi^2}\right) \left(\frac{\pi^2}{3} - 1\right) = 0$$

or

$$P + \frac{F_o h}{4} \left(\frac{2}{\pi^2}\right) \left(\frac{\pi^2}{3} - 1\right) = \frac{\pi^2 EI}{L_e^2}$$

where

$$L_e^2 = \frac{h^2}{\sqrt{1 + k^2 \left(3 - 2\frac{d}{h}\right)}}$$

for $d < 1.5\,h$ and for $d > 1.5\,h$, $L_e = h$.

The lateral load distribution q(x) shown in Figure 99 can be represented by

$$q(x) = q_{oy} \cos\frac{\pi x}{h}$$

The deflection function from Equations A1 and A19a for n = 2 is

$$y = \frac{\int_o^h q(x) \sin\frac{2\pi x}{h} dx + \sum_{i=1}^{N} Q_i \sin\frac{2\pi C_i}{h}}{\frac{16\pi^2}{2h}\frac{EI\pi^2}{h^2} - \frac{\pi^2 4}{2h}P + \frac{\beta h}{2} - \frac{F_o}{4}\left(\frac{4\pi^2}{3} - 1\right)} \sin\frac{2\pi x}{h}$$

or

$$y = \frac{h}{8\pi^2 P_{cr}} \left[\frac{\int_o^h q(x) \sin\frac{2\pi x}{h} dx + \sum_{i=1}^{N} Q_i \sin\frac{2\pi C_i}{h}}{1 - \frac{P}{4P_{cr}} - \frac{F_o h}{4P_{cr}} \frac{1}{8\pi^2}\left[\frac{4\pi^2}{3} - 1\right]}\right] \sin\frac{2\pi x}{h} \qquad (A27)$$

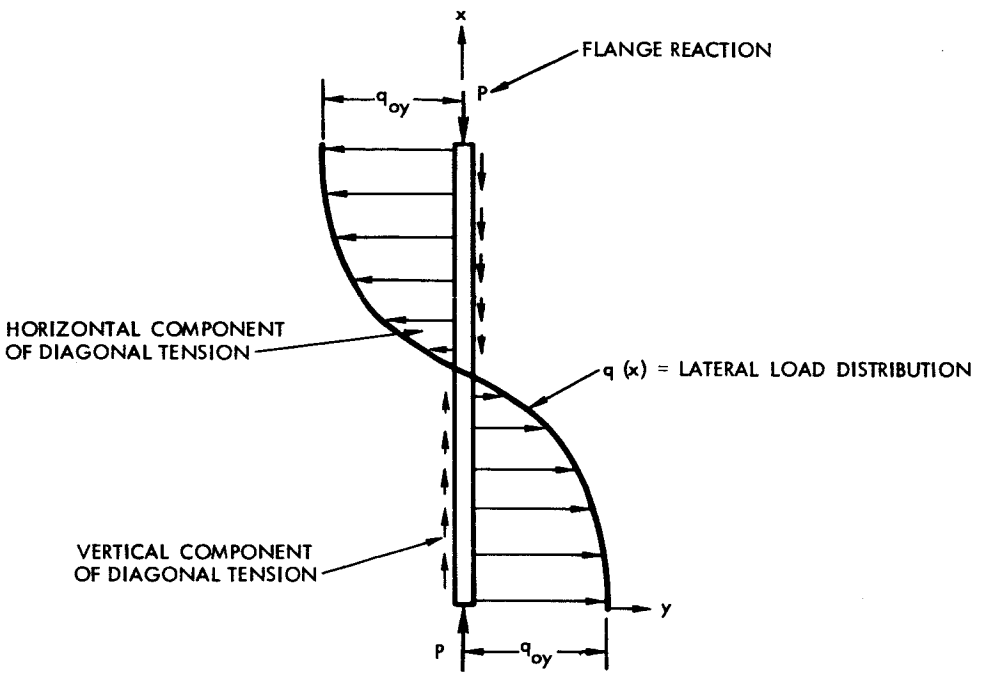

Figure 99. Lateral Loading of Upright in the Plane of the Web

The integral in the deflection function Equation A27 can be evaluated as

$$\int_o^h q_{oy} \cos\frac{\pi x}{h} \sin\frac{2\pi x}{h}\, dx = \frac{2}{3}\frac{q_{oy}\, h}{\pi}$$

hence

$$y = \frac{h}{8\pi^2 P_{cr}} \left[\frac{\frac{2}{3\pi} q_{oy} h + \sum_{i=1}^{N} Q_i \sin\frac{2\pi C_i}{h}}{1 - \frac{P}{4P_{cr}} - \frac{F_o h}{4P_{cr}} \frac{1}{8\pi^2}\left(\frac{4\pi^2}{3} - 1\right)} \right] \sin\frac{2\pi x}{h}$$

The slope and stress at any point x then becomes

$$\theta = \frac{1}{4\pi P_{cr}} \left[\frac{\frac{2h}{3\pi} q_{oy} + \sum_{i=1}^{N} Q_i \sin\frac{2\pi C_i}{h}}{1 - \frac{P}{4P_{cr}} - \frac{F_o h}{4P_{cr}} \frac{1}{8\pi^2}\left(\frac{4\pi^2}{3} - 1\right)} \right] \cos\frac{2\pi x}{h}$$

and

$$\sigma_{z\ \text{bending}} = \frac{EI_z}{2hP_{cr}Z}\left[\frac{\frac{2h}{3\pi}q_{oy} + \sum_{i=1}^{N} Q_i \sin\frac{2\pi C_i}{h}}{1 - \frac{P}{4P_{cr}} - \frac{F_o h}{4P_{cr}}\frac{1}{8\pi^2}\left(\frac{4\pi^2}{3} - 1\right)}\right] \sin\frac{2\pi x}{h}$$

Again to this bending stress add the compressive stress due to axial loads to get total stress as

$$\sigma_z = \sigma_{z\ \text{bending}} + \sigma_{comp} + \sigma_{local}$$

The bending stress can be easily computed for

$$\frac{P}{4P_{cr}} + \frac{F_o h}{4P_{cr}}\frac{1}{8\pi^2}\left[\frac{4\pi^2}{3} - 1\right] < 1$$

by use of Figure 99 where the amplification factor was defined as

$$\text{Amplification factor} = A_{anti} = \frac{1}{1 - \frac{P}{4P_{cr}} - \frac{F_o h}{4P_{cr}}\frac{1}{8\pi^2}\left(\frac{4\pi^2}{3} - 1\right)}$$

where P_{cr} to be used here is that critical load necessary to buckle in the first buckling mode, i.e., the critical buckling load required for antisymmetric buckling (two half-waves) is greater than lowest symmetrical buckling (one-half-wave) by a factor of four times when P acts alone.

APPENDIX B
NUMERICAL EXAMPLES

STRAIGHT BEAM NUMERICAL EXAMPLE

Partial-tension-field beam is exposed to the vertical and lateral loading. Determine the stresses in the web, considering different loading sequences.

SYSTEM

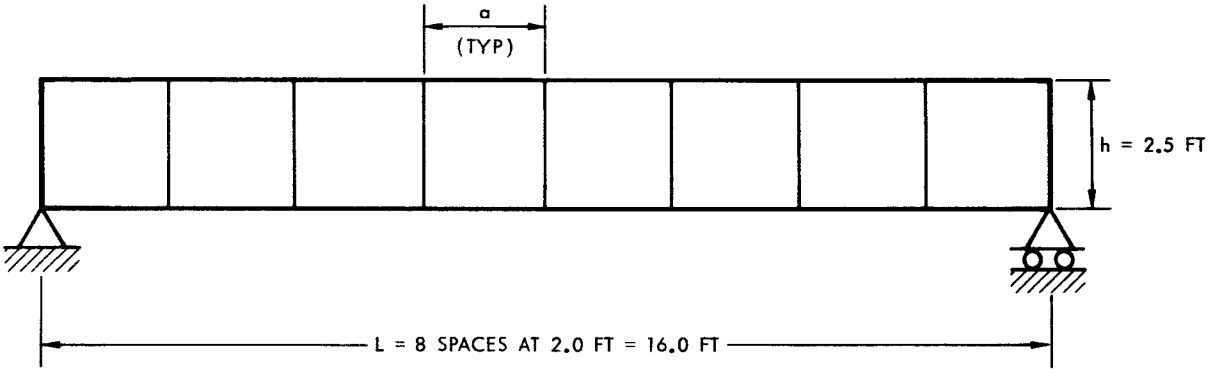

The 7075-T6 aluminum alloy beam is symmetrical about ℄. The thickness of the webs t = 0.05 inch. For this example, assume the flanges and stiffeners to be rigid enough in comparison with the web - flexibility.

LOADING

Vertical loading: g = 0.50 k per foot

Lateral loading: p = 0.10 psi

STATICAL ANALYSIS

Shear diagram due to the vertical loading g:

$$\text{Reaction } R_A = gL/2 = 1/2 \times 16 \text{ ft} \times 0.5 = 4^k$$

$$V_1 = R_A - ga = 4 - 0.5 \times 2 = 3^k$$

$$V_2 = V_1 - ga = 3 - 1 = 2^k$$

$$V_3 = V_2 - ga = 2 - 1 = 1^k$$

$$V_4 = V_3 - ga = 1 - 1 = 0^k$$

Moment diagram due to vertical loading:

$$M_1 = R_A \times a - ga^2/2 = 7^{k\text{-ft}}$$

$$M_2 = R_A \times 2a - g(2a)^2/2 = 12^k$$

$$M_3 = \text{similar} = 15^k$$

$$M_4 = \text{similar} = 16^{k\text{-ft}}$$

Check:

$$\max M = M_4 = gL^2/8 = 0.5 \times 16^2/8 = 16^{k\text{-ft}}$$

INVESTIGATION OF VERTICAL LOADING ONLY

Maximum shear for the first bay will be assumed as $V_{max} = 4^k$; for the second bay, maximum shear will be assumed $V_{max} = 3^k$.

First Bay (see Figure 51).

$$\tau_o = V/th = \frac{4000}{0.05 \times 30 \text{ in.}} = 2680 \text{ psi}$$

The critical shear (see Equation 1-2) is:

$$\tau_{cr} = k_{ss} E \left(\frac{t}{d}\right)^2 \left[R_h + \frac{1}{2}(R_d - R_h)\left(\frac{d}{h}\right)^3\right]$$

The web will be calculated as a very thin one (in accordance with Figure 24).

$$a/t = \frac{24}{0.05} = 480$$

Assuming a simple supporting on all four sides will be $R_h = R_d = 1.0$.

Modulus of Elasticity: $E = 10.3 \times 10^6$ psi.

Determination of k_{ss} from Figure 13, page 19 is as follows:

$$\frac{h}{d} = \frac{2.5}{2.0} = 1.25 \Rightarrow k_{ss} = 7.25$$

Consequently

$$\tau_{cr} = 7.25 \times 10.3 \times 10^6 \left(\frac{0.05}{24.0}\right)^2 \cdot 1 = 320 < 2680 \text{ psi}$$

The postbuckling range governs.

Determination of the factor k is as follows:

From the graph (Figure 5),

$$\frac{\tau_o}{\tau_{cr}} = \frac{2680}{320} = 8.4 \Rightarrow k = 0.44$$

For α, assume 45 degrees in order to simplify the calculation (see page 8).

$$\sigma_c = -\tau_o (1-k) \sin 2\alpha = -2680 \times (1 - 0.44) = -1500 \text{ psi}$$

$$\sigma_t = \frac{2 k \tau_o}{\sin 2\alpha} + \tau_o (1-k) \sin 2\alpha = \frac{2 \times 0.44 \times 2680}{1} + 1500 = +3850 \text{ psi}$$

Second Bay (see Figure 51 for flow diagram.)

$$\tau_o = V/th = \frac{3000 \text{ lb}}{0.05 \times 30} = 2000 \text{ psi}$$

Factor k (Figure 5):

$$\frac{\tau_o}{\tau_{cr}} = \frac{2000}{320} = 6.25 \Rightarrow k = 0.38, \ \alpha \approx 45 \text{ degrees}$$

In accordance with the equations on page 8,

$$\sigma_c = -\tau_o (1-k) \sin 2\alpha = -2000 \times 0.62 = -1240 \text{ psi}$$

$$\sigma_t = \frac{2 k \tau_o}{\sin 2\alpha} + \tau_o (1-k) \sin 2\alpha = \frac{2 \times 0.38 \times 2000}{1} + 1240 = +2760 \text{ psi}$$

INVESTIGATION OF THE LATERAL LOADING ONLY

(See Figure 51, page 97, and equations on page 49.)

$$U = p^2 E \left(\frac{h}{t}\right)^2 = 0.1^2 \times 10.3 \times 10^6 \times \left(\frac{30}{0.05}\right)^2 = 37 \times 10^9$$

$$\sqrt[3]{U} = 3330$$

Stresses: (From Figure 51, obtain η_2 and η_3)

$$\sigma_a = \eta_2 \sqrt[3]{U} = 0.26 \times 3330 = 870 \text{ psi}$$

$$\sigma_b = \eta_3 \sqrt[3]{U} = 0.19 \times 3330 = 635 \text{ psi}$$

Corresponding with $\alpha = 45$ degrees

$$_H\sigma_1 = {}_H\sigma_2 \approx \frac{870 + 635}{2} = 755 \text{ psi}$$

SIMULTANEOUS CONSIDERATION OF BOTH, VERTICAL AND LATERAL LOADING

First Bay

$$\sigma_c = 1500$$

$$_H\sigma_1 = \frac{755}{745} > \tau_{crit} = 320 \text{ psi}$$

(the post-buckling range governs)

The General Procedure ("Frozen Stress" Assumption Valid)

Assume that both loadings will be applied at the same time, starting from zero, and we want the web to buckle under $\tau^* = 446$ psi. Then the corresponding p^* will be determined. (See equations on page 9 and Figure 51.)

$$\sigma^* = \tau^* - \tau_{cr} = 446 - 320 = 126 \text{ psi}$$

$$\sigma_a^* = \sigma^*/2 = 63 \text{ psi}$$

$$p^* = \frac{\sigma_a^* \tau}{\eta_2 \text{ (longer side)}} \sqrt{\frac{\sigma_a^*}{\eta_2 E}} =$$

$$= \frac{63 \times 0.05}{0.26 \times 30 \text{ in.}} \sqrt{\frac{63}{0.26 \times 10.3 \times 10^6}} = 0.001\,96 \text{ psi}$$

Consequently, by the catenary system, the following remaining lateral loading will be taken (see page 95):

$$p'' = p - p^* = 0.1 - 0.00196 = 0.09804$$

$$\frac{\tau_o}{\tau^*} = \frac{2680}{446} = 6.01 \Rightarrow k = 0.37$$

The compressive stress will be

$$\sigma_I = -\tau_o (1-k^*) \sin 2\alpha + \sigma^*$$

$$= -2680 (1 - 0.37) + 126 = -1559$$

Tensile prestressing:

$$\sigma_{II}' = \frac{2 k^* \tau_o}{\sin 2\alpha} + \tau_o (1-k^*) \sin 2\alpha + \sigma^* =$$

$$= \frac{2 \times 0.37 \times 2680}{1} + 1685 + 126 = 3796 \text{ psi}$$

$$H_o = \sigma_{II}' A = 3796 \times 1 \times 0.05 = 189 \text{ lb}$$

Deflection at buckling:

$$\delta = \eta_1 \text{ (longer side)} \sqrt[3]{\frac{p^* \text{ (longer side)}}{Et}} =$$

$$= 0.26 \times 30 \sqrt[3]{\frac{0.00196 \times 30}{10.3 \times 10^6 \times 0.05}} = 0.0378 \text{ in.}$$

To find σ_{II}, enter the following data into the FORTRAN program:

1. $H_o = 189$ lb
2. $A = 1 \times 0.05$ in.^{2}
3. $\delta = 0.0378$ in.
4. $p'' = 0.09804$ lb per inch
5. $E = 10.3 \times 10^6$ psi

The output is H = 250.9 pounds; y_{max} = 0.05645

Consequently,

$$\sigma_{II} = \frac{250.9}{0.05} = 5018 \text{ psi}$$

Assume that the beam is vertically preloaded. Then the web will buckle at $\tau^* = \tau_{cr}$. Total p will be applied to the postbuckling stage only. Consequently:

$$p^* = o; \quad \sigma^* = o$$

$$\frac{\tau_o}{\tau_{cr}} = \frac{2680}{320} = 8.4 \Rightarrow k = 0.44$$

$$\sigma_I = -\tau_o (1-k) \sin 2\alpha + \sigma^* =$$

$$-2680 (1-0.44) + 0 = -1500 \text{ psi}$$

$$\sigma'_{II} = \frac{2k\tau_o}{\sin 2\alpha} + \tau_o (1-k) \sin 2\alpha =$$

$$\frac{2 \times 0.44 \times 2680}{1} + 1500 = + 3850$$

The component σ_{II} will be obtained from the FORTRAN program with the following input:

1. $H_o = 3850 \times 1 \times 0.05 = 193$ lb
2. $A = 1 \times 0.05$ in.^{2}
3. $E = 10.3 \times 10^6$ psi
4. $\delta = 0$
5. $p = 0.1$ lb/in.^{2}

The output is H = 199.4 lb; y = 0.07247 in. Consequently, σ_{II} = 199.4/1.0 x 0.05 = 3988 psi.

Assume that the beam is laterally preloaded, then

$$\sigma^* = {}_H\sigma_1 = 755 \text{ psi}$$

$$\sigma^* = \tau^* - \tau_{cr}$$

$$\tau^* = \sigma^* + \tau_{cr} = 755 + 320 = 1075 \text{ psi}$$

$$\frac{\tau_o}{\tau^*} = \frac{2680}{1075} = 2.5 \Rightarrow k^* = 0.2$$

$$\sigma_I = -\tau_o (1-k^*) \sin 2\alpha + \sigma^*$$

$$= -2680 (1 - 0.2) + 755 = -1385 \text{ psi}$$

$$\sigma'_{II} = +\frac{2k^*\tau_o}{\sin 2\alpha} + \tau_o (1-k^*) \sin 2\alpha + \sigma^*$$

$$= \frac{2 \times 0.2 \times 2680}{1} + 2680 \times 0.8 + 755 = 3965 \text{ psi}$$

In the above case, $\sigma'_{II} = \sigma_{II}$, because whole p was taken as prestressing.

Alternate General Procedure ("Frozen Stress" Assumption Abolished)

(See page 95 and Figure 52, page 99.)

$$\frac{\tau_o}{\tau_{cr}} = \frac{2680}{320} = 8.40 \Rightarrow k = 0.44$$

$$\sigma_I = -\tau_o (1-k) \sin 2\alpha = -2680 (1-0.44) = -1500 \text{ psi}$$

$$\sigma'_{II} = \frac{2k\tau_o}{\sin 2\alpha} + \tau_o (1-k) \sin 2\alpha$$

$$= 2 \times 0.44 \times 2680 + 1500 = +3850 \text{ psi}$$

The component σ_{II} will be obtained from the FORTRAN program with the following input:

1. $H_o = 3850 \times 1 \times 0.05$ in. = 193 lb
2. $A = 1 \times 0.05 \text{ in.}^2$

3. $p = 0.1$ lb per in.^{2}

4. $\delta = 0$

The output is H = 199.4 lb; Y = 0.07247. Consequently, σ_{II} = 199.4/1 x 0.05 = 3988 lb.

Second Bay $\sigma_c = 1240$

$$\sigma_{H\ 1} = \frac{755}{485 \text{ psi} > \tau_{cr} = 320 \text{ psi}}$$ (See page 219.)

Postbuckling range governs

The analysis will not be provided since it is similar to the analysis presented for the first bay.

Analysis of Uprights and Flanges

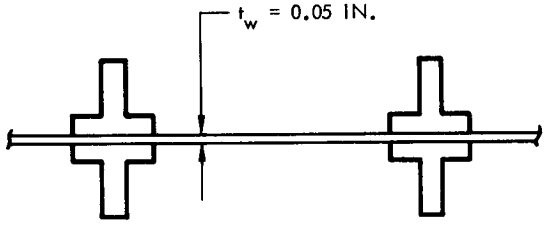

GIVEN: $A_U = 0.5$ IN.^{2}
$\sigma_{DESIGN} = 40$ ksi

VERTICAL LOAD ONLY

A numerical example will be made to illustrate the equations to be used for vertical loading. Consider double upright of "T" shape with cross sectional area of 0.5 square inch.

Stress Consideration:

The stress in the upright due to partial tension diagonal folds (see page 26) is as follows:

$$\sigma_U = - \frac{k \tau \tan \alpha}{\frac{A_U}{d t_w} + 0.5 (1-k)} \qquad (B1)$$

where k = 0.44; τ = 3850 psi; and α = 45 degrees have been determined in the web analysis, therefore,

$$\sigma_U = - \frac{0.44\ (3850)\ \tan\ 45°}{\frac{0.5}{(24)\ (0.05)} + 0.5\ (1-0.44)} = -2430 \text{ psi (compression)}$$

The formula

$$\sigma_U = \frac{-P}{A}$$

where (see page 110):

$$A = A_U + t_w d\ (0.5)\ (1-k)$$

$$P = t_w d\ (\sigma_T \sin \alpha + \sigma_c \cos \alpha) \text{ (for } \alpha = 45°)$$

presented in Section III can also be used. From the analysis of the web

σ_T = + 3850 psi (tension diagonal fold direction)

σ_c = - 1500 psi (compression perpendicular to diagonal fold direction)

Hence

$$\sigma_U = \frac{-P}{A} = - \frac{t_w d\ (\sigma_T \sin \alpha + \sigma_c \cos \alpha)}{A_U + t_w d\ (0.5)\ (1-k)} \qquad \text{(B2)}$$

$$= - \frac{(0.05)\ (24)\ (3850 \sin 45° - 1500 \cos 45°}{0.5 + 0.05\ (24)\ (0.5)\ (1-0.44)}$$

= - 2400 psi (compression)

Comparison between the two stresses show that only 1 percent variation exists between the two techniques. This justification should be mentioned since $\sigma_U = \frac{-P}{A}$ is used for combined loading analysis. Since, σ_U is less than σ design, the upright will not fail due to stress.

Stability Consideration

Column Behavior

The upright should be investigated for column buckling. The d/h ratio is $\frac{d}{h} = \frac{24}{30} = 0.8$. Since $d < 1.5h$, use (see page 26).

$$L_e = \frac{h}{\sqrt{1 + k^2\left(3 - \frac{2d}{h}\right)}} = \frac{30}{\sqrt{1 + (0.44)^2\left(3 - \frac{2\,(24)}{30}\right)}}$$

or

$$L_e = 26.6 \text{ in.}$$

The critical load using the effective length $L_e = 26.6$ inches is (See Equation A 21, page 209.)

$$P_{cr} = \frac{\pi^2 E I}{L_e^2}$$

where

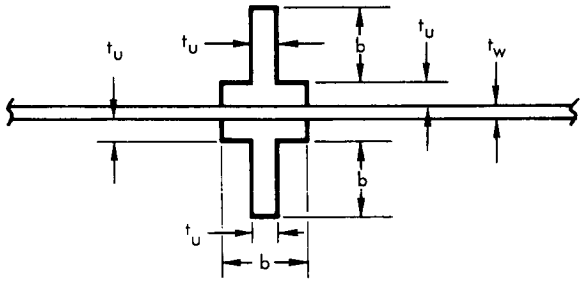

Given:

$t_u = 0.18$ in.

$b = 0.7$ in.

$t_w = 0.05$ in.

$E_{aluminum} = 10.3 \times 10^6$ psi

$$I = \frac{b\,(2\,t_u + t_w)^3}{12} + \frac{(2\,b + t_w)^3\,t_u}{12}$$

$$= \frac{0.7\left[2\,(0.18 + 0.05)\right]^3}{12} + \frac{\left[2\,(0.7) + 0.05\right]^3\,(0.18)}{12}$$

$$= 4.97 \times 10^{-2} \text{ in.}^4$$

Therefore

$$P_{cr} = \frac{\pi^2 \ (10.3 \times 10^6) \ (4.97 \times 10^{-2})}{(26.6)^2} = 7110 \text{ lb (compression)}$$

or

$$\sigma_{cr} = \frac{P_{cr}}{A} = \frac{P_{cr}}{A_U + 0.5 \ d t_w \ (1-k)}$$

$$= \frac{7110}{0.5 + 24 \ (0.05) \ (0.5) \ (1-0.44)}$$

$$= 8500 \text{ psi}$$

Since $\sigma_U < \sigma_{cr}$, the upright will not buckle as a column.

Forced Crippling

$$\sigma_o = c \, k^{2/3} \left(\frac{t_u}{t_w}\right)^{1/3} \text{ ksi (See page 28.)}$$

For double upright, c = 26 (7075-T6 aluminum)

$$\sigma_o = 26 \ (0.44)^{2/3} \left(\frac{0.18}{0.050}\right)^{1/3}$$

$$\sigma_o = 23.0 \text{ ksi}$$

Since $\sigma_U < \sigma_o$, the upright will not have forced crippling.

Crippling

First we must determine the range of $\frac{A_U}{t_w d}$

$$\frac{A_U}{t_w d} = \frac{0.5}{0.05 \ (24)} = 0.41$$

Since $\frac{A_U}{t_w d} > 0.2$, Equation 1-4, page 32, governs.

$$\sigma_{cc} = \frac{\sum_{i=1}^{N} A_i \, \sigma_{cc_i}}{\sum_{i=1}^{N} A_i}$$

For σ_{cc_i} of the leg attached to the web, we should use σ_o, the forced crippling value that considers the effect of the diagonal fields. The σ_{cc_i} for the outstanding legs are taken from Figure 21 for $\frac{b}{t_u} = \frac{0.7}{0.18} = 3.9$ and is $\sigma_{cc_i} = 29$ ksi.

Therefore,

$$2\left[A_1\right]\left[\sigma_{cc_i}\right] = 2\left[0.7\,(0.18)\right]\left[23 \times 10^3\right]$$

$$2\left[A_2\right]\left[\sigma_{cc_2}\right] = 2\left[0.7\,(0.18)\right]\left[68 \times 10^3\right]$$

where the number 2 refers to two areas; i.e., one for each side of the web.

$$\sigma_{cc} = \frac{2\left[0.7\,(0.18)\right]\left[23 \times 10^3\right] + 2\left[0.7\,(0.18)\right]\left[68 \times 10^3\right]}{2\left[0.7\,(0.18)\right] + 2\left[0.7\,(0.18)\right]}$$

or

$$\sigma_{cc} = 45{,}500 \text{ psi}$$

Since $\sigma_U < \sigma_{cc}$, the upright of the outstanding leg will not cripple.

Torsional Instability (see Equation 3-47)

$$P_{cr} = \frac{C_1\left(\frac{\pi}{L}\right)^2 + EI_z\,(z_o - h_z)^2\left(\frac{\pi}{h}\right)^2 + C}{\frac{I_o}{A} - z_o^2 + h_z^2}$$

where

$A = A_U + t_w d\ 0.5\ (1-k) = 0.836\ \text{in.}^2$ (See page 110.)

$C = GJ$ (See page 119.)

$C_1 = E\ C_w = o$ (See pages 119 and 124.)

$I_o = I_x + I_y = 2\ (4.97 \times 10^{-2})\ \text{in.}^4$

$$J \approx \frac{2bt_u^3 + 2bt_u^3}{3} \approx 5.43 \times 10^{-3}\ \text{in.}^4$$

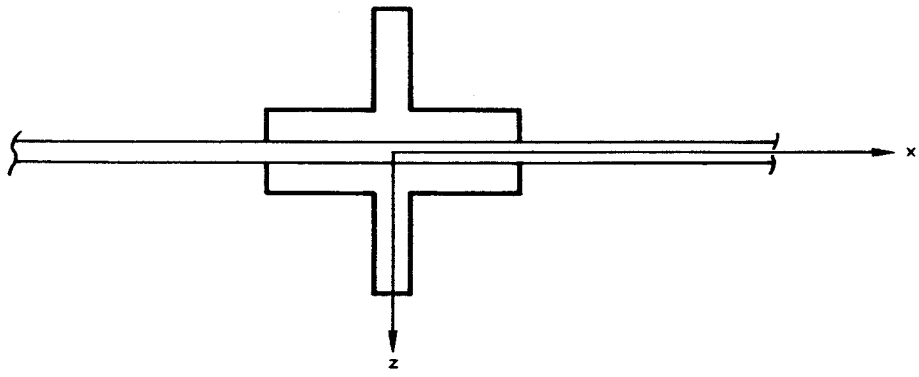

The preceding sketch shows that $z_o = h_z = 0$.

For $G = 3.9 \times 10^6$ psi for 7075-T6 aluminum alloy

$$P_{cr} = \frac{3.9 \times 10^6\ (5.43 \times 10^{-3})}{\frac{2\ (4.97 \times 10^{-2})}{0.836}} = 1.78 \times 10^5\ \text{lb}$$

and

$$\sigma_{cr} = \frac{P_{cr}}{A} = \frac{1.78 \times 10^5}{0.836} = 2.13 \times 10^5\ \text{psi}$$

Since $\sigma_U < \sigma_{cr}$, the upright will definitely not fail in torsional buckling.

LATERAL LOADING ONLY

The same cross-sectional area of the upright will be used to illustrate a numerical example for partial-tension-field beams subjected to only lateral pressure of 0.1 psi.

Stress Analysis

The distributed force acting on the upright as shown in the sketch below is q = pd or q = 0.1 (24) = 2.4 lb/in.

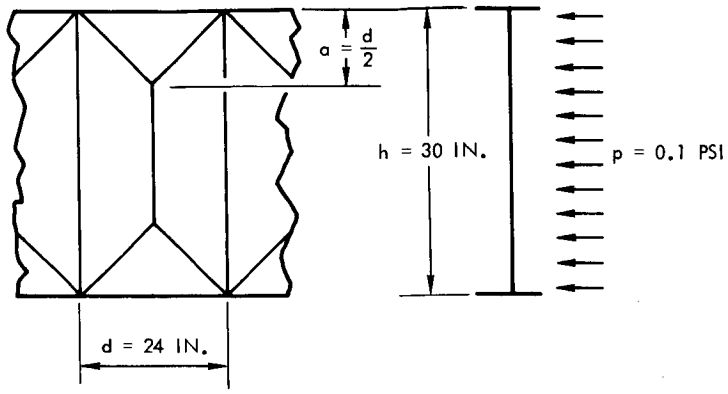

From Table 2, (page 58) the bending moment in the upright is

$$M_u = q\left(\frac{h^2}{8} - \frac{a^2}{6}\right)$$

or

$$M_u = 2.4\left(\frac{30^2}{8} - \frac{12^2}{6}\right) = 213 \text{ in.-lb}$$

The bending stress is

$$\sigma_{bend} = \pm\frac{Mc}{I} = \frac{213\ (0.7)}{4.97 \times 10^{-2}} = 3000 \text{ psi}$$

The tensile stress σ_t = 870 psi as calculated in the web analysis induces compressive stress in the upright of

$$\sigma_{compression} = \frac{P}{A_U} = \frac{\sigma_t t_w d}{A_U} = \frac{870\ (0.050)\ (24)}{0.5} = 2100 \text{ psi}$$

The total stress in upright is

$$\sigma_{U_{max}} = \sigma_{bend} + \sigma_{compression}$$

$$\sigma_{U_{max}} = 3000 + 2100 = 5100 \text{ lb per in.}^2 \text{ (compression)}$$

Since $\sigma_{u_{max}}$ is less than (1) σ_{cr} due to column buckling (2) σ_o due to forced crippling, (3) σ_{cc} due to crippling, (4) σ_{cr} due to torsional buckling, and (5) σ_{Design} design allowable, the upright will not fail.

COMBINED LOADING

Consider the combined loading of p = 0.1 psi and V = 0.5 k on the partial-tension field beam.

Stress Analysis

Stress in the upright due to lateral deflection of the upright will first be considered (deflection out of the plane of the web). The lateral load intensity acting on the upright is (see page 103)

$$q_{oz} = \frac{p\pi d\left(h - \frac{d}{2}\right)}{2h}$$

or

$$q_{oz} = \frac{(0.1)\pi\ (24)\ \left(30 - \frac{24}{2}\right)}{2\ (30)} = 2.26 \text{ lb per in.}$$

The bending stress at $x = \frac{h}{2}$ (maximum stress point) from Equation 3-20 of Section III is

$$\sigma_{\substack{bend \\ y}} = \frac{2\,EI_y\,A_{sym}}{P_{cr}\,h\,Z_y}\left[\frac{q_{oz}\,h}{2} + \sum_{i=1}^{N} Q_n \sin\frac{\pi c_i}{h}\right]$$

where

$$A_{sym} = \frac{1}{1 - \frac{P}{P_{cr}} - \frac{F_o h}{4\,P_{cr}}\left(\frac{2}{\pi^2}\right)\left(\frac{\pi^2}{3} - 1\right)}$$

$$Q_n = T_n \sin\phi_n + T_{\dot{n}} \sin\phi_{\dot{n}}$$

$$Z_y = \frac{I_y}{c}$$

Since the slope $\phi_n \approx \phi_{\dot{n}} \approx 0$, $Q_n = 0$.

The bending stress reduces to

$$\sigma_{\substack{\text{bend} \\ y}} = \frac{E\, c\, q_{oz}\, A_{sym}}{P_{cr}}$$

For $d < h$ (since our $d = 0.8h$) it is recommended that F_o be included in P where P is defined by (see page 110)

$$P = \frac{\sigma_T\, t_w d\, \sin\alpha\, (1 + \tan\alpha)}{2} + \frac{\sigma_c\, t_w d\, \cos\alpha\, (1 + \tan\alpha)}{2}$$

Thus, for $d < h$, A_{sym} reduces to

$$A_{sym} = \frac{1}{1 - \frac{P}{P_{cr}}}$$

From web analysis and FORTRAN

$$\sigma_T = 5018 \text{ psi}$$

$$\sigma_c = -1559 \text{ psi}$$

$$\alpha = 45 \text{ degrees}$$

$$P = \frac{5018\ (0.05)\ (24)\ \sin 45^\circ\ (1 + \tan 45^\circ)}{2}$$

$$+ \frac{(-1559)\ (0.05)\ (24)\ \cos 45^\circ\ (1 + \tan 45^\circ)}{2}$$

or

$$P = 2935 \text{ lb}$$

$$A_{sym} = \frac{1}{1 - \frac{2935}{7100}} = 1.70$$

$$\sigma_{bend} = \frac{10.3 \times 10^6 \ (0.7) \ (2.26) \ (1.70)}{7110} = 3893 \text{ psi}$$

The value of A_{sym} can also be obtained from Figure 63 for $\frac{P}{P_{cr}} = 0.32$ and $\frac{F_o h}{4} = 0$.

The compressive stress for $d < h$ is (see Equation 3-21)

$$\sigma_{compression} = \frac{P}{A} = \frac{P}{A_U + 0.5 \, t_w d \ (1-k)} = \frac{2935}{0.836} = 3510 \text{ psi}$$

$$\sigma_U = \sigma_{bend} + \sigma_{compression} = 3893 + 3510 = 7403 \text{ psi}$$

The upright will not fail in strength since $\sigma_U < \sigma_{Design}$. Since $\sigma_U < \sigma_{cr}$ where $\sigma_{cr} = 8500$ psi, the upright will not fail in column buckling. The upright will not buckle in forced crippling, crippling, or torsional buckling since $\sigma_U < \sigma_o$, $\sigma_U < \sigma_{cc}$, and $\sigma_U < \sigma_{cr}$.

Now consider the stresses in the upright when the upright deflects in the plane of the web.

Force intensity R_o is (see page 103)

$$R_o = \sigma_T \, t_w \cos \alpha + \sigma_c \, t_w \sin \alpha$$

$$R_o = 5018 \ (0.05) \cos 45° - 1559 \ (0.05) \sin 45°$$

or

$$R_o = 122 \text{ lb/in.}$$

At $x = \frac{h}{2}$ (from Equation 3-24)

$$\sigma_{\substack{bend \\ z}} = \frac{EI_Z \, A_{Anti}}{2h \, P_{cr} \, Z_z} \left[\frac{2}{3\pi} R_o h \right] = \frac{E \, A_{Anti} \, R_o c}{3\pi \, P_{cr}}$$

where

$$A_{anti} = \frac{1}{1 - \frac{P}{4\,P_{cr}}} = 1.09 \text{ for } d < h$$

$$\sigma_{bend} = \frac{10.3 \times 10^6 \,(1.09)\,(122)\,(0.7)}{3\pi\ 7110} = 14,298 \text{ psi}$$

$$\sigma_U = \sigma_{bend} + \sigma_{compression} = 14,298 + 3510 = 17,808 \text{ psi}$$

Since $\sigma_U < \sigma_{design}$, the upright will not fail due to material.

Stability Criteria

The stress in the upright ($\sigma_U = 17,808$) must be less than the following buckling criteria or failure will exist.

1. Column behavior for antisymmetric buckle shape

$$\sigma_{cr_{Anti}} = 4\,\sigma_{cr_{sym}} = 4\,(8500) = 34,000 \text{ psi}$$

$$\sigma_U < \sigma_{cr_{Anti}}$$

Therefore, upright will not fail in column buckling in the antisymmetric mode.

2. Forced crippling

$$\sigma_o = 23,000 \text{ psi}$$

$$\sigma_U < \sigma_o$$

Therefore, upright will not fail due to force crippling.

3. Crippling

$$\sigma_{cc} = 26,000 \text{ psi}$$

$$\sigma_U < \sigma_{cc}$$

Therefore, upright will not fail due to crippling.

4. Torsional instability

$$\sigma_{cr} = 2.13 \times 10^5 \text{ psi}$$

$$\sigma_U < \sigma_{cr}$$

Therefore, upright will not fail due to torsional instability.

CURVED BEAM NUMERICAL EXAMPLE

To demonstrate the analysis procedure, a curved semitension field beam web will be analyzed. It is assumed that the beam is a section of a cylindrical structure loaded as shown in Figure 100.

The structural configuration is indicated as follows:

Geometry:

$A_{FL} = 0.75$ in.^{2} $\quad R = 122.5$ in.

$A_U = 0.50$ in.^{2} $\quad d = 30$ in.

$t = 0.025$ in. $\quad h = 24$ in.

Double uprights and flanges with pinned joints.

Material properties (7075-T6 aluminum alloy):

$\mu = 0.32$

$\sigma_{ty} = 64.5$ ksi

$\sigma_{bru} = 108\text{-}137$ ksi $(e/D = 1.5\text{-}2.0)$

$\sigma_{tu} = 72$ ksi

$E = 10.3 \times 10^6$ psi

Loading:

$2S = 40,000$ lb

$p = 1$ psi (internal pressure)

Compute critical web shear buckling stress (no lateral pressure loading) as follows:

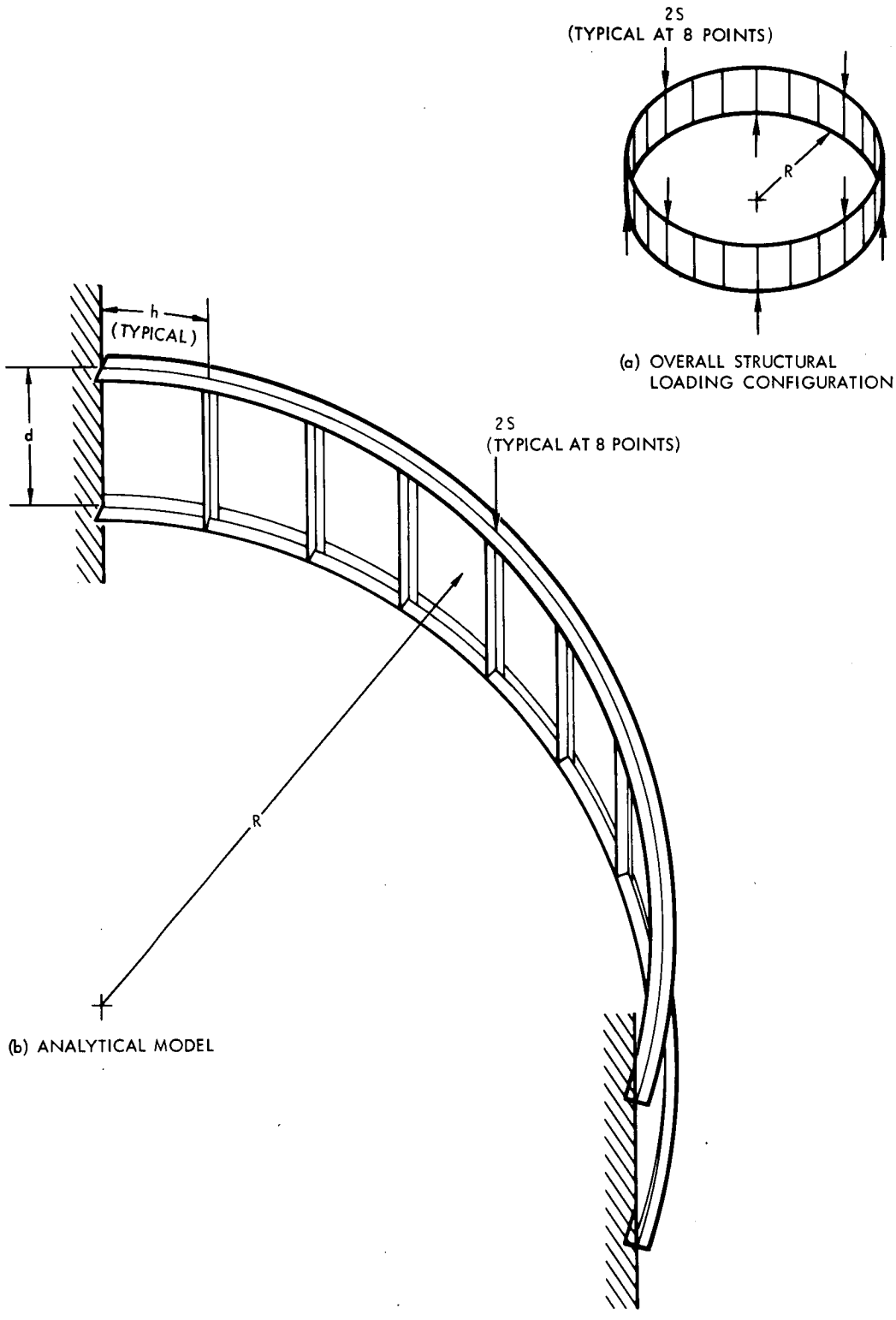

Figure 100. Curved Beam Numerical Example Configuration

$$\tau_{cr} = k_s \frac{\pi^2 Eh^2}{12 R^2 Z^2} \qquad \text{(See Equation 4-3.)}$$

$$d/h = 30/24 = 1.25$$

$$Z = \frac{h^2}{Rt}\sqrt{1 - \mu^2} = \frac{(24)^2}{122.5\,(0.025)}\sqrt{1-(0.32)^2}$$

$$= 179$$

k_s (Figure 74) = 41

$$\tau_{cr} = 41\,\frac{(3.1416)^2\ 10.3\ (10)^6\ (24)^2}{12\,(122.5)^2\,(179)^2}$$

$$= 417 \text{ psi}$$

Compute p^o_{cr} as follows:

$$p^o_{cr} = -0.92\,\frac{Et^2}{dR}\sqrt{\frac{t}{R}} \qquad \text{(See Equation 4-63.)}$$

$$= -0.92\,\frac{10.3\ (10^6)\,(0.025)^2}{30\,(122.5)}\sqrt{\frac{0.025}{122.5}}$$

$$= -0.023 \text{ psi}$$

$$\left(\frac{\tau^*}{\tau_{cr}}\right)^2 + \frac{p*}{p^o_{cr}} = 1 \qquad \text{(See Equation 4-59.)}$$

$$\left(\frac{\tau^*}{417}\right)^2 + \frac{1}{-0.023} = 1$$

$$\frac{\tau^*}{417} = \sqrt{1 + 43.48}$$

$$\tau^* = 2780 \text{ psi}$$

Applied $\tau = \frac{S}{dt} = 20,000/(30)\ 0.025$

$$= 26,700 \text{ psi}$$

Therefore, the web is buckled under this combination of loads. To find the maximum internal pressure at which the applied vertical loading will cause buckling, Equation 4-59 may be used again.

$$\left(\frac{26,700}{417}\right)^2 + \frac{p^*}{-0.023} = 1$$

$$p^* = 0.023\,(1 - 4090.)$$

$$= 94 \text{ psi}$$

This is not a reasonable pressure because the membrane stresses of the web would reach ultimate value before this pressure could be applied.

The value of the diagonal tension factor, k, is found by using Figure 80.

$$\frac{\tau}{\tau_{cr}} = \frac{26,700}{417} = 64$$

$$300\,\frac{td}{Rh} = 300\,\frac{0.025\,(30)}{122.5\,(24)}$$

$$= 0.0765$$

From Figure 80, k = 0.78

To compute the angle of diagonal tension, α, use Figure 81.

$$\frac{\frac{h}{R}\sqrt{\frac{E}{\tau}}}{\sqrt{1 + R_R}} = \frac{\frac{24}{122.5}\sqrt{\frac{10.3\,(10^6)}{26,700}}}{\sqrt{1 + \frac{30\,(0.025)}{0.75}}}$$

$$= 2.72$$

$$\frac{1 + Rs}{1 + R_R} = \frac{1 + \frac{24\,(0.025)}{0.5}}{1 + \frac{30\,(0.025)}{0.75}}$$

$$= 1.1$$

From Figure 81.

$$\alpha_{PDT} = 43.3°$$

To estimate α, use Figure 81(C).

For $k = 0.78$

$$\alpha / \alpha_{PDT} = 0.95$$

$$\alpha = 0.95\ (43.4)$$

$$= 41.2°$$

The data curve of this figure is based on $\frac{A_U}{ht} = 1.00 = \frac{A_{FL}}{dt}$

In this case,

$$\frac{A_U}{ht} = \frac{0.5}{24\ (0.025)} = 0.83$$

and

$$\frac{A_{FL}}{dt} = \frac{0.75}{30\ (0.025)} = 1.00$$

In computing stress in post-buckled catenary elements, the initial conditions of the catenary are

Length (Figure 78):

$$\text{Length} = \theta_2\, r_2$$

$$\theta_2 = \cos^{-1}\left[2\left(\frac{1 - K_1^2}{1 + K_1^2}\right)^2 - 1\right] \quad \text{(See Equation 4-5.)}$$

$$K_1 = \frac{\left(1 - \cos\frac{h}{2R}\right)\sin\alpha}{\sin\frac{h}{2R}} \quad \text{(See Equation 4-6.)}$$

$$= \frac{\left(1 - \cos\frac{24}{245}\right)\ \sin 41.2°}{\sin\frac{24}{245}}$$

$$= \frac{0.00486\,(0.65869)}{0.09691}$$

$$= 0.0320123$$

$$\theta_2 = \cos^{-1}\left[2\left(\frac{1 - 0.0010248}{1 + 0.0010248}\right)^2 - 1\right]$$

$$= \cos^{-1}(0.9918164) = 7.33333 \text{ degrees}$$

$$= 0.12798 \text{ radians}$$

Then, as per Equation 4-7, it follows

$$r_2 = \frac{R\dfrac{\sin^2\frac{\theta_1}{2}}{\sin^2\alpha} + R\left(1 - \cos\dfrac{\theta_1}{2}\right)^2}{2\left(1 - \cos\dfrac{\theta_1}{2}\right)}$$

$$= \frac{122.5\dfrac{\sin^2\frac{24}{245}}{(0.65869)^2} + 122.5\left(1 - \cos\dfrac{24}{245}\right)^2}{2\left(1 - \cos\dfrac{24}{245}\right)}$$

$$= 281 \text{ in.}$$

Initial length of the catenary element is

$$S = \theta_2 r_2$$

$$= 35.99 \approx 36. \text{ in.}$$

Initial stress in the catenary element is

$$\sigma_{II}' = \frac{2k\,\tau_o}{\text{Sin } 2\alpha} + \tau_o\,(1-k)\sin 2\alpha \text{ (See Equation 4-9.)}$$

$$= \frac{2\,(0.78)\,26,700}{\text{Sin } 82.4} + 26,700\,(1 - 0.78)\,\sin\,(82.4)^\circ$$

$$= 42,020 + 5,822$$

$$= 47,840 \text{ psi}$$

The initial catenary end load is $47,840\,(0.025) = 119.6$ lb.

Initial deflection (before panel buckles) is

$$\delta = R\left(1 - \cos\frac{h}{2R}\right)$$

$$= 122.5\left(1 - \cos\frac{24}{245}\right)$$

$$= 0.587 \text{ in.}$$

After buckling, the panel is flat and initial catenary deflection is assumed to be zero before lateral pressure loading is applied.

Initial catenary conditions:

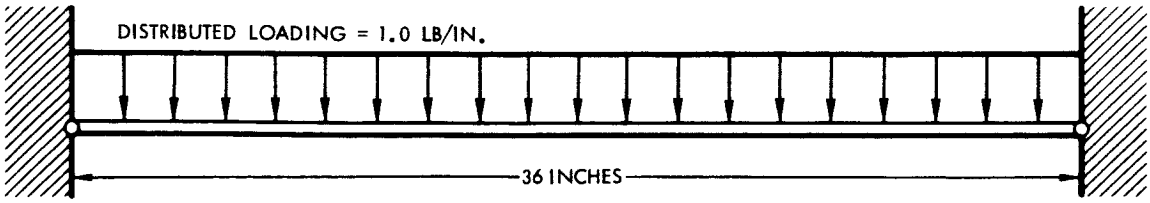

Initial tension in the element equals 119.6 pounds (before pressure load is applied); the element cross-section equals 1 x 0.025 in.; E = 10.3 (10^6) psi.

This input data applied in the FORTRAN program of the appendix produces the final element loading due to the total combined loading, and the maximum element deflection. These values are:

$$\sigma_{II} = \frac{H}{A} = \frac{289}{0.025} = 11,560 \text{ psi}$$

$$y = 0.56 \text{ inches}$$

The ultimate tensile stress of the material is 72 ksi. This value of 72 ksi must be reduced by any effect due to stress concentrations at the edges of the sheet at the upright and flange attachments and compared to σ_{II}.

APPENDIX C

FORTRAN

FORTRAN IV PROGRAM FOR CATENARY ANALYSIS

The following paragraphs present the details on the use of the FORTRAN IV IBM (7094) digital computer program developed for the analysis of extensible catenary with an initial zero deflection which is prestressed before the erection and then loaded with the arbitrary loading P_i. The program also computes an approximate solution for a prestressed extensible catenary with an initial deflection and arbitrary loadings.

The essential features of the S&ID catenary with vertical loading analysis program (8K-RB2) are described. The program may be used to analyze the behavior of catenary under different loading. The description of the method of analysis, assumptions, and input and output format explains how the program operates.

ANALYSIS

A catenary system prestressed with applied loading and zero deflection is shown in Figure 101. A prestressed catenary system with applied loading and an initial deflection is shown in Figure 102. The loading P_N and distance X_N are arbitrary in both figures.

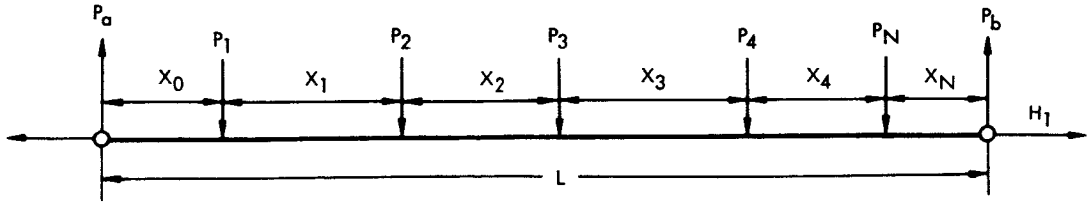

Figure 101. Prestressed Catenary System With Applied Loading and Zero Deflection

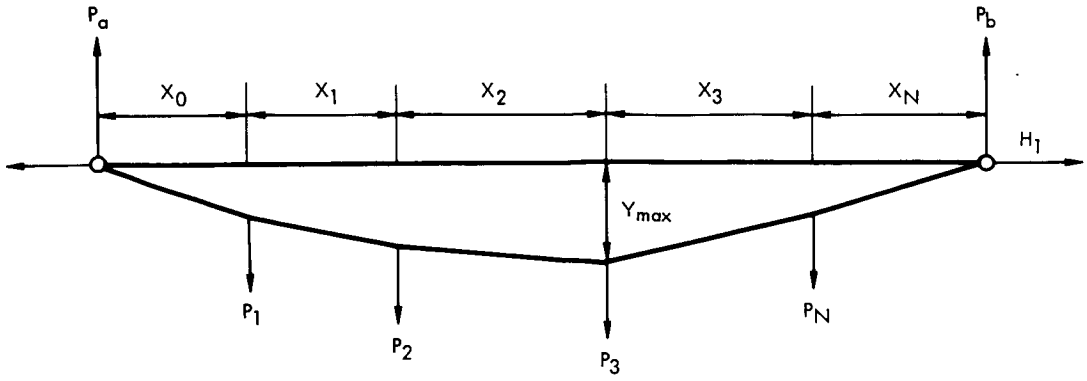

Figure 102. Prestressed Catenary System With Applied Loading and An Initial Deflection

Utilizing the applied loading and distances, the FORTRAN IV program computes the following numerical data:

a. Vertical Reactions

b. Shears

c. Moments

If the pretensioned catenary (with H_1) is erected before the loading is applied, then the initial deflection is equal to zero. The program computes the "extensible" horizontal tension (H) from the equation

$$2L\,(H^3 - H^2\,H_1) - ZAE = 0 \qquad (C1)$$

by the cubic subroutine, and uses the horizontal tension to solve for the deflection Y (I) = Moment/H, tension $T = \sqrt{Shear^2 + H^2}$, and total span length S. The analysis is now completed for Figure 101. The final extensible shape of loaded catenary is determined.

In the second case when the initial deflection is not equal to zero the program computes the inextensible horizontal tension due to loading P_i without prestressing consideration.

Horizontal tension

$$H_o = \frac{M_{max}}{Y_{max}} \qquad (C2)$$

Total span of inextensible length

$$S = S + EL\ (I) \tag{C3}$$

The horizontal tension for the extensible catenary is now computed from the cubic equation.

$$2H^3 L (1 + \alpha^2) + 2H^2 EA \left[S - L\left(1 + \frac{1}{2}\alpha^2\right)\right] + Z(2H - EA) = 0 \tag{C4}$$

by the cubic subroutine, considering loading P_i only, without pretensioning.

This extensible horizontal tension is now added to the prestressing extensible horizontal tension to obtain the final horizontal tension.

$$H_{final} = H + H_1 \tag{C5}$$

Maximum final deflection

$$Y_{final} = \frac{M_{max}}{H_{final}} + Y_{max} \tag{C6}$$

PROGRAM DETAILS

Input Data

Figure 103 is a flow chart of the program. The source deck listing for the program is shown in Figure 104. Figure 105 provides the input data. Figure 106 gives the first example of some initial deflection. Figure 107 gives the example of initial zero deflection.

The input data cards will be sorted on columns 73 through 80 before the analysis is begun. Therefore, any cards which have improper sequence numbers will generate an error in the analysis.

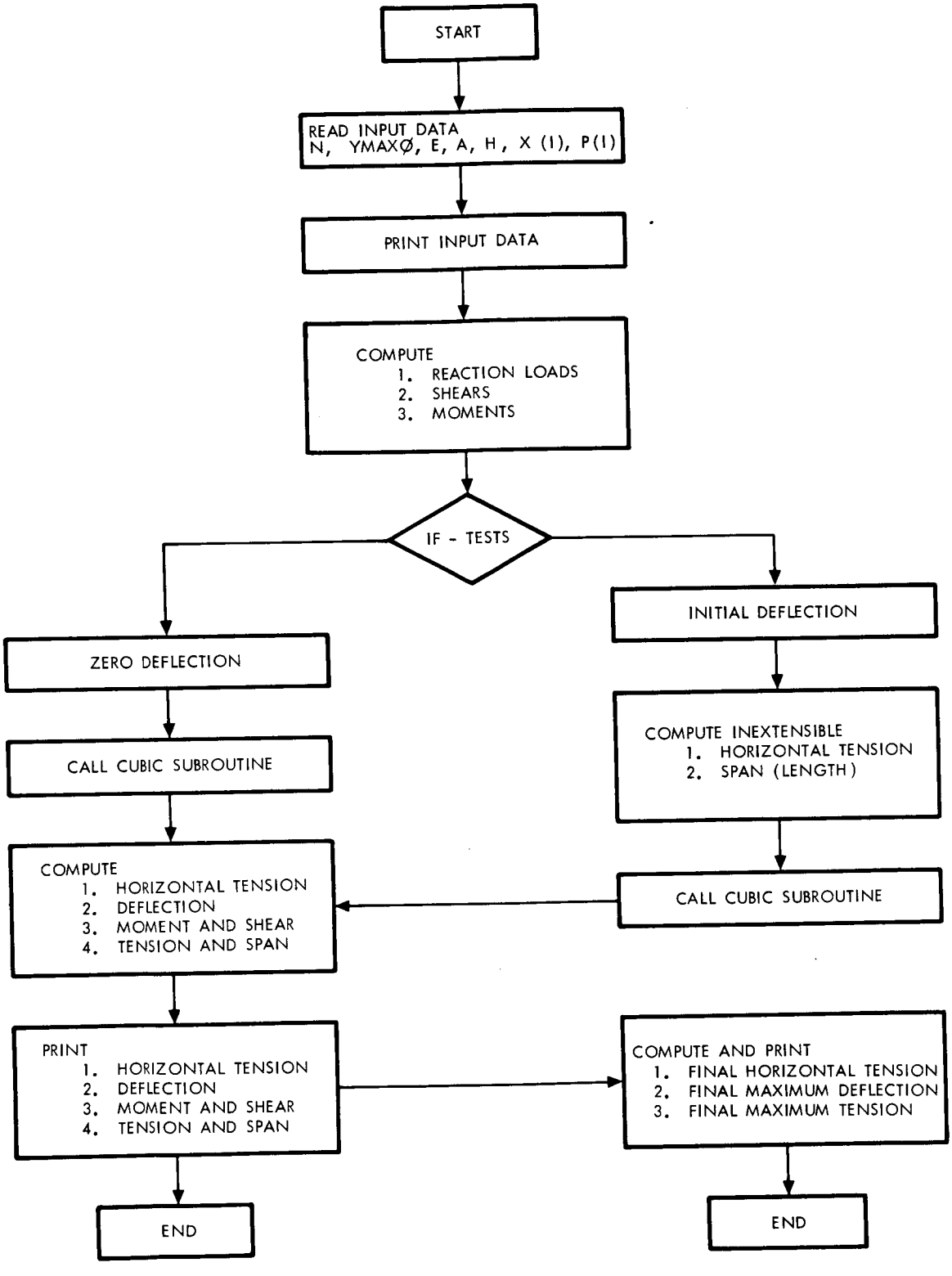

Figure 103. Flow Chart of the Program

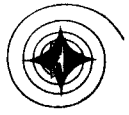

```
                                                                    02/07/86
          8K-RB2     -  EFN   SOURCE STATEMENT  -  IFN(S)  -

C      PARTIAL TENSION FIELD BEAMS                          DECK 8K-RB2      00000010
C                                                           RON BEREZNAK     00000020
C      APPLICATION OF THE CATENARY SOLUTIONS TO PARTIAL TENSION BEAMS        00000030
C     NOMENCLATURE  FOR  DATA                                               00000040
C       N     NO. OF INCREMENTS                                             00000050
C       E     MODULUS  OF  ELASTICITY                                       00000060
C       YMAX  MAXIMUM  DEFLECTION                                           00000070
C       H1    PRESTRESSING  TENSION                                         00000080
C       A     AREA                                                          00000090
C       X(I)  HORIZONTAL DISTANCES BETWEEN LOADS                            00000100
C       P(I)  APPLIED  LOADING                                              00000110
                                                                            00000120
      DIMENSION XO(1),X(100),FO(1),F(100),P(100), EMO(1),EM(100),T(100),    00000130
     1COSA(100), Y(100), TP(100), EQ(5), EL(100), COSAA(100), ELA(100),     00000131
     2FO2(1),F2(100), Q(8), CAPY(100)                                       00000132
      L = 0                                                                 00000133
    5 READ(5,10) N, YMAXO, E, A, H1,   (X(I),I=L,N), (P(I),I=1,N)           00000140    2
   10 FORMAT (1I12/4E12.8/(6E12.8) )                                        00000150
      WRITE(6,15) N, YMAXO, E, A, H1,  (X(I),I=L,N), (P(I),I=1,N)           00000160   16
   15 FORMAT(1H1////11X,11HINPUT  DATA/5X,1I12/5X,1P4E15.4/(5X,6E15.4))     00000170
   17 PA  = 0.                                                              00000180
      YMAX = YMAXO                                                          00000190
      SUMP = 0.                                                             00000200
      DO 30 I = 1,N                                                         00000210
      SUMX = 0.                                                             00000220
      DO 20 J = I,N                                                         00000230
   20 SUMX = SUMX + X(J)                                                    00000240
      SUMP = SUMP + P(I)                                                    00000250
   30 PA   = PA + P(I) * SUMX                                               00000260
      ELL  = 0.                                                             00000270
      DO 40  I = L,N                                                        00000280
   40 ELL  = ELL + X(I)                                                     00000290
      PA   = ABS (PA)/ELL                                                   00000300
      PB   = ABS (SUMP) - PA                                                00000310
      F(L) = PA                                                             00000320
      Z    = 0.                                                             00000330
```

Figure 104. Listing of Source Deck for the Catenary (Sheet 1 of 4)

```
                                                        02/07/86
       8K-RB2      -  EFN   SOURCE STATEMENT  -  IFN(S)  -
    DO 50 I = 1,N                                        00000340
    F(I) = F(I-1) + P(I)                                 00000350
    F2(I)= F(I)**2                                       00000360
 50 Z    = Z  + F2(I) * X(I)                             00000370
    F02  = PA**2                                         00000380
    Z    = Z + F02 * X(L)                                00000390
    EMO  = 0.                                            00000400
    EMAX = 0.                                            00000410
    N1   = N + 1                                         00000420
    IF(YMAX.EQ.0.) GO TO  96                             00000425
    DO 60 I = 1,N1                                       00000430
    EM(I)= EM(I-1) + X(I-1) *F(I-1)                      00000440
    IF(EMAX - EM(I)) 55,60,60                            00000450
 55 EMAX = EM(I)                                         00000460
    IMAX = I                                             00000470
 60 CONTINUE                                             00000480
 61 HO   = EMAX/YMAX                                     00000490
    DO 65  I = 1,N1                                      00000492
 65 Y(I) = EM(I)/HO                                      00000510
    HO2  = HO**2                                         00000520
    S    = 0.                                            00000530
    DO 75  I = L,N                                       00000540
 72 T(I) = SQRT(F2(I) +  HO2)                            00000550    98
    COSA(I)= HO/T(I)                                     00000570
    EL(I)= X(I)/COSA(I)                                  00000580
 75 S    = S  + EL(I)                                    00000590
 86 WRITE(6,87) S,HO,EMO,(Y(I),I=1,N)                    00000700    109
 87 FORMAT (1H1,21X, 60HPARTIAL TENSION FIELD BEAMS ** STRESS AND STRA00000710
   1IN IN CATENARY////5X,30HINEXTENSIBLE CATENARY LENGTH = , 1PE13.6  00000711
   2//10X,20HHORIZONTAL TENSION = ,1PE11.3 /10X,19HSHAPE - Y(I) VALUES00000712
   3/(15X,6E15.3) )                                      00000713
    WRITE(6,90)(T(I), I = L,N)                           00000720    117
 90 FORMAT(10X,19HTENSION IN CATENARY/(15X, 1P6E15.3)  ) 00000730
 95 ALF2 = 0.                                            00000740
    EQ(1)= 0.                                            00000760
    EQ(2)= 2.*ELL*(1.+ ALF2)                             00000770
    EQ(3) =2.*E*A*(S -ELL*(1.+.5*ALF2) )                 00000780
```

Figure 104. Listing of Source Deck for the Catenary (Sheet 2 of 4)

```
                                                                    02/07/86
      8K-RB2     -  EFN   SOURCE STATEMENT  -  IFN(S)  -

     EQ(4) = 2.* Z                                                  00000790
     EQ(5) = -E * Z  * A                                            00000800
     GO TO 98                                                       00000805
  96 DO 97 I = 1,N1                                                 00000810
  97 EM(I)= EM(I-1) + X(I-1) *F(I-1)                                00000811
     EQ(1)=0.                                                       00000813
     EQ(2)= 1.                                                      00000814
     EQ(3)  =  -  H1                                                00000815
     EQ(4)= 0.                                                      00000816
     EQ(5)= -Z*A*E /(2.*ELL)                                        00000817
  98 FLAG = 1.E +10                                                 00000819
     TOL  = 0.                                                      00000820
     CALL QARTIC(EQ,Q,TOL, MTYPE,FLAG)                              00000830    138
     H    = 0.                                                      00000840
     DO 110   I= 2,8,2                                              00000850
     IF(Q(I) - 1.E+10)100,110,100                                   00000860
 100 IF(Q(I) ) 110,105,110                                          00000870
 105 IF(H-Q(I-1))107,110,110                                        00000880
 107 H    = Q(I-1)                                                  00000890
 110 CONTINUE                                                       00000900
     IF(H) 123,120,123                                              00000910
 120 WRITE (6,121)                                                  00000920    157
 121 FORMAT(10X,40HTHE ONLY REAL ROOT WAS NEGATIVE OR ZERO.  )      00000930
     GO TO 5                                                        00000940
 123 H2   = H**2                                                    00000950
     SS  = 0.                                                       00000951
     DO  125  I = 1,N1                                              00000960
 125 CAPY(I) =  EM(I)/H                                             00000970
     DO 130  I = L,N                                                00000980
     TP(I)= SQRT(F2(I) + H2)                                        00000990    172
     COSAA(I) =  H/TP(I)                                            00000991
     ELA(I) = X(I)/COSAA(I)                                         00000992
 130 SS  = SS + ELA(I)                                              00000993
     WRITE(6,140) SS, H,  (I, CAPY(I),P(I),EM(I),F(I), I=1,N)       00001000    182
 140 FORMAT(///5X,28HEXTENSIBLE CATENARY LENGTH =,1PE13.6//10X,20HHORIZ00001010
    1ONTAL TENSION =,1PE11.3////9X,1HI,10X,7HCAPY(I), 10X, 4HLOAD, 13X,00001011
    2 6HMOMENT, 13X, 5HSHEAR //(I10,  4E18.5) )                     00001012
```

Figure 104. Listing of Source Deck for the Catenary (Sheet 3 of 4)

```
                                                                    02/07/86
      8K-RB2     -  EFN   SOURCE STATEMENT  -  IFN(S)  -

    WRITE (6,160) (TP(I), I=L,N)                                    00001020    192
160 FORMAT (10X, 19HTENSION IN CATENARY / (15X, 1P6E15.3) )         00001030
    IF (YMAX.EQ.0.) GO TO  200                                      00001035
    H3  = H1 + H                                                    00001036
    H4  = H3 **2                                                    00001037
    CAPYY =  EMAX/H3                                                00001038
    TPP =  SQRT (F02 + H4)                                          00001039    202
    WRITE (6,170) H3,CAPYY, TPP                                     00001040    203
170 FORMAT(/5X,26HFINAL HORIZONTAL TENSION =,1PE11.3/10X,26HFINAL MAXI00001041
   1MUM DEFLECTION =,1PE11.3/10X,23HFINAL MAXIMUM TENSION =,1PE11.3 ) 00001042
200 CONTINUE                                                        00001048
    GO TO  5                                                        00001050
    END                                                             00001060
```

Figure 104. Listing of Source Deck for the Catenary (Sheet 4 of 4)

Data Page 1

	N	Number of Increments
2 0 0 0 0 0 0 1		
	YMAXO	Maximum Deflection
	E	Modulus of Elasticity
	A	Area
	H_1	Prestressing Tension
2 0 0 0 0 0 0 2		
	X_0	Distance Between Applied Load
	X_1	Distance Between Applied Load
	X_2	Distance Between Applied Load
	X_N	Distance Between Applied Load
	P_1	Applied Load
2 0 0 0 0 0 0 3	P_2	Applied Load
	P_N	Applied Load
2 0 0 0 0 0 0 4		

Figure 105. Input Data

```
 INPUT  DATA
    10
3.7800E-02     1.0300E 07     5.0000E-02     1.8900E 02
1.7000E 00     3.4000E 00     3.4000E 00     3.4000E 00     3.4000E 00     3.4000E 00
3.4000E 00     3.4000E 00     3.4000E 00     3.4000E 00     1.7000E 00    -3.3330E-01
-3.3330E-01    -3.3330E-01    -3.3330E-01    -3.3330E-01    -3.3330E-01    -3.3330E-01
-3.3330E-01    -3.3330E-01    -3.3330E-01
```

Figure 106. Example No. 1—Initial Deflection (Sheet 1 of 2)

OUTPUT DATA

PARTIAL TENSION FIELD BEAMS ** STRESS AND STRAIN IN CATENARY

INEXTENSIBLE CATENARY LENGTH = 3.400010E 01

HORIZONTAL TENSION = 3.747E 02

SHAPE - Y(I) VALUES

0.000E-39	7.560E-03	1.966E-02	2.873E-02	3.478E-02	3.780E-02
3.780E-02	3.478E-02	2.873E-02	1.966E-02	7.560E-03	

TENSION IN CATENARY

3.747E 02	3.747E 02	3.747E 02	3.747E 02	3.747E 02	3.747E 02
3.747E 02	3.747E 02	3.747E 02	3.747E 02	3.747E 02	

EXTENSIBLE CATENARY LENGTH = 3.400357E 01

HORIZONTAL TENSION = 6.192E 01

I	CAPY(I)	LOAD	MOMENT	SHEAR
1	4.57505E-02	-3.33300E-01	2.83305E 00	1.33320E 00
2	1.18951E-01	-3.33300E-01	7.36393E 00	9.99900E-01
3	1.73852E-01	-3.33300E-01	1.07656E 01	6.66600E-01
4	2.10452E-01	-3.33300E-01	1.30320E 01	3.33300E-01
5	2.28753E-01	-3.33300E-01	1.41652E 01	-8.19564E-08
6	2.28753E-01	-3.33300E-01	1.41652E 01	-3.33300E-01
7	2.10452E-01	-3.33300E-01	1.30320E 01	-6.66600E-01
8	1.73852E-01	-3.33300E-01	1.07656E 01	-9.99900E-01
9	1.18951E-01	-3.33300E-01	7.36593E 00	-1.33320E 00
10	4.57505E-02	-3.33300E-01	2.83305E 00	-1.66650E 00

TENSION IN CATENARY

6.192E 01	6.194E 01	6.193E 01	6.193E 01	6.192E 01	6.192E 01
6.192E 01	6.193E 01	6.193E 01	6.194E 01	6.195E 01	

FINAL HORIZONTAL TENSION = 2.509E 02

FINAL MAXIMUM DEFLECTION = 5.645E-02

FINAL MAXIMUM TENSION = 2.509E 02

Figure 106. Example No. 1—Initial Deflection (Sheet 2 of 2)

```
 INPUT  DATA
     10
 0.0000E-39      1.0300E 07      5.0000E-02      1.9300E 02
 1.7000E 00      3.4000E 00      3.4000E 00      3.4000E 00      3.4000E 00      3.4000E 00
 3.4000E 00      3.4000E 00      3.4000E 00      3.4000E 00      1.7000E 00     -3.4000E-01
-3.4000E-01     -3.4000E-01     -3.4000E-01     -3.4000E-01     -3.4000E-01     -3.4000E-01
-3.4000E-01     -3.4000E-01     -3.4000E-01

 OUTPUT DATA

EXTENSIBLE CATENARY LENGTH = 3.400036E 01

 HORIZONTAL TENSION =  1.994E 02

 I          CAPY(I)          LOAD          MOMENT          SHEAR
 1       1.44960E-02     -3.40000E-01     2.89000E 00      1.36000E 00
 2       3.76895E-02     -3.40000E-01     7.51400E 00      1.02000E 00
 3       5.50847E-02     -3.40000E-01     1.09820E 01      6.80000E-01
 4       6.66814E-02     -3.40000E-01     1.32940E 01      3.40000E-01
 5       7.24798E-02     -3.40000E-01     1.44500E 01     -8.19564E-08
 6       7.24798E-02     -3.40000E-01     1.44500E 01     -3.40000E-01
 7       6.66814E-02     -3.40000E-01     1.32940E 01     -6.80000E-01
 8       5.50847E-02     -3.40000E-01     1.09820E 01     -1.02000E 00
 9       3.76895E-02     -3.40000E-01     7.51400E 00     -1.36000E 00
10       1.44960E-02     -3.40000E-01     2.89000E 00     -1.70000E 00
 TENSION IN CATENARY
                1.994E 02       1.994E 02       1.994E 02       1.994E 02       1.994E 02       1.994E 02
                1.994E 02       1.994E 02       1.994E 02       1.994E 02       1.994E 02
```

Figure 107. Example No. 2—Initial Zero Deflection

Data Page 1

Card 20000001

Number of increments

Card 20000002

Maximum deflection
Modulus of elasticity
Area
Prestressing Tension

Card 20000003 or 4 . . . i

Distance between applied load
Applied load

Output Format

Figures 106 and 107 describe the output format of the program:

Output Data For Zero Deflection

Extensible catenary length
Horizontal tension

CAPY (I) Load Moment Shear
(deflection)

Output Data For Initial Deflection

Inextensible catenary length
Horizontal tension
Shape

Extensible catenary length
Horizontal tension

CAPY (I) Load Moment Shear

Final horizontal tension
Final maximum deflection
Final maximum tension

The FORTRAN program which determines the stress and deflection of a pretensioned catenary with the initial deflection (due to unknown loading) is an approximate one. The prerequisite for the usage of this program is a comparatively large prestressing and very small lateral loading. These prerequisites are always satisfied in the case of partial-tension-field beams. The program will handle both components independently: pretensioning and lateral loading. The resulting stresses will be added algebraically, and this is an approximation. In reality the stresses will be smaller; consequently, the program is on the safe side. The maximum deflection, however, will be obtained by Equation C6.

The FORTRAN program which determines the stress and deflection of a pretensioned catenary with zero initial deflection is an exact one. It may be safely used instead of the first one, which was described above, if the initial deflection is very small.

SUMMARY

Given the input data of area, length, deflection, applied load, and initial tension, the FORTRAN IV program can compute two separate analyses depending on "zero deflection" or "initial deflection." The source deck of the program takes less than thirty seconds execution time on the IBM 7094 and requires less than 400 lines printout per case.

FORTRAN IV PROGRAM

A digital computer program has been developed for executing Equation 4-46. A detailed description on the usage of the computer program is presented in this Appendix.

ANALYSIS

The following equation is solved numerically with the IBM 7094 computer:

$$\frac{p_b\, b^2}{2.78\sqrt[3]{A\, E\, p_b^{\,2}\, b^2}} - 0.433\sqrt{\left[a + \frac{(1. - p_b)\, R\, a}{E\, A}\right]^2 - \ell^2} = 0.5\sqrt{4R^2 - \ell^2} - R \qquad \text{(C7)}$$

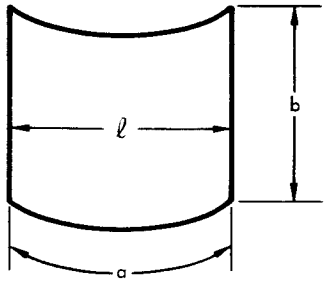

$$\ell = 2R \sin \frac{a}{R}/2$$

By setting p_b equal to some initial value (input data), the IBM program increments that value by the same amount each time until the equation is equal on both sides, or within the calculated tolerance.

PROGRAM DETAILS

Input Data

This paragraph describes the input data required for execution of the numerical procedure.

Data Page 1

Card 30000001

Number of Increments

Card 30000002

Straight Length
Curved Length
Modulus of elasticity
Area
Radius of curvature
Amount p_b is increased

Card 30000003

Tolerance

Output Format

This section describes the printout of the program.

Comparable value = $0.5 \sqrt{4R^2 - \ell^2} - R$

p_b (I) = Incremented input data

$$S(I) = \frac{p_b b^2}{2.78 \sqrt{A E p_b^2 b^2}} - 0.433 \sqrt{\left[a + \frac{(1. - p_b) Ra}{E A}\right]^2 - \ell^2} \qquad (C8)$$

If the value calculated is within the given tolerance, the program will print out only p_b S and S.

SUMMARY

The FORTRAN IV program solves the algebraic equation. The source deck of the program takes less than twenty seconds execution time on the IBM 7094 and requires less than 300 lines printout per case. Figure 108 is a listing of the source deck for algebraic equations. Figure 109 lists the input data for algebraic equations. Figure 110 lists the output data.

```
                                                               02/01/86
      BK-PB3      -  FFN    SOURCE STATEMENT  -  IFN(S)  -

C                                                  RON BEREZNAK    00000003
C      NOMENCLATURE FOR DATA                                       00000004
C        N      NO OF INCREMENTS                                   00000005
C        A      CURVED LENGTH                                      00000007
C        E      MODULUS OF ELASTICITY                              00000008
C        EL     LENGTH                                             00000009
C        B      STRAIGHT LENGTH                                    00000006
C        BA     AREA                                               00000010
C        R      RADIUS OF CURVATURE                                00000011
C        PA     AMOUNT PR IS INCREASED                             00000012
C        TOL    TOLERANCE                                          00000013
C        PR     LOADING                                            00000014
       DIMENSION  PR(1042), S (1042)                               00000019
     5 READ(5,10) N,B,A,E,    BA,R,PA,TOL                          00000020    1
    10 FORMAT(I12/(6E12.8) )                                       00000030
       THETA = (A/R)/2.                                            00000032
       EL  = 2.*R * SIN (THETA)                                    00000033    3
    15 DO 70 I = 1,N                                               00000040
       PR = 0.                                                     00000050
       AL  = PR(I)*B**2/(2.72*(BA*E*PR(I)**2 *B**2) **(1./3.) )    00000060   10
       BL= 0.433 * SQRT((A +(1.-PR(I)) *R*A/(E *BA))**2-EL**2)     00000070   13
       C = 0.5 * SQRT(4.*R**2-EL**2) -  R                          00000080   14
       S(I) = AL- BL                                               00000090
       IF(ABS(S(I)-C) - TOL) 80,80,50                              00000100
    50 PR(I+1) =   PR(I) + PA                                      00000110
    70 CONTINUE                                                    00000120
       WRITE(6,75)C,(I,PR(I),S(I), I  = 1,N)                       00000130   23
    75 FORMAT(1H1////10X,18HCOMPARABLE VALUE = ,1PE11.3////9X,1HI ,  8X, 00000140
     1 5HPR(I), 10X, 4HS(I) //(I10, 2E15.3) )                      00000141
       GO TO 5                                                     00000150
    80 WRITE(6,85) C,PR(I),S(I)                                    00000160   32
    85 FORMAT(1H1///10X,18HCOMPARABLE VALUE =,1PE11.3//10X,5HPRS =,1PE11.00000170
     13//10X3HS =,1PE11.3 )                                        00000171
       GO TO 5                                                     00000180
       END                                                         00000190
```

Figure 108 . Listing of the Source Deck for Algebraic Equations

FORTRAN FIXED 10 DIGIT DECIMAL DATA

DECK NO. _____ PROGRAMMER _____ DATE _____ PAGE _____ of _____ JOB NO. _____

NUMBER	IDENTIFICATION	DESCRIPTION DO NOT KEY PUNCH Data Page 1
		N Number of Increments
	73 80	
	3 0 0 0 0 0 0 1	
		b Straight Length
		a Curved Length
		E Modulus of Elasticity
		BA Area
		R Radius of Curvature
	3 0 0 0 0 0 0 2	PA Amount p_b is Increased
		TOL Tolerance
	3 0 0 0 0 0 0 3	

FORM 114-C-17 REV. 7-58

Figure 109. Input Data for Algebraic Equations

COMPARABLE VALUE = -2.344E 00

I	PR(I)	S(I)
1	0.000E-39	-2.431E 00
2	1.000E-03	-2.378E 00
3	2.000E-03	-2.364E 00
4	3.000E-03	-2.355E 00
5	4.000E-03	-2.347E 00
6	5.000E-03	-2.340E 00
7	6.000E-03	-2.335E 00
8	7.000E-03	-2.330E 00
9	8.000E-03	-2.325E 00
10	9.000E-03	-2.321E 00
11	1.000E-02	-2.317E 00
12	1.100E-02	-2.313E 00
13	1.200E-02	-2.309E 00
14	1.300E-02	-2.306E 00
15	1.400E-02	-2.303E 00
16	1.500E-02	-2.300E 00
17	1.600E-02	-2.297E 00
18	1.700E-02	-2.294E 00
19	1.800E-02	-2.291E 00
20	1.900E-02	-2.289E 00
21	2.000E-02	-2.286E 00
22	2.100E-02	-2.284E 00
23	2.200E-02	-2.281E 00
24	2.300E-02	-2.279E 00
25	2.400E-02	-2.277E 00
26	2.500E-02	-2.275E 00
27	2.600E-02	-2.273E 00
28	2.700E-02	-2.271E 00
29	2.800E-02	-2.269E 00
30	2.900E-02	-2.267E 00
31	3.000E-02	-2.265E 00
32	3.100E-02	-2.263E 00
33	3.200E-02	-2.261E 00

Figure 110. Output Data

REFERENCES

1. Kuhn, Paul, Stresses in Aircraft and Shell Structures. New York: McGraw-Hill Book Company, Inc. (1956).

2. Wagner, Herbert, Flat Sheet Metal Girders with Very Thin Metal Web. Part I – General Theories and Assumptions. NACA TM 604, (1931).

3. Wagner, Herbert, Flat Sheet Metal Girders with Very Thin Metal Web. Part II – Sheet Metal Girders with Spars Resistant to Bending. Oblique Uprights – Stiffness. NACA TM 605 (1931).

4. Wagner, Herbert, Flat Sheet Metal Girders with Very Thin Metal Web. Part III – Sheet Metal Girders with Spars Resistant to Bending. The Stress in Uprights – Diagonal Tension Fields. NACA TM 606 (1931).

5. Moness, E., Flat Plates Under Normal Loads. Douglas Aircraft Co., Rept. 1862, Part I through VII.

6. Levy, S., D. Goldenberg and G. Fibritosky. Simply Supported Long Rectangular Plate Under Combined Axial Load and Normal Pressure. NACA TN 949 (1944).

7. Woolley, R. M., J. N. Corrick, and S. Levy. Clamped Long Rectangular Plate Under Combined Axial Load and Normal Pressure. NACA TN 1047, (1946).

8. Arbuzov. "Analysis of High Beams Based on Ultimate Condition," Oborongiz (1963), (In Russian).

9. Timoshenko, S. P., and J. M. Gere, Theory of Elastic Stability. Second ed., New York: McGraw-Hill Book Company, Inc., (1961).

10. Structures Manual. NAA, S&ID.

11. Moore, R. L. and C. Westcoat. Torsion Tests of Stiffened Cylinders. NACA W. R. No. 4E31, 1944.

12. Romashevski, A. J., "Investigation of Behavior of Beams Systems With a Thin Web and Nonparallel Flanges." CAGI, Trudi No.203 (1935), (In Russian).

13. Romashevski, A.J., "Investigation of Behavior of Beam With a Thin Web." CAGI, Technical Notes No. 58 (1935)., (In Russian).

14. Strigunov, V.M., Theoretical and Experimental Investigation of Behavior of Thin-Walled Beams, CAGI, Trudi No. 349 (1938). Thu

15. Strigunov, V.M., Investigation of Behavior and Method of Analysis of a Beam on Two Supports, With Thin Web. CAGI, Technical Notes No. 58 (1935).

16. Marinkovic, M., "Statica Odredjenich Nosaca", Beograd (1952), (In Serbian).

17. Heinrich Hertel. "Leichtbau", Spring Verlog 1960.

18. Timoshenko, S. Theory of Plates and Shells. New York: McGraw-Hill Book Company, Inc. (1940).

19. Sechler, E.E., and L.G. Dunn. Airplane Structural Analysis and Design. New York: John Wiley & Sons, Inc., (1942).

20. Kauai Tadahiku, and Bruno Thurlinann. Influence Surfaces for Moments in Slabs Continuous Over Flexible Cross Beams. International Association for Bridges and Struct. Engineering, Zürich, Switzerland (1957).

21. Thurlinann, Bruno. Influence Surfaces for Support Moments of Continuous Slabs. Publication of International Association for Bridges and Structural Engineering, Zürich Switzerland (1956).

22. Föppl, A. and Ludwig Föppl. Drang und Zwang. München und Berlin: Verlag von R. Oldenburg, (1941).

23. Uniformly Distributed Hydrostatic Pressure. NACA TM 965.

24. Flat Plates Under Normal Loads. Douglas Aircraft Co., Report 1862.

25. Niles, A.S. and J.S. Newell, "Airplane Structures," Vol. II, 1938.

26. Beton-Kalender, 1965, Taschenbuch für Beton und Stahlbetonbau Sowie die Verwandten Fächer, Berlin — München, p. 203.

27. Niles, A.J., and J.J. Newell, "Airplane Structures," Vol. I, 3rd Edition, 1943, p. 126.

28. Wang, C. Applied Elasticity. New York: McGraw-Hill Book Company, Inc., (1953).

29. Pippard, M. B. E., and J. F. Baker. The Analysis of Engineering Structures, London: Edward Arnold & Co.

30. Kuhn, P., J. P. Peterson, and L. R. Levin. A Summary of Diagonal Tension: Parts I and II. NACA T. N. 2661 and 2622.

31. Denke, Paul H. "Strain Energy Analysis of Incomplete Tension Field Web-Stiffener Combinations," J. Aeron. Sci., Vol. 11, No. 1, (1944) pp. 25-40.

32. Denke, Paul H. "Analysis and Design of Stiffened Shear Webs," J. Aeron. Sci., Vol. 17, No. 4, (1950) pp. 216-231.

33. Kuhn, P., "Investigations on the Incompletely Developed Plane Diagonal-Tension Field". NASA Report No. 697 (1940).

34. Timoshenko, S. P. Theory of Elastic Stability. New York: McGraw-Hill Book Company, Inc. (1936).

35. Moisseiff, L. S., Design Specifications for Bridges and Structures of Aluminum Alloy 27S-T. Pittsburg: Aluminum Company of America (1940).

36. Alcoa Structural Handbook. Aluminum Co. of America, Pittsburg, Penna., (1956).

37. Marjin, V. A. "Stability of Cylindrical Panel Against Shear", Moscow (1959), (In Russian).

38. Marjin, V. A. "Stability of Cylindrical Shell Against Torsion and Internal Pressure", Moscow (1959), (In Russian).

39. Gerard, G., and Herbert Becker. Handbook of Structural Stability. Part III. "Buckling of Curved Plates and Shells". NACA TN 3783 (August 1957).

40. Carslaw, H. S. Fourier's Series and Integrals. Third ed., Dover, New York (1930).

41. Langhaar, H. L. Energy Methods in Applied Mechanics. John Wiley & Sons, Inc. (1962).